

## 5. Stress physiology

HJ De Boeck (editor)

Ecophysiology integrates biology, chemistry, and physics to study how individual organisms sense and respond to changes in their environment. Because they are largely immobile, plants are restricted to responding to changing conditions through phenotypic plasticity. This has led to a series of adaptations, often through adjustments in gene expression leading to changes in hormone synthesis, osmotic balance, etc. (Larcher, 2003; Schulze et al., 2005). Some responses to changes in the environment are slow and these often relate to morphological adjustments such as increased root growth in response to drought via abscisic acid. Other responses are much faster, among which many adjustments (such as stomatal conductance) are to the large fluctuations in temperature, radiation, and air humidity plants experience within a single day.

In uncovering how climate- and other global-change drivers will affect plants and ecosystems, studying ecophysiology provides a mechanistic way to predict when tolerance limits are exceeded and therefore when changes can be expected in the functioning of individual plants, species, and entire ecosystems. Measuring tools and analytical procedures have become increasingly sophisticated, yet the interpretation can be challenging as physiological responses may vary considerably with context-dependent factors such as microclimate and acclimation. For example, heat stress effects may be misinterpreted if tissue temperature is not directly determined and only air temperatures are used (De Boeck et al., 2016; Michaletz et al., 2016), and if measurements are made on plants that have been exposed to relatively high temperatures earlier in their growing season (leading to hardening and muted responses to heat) as opposed to plants that were not exposed (Neuner & Buchner, 2012). Moreover, many ecophysiological measurements are made at the leaf level and scaling up to whole organisms or even ecosystems is usually not straightforward.

In the stress physiology chapter (5), we describe a series of physiological or related measurements useful in climate-change biology. These focus mostly on their use as indicators of stress, be it through the determination of compounds (e.g. chlorophyll and carotenoid content, non-structural carbohydrates), traits and variables such as reflectance, leaf hydraulic conductivity, and leaf thermal properties, to measurements that directly assess stress (through Fv/Fm) and general approaches for determining tolerance.

## References

- De Boeck, H. J., Velde, H. V. D., Groote, T. D., & Nijs, I. (2016). Ideas and perspectives: Heat stress: more than hot air. *Biogeosciences*, 13(20), 5821-5825.
- Larcher, W. (2003). *Physiological Plant Ecology: Ecophysiology and Stress Physiology of Functional Groups*. Springer Science & Business Media.
- Michaletz, S. T., Weiser, M. D., McDowell, N. G., Zhou, J., Kaspari, M., Helliker, B. R., & Enquist, B. J. (2016). The energetic and carbon economic origins of leaf thermoregulation. *Nature Plants*, 2, 16147.

Neuner, G., & Buchner, O. (2012). Dynamics of tissue heat tolerance and thermotolerance of PS II in alpine plants. In C. Lütz (Ed.), *Plants in Alpine Regions: Cell Physiology of Adaption and Survival Strategies* (pp. 61-74). Vienna: Springer.

Schulze, E. D., Beck, E., & Müller-Hohenstein, K. (2005). Environment as stress factor: stress physiology of plants. In *Plant Ecology* (pp. 7-22). Berlin: Springer.

How to cite a protocol:

E.g. To measure the leaf thermal time constant we used the methods described in protocol 5.6 Leaf thermal traits in the Supporting Information S5 Stress physiology in Halbritter et al. (2020).

Halbritter et al. (2020) The handbook for standardised field and laboratory measurements in terrestrial climate-change experiments and observational studies (ClimEx). *Methods in Ecology and Evolution*, 11(Issue) pages.

How to cite an updated protocol version:

E.g. To measure the leaf thermal time constant we used the methods described in protocol 5.6 Leaf thermal traits in the Supporting Information S5 Stress physiology in Halbritter et al. (2020), using the updated protocol version, Date, available in the online version: [www.climexhandbook.uib.no](http://www.climexhandbook.uib.no).

Halbritter et al. (2020) The handbook for standardised field and laboratory measurements in terrestrial climate-change experiments and observational studies (ClimEx). *Methods in Ecology and Evolution*, 11(Issue) pages.

## Table of contents

5.1 Chlorophyll fluorescence.....	402
5.2. Chlorophyll and carotenoid content .....	413
5.3. Non-structural carbohydrates.....	422
5.4 Lethal dose (LD50) to quantify stress tolerance exemplified by frost tolerance .....	431
5.5 Leaf temperature .....	440
5.6 Leaf thermal traits.....	450
5.7 Stomatal conductance .....	458
5.8 Psychrometry for water potential measurements.....	465
5.9 Pressure-volume curve – TLP, $\epsilon$ , $\Psi_0$ .....	472
5.10 Maximum leaf hydraulic conductance .....	477

5.11 Metabolomic profiling in plants using mass-spectrometry.....	483
5.12 Reflectance assessment of plant physiological status .....	490
5.13 Stable isotopes of water for inferring plant function.....	498
5.14 BVOC emissions from plants and soils .....	515
5.15 Water-use efficiency .....	522
5.16 Leaf hydraulic vulnerability to dehydration .....	534

## 5.1 Chlorophyll fluorescence

**Authors:** Lembrechts JJ<sup>1</sup>, Zinnert JC<sup>2</sup>, Mänd P<sup>3</sup>, De Boeck HJ<sup>1</sup>

**Reviewer:** Porcar Castell A<sup>4</sup>

**Measurement unit:**  $F_v/F_m$  or related variables; **Measurement scale:** leaf part; **Equipment cost:** €€–€€€; **Running costs:** €; **Installation effort:** low; **Maintenance effort:** medium (frequent recording); **Knowledge need:** medium to high (for interpretation); **Measurement mode:** manual

Chlorophyll fluorescence can be used as an indirect non-invasive measurement of photosystem II (PSII) efficiency. The principle underlying it is relatively simple. The fate of light energy absorbed by chlorophyll molecules in a leaf is one of the following: (i) it can be used to drive photosynthesis, (ii) excess energy can be dissipated as heat, or (iii) the energy can be re-emitted as light with a longer wavelength (Maxwell & Johnson, 2000), a process called chlorophyll fluorescence. These three processes occur in competition, as they rely on the same energy source – the absorbed photons. Hence, measuring the yield of chlorophyll fluorescence can provide information on changes in both the efficiency of photochemistry and heat dissipation (Kautsky & Hirsch, 1931; Maxwell & Johnson, 2000).

The proven effects of both abiotic and biotic stressors on this energy partitioning in PSII (and the subsequent fluorescence yield), combined with the ease of the measurements, have made chlorophyll fluorescence a widely applied technique as an indicator of stress in leaves, in climate-change studies, and beyond (Lichtenthaler, 1988; Lichtenthaler & Miehé, 1997; Ogaya & Peñuelas, 2003; Souza et al., 2004; Takahashi & Murata, 2008). Applications include its role as an indicator of crop performance and tree vitality (Lichtenthaler et al., 1986; Baker & Rosenqvist, 2004), as well as of abiotic (e.g. drought or heat stress; Havaux, 1992; Ogaya & Peñuelas, 2003) and biotic (e.g. plant-pathogen interactions; Lang, 1995; Chaerle et al., 2004) stressors, showing its versatility as a tool to study plant responses to environmental factors in a wide range of observational and experimental studies.

### 5.1.1 What and how to measure?

#### *Phenomenology*

When a leaf is transferred from darkness to light, excitation energy captured by chlorophyll molecules in the antenna is rapidly transferred to open/oxidised reaction centres of photosystem II (PSII), progressively reducing them (Maxwell & Johnson, 2000). During the first seconds of illumination, this gives rise to an increase in the yield of chlorophyll fluorescence (the Kautsky effect, Kautsky & Hirsch, 1931). When the light input is sustained, however, the fluorescence level typically starts to fall again, over a timescale of seconds to minutes. This so-called fluorescence quenching results from the two above-mentioned processes competitively using the same incoming energy: “photochemical quenching”, the use of excitation energy in photosynthesis, and “non-photochemical quenching”, the use of excitation energy in heat dissipation. Over time, various measurement techniques have been developed to measure fluorescence yield and disentangle these different quenching components, ranging from traditional measurements on single, dark-adapted leaves, over

pulse amplitude modulated (PAM) measurements to large-scale remote sensing assessments of whole canopies using passive fluorescence methods.

### **Where to start**

Krause & Weis (1991), Lazár (2015), Lichtenthaler (1988), Maxwell & Johnson (2000), Murchie & Lawson (2013), Souza et al. (2004)

### **Main instrumentation**

#### **a) Dark-adapted measurements**

Dark-adapted fluorescence measurements are used to mimic night conditions by avoiding the variation in fluorescence and quenching caused by instantaneous illumination (Porcar-Castell, 2011). The purpose of this dark acclimation is to re-oxidise the electron acceptors in PSII (which takes only a few seconds) and to relax all the reversible non-photochemical quenching, which may take a few minutes or hours, depending on plant species, temperature, stress levels, and prior light conditions (Demmig-Adams & Adams, 2006; Porcar-Castell et al., 2014).

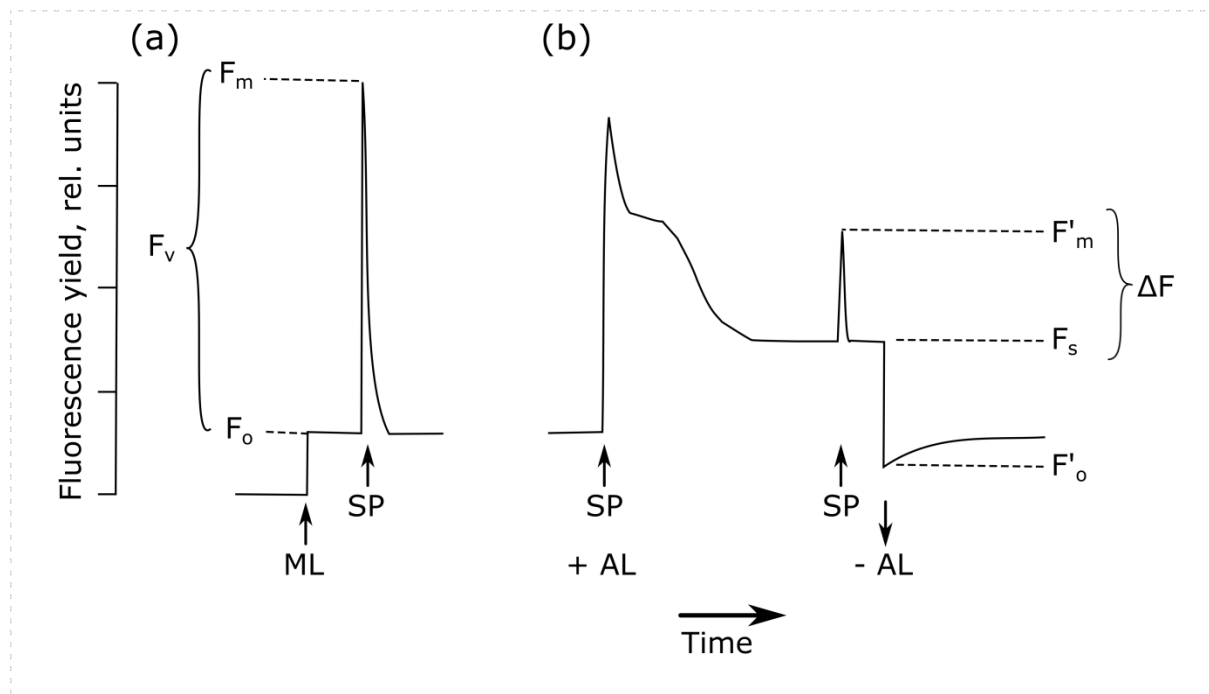


**Figure 5.1.1** Measurement of chlorophyll fluorescence (in relative units) on a dark-adapted leaf (a) and with the pulse amplitude modulation method (b). ML = measuring light, SP = saturating light pulse. AL = actinic (background) light. For the explanation of the different F-values, see main text. Adapted from van Kooten and Snel (1990).

After dark-adaptation, background fluorescence ( $F_o$ ) is measured with a measuring light too weak to start photochemical reactions (Figure 5.1.1, Bolhàr-Nordenkampf & Öquist, 1993). Subsequent application of a high intensity, short duration flash of light to this dark-adapted leaf closes all

reaction centres (Maxwell & Johnson, 2000). The fluorescence yield reaches a value equivalent to that which would be attained in the absence of any photochemical quenching, the maximum fluorescence,  $F_m$ . The difference between  $F_o$  and  $F_m$  is the variable fluorescence,  $F_v$ . It has been shown theoretically and empirically that  $F_v / F_m$  (i.e.  $(F_m - F_o) / F_m$ ) is a robust indicator of the maximum quantum yield of PSII chemistry (Butler, 1978). For unstressed leaves, the value of  $F_v / F_m$  is fairly consistent, with observed values of  $0.832 \pm 0.004$ , correlating with the maximum quantum yield of photosynthesis (Björkman & Demmig, 1987), while a stressor would reduce this value. Dark-adapted or pre-dawn  $F_v / F_m$  thus provides a useful relative indication of substantial photoinhibition or down-regulation of PSII in relation to non-specific stressors (Murchie & Lawson, 2013), although it is worth noting that it cannot be used as an accurate quantitative value of the quantum yield, among others due to the significant variation in this value depending on leaf morphology, species, and fluorometer (Baker, 2008). More detailed measurements of the rise from  $F_o$  to  $F_m$  at a resolution of  $\mu\text{s}$  and the specific pattern – called O-J-I-P – this transition follows, can provide additional insights in the photochemical efficiency of PSII (Strasser & Govindjee, 1992).

The timing of dark-adaptation is thus crucial to acquire accurate measurements of  $F_v / F_m$ . Often, a period of 15 to 20 minutes is recommended. It has, however, been shown that low levels of quenching can still be observed after a whole night or even 24 hours of dark-adaption (Baker, 2008). There are indeed different types of non-photochemical quenching with different temporal components, being either rapidly or slowly reversible non-photochemical quenching (Porcar-Castell, 2011; Lazár, 2015). As one can never be sure that all samples have been dark-adapted for the same time, pre-dawn conditions are often preferred in the field for stress assessments (Maxwell & Johnson, 2000; Murchie & Lawson, 2013). If this cannot be achieved, leaf clips – usually provided with the fluorometer – can be used to dark-adapt a leaf (or leaf part) for a fixed period of time at any time of the day (Figure 5.1.2).

Modern handheld fluorometers (both plant efficiency analysers (PEA) and pulse amplitude modulated (PAM) fluorometers) automatically provide all the mentioned F-values after initiating the necessary measurement light and saturating light pulse, making the actual measurements easy, fast, and practical to perform in-situ without harvesting the leaves. For a good overview of the many possible pitfalls in the interpretation of these measurements, see Murchie & Lawson (2013).



**Figure 5.1.2** Dark adaption clips and optical sensor unit (with measurement light) of a plant efficiency analyser (PEA). The dark adaption clip is installed on a leaf and the metal shutter is used to close the measurement hole. After dark adaption time of 15-20 minutes, the sensor unit is placed on the clip, the shutter is opened and the measurement light flashed. Photo Jonas Lambrechts.

### b) Light-adapted measurements

Measurement of chlorophyll fluorescence has become even more versatile with “modulated” fluorometers, which rely on the selective monitoring of the fluorescence yield from rapid repetitive high-frequency light pulses with a measuring beam, while the detector is tuned to detect only fluorescence excited by the measuring light (Quick & Horton, 1984; Schreiber et al., 1986; Maxwell & Johnson, 2000; Souza et al., 2004). This approach allows the measurement of fluorescence dynamics under illumination, as the recorded fluorescence is coming from a modulated light source of constant intensity instead of from ambient light. So, while ambient fluorescence is controlled by both incoming light and current PSII energy partitioning status, PAM fluorescence is only controlled by the current PSII energy partitioning status, allowing one to probe PSII much more easily.

The light-adapted measurement can be used to estimate changes in the quantum yield of PSII (i.e. the proportion of light absorbed by chlorophyll in PSII that is used in photochemistry; Genty et al., 1989; Maxwell & Johnson, 2000).  $\Delta F / F'_m$  is calculated as the relationship between maximal fluorescence in a light-adapted leaf after a saturating pulse of light ( $F'_m$ ) and steady-state fluorescence prior to any saturating pulse ( $F_s$  or  $F_t$ , depending on the source):  $(F'_m - F_s) / F'_m$  (Figure 5.1.1). Since  $\Delta F / F'_m$  changes with light intensity, it is important to compare samples at similar levels of photosynthetically active radiation (PAR) (Murchie & Lawson, 2013). Other approaches have restricted measurements to conditions of saturating PAR for photosynthesis (Murchie & Lawson, 2013).



**Figure 5.1.3** Leaf clip of a pulse amplitude modulated (PAM) fluorometer, with different light sources from above and below. A leaf – potentially still attached to the plant – is held underneath the horizontal plate. Photo: Jonas Lambrechts.

conditions are used for each measurement. Again, interpretation of the results can encounter several pitfalls; for a good overview see Murchie & Lawson (2013).

### c) New fluorescence methods: solar-induced fluorescence

More recent developments in the field now allow remote measurements of solar-induced chlorophyll fluorescence (SIF), providing new ways to track photosynthesis and gross primary productivity of

For a description of additional parameters provided by the PAM methodology, see section 5.1.2 *Special cases, emerging issues, and challenges*. Modern PAM-fluorometers are easy to use, and only require the attachment of a leaf clip to the leaf and one click of a button to initiate the necessary measurement pulses (Figure 5.1.3). In contrast to dark-adapted measurements, the timing of measurements is less critical, yet one might want to make sure comparable

terrestrial ecosystems (Meroni et al., 2009; Frankenberg et al., 2011; Guanter et al., 2014). Importantly, the spatiotemporal and methodological context of these new applications is very different from the traditional methods described above, both in terms of phenomenology as well as in terms of instrumentation (Porcar-Castell et al., 2014). For example, unlike PAM, SIF can only be estimated within very narrow spectral bands where the radiation reaching the Earth's surface has been greatly attenuated due to gas absorption, either in the solar photosphere (Fraunhofer lines) or Earth's atmosphere (e.g. oxygen bands). Because SIF is not based on PAM measurements, nor can it be measured under saturating pulses, its interpretation is much more complex than that of PAM fluorescence. This is a rapidly expanding field however, in which ground instrumentation is being developed (e.g. Porcar-Castell et al., 2014) and in which new space missions are providing increasing amounts of data. Overall, connecting active PAM and passive SIF measurements may provide new opportunities for upscaling ecological hypotheses from the leaf to the canopy and landscape levels.

### **Where to start**

Baker (2008), Björkman & Demmig (1987), Bolhàr-Nordenkampf & Öquist (1993), Butler (1978), Genty et al. (1989), Porcar-Castell et al. (2014), Quick & Horton (1984)

#### **5.1.2 Special cases, emerging issues, and challenges**

##### **Special cases**

PAM fluorescence measurement devices have been adapted recently for continuous field monitoring (MONI-PAM; Porcar-Castell et al., 2008). Such instruments measure chlorophyll fluorescence, PAR, and temperature in the field over a certain period, on exactly the same leaf area and thus facilitate the estimation of both rapidly reversible and sustained non photochemical quenching.

*In vivo* fluorescence measurement techniques, as described here, have also been adapted for use in aquatic environments on lower photosynthetic organisms such as algae. The assessment of largely identical fluorescence parameters is possible (Campbell et al., 1998; Kromkamp & Forster, 2003), although alternative fluorometers and some modifications of the above-mentioned parameters might be needed (Campbell et al., 1998).

Chlorophyll fluorescence measurements are often combined with other techniques and instrumentation and help provide a unique research tool to answer a myriad of other questions. For example, combining chlorophyll fluorescence with infra-red gas exchange (IRGA; also see protocols 5.7 Stomatal conductance and 5.15 Water-use efficiency) techniques provides information on the correlation between PSII photosynthetic efficiency and the CO<sub>2</sub> assimilation rate by eliminating photorespiration (Murchie & Lawson, 2013). Such exercises, however, require good insights into the processes at hand to avoid misinterpretation. For example, the abovementioned technique often relies on absolute estimates of the electron transport rate (ETR) through fluorescence, yet the latter is based on several assumptions (see below *Challenges b) Light-adapted measurements*; e.g. Yin et al., 2009).

## **Challenges**

### **a) Dark-adapted measurements**

With  $F_v / F_m$  being so easy to measure in dark-adapted leaves, it has proven an invaluable measure of plant stress. Its interpretation, however, is not always straightforward (Murchie & Lawson, 2013). First, it is not easy to assess the underlying cause of the decline in the performance of PSII as assessed through  $F_v / F_m$ . Certain stress conditions such as drought might not only inactivate PSII reaction centres and reduce  $F_v / F_m$  through a rise in  $F_o$ , but they might also change the optical properties of the leaf, in which case the individual observed values of  $F_m$  and  $F_o$  may be a result of changes in leaf absorptance (Murchie & Lawson, 2013). This will affect the estimation of NPQ but has, *a priori*, no effect on  $F_v / F_m$  since the reduction in  $F$  due to absorption cancels out in the ratio. Additionally, a decline in  $F_v / F_m$  does not necessarily imply that the photosynthetic performance of the plant is compromised (Demmig-Adams & Adams, 2006; Murchie & Niyogi, 2011; Murchie & Lawson, 2013). It is worth mentioning that a sufficiently high light intensity is necessary to induce closure of PSII (Takahashi & Murata, 2008) before a difference in  $F_v / F_m$  is observed between treatments.  $F_v / F_m$  measurements as an indicator of stress are also limited to leaves: stress in other plant parts might not be reflected by a reduction in fluorescence yield (Murchie & Lawson, 2013). In that regard, leaf selection itself is also important. One should note that fluorescence measurements are highly heterogeneous at the within-plant level, especially under stress conditions. Comparing leaves in similar conditions, for example consistently working with the youngest fully expanded leaf or with leaves growing under similar light regimes, can help to reduce such measurement noise.

### **b) Light-adapted measurements**

The electron transport rate (ETR,  $\mu\text{mol photon m}^{-2} \text{ s}^{-1}$ ) can be derived from the quantum yield as measured by the PAM, by multiplying  $\Delta F / F'_m$  with the light intensity (PAR), fractional absorptance of light by the leaf (measured using an integrating sphere), and the partitioning of energy between PSII and PSI (0.5, yet dependent on wavelength of the light, time, and species; Maxwell & Johnson, 2000). This requires an accurate determination of the incident PAR on the leaf, the proportion of incident PAR that is absorbed by the leaf, and the fraction of absorbed PAR that is received by PSII. As it is not generally practical to measure the fractional absorptance of light (but see Olascoaga et al., 2016), it is often estimated as 0.84 for C<sub>3</sub> plants (Björkman & Demmig, 1987). The need for such general assumptions suggests it is best to avoid using ETR to draw conclusions between samples. Alternatively, ETR can be expressed in relative changes among samples by multiplying  $\Delta F / F'_m$  by PAR (Maxwell & Johnson, 2000).

The PAM measuring systems can be used to disentangle the various sources of fluorescence quenching as either photochemical or non-photochemical quenching (Roháček & Barták, 1999), allowing a more detailed assessment of the processes driving photosynthesis and energy dissipation. The first saturating light pulse on a dark-adapted leaf closes all reaction centres ( $qP = 0$ ) and causes fluorescence to rise to the peak value  $F_m$ . Next, a continuous actinic light source induces both photochemical and non-photochemical quenching, together dictating the level of fluorescence. Once both types of quenching reach a steady state, fluorescence will be constant (steady-state fluorescence,  $F_s$ ). Subsequent saturating light pulses will now result in peaks with the maximal fluorescence level  $F'_m$ , lower than the initial  $F_m$  due to the initiation of non-photochemical quenching.

The photochemical quenching ( $qP$ ) can then be calculated as  $(F'_m - F_s) / (F'_m - F'_o)$ , with  $F'_o$  the new level of background fluorescence when actinic light is switched off again (van Kooten & Snel, 1990). While this parameter appears very similar to  $\Delta F / F'_m$  described in 1.2b,  $qP$  gives an indication of the proportion of PSII reaction centres that are open, in contrast to the proportion of absorbed energy being used in photochemistry described by  $\Delta F / F'_m$ .

At the time of the short saturating light pulses, all PSII acceptors will be reduced, again inhibiting all photochemical quenching. All remaining quenching compared to the dark-adapted control ( $F_m$ ) thus has to be non-photochemical (Schreiber et al., 1986), allowing the calculation of  $qN$  as  $(F_m - F'_m) / (F_m - F'_o)$ . Throughout the years, many alternative quenching parameters have been proposed, tackling several issues with the two listed. For more details see Roháček (2002) and Lazár (2015).

### Selection of leaves

Care must be taken when making comparisons with light-adapted measurements as  $\Delta F / F'_m$  can vary based on light levels and the light saturation behaviour of plants growing under different field conditions (Maxwell & Johnson, 2000). Comparative measurements can be obtained by standardising light levels among plants or capturing a range of light conditions on one plant. Commonly, light-saturated, fully expanded leaves are selected when taking measurements in open environments. In shaded environments, light-adapted parameters will quickly change based on sunflecks (Adams et al., 1999; Maxwell & Johnson, 2000).

### 5.1.3 References

#### *Theory, significance, and large datasets*

Baker (2008), Kautsky & Hirsch (1931), Krause and Weis (1991), Maxwell & Johnson (2000), Schreiber et al. (1995)

#### *More on methods and existing protocols*

Campbell et al. (1998), Kolber et al. (2005), Lazár (2015), Maxwell & Johnson (2000), Murchie & Lawson (2013)

### All references

- Adams, W., Demmig-Adams, B., Logan, B., Barker, D., & Osmond, C. B. (1999). Rapid changes in xanthophyll cycle-dependent energy dissipation and photosystem II efficiency in two vines, *Stephania japonica* and *Smilax australis*, growing in the understory of an open Eucalyptus forest. *Plant, Cell & Environment*, 22(2), 125-136.
- Baker, N. R. (2008). Chlorophyll fluorescence: a probe of photosynthesis in vivo. *Annual Review of Plant Biology*, 59, 89-113.

- Baker, N. R., & Rosenqvist, E. (2004). Applications of chlorophyll fluorescence can improve crop production strategies: an examination of future possibilities. *Journal of Experimental Botany*, 55(403), 1607-1621.
- Björkman, O., & Demmig, B. (1987). Photon yield of O<sub>2</sub> evolution and chlorophyll fluorescence characteristics at 77K among vascular plants of diverse origins. *Planta*, 170(4), 489-504.
- Bolhàr-Nordenkampf, H., & Öquist, G. (1993). Chlorophyll fluorescence as a tool in photosynthesis research. In D. O. Hall, J. M. O. Scurlock, H. R. Bolhàr-Nordenkampf, R. C. Leegood, & S. P. Long (Eds.), *Photosynthesis and Production in a Changing Environment* (pp. 193-206). Netherlands: Springer.
- Butler, W. L. (1978). Energy distribution in the photochemical apparatus of photosynthesis. *Annual Review of Plant Physiology*, 29(1), 345-378.
- Campbell, D., Hurry, V., Clarke, A. K., Gustafsson, P., & Öquist, G. (1998). Chlorophyll fluorescence analysis of cyanobacterial photosynthesis and acclimation. *Microbiology and Molecular Biology Reviews*, 62(3), 667-683.
- Chaerle, L., Hagenbeek, D., de Bruyne, E., Valcke, R., & van der Straeten, D. (2004). Thermal and chlorophyll-fluorescence imaging distinguish plant-pathogen interactions at an early stage. *Plant and Cell Physiology*, 45(7), 887-896.
- Demmig-Adams, B., & Adams, W. W. (2006). Photoprotection in an ecological context: the remarkable complexity of thermal energy dissipation. *New Phytologist*, 172(1), 11-21.
- Frankenberg, C., Fisher, J. B., Worden, J., Badgley, G., Saatchi, S. S., Lee, J. E., ... Kuze, A. (2011). New global observations of the terrestrial carbon cycle from GOSAT: Patterns of plant fluorescence with gross primary productivity. *Geophysical Research Letters*, 38(17) GL048738.
- Genty, B., Briantais, J.-M., & Baker, N. R. (1989). The relationship between the quantum yield of photosynthetic electron transport and quenching of chlorophyll fluorescence. *Biochimica et Biophysica Acta - General Subjects*, 990(1), 87-92.
- Guanter, L., Zhang, Y., Jung, M., Joiner, J., Voigt, M., Berry, J. A., ... Lee, J.-E. (2014). Global and time-resolved monitoring of crop photosynthesis with chlorophyll fluorescence. *Proceedings of the National Academy of Sciences USA*, 111(14), E1327-E1333.
- Havaux, M. (1992). Stress tolerance of photosystem II in vivo: antagonistic effects of water, heat, and photoinhibition stresses. *Plant Physiology*, 100(1), 424-432.
- Kautsky, H., & Hirsch, A. (1931). Neue versuche zur kohlensäureassimilation. *Naturwissenschaften*, 19(48), 964-964.
- Kolber, Z., Klimov, D., Ananyev, G., Rascher, U., Berry, J., & Osmond, B. (2005). Measuring photosynthetic parameters at a distance: laser induced fluorescence transient (LIFT) method for remote measurements of photosynthesis in terrestrial vegetation. *Photosynthesis Research*, 84(1-3), 121-129.
- Krause, G., & Weis, E. (1991). Chlorophyll fluorescence and photosynthesis: the basics. *Annual Review of Plant Biology*, 42(1), 313-349.

- Kromkamp, J. C., & Forster, R. M. (2003). The use of variable fluorescence measurements in aquatic ecosystems: differences between multiple and single turnover measuring protocols and suggested terminology. *European Journal of Phycology*, 38(2), 103-112.
- Lang, M. (1995). Studies on the blue-green and chlorophyll fluorescences of plants and their application for fluorescence imaging of leaves. *Karlsruhe Contribution to Plant Physiology*, 29, 1-110.
- Lazár, D. (2015). Parameters of photosynthetic energy partitioning. *Journal of Plant Physiology*, 175, 131-147.
- Lichtenthaler, H. K. (1988). In vivo chlorophyll fluorescence as a tool for stress detection in plants. In H. K. Lichtenthaler (Ed.), *Applications of Chlorophyll Fluorescence in Photosynthesis Research, Stress Physiology, Hydrobiology and Remote Sensing* (pp. 129-142). Netherlands: Springer.
- Lichtenthaler, H. K., & Miehé, J. A. (1997). Fluorescence imaging as a diagnostic tool for plant stress. *Trends in Plant Science*, 2(8), 316-320.
- Lichtenthaler, H., Buschmann, C., Rinderle, U., & Schmuck, G. (1986). Application of chlorophyll fluorescence in ecophysiology. *Radiation and Environmental Biophysics*, 25(4), 297-308.
- Maxwell, K., & Johnson, G. N. (2000). Chlorophyll fluorescence—a practical guide. *Journal of Experimental Botany*, 51(345), 659-668.
- Meroni, M., Rossini, M., Guanter, L., Alonso, L., Rascher, U., Colombo, R., & Moreno, J. (2009). Remote sensing of solar-induced chlorophyll fluorescence: Review of methods and applications. *Remote Sensing of Environment*, 113(10), 2037-2051.
- Murchie, E. H., & Lawson, T. (2013). Chlorophyll fluorescence analysis: a guide to good practice and understanding some new applications. *Journal of Experimental Botany*, 64(13), 3983-3998.
- Murchie, E. H., & Niyogi, K. K. (2011). Manipulation of photoprotection to improve plant photosynthesis. *Plant Physiology*, 155(1), 86-92.
- Ogaya, R., & Peñuelas, J. (2003). Comparative field study of *Quercus ilex* and *Phillyrea latifolia*: photosynthetic response to experimental drought conditions. *Environmental and Experimental Botany*, 50(2), 137-148.
- Olascoaga, B., Mac Arthur, A., Atherton, J., & Porcar-Castell, A. (2016). A comparison of methods to estimate photosynthetic light absorption in leaves with contrasting morphology. *Tree Physiology*, 36(3), 368-379.
- Porcar-Castell, A. (2011). A high-resolution portrait of the annual dynamics of photochemical and non-photochemical quenching in needles of *Pinus sylvestris*. *Physiologia Plantarum*, 143(2), 139-153.
- Porcar-Castell, A., Pfundel, E., Korhonen, J. F., & Juurola, E. (2008). A new monitoring PAM fluorometer (MONI-PAM) to study the short-and long-term acclimation of photosystem II in field conditions. *Photosynthesis Research*, 96(2), 173-179.
- Porcar-Castell, A., Tyystjärvi, E., Atherton, J., van der Tol, C., Flexas, J., Pfundel, E. E., ... Berry, J. A. (2014). Linking chlorophyll *a* fluorescence to photosynthesis for remote sensing applications: mechanisms and challenges. *Journal of Experimental Botany*, 65(15), 4065-4095.

- Quick, W., & Horton, P. (1984). Studies on the induction of chlorophyll fluorescence in barley protoplasts. II. Resolution of fluorescence quenching by redox state and the transthalakoid pH gradient. *Proceedings of the Royal Society of London B: Biological Sciences*, 220(1220), 361-370.
- Roháček, K. (2002). Chlorophyll fluorescence parameters: the definitions, photosynthetic meaning, and mutual relationships. *Photosynthetica*, 40(1), 13-29.
- Roháček, K., & Barták, M. (1999). Technique of the modulated chlorophyll fluorescence: basic concepts, useful parameters, and some applications. *Photosynthetica*, 37(3), 339.
- Schreiber, U., Schliwa, U., & Bilger, W. (1986). Continuous recording of photochemical and non-photochemical chlorophyll fluorescence quenching with a new type of modulation fluorometer. *Photosynthesis Research*, 10(1-2), 51-62.
- Schreiber, U., Bilger, W., & Neubauer, C. (1995). Chlorophyll fluorescence as a nonintrusive indicator for rapid assessment of in vivo photosynthesis. In E.-D. Schultze, & M. M. Caldwell (Eds.), *Ecophysiology of Photosynthesis* (pp. 49-70). Berlin: Springer.
- Souza, R., Machado, E., Silva, J., Lagôa, A., & Silveira, J. (2004). Photosynthetic gas exchange, chlorophyll fluorescence and some associated metabolic changes in cowpea (*Vigna unguiculata*) during water stress and recovery. *Environmental and Experimental Botany*, 51(1), 45-56.
- Strasser, R. J., & Govindjee (1992). The Fo and the O-J-I-P fluorescence rise in higher plants and algae. In J. H. Argyroudi-Akoyunoglou (Ed.), *Regulation of Chloroplast Biogenesis* (pp. 423-426). Boston: Springer.
- Takahashi, S., & Murata, N. (2008). How do environmental stresses accelerate photoinhibition? *Trends in Plant Science*, 13(4), 178-182.
- van Kooten, O., & Snel, J. F. (1990). The use of chlorophyll fluorescence nomenclature in plant stress physiology. *Photosynthesis Research*, 25(3), 147-150.
- Yin, X., Struik, P. C., Romero, P., Harbinson, J., Evers, J. B., van der Putten, P. E. L., & Vos, J. A. N. (2009). Using combined measurements of gas exchange and chlorophyll fluorescence to estimate parameters of a biochemical C<sub>3</sub> photosynthesis model: a critical appraisal and a new integrated approach applied to leaves in a wheat (*Triticum aestivum*) canopy. *Plant, Cell & Environment*, 32(5), 448-464.

**Authors:** Lembrechts JJ<sup>1</sup> Zinnert JC<sup>2</sup>, Mänd P<sup>3</sup>, De Boeck HJ<sup>1</sup>

**Reviewer:** Porcar Castell A<sup>4</sup>

## Affiliations

<sup>1</sup> Centre of Excellence PLECO (Plants and Ecosystems), Biology Department, University of Antwerp, Wilrijk, Belgium

<sup>2</sup> Department of Biology, Virginia Commonwealth University, Richmond, USA

<sup>3</sup> Institute of Ecology and Earth Sciences, Tartu University, Tartu, Estonia

<sup>4</sup> Optics of Photosynthesis Laboratory, Institute for Atmospheric and Earth System Research/Forest Sciences, University of Helsinki, Helsinki, Finland

## 5.2. Chlorophyll and carotenoid content

**Authors:** Mänd P<sup>1</sup>

**Reviewers:** Porcar Castell A<sup>2</sup>, Linder S<sup>3</sup>

**Measurement unit:** mg cm<sup>-2</sup>, mg g<sup>-1</sup>; **Measurement scale:** leaf-level; **Equipment costs:** €–€€; **Running costs:** €; **Installation effort:** medium; **Maintenance effort:** low; **Knowledge:** medium; **Measurement mode:** manual

Chlorophylls and carotenoids are plant pigments which absorb light energy for use in photosynthesis. There are two main chlorophyll (Chl) pigments in higher plants (Chl a and Chl b) and several hundred different carotenoids (Car). However, only six carotenoids are ubiquitous among higher plants (Esteban et al., 2015). The pigment content of plants is species-specific and changes with season and leaf age (Linder, 1972), but also depends on environmental parameters, mainly light conditions (Demmig-Adams & Adams, 1992; Niinemets & Valladares, 2004). Shade plants usually have higher chlorophyll concentrations per unit leaf mass and a lower ratio of Car:Chl and Chl a:b (Niinemets et al., 1998). Light-harvesting protein complexes in plant photosystems (mainly LHCII) are rich in Chl b, in contrast to the core reaction centre complexes of plant photosystems that consist only of Chl a. Thus, an increase in antenna (LHC) size will be reflected as a decrease in the Chl a:b ratio. Under low light there is no need to invest so much on reaction centres and electron transport chain constituents and resources are invested instead in building larger antennae (Eichelmann et al., 2005). The chlorophyll content of leaves and ratio of Chl a:b are furthermore known to change as a response to climate- and global-change drivers, such as air pollution (Tripathi & Gautam, 2007), drought (Anjum et al., 2011), salt stress (Santos, 2004), and iron deficiency (Belkhodja et al., 1998). In addition to light harvesting, the carotenoids play an important role in the photoprotection of the photosystems, which is why the Car:Chl ratio depends mainly on light conditions (Demmig-Adams, 1990).

The conversion of a carotenoid violaxanthin to zeaxanthin is the main pathway in the regulation of heat dissipation of photosystem II (PSII) energy, when PSII encounters excess energy that exceeds the photosynthetic capacity of the photosystem (Young, 1991). In fact, most plants experience excess light on a daily basis, although in the case of stressed plants, photosynthetic capacity declines even more and excess light needs to be redirected to avoid photodamage (Ort, 2001). Thus, the content of photoprotective pigments tends to increase in stressed environments, as has been observed in cases of nitrogen starvation (Jalal et al., 2013) or drought (Colom & Vazzana, 2003). Chlorophyll content is used also as an indicator of the nitrogen (N) status of leaves while N is needed for chlorophyll production (Linder, 1980; Muñoz-Huerta et al., 2013). Pigment content also affects the optical properties of leaves including their spectral reflectance (Vogelmann, 1993; Gitelson et al., 2003; Atherton et al., 2017). A large number of indices, mostly based on reflectance (see section 5.2.2) (Peñuelas et al., 1995; Sims & Gamon, 2002; Gamon et al., 2016) but also on fluorescence ratios (e.g. Gitelson et al., 1998), has been developed in order to link changes in plant pigment concentrations to optical measurements. The advantage of these indices is that they can be used to track changes in leaf pigment concentrations on a non-destructive basis (when applied at the leaf level), or to track vegetation greenness and pigment dynamics (when applied at the canopy and landscape scales via remote sensing) (Sims & Gamon, 2002; Inoue et al., 2016). As such, the more effective and less-

laborious remote quantification of the content of pigments could give us an opportunity to detect early on severe changes in pigment content, indicating stress in plants and/or whole canopies.

### 5.2.1 What and how to measure?

#### ***Gold standard***

Extraction of chlorophyll from plant materials requires organic solvents that diffuse through plant tissue, increasing the permeability of chloroplast membranes and disrupting the chlorophyll-protein complexes (Hosikian et al., 2010). After solubilising the pigments, the pigment content of the extracts is quantified by spectrophotometric (Lichtenthaler, 1987; Porra et al., 1989) or high-performance liquid chromatography (HPLC) measurements (Wright et al., 1991; Dunn et al., 2004). In general, HPLC measurements are more time-consuming, labour-intensive, and costly than spectrometric analysis of pigments. But when individual carotenoid concentrations are required, HPLC measurements must be done (Dunn et al., 2004). Most often, plant photosynthetic pigments are extracted using 80% acetone for chlorophyll and pure acetone for polar carotenoids (Dunn et al., 2004; Vicas et al., 2010). The buffering of aqueous acetone (80% acetone) at pH 7.8 (e.g. acetone/Tris buffer solution, 80:20 vol:vol, pH = 7.8) is recommended to avoid the pheophytin formation by loss of the Mg atom in the presence of extracted metabolic acids (Porra, 2002). Most often Tris or sodium phosphate buffers have been used (e.g. Porra et al., 1989; Sims & Gamon, 2002). Other solvents, such as methanol, ethanol, *N,N* – dimethylformamide (DMF), DMSO, diethyl-ether, or dimethyl-sulphoxide can be used as well.

Extinction coefficients have been provided for a number of different solutes (Lichtenthaler, 1987; Wellburn, 1994; Porra, 2002; Vicas et al., 2010) and need to be used when calculating the pigment contents. The choice of solvent often depends on the type of plant material (Wellburn, 1994; Dunn et al., 2004). In most solutes, the leaf tissue needs to be homogenised first (adding solvent to the sample when grinding) and centrifuged or filtered after pigments have been solubilised. For pigment calculations, the total volume of solute added to the sample during different stages of grinding and washing the mortar from sample-residuals must be collected, recorded, and taken into account during the quantification. Some solutes, such as DMF can be used for determining Chl content in intact tissues if chlorophyll content is low enough (Inskeep & Bloom, 1985). Many solvents require precautionary measures because of their toxicity.

The incubation time of tissues in solvents for extraction depends on the solvent and on the size of the material and also on the species (Minocha et al., 2009). A thumb-rule is that if the leaflet or pellet of leaf residuals look greenish after the extraction then not all chlorophylls have been solubilised, if the leaf material looks yellowish some carotenoids have not solubilised, and when the leaf material is white (or any other colour but not green or yellowish) then the incubation time is long enough. The extraction process can be repeated if the plant material still contains pigments, the total volume of solute needs to be taken into account. During incubation in solute the intact tissues must be stored in dark probes with corks to avoid vaporising of the solvent.

### **Bronze standard**

As traditional measurements of plant pigments are destructive, there is a less laborious and non-destructive method for estimating leaf Chl content using optical chlorophyll meters, which are portable and easy to use (e.g. Netto et al., 2005). In addition, new devices are being developed for simultaneous estimation of more than one plant pigment, such as content of Chl, nitrogen, flavonols, and anthocyanins of the leaf. The Chl content in most of the chlorophyll meters is estimated by measuring the ratio of transmission of near-infrared (NIR) to red wavelengths. It is assumed that transmission of red light is affected both by Chl and other cell structures, while transmission of NIR is not affected by Chl. However, in order to quantify the readings of an optical chlorophyll meter, a correlative dataset of non-destructively gained Chl estimations v. Chl contents from destructive measurements is required. This is because at the near-infrared region, leaf thickness, structure, and consequent internal light scattering affect the light transmission (Parry et al., 2014). The correlative dataset must be done separately for every species. Also one must be aware that optical estimations of Chl content appear to be less accurate if Chl content increases (Richardson et al., 2002). As Chl in leaves is distributed unevenly, it is recommended that a few optical measurements be made from one leaf and take an average for the whole leaf Chl estimation.

### ***Installation, field operation, maintenance, and interpretation of the data***

Leaf samples (e.g. using a cork drill) or whole leaves for pigment content measurements should be collected under comparable light conditions (Demmig-Adams & Adams, 1992) and age (Linder, 1972). Pigments in leaves are not distributed evenly, so in order to get results that can be readily compared, all leaf discs should be taken from same leaf region. Leaves or leaf discs (of known area) must preferentially be frozen as soon as possible (e.g. transported in liquid nitrogen) and stored at -80 °C in the dark to sustain the plant material until pigment analysis. If leaf samples are collected from very moist or wet conditions and/or stored for longer periods or transported in unstable conditions before extraction, it is recommended to lyophilise the samples. Such samples can be stored at room temperatures for days allowing easy transportation if kept away from moisture (Tausz et al., 2003). In the field, it is not always possible to freeze or freeze-dry pigment samples, in which case alternative (less recommended) methods for sampling and preserving plant pigments are available (Esteban et al., 2009). It is also recommended to collect parallel samples (e.g. nearby leaf) for determination of total area and fresh and dry weights. This will enable the quantification of leaf pigments on a mass or area basis. The mass of lyophilised samples (for estimation of dry mass) can be measured for calculations of pigment concentrations. Pigments should be extracted in dim light. Common problems that can be encountered during plant pigment analysis are errors in sample collection, preservation, labelling, biomass, and leaf area measurements, as well as incomplete extraction, instruments not working correctly, false compound identification, pipetting errors, confusion in units, etc. (Fernández-Marín et al., 2015).

### **Where to start**

Dunn et al. (2004), Esteban et al. (2009), Hosikian et al. (2010), Minocha et al. (2009), Porra (2002)

## 5.2.2 Special cases, emerging issues, and challenges

Estimating canopy-pigment contents remotely enables the monitoring of plant parameters over much larger spatial and temporal scales. Reflectance indices (see Table 5.2.1) and fluorescence indices (e.g. Gitelson et al., 1998) have been developed enabling remote estimations of chlorophyll and carotenoid contents. For instance, in global carbon budget models, PRI (Table 5.2.1) is used, as this index correlates with changes in pigment pools of plant canopies (Gamon et al., 1992; Gitelson et al., 2017). Recently, an index tracking Chl:Car ratios and photosynthetic activity of evergreen trees was introduced (Gamon et al., 2016). There has even been an attempt to use the reflectance spectra of the regions of different tree biochemical constituents that change seasonally (e.g. pigments) to classify trees remotely (Kozhoridze et al., 2016). However, one must always be aware of the effect of canopy structure and overlapping wavelength regions on reflectance while using remote estimations of plant parameters (Mänd et al., 2010).

**Table 5.2.1** Vegetation indices for estimations of leaf pigment content (most-cited or recently developed and repeatedly cited indices). Table modified and provided with permission from COST Action ES0903.  $R_x$  means the reflectance ( $R$ ) at wavelength  $x$ .  $D_x$  shows the first derivative ( $D$ ) of reflectance at the respective wavelength  $x$ .

Index	Formula	Used for	Reference
Simple Ratios (SR)	$SR=R_{NIR}/R_{RED}$	Greenness	Jordan, 1969
Chlorophyll Index (CI)	$CI=(R_{750}-R_{705})/(R_{750}+R_{705})$	Chlorophyll content	Gitelson & Merzlyak, 1994
Canopy Chlorophyll Index (CCI)	$CCI=D_{720}/D_{700}$	Canopy chlorophyll content	Sims et al., 2006
Normalized Difference Vegetation Index (NDVI)	$NDVI=(R_{NIR}-R_{RED})/(R_{NIR}+R_{RED})$	Greenness	Myneni et al., 1997
Structural Insensitive Pigment Index (SIPI)	$SIPI=(R_{800}-R_{445})/(R_{800}-R_{680})$	Carotenoid:Chlorophyll ratio	Peñuelas et al., 1995
Modified Chlorophyll Absorption in Reflectance Index (MCARI)	$MCARI=[(R_{700}-R_{670})-0.2(R_{700}-R_{550})] (R_{700}/R_{670})$	Canopy Chlorophyll content	Daughtry et al., 2000
Transformed Chlorophyll Absorption in Reflectance Index (TCARI)	$TCARI=3[(R_{700}-R_{670})-0.2(R_{700}-R_{550})] (R_{700}/R_{670})$	Canopy Chlorophyll content	Haboudane et al., 2002
Photochemical Reflectance Index (PRI)	$PRI=(R_{531}-R_{570})/(R_{531}-R_{570})$	Photosynthetic light use efficiency and leaf pigment contents	Gamon et al., 1992

### 5.2.3. References

#### **Theory, significance, and large datasets**

Demmig-Adams & Adams (1992), Fernández-Marín (2015), Niinemets et al. (1998), Ort (2001), Richardson et al. (2002)

#### **More on methods and existing protocols**

Lichtenthaler (1987), Porra et al. (1989), Vicas et al. (2010), Wellburn (1994), Wright et al. (1991)

#### **All references**

- Anjum, S. A., Xie, X. Y., Wang, L. C., Saleem, M. F., Man, C., & Lei, W. (2011). Morphological, physiological and biochemical responses of plants to drought stress. *African Journal of Agricultural Research*, 6(9), 2026-2032.
- Atherton, J., Olascoaga, B., Alonso, L., & Porcar-Castell, A. (2017). Spatial variation of leaf optical properties in a boreal forest is influenced by species and light environment. *Frontiers in Plant Science*, 8, a309.
- Belkhodja, R., Morales, F., Sanz, M., Abadía, A., & Abadía, J. (1998). Iron deficiency in peach trees: effects on leaf chlorophyll and nutrient concentrations in flowers and leaves. *Plant and Soil*, 203(2), 257-268.
- Colom, M. R., & Vazzana, C. (2003). Photosynthesis and PSII functionality of drought-resistant and drought-sensitive weeping lovegrass plants. *Environmental and Experimental Botany*, 49(2), 135-144.
- Daughtry, C. S. T., Walthall, C. L., Kim, M. S., de Colstoun, E. B., & McMurtrey, J. E. (2000). Estimating corn leaf chlorophyll concentration from leaf and canopy reflectance. *Remote Sensing of Environment*, 74(2), 229-239.
- Demmig-Adams, B. (1990). Carotenoids and photoprotection in plants: a role for the xanthophyll zeaxanthin. *Biochimica et Biophysica Acta - Bioenergetics*, 1020(1), 1-24.
- Demmig-Adams, B., & Adams, W. W. (1992). Photoprotection and other responses of plants to high light stress. *Annual Review of Plant Biology*, 43(1), 599-626.
- Dunn, J. L., Turnbull, J. D., & Robinson, S. A. (2004). Comparison of solvent regimes for the extraction of photosynthetic pigments from leaves of higher plants. *Functional Plant Biology*, 31(2), 195-202.
- Eichelmann, H., Oja, V., Rasulov, B., Padu, E., Bichele, I., Pettai, H., ... Laisk, A. (2005). Adjustment of leaf photosynthesis to shade in a natural canopy: reallocation of nitrogen. *Plant, Cell & Environment*, 28(3), 389-401.
- Esteban, R., Balaguer, L., Manrique, E., de Casas, R. R., Ochoa, R., Fleck, I., ... Lorenzo, R. (2009). Alternative methods for sampling and preservation of photosynthetic pigments and tocopherols in plant material from remote locations. *Photosynthesis Research*, 101(1), 77-88.

- Esteban, R., Moran, J. F., Becerril, J. M., & García-Plazaola, J. I. (2015). Versatility of carotenoids: An integrated view on diversity, evolution, functional roles and environmental interactions. *Environmental and Experimental Botany*, 119, 63-75.
- Fernández-Marín, B., Artetxe, U., Barrutia, O., Esteban, R., Hernández, A., & García-Plazaola, J. I. (2015). Opening Pandora's box: cause and impact of errors on plant pigment studies. *Frontiers in Plant Science*, 6, a148.
- Gamon, J. A., Peñuelas, J., & Field, C. B. (1992). A narrow-waveband spectral index that tracks diurnal changes in photosynthetic efficiency. *Remote Sensing of Environment*, 41(1), 35-44.
- Gamon, J. A., Huemmrich, K. F., Wong, C. Y., Ensminger, I., Garrity, S., Hollinger, D. Y., ... Peñuelas, J. (2016). A remotely sensed pigment index reveals photosynthetic phenology in evergreen conifers. *Proceedings of the National Academy of Sciences USA*, 113(46), 13087-13092.
- Gitelson, A. A., & Merzlyak, M. N. (1994). Spectral reflectance changes associated with autumn senescence of *Aesculus hippocastanum* L. and *Acer platanoides* L. leaves. Spectral features and relation to chlorophyll estimation. *Journal of Plant Physiology*, 143(3), 286-292.
- Gitelson, A. A., Buschmann, C., & Lichtenthaler, H. K. (1998). Leaf chlorophyll fluorescence corrected for re-absorption by means of absorption and reflectance measurements. *Journal of Plant Physiology*, 152(2-3), 283-296.
- Gitelson, A. A., Gritz, Y., & Merzlyak, M. N. (2003). Relationships between leaf chlorophyll content and spectral reflectance and algorithms for non-destructive chlorophyll assessment in higher plant leaves. *Journal of Plant Physiology*, 160(3), 271-282.
- Gitelson, A. A., Gamon, J. A., & Solovchenko, A. (2017). Multiple drivers of seasonal change in PRI: Implications for photosynthesis 2. Stand level. *Remote Sensing of Environment*, 190, 198-206.
- Haboudane, D., Miller, J. R., Tremblay, N., Zarco-Tejada, P. J., & Dextraze, L. (2002). Integrated narrow-band vegetation indices for prediction of crop chlorophyll content for application to precision agriculture. *Remote Sensing of Environment*, 81(2), 416-426.
- Hosikian, A., Lim, S., Halim, R., & Danquah, M. K. (2010). Chlorophyll extraction from microalgae: a review on the process engineering aspects. *International Journal of Chemical Engineering*, 2010, a391632.
- Inoue, Y., Guérif, M., Baret, F., Skidmore, A., Gitelson, A., Schlerf, M., ... Olioso, A. (2016). Simple and robust methods for remote sensing of canopy chlorophyll content: a comparative analysis of hyperspectral data for different types of vegetation. *Plant, Cell & Environment*, 39(12), 2609-2623.
- Inskeep, W. P., & Bloom, P. R. (1985). Extinction coefficients of chlorophyll a and b in N, N-dimethylformamide and 80% acetone. *Plant Physiology*, 77(2), 483-485.
- Jalal, K. C. A., Shamsuddin, A. A., Rahman, M. F., Nurzatul, N. Z., & Rozihan, M. (2013). Growth and total carotenoid, chlorophyll a and chlorophyll b of tropical microalgae (*Isochrysis* sp.) in laboratory cultured conditions. *Journal of Biological Sciences*, 13(1), 10-17.
- Jordan, C. F. (1969). Derivation of leaf-area index from quality of light on the forest floor. *Ecology*, 50(4), 663-666.

- Kozhordize, G., Orlovsky, N., Orlovsky, L., Blumberg, D. G., & Golan-Goldhirsh, A. (2016). Remote sensing models of structure-related biochemicals and pigments for classification of trees. *Remote Sensing of Environment*, 186, 184-195.
- Lichtenthaler, H. K. (1987). Chlorophylls and carotenoids: pigments of photosynthetic biomembranes. *Methods in Enzymology*, 148, 350-382.
- Linder, S. (1972). Seasonal variation of pigments in needles. A study of Scots pine and Norway spruce seedling grown under different nursery conditions. *Studia Forestalia Suecica*, 100, 1-37.
- Linder, S. (1980). Chlorophyll as an indicator of nitrogen status of conifer needles. *New Zealand Journal of Forestry Science*, 10, 166-175.
- Mänd, P., Hallik, L., Peñuelas, J., Nilson, T., Duce, P., Emmett, B. A., ... Schmidt, I. K. (2010). Responses of the reflectance indices PRI and NDVI to experimental warming and drought in European shrublands along a north–south climatic gradient. *Remote Sensing of Environment*, 114(3), 626-636.
- Minocha, R., Martinez, G., Lyons, B., & Long, S. (2009). Development of a standardized methodology for quantifying total chlorophyll and carotenoids from foliage of hardwood and conifer tree species. *Canadian Journal of Forest Research*, 39(4), 849-861.
- Muñoz-Huerta, R. F., Guevara-Gonzalez, R. G., Contreras-Medina, L. M., Torres-Pacheco, I., Prado-Olivarez, J., & Ocampo-Velazquez, R. V. (2013). A review of methods for sensing the nitrogen status in plants: advantages, disadvantages and recent advances. *Sensors*, 13(8), 10823-10843.
- Myneni, R. B., Keeling, C. D., Tucker, C. J., Asrar, G., & Nemani, R. R. (1997). Increased plant growth in the northern high latitudes from 1981 to 1991. *Nature*, 386(6626), 698.
- Netto, A. T., Campostrini, E., de Oliveira, J. G., & Bressan-Smith, R. E. (2005). Photosynthetic pigments, nitrogen, chlorophyll a fluorescence and SPAD-502 readings in coffee leaves. *Scientia Horticulturae*, 104(2), 199-209.
- Niinemets, Ü., & Valladares, F. (2004). Photosynthetic acclimation to simultaneous and interacting environmental stresses along natural light gradients: optimality and constraints. *Plant Biology*, 6(03), 254-268.
- Niinemets, Ü., Bilger, W., Kull, O., & Tenhunen, J. D. (1998). Acclimation to high irradiance in temperate deciduous trees in the field: changes in xanthophyll cycle pool size and in photosynthetic capacity along a canopy light gradient. *Plant, Cell & Environment*, 21(12), 1205-1218.
- Ort, D. R. (2001). When there is too much light. *Plant Physiology*, 125(1), 29-32.
- Parry, C., Blonquist, J., & Bugbee, B. (2014). In situ measurement of leaf chlorophyll concentration: analysis of the optical/absolute relationship. *Plant, Cell & Environment*, 37(11), 2508-2520.
- Peñuelas, J., Baret, F., & Filella, I. (1995). Semi-empirical indices to assess carotenoids/chlorophyll a ratio from leaf spectral reflectance. *Photosynthetica*, 31(2), 221-230.
- Porra, R. J. (2002). The chequered history of the development and use of simultaneous equations for the accurate determination of chlorophylls a and b. *Photosynthesis Research*, 73(1-3), 149-156.

- Porra, R. J., Thompson, W. A., & Kriedemann, P. E. (1989). Determination of accurate extinction coefficients and simultaneous equations for assaying chlorophylls a and b extracted with four different solvents: verification of the concentration of chlorophyll standards by atomic absorption spectroscopy. *Biochimica et Biophysica Acta - Bioenergetics*, 975(3), 384-394.
- Richardson, A. D., Duigan, S. P., & Berlyn, G. P. (2002). An evaluation of noninvasive methods to estimate foliar chlorophyll content. *New Phytologist*, 153(1), 185-194.
- Santos, C. V. (2004). Regulation of chlorophyll biosynthesis and degradation by salt stress in sunflower leaves. *Scientia Horticulturae*, 103(1), 93-99.
- Sims, D. A., & Gamon, J. A. (2002). Relationships between leaf pigment content and spectral reflectance across a wide range of species, leaf structures and developmental stages. *Remote Sensing of Environment*, 81(2), 337-354.
- Sims, D. A., Luo, H., Hastings, S., Oechel, W. C., Rahman, A. F., & Gamon, J. A. (2006). Parallel adjustments in vegetation greenness and ecosystem CO<sub>2</sub> exchange in response to drought in a Southern California chaparral ecosystem. *Remote Sensing of Environment*, 103(3), 289-303.
- Tausz, M., Wonisch, A., Grill, D., Morales, D., & Jiménez, M. S. (2003). Measuring antioxidants in tree species in the natural environment: from sampling to data evaluation. *Journal of Experimental Botany*, 54(387), 1505-1510.
- Tripathi, A. K., & Gautam, M. (2007). Biochemical parameters of plants as indicators of air pollution. *Journal of Environmental Biology*, 28(1), 127.
- Vicas, S., Laslo, V., Pantea, S., & Bandici, G. (2010). Chlorophyll and carotenoids pigments from Mistletoe (*Viscum album*) leaves using different solvents. *Analele Universitatii din Oradea, Fascicula Biologie*, 17(2), 213-218.
- Vogelmann, T. C. (1993). Plant tissue optics. *Annual Review of Plant Biology*, 44(1), 231-251.
- Wellburn, A. R. (1994). The spectral determination of chlorophylls a and b, as well as total carotenoids, using various solvents with spectrophotometers of different resolution. *Journal of Plant Physiology*, 144(3), 307-313.
- Wright, S. W., Jeffrey, S. W., Mantoura, R. F. C., Llewellyn, C. A., Bjørnland, T., Repeta, D., & Welschmeyer, N. (1991). Improved HPLC method for the analysis of chlorophylls and carotenoids from marine phytoplankton. *Marine Ecology Progress Series*, 77, 183-196.
- Young, A. J. (1991). The photoprotective role of carotenoids in higher plants. *Physiologia Plantarum*, 83(4), 702-708.

**Authors:** Mänd P<sup>1</sup>

**Reviewers:** Porcar Castell A<sup>2</sup>; Linder S<sup>3</sup>

## Affiliations

<sup>1</sup> Institute of Ecology and Earth Sciences, University of Tartu, Tartu, Estonia

<sup>2</sup> Optics of Photosynthesis Laboratory, Institute for Atmospheric and Earth System Research/Forest Sciences, University of Helsinki, Helsinki, Finland

<sup>3</sup> Southern Swedish Forest Research Centre, Alnarp, Sweden

## 5.3. Non-structural carbohydrates

**Authors:** McDowell NG<sup>1</sup>, Hoch G<sup>2</sup>, Landhäusser SM<sup>3</sup>

**Reviewer:** Dickman LT<sup>4</sup>

**Measurement unit:** percent dry weight; **Measurement scale:** grinding unit, spectrophotometer, water bath, etc.; **Equipment costs:** €€€; **Running costs:** €; **Installation effort:** medium; **Maintenance effort:** medium; **Knowledge need:** medium; **Measurement mode:** manual

Non-structural carbohydrates (NSCs) provide the energy to sustain growth, reproduction, metabolism, and survival in plants (Chapin et al., 1990). NSC concentrations measured and scaled appropriately provide insight into carbon allocation, storage, and utilisation patterns (Dietze et al., 2014; Martinez-Vilalta et al., 2016). NSCs are simple sugars including glucose, fructose, and sucrose, as well as oligo- and polysaccharides such as starch. Lipids, while not carbohydrates, are another important energy source in some plants (Hoch & Körner, 2003; Hoch et al., 2003). NSC concentrations in plants are sensitive to water availability (Würth et al., 2005; Dickman et al., 2015), CO<sub>2</sub> (Bader et al., 2013; Hartmann et al., 2013; Quirk et al., 2013), soil and air temperature (Hoch & Körner, 2012; Karst & Landhäusser, 2014), growth rates (Sulpice et al., 2009; Hummel et al., 2010), injury (Landhäusser & Lieffers, 2012; Wiley et al., 2016), regeneration (Landhäusser & Lieffers, 2002; Paula & Ojeda, 2009), shade (Marshall, 1986; Weber et al. 2019), nutrients (Linder, 1995), and season (Ericsson & Persson, 1980). NSC availability has also been implicated in maintenance and repair of xylem hydraulic conductivity (McDowell et al., 2011; O'Brien et al., 2014; Trifiliò et al. 2019). NSC measurement and understanding of function has expanded significantly in the last decade to address both crop and wildland questions, driven in particular by climate change and other global changes and associated pressures on plant growth, yield, and survival.

### 5.3.1 What and how to measure?

#### *Measurement principles and challenges*

To measure NSC a plant tissue sample is ground and the sugars and starch molecules extracted, refined, and finally quantified by either spectrometry or chromatography. Many methods have been used for the collection, preparation, and analysis of NSC samples. Unfortunately, comparison across 29 international laboratories revealed that this variety of methods results in a wide range of NSC concentrations reported for the same samples, presenting a challenge for inter-lab comparisons (Quentin et al., 2015). Luckily, most published studies on NSCs include samples processed only at one lab, allowing valid within-study comparisons of NSCs (e.g. among experimental treatments). There are no accepted reference standards for NSC: particularly not any that are appropriate for plant tissues with complex matrices. Because no method has yet been determined to be the most accurate, in this chapter we present a “reference” method building on the results of Quentin et al. (2015) and Landhäusser et al. (2018) who suggested some approaches to reduce variability across laboratories. Rather than re-state all of the methods as presented in Quentin et al. (2015) and Landhäusser et al. (2018), we have focused on identifying the sources of variability amongst methods

so that scientists may minimise errors and maximise reproducibility of NSC results within and across laboratories.

The main sources of variability in the field are 1) inconsistency in sample collection (e.g. dissimilar tissues, organ size (such as roots or twigs of different diameter, and timing of collection), and 2) subsequent handling of samples (e.g. field storage, lab preparation). In the laboratory, the main sources of variability lie in 1) the precision and execution of basic laboratory procedures (e.g. preparation of chemical solutions and dilutions, inconsistencies in pipetting and weighing), 2) the failure to use internal standards and calibrations with every analytical run, and 3) calculation errors. When starting a new experiment or laboratory studying NSCs, we suggest these are the most critical focal areas to develop because they are the major sources of variation that impede reproducibility and comparability within and among laboratories.

### ***Sample collection, preparation, and analysis***

Fundamentally, the process of determining NSCs starts with sample collection, proceeds through preparation, including grinding of samples into powder, and ends with analysis (Figure 5.3.1). To compare NSC among experimental treatments it can be important to collect samples at the same time of day, as NSCs can vary over a 24-hour period (Landhäuser, 2011). Likewise, plant organs differ substantially in their NSC concentrations depending on the species and its phenological condition (e.g. Würth et al., 2005; Landhäuser & Lieffers, 2003; Dickman et al., 2015; Martinez-Vilalta et al., 2016), thus wise selection, timing, and consistent sampling are essential. For example, if NSC pools in plants are compared across different locations, it is imperative to confirm that the sampled plants are at the same phenological and developmental stage in all locations. This is especially important if plants are sampled across elevational transects (Hoch, 2015). In boreal conifers there is a pronounced seasonal variation in foliar starch reserves (e.g. Ericsson & Persson, 1980; Linder, 1995) which must be considered when estimating concentrations of other foliar elements. Finally, it should be taken into account that NSC concentrations can vary significantly even for the same tissue type within a single plant individual, for example along a light gradient within a tree canopy, or within tree stems from the youngest to the oldest wood fraction. It is therefore valuable to consistently sample within the same light environment and age class, or to sample across ages and conditions to produce an “average” value.

Another potentially critical step in sample collection is to ensure that enzymatic activity that can metabolise NSCs is halted after sampling so that measured concentrations represent the condition of the plant at the time of sampling and are not influenced by sample degradation after collection. This can be done by rapidly freezing the sample in dry ice or liquid nitrogen, followed soon after by microwaving or freeze drying. Currently it is unknown how long samples can sit between sampling and the cessation of enzymatic activity without influencing the results. Maintaining dry samples until further processing is therefore essential.

Grinding of material is typically done with a ball-mill. The critical step in creating powdered samples is to grind the material to < 0.15 mm particle size to allow for complete extraction and solubilisation of NSCs (Quentin et al., 2015). Dried and powdered samples are stored dry over desiccant and should be re-dried immediately before weighing, along with internal laboratory standards and blanks to allow for internal calibration and procedural checking.

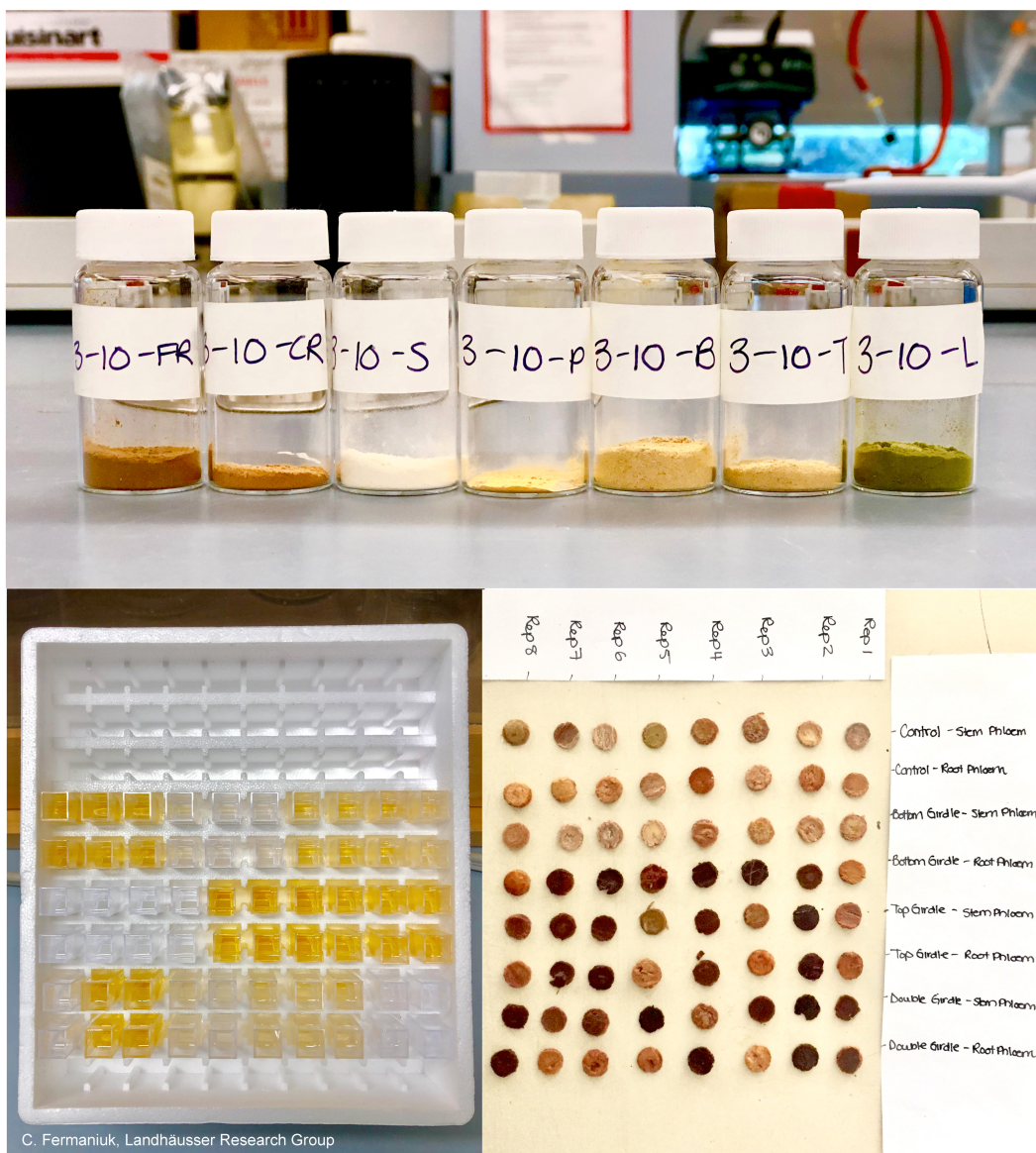


**Figure 5.3.1** Careful sample collection, grinding, extraction, and analyses of plant tissue samples are all critical steps to quality NSC quantification procedures. Photo: Landhäuser Research Lab/Coral Fermaniuk.

### Chemical analysis

All methods described here first extract the water or ethanol-soluble sugars and then analyse starch from the pellet after degradation to glucose-units. The steps following sample preparation include extraction of NSCs and separation into soluble sugars (supernatant after centrifugation) and starch (contained in the insoluble tissue pellet), followed by spectrophotometric or HPLC measurement of the soluble sugars.

For the quantification of soluble sugars, three general approaches are commonly used: (1) colorimetric-photometric (Dubois et al., 1956; Ashwell, 1957; Miller, 1959; Buysse & Merckx, 1993; Chow & Landhäuser, 2004); (2) enzymatic-photometric (Wong, 1990; Hoch et al., 2003; Sevanto et al., 2014); and (3) chromatographic (Raessler et al., 2010). Approaches (1) and (2) have the

advantage of being fast and relatively economical methods, but approach (1) does not distinguish between the low molecular weight sugars (i.e. mono- and oligosaccharides are lumped together), while approach (2) can quantify individual sugars of interest in an aqueous solution through a series of enzyme-catalysed reactions, but is complicated by issues of enzyme specificity and the need to adjust enzyme concentrations with each new sample type. Approach (3) has the advantage of allowing all low molecular weight sugars to be quantified separately, and chromatographic analyses are more sensitive. However, approach (3) requires more time-intensive analyses (i.e. lower sample throughput) and is more expensive. The greatest challenge with all three approaches is to quantitatively extract all sugars without extracting structural carbon compounds (e.g. hemicellulose).

### **a) Sugar extraction**

For the extraction of low molecular weight sugars, one should preferentially use ethanol (Landhäuser et al. 2018). Water extraction cannot be recommended as starch gelatinises in water, which reduces the amount of starch in the pellet and underestimates starch concentrations. If water extraction is necessary, two separate samples must be run: one for soluble sugar analyses and one for total NSC analyses (i.e. soluble sugar and starch analysis combined) and then subtract the soluble sugar concentration (sample 1) from the total concentration (sample 2) to calculate the starch concentration of the sample.

### **b) Starch degradation**

To estimate starch in tissue samples, most methods convert the starch polymer to glucose hydrolysate, which is subsequently assayed. A crucial issue is the exhaustive degradation of starch in plant tissue, since an incomplete hydrolysis of starch will lead to an underestimation of the real starch concentration. In contrast, the actual starch concentration will be overestimated if methods are used that also degrade glucose from polymers other than starch. Acid hydrolysis using sulphuric or hydrochloric acid is considered the simplest and most rapid method to hydrolyse starch and is often found in the NSC literature. This approach has been found to be inaccurate as it can digest structural components (e.g. cellulose and hemicelluloses, which also contain glucose units) in the tissue even at low acid concentrations (Marshall, 1986; Chow & Landhäuser, 2004). Therefore we believe that the most reliable method to determine starch concentrations is an enzymatic degradation. We suggest using a stepwise degradation with amylase and then amyloglucosidase. It is important to apply enzymes in surplus to ensure complete degradation of starch to glucose, and to use the enzymes in sequence (amylase first) since amyloglucosidase is not specific to starch and will degrade additional malto-oligosaccharides if applied before amylase. It is also essential to maintain consistent conditions for enzymatic degradation across samples (e.g. time and temperature).

### **c) Calculations**

NSC is calculated as the sum of all measured low molecular sugars determined by the respective methods plus starch. With the hydrolysis of starch, each glucose-unit accepts one H<sub>2</sub>O molecule. Hence, when calculating the amount of starch within a sample, the amount of starch-derived glucose after degradation has to be corrected by subtracting the mass of this H<sub>2</sub>O from the molar mass of glucose (i.e. 180 g per mol (Glc) – 18 g per mol (H<sub>2</sub>O) = 162 g per mol). Thus, the measured mass of glucose derived from the starch contained in the sample has to be reduced by 10%. More detailed descriptions of calculations based on the different quantification methods are provided in Landhäuser et al. (2018).

#### **d) A note on units**

Commonly, the NSC content of plant tissue is presented as a concentration relative to the total dry matter (either as  $\text{mg g}^{-1}$  or as % dry matter). It is important to note that these concentrations are not only dependent on the numerator (i.e. the amount of NSC), but also on the denominator (i.e. the total dry mass), which is largely driven by the amount of cell wall compounds in plant tissue. Hence, special attention must be paid in situations where NSC is compared from samples with different cell wall fractions (e.g. leaves with different specific leaf area, or wood samples with different wood densities). In such cases, it is advisable to report NSC concentrations on a volume basis ( $\text{mg cm}^{-3}$ ; e.g. see Hoch, 2008).

#### **Where to start**

Chapin et al. (1990), Landhäusser et al. (2018), Martinez-Vilalta et al. (2016), Quentin et al. (2015)

### **5.3.2 Special cases, emerging issues, and challenges**

#### **Alternative approaches**

An alternative approach to the wet chemical quantification of NSC in plant tissue might be the use of near-infrared spectrometry (NIRS) on bulk plant powder. Previous attempts to quantify NSC in different tissue types showed promising results (Decruyenaere et al., 2012; Ramirez et al., 2015; Quentin et al., 2016). However, NIRS analyses of NSC require separate calibrations with wet chemical methods for each tissue type. Therefore, this method is mainly applicable for investigations of large numbers of samples from the same tissue type.

#### **Next steps towards standard procedures for NSC quantification**

Until recently there were no unified standard procedures for sample collection, handling, NSC extraction, or starch digestion that could be used by scientists (Smith & Zeeman, 2006). However Landhäusser et al. (2018) provide very detailed step-by-step procedures and protocols for the three soluble sugar quantification methods and enzymatic starch quantification described earlier, which should help reduce inconsistencies in laboratory procedures that have been responsible for the large variability and erroneous results. There are currently no universal and international NSC sample standards for plant material with precisely known starch and sugar concentrations. To improve comparability of NSC among different laboratories, international plant standards for NSC are highly desirable.

### **5.3.3 References**

#### **Theory, significance, and large datasets**

Chapin et al. (1990), Landhäusser et al. (2018), Martinez-Vilalta et al. (2016), McDowell (2011), Quentin et al. (2015)

### **More on methods and existing protocols**

Chow & Landhäusser (2004), Dickman et al. (2015), Hoch et al. (2003), Landhäusser et al. (2018), Raessler et al. (2010)

### **All references**

- Ashwell, G. (1957). Colorimetric analysis of sugars. *Methods in Enzymology*, 3, 73-105.
- Bader, M. K. F., Leuzinger, S., Keel, S. G., Siegwolf, R. T. W., Hagedorn, F., Schleppi, P., & Körner, C. (2013). Central European hardwood trees in a high-CO<sub>2</sub> future: synthesis of an 8-year forest canopy CO<sub>2</sub> enrichment project. *Journal of Ecology*, 101, 1509-1519.
- Buyssse, J. & Merckx, R. (1993). An improved colorimetric method to quantify sugar content of plant tissue. *Journal of Experimental Botany*, 44, 1627-1629.
- Chapin, F. S., Schulze, E. D., & Mooney H. A. (1990). The ecology and economics of storage in plants. *Annual Review of Ecology and Systematics*, 21(1), 423-447.
- Chow, P. S., & Landhäusser, S. M. (2004). A simplified method for measuring sugar and starch content in woody-plant tissues. *Tree Physiology*, 24, 1129-1136.
- Decruyenaere, V., Clément, C., Agneesens, R., Losseau, C., & Stilmant, D. (2012). Development of near-infrared spectroscopy calibrations to quantify starch and soluble sugar content in the roots of *Rumex obtusifolius*. *Weed Research*, 52(1), 1-5.
- Dickman, L. T., McDowell, N. G., Sevanto, S., Pangle, R. E., Pockman, W. T. (2015). Carbohydrate dynamics and mortality in a piñon-juniper woodland under three future precipitation scenarios. *Plant, Cell & Environment*, 38(4), 729-739.
- Dietze, M. C., Sala, A., Carbone, M. S., Czimczik, C. I., Mantooth, J. A., Richardson, A. D., & Vargas, R. (2014). Nonstructural carbon in woody plants. *Annual Review of Plant Biology*, 29(65), 667-687.
- Dubois, M., Gilles, K. A., Hamilton, J. K., Rebers, P. A., & Smith, F. (1956). Colorimetric method for determination of sugars and related substances. *Analytical Chemistry*, 28, 350-356.
- Ericsson, A., & Persson, H. (1980). Seasonal changes in starch reserves and growth of fine roots of 20-year-old scots pines. *Ecological Bulletins*, 32, 239-250.
- Hartmann, H., Ziegler, W., Kolle, O., & Trumbore, S. (2013). Thirst beats hunger – declining hydration during drought prevents carbon starvation in Norway spruce saplings. *New Phytologist*, 200, 340-349.
- Hoch, G. (2008). The carbon supply of *Picea abies* trees at a Swiss montane permafrost site. *Plant Ecology & Diversity*, 1, 13-20.
- Hoch, G. (2015) Carbon reserves as indicators for carbon limitation in trees. In U. Lüttge, & W. Beyschlag (Eds.), *Progress in Botany* (pp. 321-346). Cham: Springer.
- Hoch, G., & Körner, C. (2003). The carbon charging of pines at the climatic treeline: a global comparison. *Oecologia*, 135, 10-21.

- Hoch, G., & Körner, C. (2012). Global patterns of mobile carbon stores in trees at the high-elevation tree line. *Global Ecology and Biogeography*, 21, 861-871.
- Hoch, G., Richter, A., & Körner, C. (2003). Non-structural carbon compounds in temperate forest trees. *Plant, Cell & Environment*, 26, 1067-1081.
- Hummel, I., Pantin, F., Sulpice, R., Piques, M., Rolland, G., Dauzat, M., ... Gibon, Y. (2010). *Arabidopsis* plants acclimate to water deficit at low cost through changes of carbon usage: an integrated perspective using growth, metabolite, enzyme, and gene expression analysis. *Plant Physiology*, 154(1), 357-372.
- Karst, J., & Landhäusser, S. M. (2014). Low soil temperatures increase carbon reserves in *Picea mariana* and *Pinus contorta*. *Annals of Forest Science*, 71, 371-380.
- Landhäusser, S. M. (2011). Aspen shoots are carbon autonomous during bud break. *Trees*, 25, 531-536.
- Landhäusser, S. M., & Lieffers, V. J. (2002). Leaf area renewal, root retention and carbohydrate reserves in a clonal tree species following aboveground disturbance. *Journal of Ecology*, 90, 658-665.
- Landhäusser, S. M., & Lieffers, V. J. (2003). Seasonal changes in carbohydrate reserves in mature northern *Populus tremuloides* clones. *Trees*, 17, 471-476
- Landhäusser, S. M., & Lieffers, V. J. (2012). Defoliation increases risk of carbon starvation in root systems of mature aspen. *Trees*, 26, 653-661.
- Landhäusser, S. M., Chow, P. S., Dickman, L. T., Furze M., Kuhlman, I., Schmid S., ... Adams, H. D (2018). Standardized protocols and procedures can precisely and accurately quantify non-structural carbohydrates. *Tree Physiology*, 38, 1764-1778.
- Linder, S. (1995). Foliar analysis for detecting and correcting nutrient imbalances in Norway spruce. *Ecological Bulletins(Copenhagen)*, 44, 178-190.
- Marshall, J. D. (1986). Drought and shade interact to cause fine-root mortality in Douglas-fir seedlings. *Plant and Soil*, 91, 51-60.
- Martinez-Vilalta, J., Sala, A., Asensio, D., Galiano, L., Hoch, G., ... Lloret, F. (2016). Dynamics of non-structural carbohydrates in terrestrial plants: a global synthesis. *Ecological Monographs*, 86, 495-516.
- McDowell, N.G. (2011). Mechanisms linking drought, hydraulics, carbon metabolism, and vegetation mortality. *Plant Physiology*, 155(3), 1051-1059.
- McDowell, N. G., Beerling, D. J., Breshears, D. D., Fisher, R. A., Raffa, K. F., & Stitt, M. (2011). The interdependence of mechanisms underlying climate-driven vegetation mortality. *Trends in Ecology & Evolution*, 26(10), 523-532.
- Miller, G. L. (1959). Use of dinitrosalicylic acid reagent for determination of reducing sugar. *Analytical Chemistry*, 31(3), 426-428.

- O'Brien, M. J., Leuzinger, S., Philipson, C. D., Tay, J., & Hector, A. (2014). Drought survival of tropical tree seedlings enhanced by non-structural carbohydrate levels. *Nature Climate Change*, 4(8), 710-714.
- Paula, S., & Ojeda, F. (2009). Belowground starch consumption after recurrent severe disturbance in three resprouter species of the genus *Erica*. *Botany*, 87, 253-259.
- Quentin, A. G., Pinkard, E. A., Ryan, M. G., Tissue, D. T., Baggett, L. S., Adams, H. D., ... Woodruff, D. R. (2015). Non-structural carbohydrates in woody plants compared among laboratories. *Tree Physiology*, 35(11), 1146-1165.
- Quentin, A. G., Rodemann, T., Doutreleau, M.-F., Moreau, M., Davies, N. W., & Millard, P. (2016). Application of near-infrared spectroscopy for estimation of non-structural carbohydrates in foliar samples of *Eucalyptus globulus* Labilladière. *Tree Physiology*, 37(1), 131-141.
- Quirk, J., McDowell, N. G., Leake, J. R., Hudson, P. J., & Beerling, D. J. (2013). Increased susceptibility to drought-induced mortality in *Sequoia sempervirens* (Cupressaceae) trees under Cenozoic atmospheric carbon dioxide starvation. *American Journal of Botany*, 100(3), 582-591.
- Raessler, M., Wissuwa, B., Breul, A., Unger, W., & Grimm, T. (2010). Chromatographic analysis of major non-structural carbohydrates in several wood species – an analytical approach for higher accuracy of data. *Analytical Methods*, 2, 532-538.
- Ramirez, J. A., Posada, J. M., Handa, I. T., Hoch, G., Vohland, M., Messier, C., & Reu, B. (2015). Near-infrared spectroscopy (NIRS) predicts non-structural carbohydrate concentrations in different tissue types of a broad range of tree species. *Methods in Ecology and Evolution*, 6, 1018-1025.
- Sevanto, S., McDowell, N. G., Dickman, L. T., Pangle, R., Pockman, W. T. (2014). How do trees die? A test of the hydraulic Failure and carbon starvation hypotheses. *Plant, Cell & Environment*, 37, 153-161.
- Smith, A. M. & Zeeman, S. C. (2006). Quantification of starch in plant tissues. *Nature Protocols*, 1, 1342-1345.
- Sulpice, R., Pyl, E. T., Ishihara, H., Trenkamp, S., Steinfath, M., Witucka-Wall, H., ... Stitt, M. (2009). Starch as a major integrator in the regulation of plant growth. *Proceedings of the National Academy of Sciences USA*, 106(25), 10348-10353.
- Trifilò, P., Kiorapostolou, N., Petruzzellis, F., Vitti, S., Petit, G., Lo Gullo, M. A., ... Casolo, V. (2019). Hydraulic recovery from xylem embolism in excised branches of twelve woody species: relationships with parenchyma cells and non-structural carbohydrates. *Plant Physiology and Biochemistry*, 139, 513-520.
- Weber, R., Gessler, A., & Hoch G. (2019). High carbon storage in carbon-limited trees. *New Phytologist*, 222(1), 171-182.
- Wiley, E., Rogers, B. J., Hodgkinson, R., & Landhäusser, S. M. (2016). Nonstructural carbohydrate dynamics of lodgepole pine dying from mountain pine beetle attack. *New Phytologist*, 209, 550-562.
- Wong, S. C. (1990). Elevated atmospheric partial-pressure of CO<sub>2</sub> and plant-growth. 2 - Nonstructural carbohydrate content in cotton plants and its effect on growth-parameters. *Photosynthesis Research*, 23, 171-180.

Würth, M. K., Pelaez-Riedl, S., Wright, S. J., & Körner, C. (2005). Non-structural carbohydrate pools in a tropical forest. *Oecologia*, 143(1), 11-24.

**Authors:** McDowell NG<sup>1</sup>, Hoch G<sup>2</sup>, Landhäusser SM<sup>3</sup>

**Reviewer:** Dickman LT<sup>4</sup>

### Affiliations

<sup>1</sup> Pacific Northwest National Laboratory, Richland Washington, USA

<sup>2</sup> Department of Environmental Sciences - Botany, University of Basel, Basel, Switzerland

<sup>3</sup> Department of Renewable Resources, University of Alberta, Edmonton, Canada

<sup>4</sup> Earth and Environmental Sciences Division, Los Alamos National Laboratory, Los Alamos, USA

## 5.4 Lethal dose (LD<sub>50</sub>) to quantify stress tolerance exemplified by frost tolerance

**Authors:** Kreyling J<sup>1</sup>, Lembrechts JJ<sup>2</sup>, De Boeck HJ<sup>2</sup>

**Reviewer:** Lenz A<sup>3</sup>

**Measurement unit:** same as unit of interest, e.g. °C; **Measurement scale:** for frost tolerance: temperature test chamber; **Equipment costs:** €€€; **Running costs:** €; **Installation effort:** medium; **Maintenance effort:** low; **Knowledge need:** medium; **Measurement mode:** manual measurement

Our understanding of plant ecology hinges largely on studies exploring stress responses and explaining their specific mechanisms. Generally, stress has a physiological impact, leading to the loss of tissue or a severe restriction of physiological processes (Körner, 2012). Stress responses can be gradual (eustress) with slight deviations from a reference state, or destructive leading to severe damage and the loss of tissue. Stress has a direct physiological impact and is, as such, zonal, i.e. typically associated with environmental gradients, for instance elevation (Körner, 2012). Potential stress factors include deficiency and excess of light, UV-radiation, heat, cold, frost, or drought. Stress should not be confused with disturbance, which refers to a mechanical or physical impact on plants, such as wind, burial, grazing, trampling, or soil compaction. In light of climate change and other global changes, several stress factors are intensifying, leading to renewed interest in plant stress responses (Tylianakis et al., 2008). Stress responses are simply any plant reaction to any stress factor and can be measured by a multitude of response parameters and experimental or observational methods.

Generally, studies of stress responses range from the quantification of net effects at ecosystem level such as CO<sub>2</sub>-fluxes under contrasting expression of stress (Ciais et al., 2005) to detailed molecular physiological studies (Thomashow, 1999; Munns & Tester, 2008). Most studies focus on destructive stress, which can be experimentally investigated. Plant responses to destructive stress include “escape” and “resistance”. Escape is a temporal or spatial evasion of the stress, for example shedding green leaves in autumn, or keeping meristems belowground to escape freezing stress in winter. Resistance is further subdivided into avoidance and tolerance. Avoidance implies that the stress is avoided, for example by supercooling water to survive temperatures below 0 °C. To truly be able to survive temperate, boreal, and arctic climates, plants need to be able to tolerate freezing temperatures, i.e. the water freezes within the plant and the plant survives this freezing.

### 5.4.1 What and how to measure?

A widely used concept to quantify stress tolerance is the LD (lethal dose) approach adopted from toxicology (Trevan, 1927). The median lethal dose, LD<sub>50</sub> (also called LC<sub>50</sub> for lethal concentration or LC<sub>T50</sub> for lethal concentration and time) of a given stress factor is the dose required to kill half the members of a tested population after a specified test duration. Here, its use in stress ecology is exemplified by referring to frost stress and determination of LT<sub>50</sub>, the median lethal temperature. LD<sub>50</sub> for any other stress factor can be assessed accordingly.

### **Four ways of measuring LD<sub>50</sub>**

Generally, we measure the survival of organisms or organs under controlled environmental conditions. The lethal dose is determined by regressing survival or quantitative performance of organisms or tissues against a gradient of increasing severity of a given stress factor under laboratory conditions. Ideally, the stress gradient should cover the full range from non-stressed to completely lethal conditions for the test subject, including a control at both ends. By fitting a model to the observed relation between survival and stress, the median lethal dose (LD<sub>50</sub>) is determined. The lethal temperature for 50% of the investigated population (LT<sub>50</sub>) can be determined for whole organisms or for specific plant organs such as flowers, leaves, roots, twigs, or buds. Survival or performance of the plants or of the specific organs can be determined by various methods. Here, only the measurement after simulating the stress is described. The methods to simulate the stress are described below under *Installation, field operation, maintenance, interpretation*.

**a) Direct measurement of the stress response during induction of the stress.** Cell damage can be directly quantified by differential thermal analysis (DTA). The exotherm reaction (warming peak when water freezes) of intracellular freezing (low temperature exotherm) is measured by miniature temperature thermocouples directly inserted into tissues (Räisänen et al., 2006; Pramsohler et al., 2012). The temperature of intracellular freezing is the lethal temperature of the sample. LT<sub>50</sub> values can be calculated as the median of replicates. Comparing samples to dead tissue not showing any low temperature exotherm reaction upon intracellular freezing and putting the samples into aluminium blocks can improve the precision of the method considerably (Räisänen et al., 2006). **Advantages:** This method is the most direct method to measure freezing resistance. It is objective and provides a very quick and direct test that can even be applied in the field (Pramsohler et al., 2012). **Disadvantages:** DTA is not applicable for all organs and species (Salazar-Gutiérrez et al., 2016). Before use, pre-trials are recommended as the low temperature exotherms are not always detectable for particular species and tissue types. The technical equipment for this method is different from all other methods described here.

**b) Continued monitoring under non-limiting conditions** (Sakai, 1966). After freezing stress has been induced, whole plants or organs such as twigs with buds are kept under non-stressful conditions (e.g. above freezing temperatures) for a prolonged period of time, during which their performance is regularly monitored. Since death of whole plants or plant organs is usually hard to determine, testing for regrowth or sprouting after induction of the stress is a valuable option. Monitoring times depend on the studied organisms or organs. For frost tolerance of tree buds during winter for example, monitoring can continue until leaf unfolding, which is the ultimate measure of bud survival. Uninodal (Bilavčík et al., 2012) or longer twigs (Sakai, 1966) can be kept for weeks with their bases in water if the water is changed regularly, the base is freshly cut on a weekly basis, and the upper cut (for uninodal samples) is sealed with wax or paraffin. **Advantages** of this method are that it is easily applicable and death of investigated organs is very obvious. **Disadvantages** are the long duration needed to wait until death is apparent.

**c) Visual inspection of damage immediately after the stress** (e.g. Vitasse et al., 2014). For many organs and species, damage can be visually quantified immediately after stress exposure. Freezing damage becomes apparent by the texture, odour, and discolouration of tissues caused by the oxidation of polyphenols and the decompartmentalisation of the protoplast (Sakai & Larcher, 1987). The method works well with different plant tissues such as leaves (e.g. Lenz et al., 2013, Vitasse et

al., 2014), twigs (Lindén et al., 1996), buds (Lenz et al., 2013), and roots (Kreyling et al., 2012). After an initial learning phase, the method is easily applicable to almost any tissue. Comparing the investigated sample with the dead and the alive controls allows for a correct assessment of survival. **Advantages** of the method are that different tissues can be assessed differentially at the same time. For instance, LT<sub>50</sub> values of leaf primordia and phloem and xylem tissue can be assessed in one open cut bud. **Disadvantages** are that in some species and tissues, for instance buds of *Tilia platyphyllos*, visual inspection becomes very hard since changes between alive and dead tissues are very subtle. However, after some training the method should be applicable to most tissues of most species. **Caution** should be taken to blind the samples to the stress level used, when visually assessing damage.

d) **Indirect measurements of cell damage by electrolyte leakage after the stress** (Whitlow et al. 1992). Electrolyte leakage is a proxy for cell damage. Target tissues are placed in a vial with deionised water after stress has been induced. After a certain amount of time, when the leakage of electrolytes is complete (to be determined for the samples studied), electrical conductivity of the water is measured. Thereafter, samples are killed completely (usually by autoclaving the samples), with the aim of destroying all cells. After a second waiting period, electrical conductivity of the water is measured again, corresponding to the complete leakage of dead cells. Different methods are suggested to further process the data (see Lim et al., 1998). Relative electrolyte leakage is the first value after the stress, divided by the second value after killing the sample completely. Injury is relative electrolyte leakage standardised by the electrolyte leakage of the alive control. Adjusted injury is injury standardised by electrolyte leakage of the dead control. These values (relative electrolyte leakage, injury, adjusted injury) are then fit to non-linear models. The inflection point of the non-linear function corresponds to the calculated LT<sub>50</sub> value. **Advantages:** objective and reasonably quick. **Disadvantages:** first, electrolyte leakage data give a bulk signal of all immersed tissues within the water solution. For instance, when a bud is frozen, the LT<sub>50</sub> calculated by electrolyte leakage is influenced by the LT<sub>50</sub> of leaf primordia and xylem and phloem tissue, with every organ having a different contribution. Second, fitting of non-linear functions to data is not trivial. The search for optimal starting parameters in the fitting procedure might be hard to impossible, which will lead to no data. Further, the non-linear functions are not symmetric. Thus, different functions will result in different LT<sub>50</sub> values on the same data. In addition, standardising data differently (relative electrolyte leakage, injury, adjusted injury) again leads to more variety of LT<sub>50</sub> values on the same data, decreasing the comparability of the method. **Caution** should be taken to exactly describe the method used, since a large variety is available.

An alternative method for photosynthetically active organs similar to electrolyte leakage is comparing chlorophyll fluorescence after frost to control levels (Clement & van Hasselt, 1996).

### Where to start

Lim et al. (1998), Neuner & Hacker (2012), Sakai (1966), Sutinen et al. (1992), Trevan (1927), Vitasse et al. (2014), Whitlow et al. (1992)

### Installation, field operation, maintenance, interpretation

To study freezing resistance, basically one or several freezers are needed. Commercial systems are available for differential thermal analysis, as well as for controlled freezing runs. Some laboratories developed their own systems, either for a controlled freezing in parallel in several freezers (Lenz et al., 2013), or for *in situ* freezing in several chambers (Buchner & Neuner, 2009). Here, we describe the method for controlled freezing runs in detail, excluding differential thermal analysis.

The general course of a freezing run consists of collecting samples *in situ*, bringing them to the lab, processing them as fast as possible, putting them into the freezers, running the freezing programme, and assessing freezing resistance. Some steps are more critical than others. The effect of transport to the lab has not, so far, been investigated. However, temperatures before freezing have a large effect on the freezing resistance of a plant (Lenz et al., 2016a). Thus, the temperature used should ideally not deviate from ambient temperatures. Most important is the freezing and re-warming ramp, as well as the duration of the target stress level. For the freezing ramp, caution should be taken to simulate the conditions one would like to study as naturally as possible in the laboratory. For instance, if the lethal temperature under clear sky conditions in winter are of interest, when temperatures drop below freezing by radiative cooling, slow cooling rates of  $<5\text{ K h}^{-1}$  should be chosen. Immediate exposure to freezing temperatures can cause artefacts, for example by supercooling due to too drastic cooling or warming rates (Siminovitch et al., 1978; Steffen et al., 1989). If, however, one is interested in the damaging temperature at the border of a cold lake due to temperature inversion, much faster cooling and re-warming rates should be applied, maybe even several in succession. It is a good idea to check climate records before starting freezing research, taking into account that temperatures measured at climate stations deviate from temperatures that plants actually experience (Kollas et al., 2014). The target stress level (the target temperature) depends strongly on the plant, organ, and season. Some tropical plants already experience cold damage at above freezing temperatures (see references in Larcher, 2005), while other fully cold-hardened plants may survive immersion in liquid nitrogen at  $-196\text{ }^{\circ}\text{C}$  (Sakai, 1960). Ideally, several levels below the  $\text{LT}_{50}$  and several levels above the  $\text{LT}_{50}$  are applied. Re-warming rates should be similar to freezing rates. The temperature programme is ideally set up in a way that all samples reach the same temperature while re-warming, so that damage starts to develop in all samples at the same time and no bias is introduced in measuring freezing resistance due to time-lags between the samples. Best practices involve repeated measures on the same individual (a part of it in every target freezing temperature) or a randomisation of samples to freezing temperatures, and blinding of target freezing temperatures, so that an unbiased estimate of freezing resistance is possible. See the previous section for the various methods to measure freezing resistance.

Based on these data,  $\text{LT}_{50}$  can be directly determined from logistic regression of binary data (dead or alive; Lindén et al., 1996; Vitasse et al., 2014) or by non-linear curve fitting of quantitative data such as the Richards function (Lim et al. 1998):

$$Y_T = 100(1 - e^{(b - kT)})^{\frac{-1}{d}}$$
$$\text{LT}_{50} = b - \frac{\log(1 - 0.5^d)}{k}$$

with  $Y_T$  the quantitative response variable at temperature  $T$ , and  $b$ ,  $d$ , and  $k$  being function parameters;

Or the Gompertz function (Lim et al. 1998):

$$Y_T = ae^{-be^{-kT}}$$
$$LT_{50} = -\frac{\log(\log(2)/b)}{k}$$

with the asymptote  $a$ , the  $x$ -placement parameter  $b$  and the slope-parameter  $k$ . Note that several other functions are in use, for example a symmetric function by Anderson et al. (1988):

$$Y_T = Y_{\min} \frac{Y_{\max} - Y_{\min}}{1 + e^{k(T_m - T)}}$$

with  $Y_{\min}$  the asymptotic value of the response variable in uninjured tissue,  $Y_{\max}$  the asymptotic value at maximum low-temperature stress,  $k$  the steepness of the response curve, and  $T_m$  an estimate of  $LT_{50}$ . Curve fitting can be carried out using non-linear least squares regression (a robust solution includes the `nlsLM` function in the `minpack.lm` R package; Elzhov et al. 2016). Note that many different equations can be used here, which is a drawback of this method in comparison to simple logistic regression of binary data.

*Maintenance of freezing lab:* this is dependent on conditions. If an ultra-low temperature lab is established (temperatures below  $-40^{\circ}\text{C}$ ), costs for establishment and maintenance are much higher than for a lab at warmer temperatures, which can be achieved with commercial home freezers and a clever computer program. In any case, temperature in the samples should be measured independently and used in subsequent calculations of  $LT_{50}$  values.

*Interpretation:* survival of plants is a clear binary response, dead or alive. However, the obtained lethal temperature ( $LT_{50}$ ) is a statistical value, which does not imply that all individuals out of the studied population will die at this point. In addition, neither the entire organ nor the observed tissue may be dead, resulting in a gradual response for dead. How well  $LT_{50}$  values are related to survival of plants, which is the ultimate goal, is not known. Nevertheless,  $LT_{50}$  values of excised shoots and those measured *in situ* correlate strongly, although they are not the same (Neuner et al., 1997).

The usefulness of  $LT_{50}$ , or the more general  $LD_{50}$ , is the fact that one obtains a single value in units of the studied stress factor, which has ecological importance and can (at least within one study) be compared among species and organs. It should be noted, however, that this value depends not only on the dose, i.e. the minimum temperature, but also on duration of exposure, rate of cooling and warming, and the equation used. These facts therefore need to be reported alongside the results, but make a comparison among studies applying different protocols problematic.

#### 5.4.2 Special cases, emerging issues, and challenges

Applying  $LD_{50}$  concepts to other stress factors in ecology beyond low temperature stress will not only advance stress ecology but, in the long run, also facilitate process-based projections of shifts in species composition with global change. Temporal dynamics in stress tolerance, however, need to be taken into account. Frost tolerance, for instance, does not only differ among species and populations, but also temporally over the course of the year (Lenz et al., 2013; Kreyling et al., 2015) and the phenological stage of a plant (Lenz et al., 2016b). In fact, frost tolerance responds dynamically to ambient temperatures within days (Kalberer et al., 2006; Lenz et al., 2016a; Vitra et al. 2017).

Concerning other stress factors, similar protocols as for frost tolerance can be applied. Drought tolerance, for instance, can be assessed by relative electrolyte leakage of plants or organs kept under osmotic stress which is caused experimentally by varying concentrations of polyethylene glycol in water solutions (PEG method; Premachandra & Shimada, 1987; Bajji et al., 2002).

Beyond the commonly reported LD<sub>50</sub>, other percentiles (e.g. LD<sub>10</sub>, LD<sub>90</sub>) can shed additional light on variation and range of stress tolerances.

Finally, it should be emphasised that accurate and correct measurements of the environmental variable studied is crucial. For instance, plant tissue temperature determines stress levels with regards to frost or heat. These tissue temperatures may deviate considerably from air temperatures. Using air temperatures might consequently lead to fairly nonsensical conclusions.

#### 5.4.3 References

##### ***Theory, significance, and large datasets***

Bigras et al. (2001), Chapter 4 in Snyder & de Melo-Abreu (2005), Sakai & Larcher (1987), Sakai & Weiser (1973), Thomashow (1999)

##### ***More on methods and existing protocols***

Sakai & Larcher (1987) has a good chapter on protocols and how to measure freezing resistance. See also Hincha & Zuther (2014).

##### ***All references***

- Anderson, J. A., Kenna, M. P., & Taliaferro, C. M. (1988). Cold hardiness of Midiron and Tifgreen bermudagrass. *Hortscience*, 23(4), 748-750.
- Bajji, M., Kinet, J.-M., & Lutts, S. (2002). The use of the electrolyte leakage method for assessing cell membrane stability as a water stress tolerance test in durum wheat. *Plant Growth Regulation*, 36(1), 61-70.
- Bigras, F. J., Ryypö, A., Lindstrom, A., & Sattin, E. (2001). Cold acclimation and deacclimation of shoots and roots of conifer seedlings. In F. J. Bigras, & S. J. Colombo (Eds.), *Conifer Cold Hardiness* (pp. 57-88). Dordrecht: Kluwer.
- Bilavčík, A., Zámečník, J., Grospietsch, M., Faltus, M., & Jadrná, P. (2012). Dormancy development during cold hardening of in vitro cultured *Malus domestica* Borkh. plants in relation to their frost resistance and cryotolerance. *Trees*, 26(4), 1181-1192.
- Buchner, O., & Neuner, G. (2009). A low-temperature freezing system to study the effects of temperatures to -70° C on trees in situ. *Tree Physiology*, 29(3), 313-320.
- Ciais, P., Reichstein, M., Viovy, N., Granier, A., Ogee, J., Allard, V., ... Valentini, R. (2005). Europe-wide reduction in primary productivity caused by the heat and drought in 2003. *Nature*, 437(7058), 529-533.

- Clement, J. M. A. M., & van Hasselt, P. R. (1996). Chlorophyll fluorescence as a parameter for frost hardness in winter wheat. A comparison with other hardness parameters. *Phyton-Annales Rei Botanicae*, 36(1), 29-41.
- Elzhov, T. V., Mullen, K. M., Spiess, A.-M., & Bolker, B. (2016). minpack.lm: R Interface to the Levenberg-Marquardt Nonlinear Least-Squares Algorithm Found in MINPACK, Plus Support for Bounds. <https://CRAN.R-project.org/package=minpack.lm>
- Hincha, D. K. & Zuther, E. (Eds.) (2014). *Plant Cold Acclimation*. New York: Springer.
- Kalberer, S. R., Wisniewski, M., & Arora, R. (2006). Deacclimation and reacclimation of cold-hardy plants: Current understanding and emerging concepts. *Plant Science*, 171, 3-16.
- Kollas, C., Randin, C. F., Vitasse, Y., & Körner, C. (2014). How accurately can minimum temperatures at the cold limits of tree species be extrapolated from weather station data? *Agricultural and Forest Meteorology*, 184, 257-266.
- Körner, C. (2012). *Alpine Treelines, Functional Ecology of the Global High Elevation Tree Limits*. Basel: Springer.
- Kreyling, J., Persoh, D., Werner, S., Benzenberg, M., & Wöllecke, J. (2012). Short-term impacts of soil freeze-thaw cycles on roots and root-associated fungi of *Holcus lanatus* and *Calluna vulgaris*. *Plant and Soil*, 353(1-2), 19-31.
- Kreyling, J., Schmid, S., & Aas, G. (2015). Cold tolerance of tree species is related to the climate of their native ranges. *Journal of Biogeography*, 42, 156-166.
- Larcher, W. (2005). Climatic constraints drive the evolution of low temperature resistance in woody plants. *Journal of Agricultural Meteorology*, 61(4), 189-202.
- Lenz, A., Hoch, G., Vitasse, Y., & Koerner, C. (2013). European deciduous trees exhibit similar safety margins against damage by spring freeze events along elevational gradients. *New Phytologist*, 200(4), 1166-1175.
- Lenz, A., Hoch, G., & Vitasse, Y. (2016a). Fast acclimation of freezing resistance suggests no influence of winter minimum temperature on the range limit of European beech. *Tree Physiology*, 36(4), 490-501.
- Lenz, A., Hoch, G., Körner, C., & Vitasse, Y. (2016b). Convergence of leaf-out towards minimum risk of freezing damage in temperate trees. *Functional Ecology*, 30(9), 1480-1490.
- Lim, C. C., Arora, R., & Townsend, E. C. (1998). Comparing Gompertz and Richards functions to estimate freezing injury in *Rhododendron* using electrolyte leakage. *Journal of the American Society for Horticultural Science*, 123(2), 246-252.
- Lindén, L., Rita, H., & Suojala, T. (1996). Logit models for estimating lethal temperatures in apple. *HortScience*, 31(1), 91-93.
- Munns, R., & Tester, M. (2008). Mechanisms of salinity tolerance. *Annual Review of Plant Biology*, 59, 651-681.
- Neuner, G., & Hacker, J. (2012). Ice formation and propagation in alpine plants. In C. Lütz (Ed.), *Plants in Alpine Regions* (pp. 163-174). Vienna: Springer.

- Neuner, G., Bannister, P., & Larcher, W. (1997). Ice formation and foliar frost resistance in attached and excised shoots from seedlings and adult trees of *Nothofagus menziesii*. *New Zealand Journal of Botany*, 35(2), 221-227.
- Pramsohler, M., Hacker, J., & Neuner, G. (2012). Freezing pattern and frost killing temperature of apple (*Malus domestica*) wood under controlled conditions and in nature. *Tree Physiology*, 32(7), 819-828.
- Premachandra, G. S., & Shimada, T. (1987). The measurement of cell membrane stability using polyethylene glycol as a drought tolerance test in wheat. *Japanese Journal of Crop Science*, 56(1), 92-98.
- Räisänen, M., Repo, T., Rikala, R., & Lehto, T. (2006). Does ice crystal formation in buds explain growth disturbances in boron-deficient Norway spruce? *Trees*, 20(4), 441-448.
- Sakai, A. (1960). Survival of the twig of woody plants at -196° C. *Nature*, 185(4710), 393-394.
- Sakai, A. (1966). Studies of frost hardiness in woody plants. II. Effect of temperature on hardening. *Plant Physiology*, 41(2), 353-359.
- Sakai, A., & Larcher, W. (1987). *Frost Survival of Plants*. Ecological Studies: Vol. 62. Berlin: Springer.
- Sakai, A., & Weiser, C. J. (1973). Freezing resistance of trees in North America with reference to tree regions. *Ecology*, 54(1), 118-126.
- Salazar-Gutiérrez, M. R., Chaves, B., & Hoogenboom, G. (2016). Freezing tolerance of apple flower buds. *Scientia Horticulturae*, 198, 344-351.
- Siminovitch, D., Singh, J., & La Roche, I. A. D. (1978). Freezing behavior of free protoplasts of winter rye. *Cryobiology*, 15(2), 205-213.
- Snyder, R. L., & de Melo-Abreu, J. P. (2005). *Frost Protection: Fundamentals, Practice, and Economics*. Rome: FAO
- Steffen, K. L., Arora, R., & Palta, J. P. (1989). Relative sensitivity of photosynthesis and respiration to freeze-thaw stress in herbaceous species: Importance of realistic freeze-thaw protocols. *Plant Physiology*, 89(4), 1372-1379.
- Sutinen, M. L., Palta, J. P., & Reich, P. B. (1992). Seasonal differences in freezing stress resistance of needles of *Pinus nigra* and *Pinus resinosa* – evaluation of the electrolyte leakage method. *Tree Physiology*, 11(3), 241-254.
- Thomashow, M. F. (1999). Plant cold acclimation: Freezing tolerance genes and regulatory mechanisms. *Annual Review of Plant Physiology and Plant Molecular Biology*, 50, 571-599.
- Trevan, J. W. (1927). The error of determination of toxicity. *Proceedings of the Royal Society of London Series B: Biological Sciences*, 101(712), 483-514.
- Tylianakis, J. M., Didham, R. K., Bascompte, J., & Wardle, D. A. (2008). Global change and species interactions in terrestrial ecosystems. *Ecology Letters*, 11(12), 1351-1363.
- Vitasse, Y., Lenz, A., Hoch, G., Körner, C., & Piper, F. (2014). Earlier leaf-out rather than difference in freezing resistance puts juvenile trees at greater risk of damage than adult trees. *Journal of Ecology*, 102(4), 981-988.

Vitra, A., Lenz, A., & Vitasse, Y. (2017). Frost hardening and dehardening potential in temperate trees from winter to budburst. *New Phytologist*, 216(1), 113-123.

Whitlow, T. H., Bassuk, N. L., Ranney, T. G., & Reichert, D. L. (1992). An improved method for using electrolyte leakage to assess membrane competence in plant tissues. *Plant Physiology*, 98, 198-205.

**Authors:** Kreyling J<sup>1</sup>, Lembrechts JJ<sup>2</sup>, De Boeck HJ<sup>2</sup>

**Reviewer:** Lenz A<sup>3</sup>

### Affiliations

<sup>1</sup> Experimental Plant Ecology, Institute of Botany and Landscape Ecology, University of Greifswald, Greifswald, Germany

<sup>2</sup> Centre of Excellence PLECO (Plants and Ecosystems), Biology Department, University of Antwerp, Wilrijk, Belgium

<sup>3</sup> Clinical Trial Unit Bern, Department of Clinical Research, University of Bern, Bern, Switzerland

## 5.5 Leaf temperature

**Authors:** Michaletz ST<sup>1,2,3</sup>, Blonder B<sup>4,5</sup>, De Boeck HJ<sup>6</sup>

**Reviewer:** Goldsmith GR<sup>7</sup>

**Measurement unit:** K (Kelvin); **Measurement scale:** leaf or canopy; **Equipment costs:** €€-€€€; **Running costs:** €-€€€; **Installation effort:** medium; **Maintenance effort:** medium; **Knowledge need:** medium; **Measurement mode:** manual or data logger

The temperature of plant tissues is determined both by environmental conditions (e.g. De Boeck et al., 2016) and by plant thermal traits that determine heat storage and fluxes (e.g. Michaletz et al., 2015); see [protocol 5.6 Leaf thermal traits](#)). As such, leaf temperatures can vary widely between environments, but also between plants growing under the same conditions and even within the canopy of a single plant (Leuzinger & Körner, 2007). Leaf temperatures directly impact metabolic rates and are coupled to the water cycle, thus affecting growth and fluxes of CO<sub>2</sub> and H<sub>2</sub>O (Michaletz, 2018). Furthermore, leaf temperature is also important regarding interactions between plants and ectotherm herbivores (Caillon et al., 2014). Because leaf temperatures can deviate substantially from air temperatures (differences of > 30 K have been observed in extreme cases, (cf. Neuner & Buchner, 2012), it is imperative to measure leaf temperatures to avoid erroneous conclusions that may result from use of ambient air temperatures in analyses. This is especially relevant for studies of plant and ecosystem responses to projected changes in climate, hydrology, and land use, as well as other global-change agents. Changes in microclimate (e.g. air temperature, humidity, wind, soil moisture, radiation) together with plant thermal traits (see [protocol 5.6 Leaf thermal traits](#)) will determine whether leaf temperature variation will be weakened or strengthened relative to ambient levels (helping maintain leaves near metabolic optima). Under global change, high variation can lead to more frequent deviations from optima and higher incidence of temperature stress, or could also lift temperatures closer to the optimum in cold climates (e.g. Marchand et al., 2005). The measurement of leaf and canopy temperatures is therefore essential in helping to predict responses of plants to environmental change.

### 5.5.1 What and how to measure?

Most investigators are interested in measuring the leaf operating temperature, which is the temperature at which leaf physiological processes occur. Leaf operating temperatures can be determined through direct or indirect methods. Direct methods require either contact with the leaf (thermocouples), or are achieved remotely via non-contact thermal sensors (infrared thermometers or cameras). In either case, direct methods involve *in situ* measurement of leaves on intact live plants. The main indirect method involves measurement of stable isotopes of oxygen ( $\delta^{18}\text{O}$ ) in plant tissue. This indirect method requires destructive sampling of plant tissues that are later processed and measured in the laboratory.

Thermocouples consist of a soldered bead connecting two wires that are each composed of a different metal alloy. As a result of the thermoelectric effect, the thermocouple bead will produce a voltage that is a nonlinear function of temperature. Calibration relationships allow conversion

between thermocouple bead temperature and measured voltages. Thermocouples attached to an *in situ* leaf will thus measure the leaf temperature after a period of equilibration (e.g. Hall et al., 2014).

An infrared thermometer uses radiation theory to estimate skin (surface) temperature. Based on the emissivity of the object in question and the measurement of a portion of the emitted radiation, the object's temperature is derived in accordance with the Stefan–Boltzmann law. The thermometer usually consists of a filter that permits infrared radiation to pass through and a thermopile detector, yielding two voltages from which the object's surface temperature can be established. These detectors average the radiation fluxes over a certain angular field of view, and do not provide point measurements of temperature unless placed very close to the object in question.

Infrared cameras permit imaging and point measurements across a field of view. The images produced by such cameras are not of the visible portion of the spectrum (c. 0.4–0.7 µm), but instead of the thermal/infrared portion (cameras often capture the 7–14 µm band). The measurement principle is comparable to that of infrared thermometers, where a lens made of a material that is transparent to infrared radiation (such as germanium) is used to focus radiation on an infrared-sensitive detector array. A complete image is formed that contains surface temperature information at the pixel scale. Pixel values are a nonlinear function of radiation intensity. Various calibration relationships (assuming different object and atmospheric properties) can then be employed to convert pixel values to temperature (Aubrecht et al., 2016). These calibration relationships are more sophisticated than typically used for infrared thermometers. Images are often displayed in pseudo-colour to highlight temperature differences. Imaging software then allows the selection of regions of interest, such as single leaves in an image of a canopy, depending on the available resolution (e.g. Jerbi et al., 2015).

Finally, indirect measurements of leaf temperature can be achieved through the stable isotopes of oxygen ( $\delta^{18}\text{O}$ ) of leaf tissue (see [protocol 5.13 Stable isotopes of water for inferring plant function](#)). These isotopes have different molecular masses, so that evaporation (i.e. phase change from liquid to vapour) of water molecules with a different number of neutrons requires different amounts of energy. The  $\delta^{18}\text{O}$  of leaf water is thus strongly correlated with the temperature of the leaf (though the primary temperature control is on source water, which the method accounts for). As such,  $\delta^{18}\text{O}$  has long been used for past climate reconstruction, but the method can also be applied to infer photosynthetically-weighted leaf temperatures over a period of time (e.g. the growing season) in existing vegetation (Helliker & Richter, 2008).

In the following, we focus on the advantages and disadvantages of these four methods.

### **Where to start**

Aubrecht et al. (2016), Chelle (2005), Costa et al. (2013), Jones & Vaughan (2010), Jones et al. (2009)

### ***Installation, field operation, maintenance, interpretation***

a) **Thermocouples** are widely used for measuring leaf temperature, but to obtain accurate measurements there are several points that should be considered. Since thermocouple measurements are made *in situ* on leaves of intact live plants, it is important that the thermocouple

does not affect any of the climate variables or thermal properties that control leaf temperature, such as solar radiation, leaf angle, or boundary layer development (see [protocol 5.6 Leaf thermal traits](#)). Care should be taken to avoid touching the leaf, moving the leaf out of its resting position, or shading the leaf, as these will influence the temperature of the leaf. Leaf temperature is generally measured on the abaxial side (bottom) of the leaf to avoid shading of solar radiation on the top of the leaf. It is also important to recognise that temperature measured with a thermocouple represents the temperature of the thermocouple bead and not necessarily the temperature of the leaf. Thus, care must be taken to ensure that the thermocouple temperature is in equilibrium with that of the leaf. This can be achieved using a fine-gauge bare wire thermocouple that will respond rapidly to temperature fluctuations (i.e. the thermocouple time constant should be smaller than that of the leaf). The thermocouple bead must also be maintained in direct contact with the leaf surface, which can be achieved in a number of ways. For short-term measurements, the thermocouple can simply be held against the leaf surface, but efforts should be made to prevent heat conduction from one's hand down the thermocouple wires to the thermocouple bead. This can be accomplished by wearing an insulated glove or constructing a thermocouple handle from a fine wire or paper clip. Leaf thermocouple clamps may also be constructed (Slot et al., 2016), although these should be small and lightweight so as to not interfere with the thermal boundary layer or leaf angle. The thermocouple may also be threaded into the leaf (Hanson & Sharkey, 2001), although this may cause xylem embolisms that can reduce stomatal conductance and transpirational cooling. Finally, thermocouples may also be affixed to the leaf surface using porous tape (e.g. 3 M Transpore surgical tape; Slot et al., 2016) that permits gas exchange and transpirational cooling between the leaf and atmosphere. Thermocouples affixed with porous tape were found to agree closely with infrared sensor measurements (Slot et al., 2016).

Thermocouples have some advantages over other temperature measurement methods. For example, they measure temperature over a relatively small leaf area, and are thus suitable for measurements of individual leaves (including spatial variation within leaves or leaflets). Thermocouples measure leaf temperature via conduction from the leaf into the thermocouple bead and are thus immune to the view and emissivity issues that adversely affect non-contact sensors that rely on thermal radiation (infrared sensors and cameras). For this reason, thermocouples can also be used to measure leaf temperatures within the interiors of crowns and canopies, which are difficult if not impossible to measure using non-contact methods. Finally, thermocouples are relatively simple devices and are therefore durable in outdoor weather conditions. The main disadvantages of thermocouples are that they cannot measure average temperatures over large areas and must maintain good contact between the thermocouple bead and the leaf. The latter may be especially challenging when the application requires long-term measurements in outdoor weather conditions.

**b) Infrared thermometers** are a relatively cost-efficient method for remote *in situ* measurement of leaf or canopy temperatures, with the cost per sensor amounting to a fraction (< 5%) of the cost of an infrared camera (Martínez et al., 2017). As such, they can be considered the **bronze standard** in (non-contact) thermography. Infrared thermometers give instantaneous temperature values that, depending on the view angle of the sensor (usually between 10 and 90 °) and the distance to the object, permit the determination of the average temperature of individual leaves or full canopies. Aligning a regular camera with the sensor can aid in making sure the correct area or object is monitored (Martínez et al., 2017). Measurements can be made by hand, in which case the variability

of microenvironmental variables such as wind speed should be taken into account by taking multiple measurements spread over time. This is facilitated by the high speed of each measurement, with no equilibration required (in contrast to thermocouple readings). Scanning of larger areas can be achieved by attaching the sensor to an unmanned aerial vehicle (UAV), although data interpretation may be challenging when dealing with open canopies and/or vegetation with low ground cover, as well as temporal variation in microenvironmental conditions (cf. Martínez et al., 2017). For continuous monitoring, for example in the temperature control of infrared heating arrays (De Boeck et al., 2017), sensors can be installed on a support. Usually, measurements are taken perpendicular to the surface of interest. When measuring at an angle, the area will be elliptical and thus more difficult to control. The main disadvantage of infrared thermometers is that they provide a single value of temperature averaged over their entire field of view. This means that measurements are generally only possible for leaves situated on the exterior of a crown or canopy, and that a view that includes non-leaf bodies such as branches, stems, or the ground can lead to erroneous leaf temperature estimates. This can also mask important temperature variation in heterogeneous crowns and canopies.

c) **Infrared cameras** also perform remote *in situ* measurement of leaf or canopy temperatures, and are the **gold standard** of (non-contact) thermography. They have developed rapidly over the past two decades, helped by modern commercial applications such as home energy auditing. Although still expensive, infrared cameras with relatively high resolution ( $640 \times 480$  pixels) have seen their prices drop by 50% or more during the past ten years. The main advantage of infrared cameras is that they capture a lot of information within each image, which allows comparison of different objects (e.g. species, phenotypes) under the same ambient conditions. Of course, the radiation environment may differ significantly within the same image (Morecroft & Roberts, 1999). For example, the mean irradiance (and thus temperature) will be greatest for sun-leaves, while leaves deeper within the canopy will be primarily exposed to diffuse radiation scattered by other leaves and the soil (Jones et al., 2009). The orientation of the camera relative to the sun directly affects the readings, as alignment with the solar angle will yield a larger fraction of sun-lit leaves, and hence a higher surface temperature. This is described by the bidirectional reflectance distribution function (Liang, 2005). Depending on the research question, the camera can thus be used aligned with the solar angle at the time of measurement (taking care not to self-shade), or at a fixed angle (e.g. 45 °). If readings are taken at more than one angle, both the mean canopy and leaf temperature components can be calculated, as well as the sunlit and shaded leaf temperature components (Jia et al., 2003). Another factor to keep in mind regarding the camera angle is that a greater proportion of bare soil is captured when the angle is closer to being perpendicular to the soil surface. It is possible to use infrared cameras attached to UAVs (Martínez et al., 2017), although altitudinal corrections need to be applied to account for atmospheric radiation (Jones & Vaughan, 2010). As a general rule, the camera distance from objects in a comparison should be as similar as possible to avoid complications due to distance-induced bias (Faye et al., 2016). Because emissivity plays such an important role in the derivation of surface temperature, it should ideally be determined for the canopy under study (see [protocol 5.6 Leaf thermal traits](#)). For very distant vegetation, it is more appropriate to use blackbody values (Aubrecht et al., 2016). Infrared cameras can be suspended in one place and used to take automated measurements, so that a time series is created. The large amount of data thus recorded can be rendered manageable through batch-processing via image analysis software, although finer details (e.g. specific leaves in a vegetation) usually require

researcher input as plant growth induces changes in their location within the image and/or changes in the radiation environment. Finally, calibrated temperatures can be affected by several factors, such as relative humidity of the air and sensor temperature, causing spatial or temporal variation (discussed in Aubrecht et al., 2016).

**d)  $\delta^{18}\text{O}$  of cellulose** can be used to estimate a photosynthetically-weighted leaf temperature over the period when the carbon in the cellulose was assimilated (Helliker & Richter, 2008). This is an indirect method that requires destructive sampling and laboratory measurement of plant tissues. Leaf water  $\delta^{18}\text{O}$  is influenced by source water  $\delta^{18}\text{O}$  and transpiration, both of which vary with climate variables (relative humidity and air temperature, VPD; Bögelein et al., 2017; Kahmen et al., 2011). During photosynthesis, transpiration will yield a leaf water  $\delta^{18}\text{O}$  that is in part dependent on leaf temperature. The leaf water  $\delta^{18}\text{O}$  is then incorporated into the sugars produced by photosynthesis, which ultimately become incorporated into the cellulose in plant tissue (Gessler et al., 2014). Thus, the  $\delta^{18}\text{O}$  of cellulose reflects the temperature integrated across the plant's total leaf area and through the time period when source carbon was assimilated. Unlike point measurements,  $\delta^{18}\text{O}$  estimates provide an integrated measure of variation in leaf biophysics (energy balance and biochemistry) because they quantify the “effective temperature” driving rates of leaf-level metabolism and physiology. Thus, this method provides a more time-integrated measure of the average temperature at which net photosynthesis is most productive – i.e. an average temperature of leaf metabolism. Relative to thermocouples and IR sensors, the method is simple and low-cost, making  $\delta^{18}\text{O}$  estimates of leaf temperature especially useful for global change studies that span macroecological scales of time and space.

Leaf temperature is estimated by solving a model originally developed for estimating the  $\delta^{18}\text{O}$  of plant tissue (Barbour & Farquhar, 2000). This requires data for the cellulosic  $\delta^{18}\text{O}$  of the tissue of interest, the  $\delta^{18}\text{O}$  of plant source water, air temperature, and relative humidity. Depending on the tissue source (e.g. leaf v. tree-ring cellulose), additional fractionation must be accounted for due to exchange of oxygen isotopes among different water and carbohydrate pools (see [protocol 5.13 Stable isotopes of water for inferring plant function](#)). Leaf cellulose may yield more accurate estimates of photosynthetically-weighted leaf temperature than wood cellulose, because it has a shorter phloem path length over which post-photosynthetic oxygen exchange may occur. The  $\delta^{18}\text{O}$  of source water can either be directly measured for the plant-available water, or estimated from models for  $\delta^{18}\text{O}$  of precipitation (e.g. Bowen et al., 2017). Air temperature and relative humidity should be measured on-site at a fine temporal resolution (at least hourly) so that 24 h and daytime averages can be calculated. Ideally, these should be weighted by gross primary production (GPP), but if temporal estimates of GPP are unavailable, these can be resolved for 24 h and daytime using irradiance or photosynthetically active radiation (PAR) data.

Different plant tissues can be used to estimate photosynthetically-weighted leaf temperatures corresponding to different time periods. Shorter-term estimates may be obtained using leaf cellulose (Flanagan & Farquhar, 2014), which will integrate over the time that the leaf formed and the cellulose was synthesised. Longer-term estimates can be obtained from annual growth rings from branches or increment cores of woody plants. For example, annual growth rings can be homogenised to give long-term average leaf temperatures (Helliker & Richter, 2008; Song et al., 2011), while individual rings can be analysed in order to characterise inter- or intra-annual variation.

Preparation of the plant tissue and measurements of isotopic composition are described in [protocol 5.13 Stable isotopes of water for inferring plant function](#))

## 5.5.2 Special cases, emerging issues, and challenges

In agronomy, there is much interest in using measurements of leaf temperature as a method to control precision irrigation as one image can reveal where soil water is deficient and where it is not (e.g. Padhi et al., 2012). Irrigation can thus be applied before visual stress is perceivable (Gerhards et al., 2016), which helps to avoid production losses. It should be noted that anisohydric species such as soybean and wheat are less suitable for such strategies due to the poor correlation between stomatal conductance (and therefore leaf temperature) and soil water status (cf. Costa et al., 2013). In such cases, leaf water potential is a much better (but less practical) indicator of soil water deficit. Apart from being an indicator of drought stress, increased leaf temperature can also be indicative of several plant diseases (e.g. the tobacco mosaic virus) before visual symptoms are apparent, as the infection changes water use and/or movement (Chærle et al., 2004; Oerke et al., 2011).

A concept with various applications in ecology is the thermal time constant  $\tau$  (s). This is a composite leaf trait that quantifies the thermal stability of a leaf, i.e. how rapidly leaf temperature responds to temporal variation in microclimate. It can be measured indirectly via leaf thermal traits (see [protocol 5.6 Leaf thermal traits](#) and Michaletz et al., 2015, 2016) or directly through periodic thermal forcing of a leaf or via step-changes in temperatures followed by curve-fitting through the ensuing time series data (Jones, 2014). Large time constants dampen leaf temperature variation relative to ambient and may help maintain leaves near metabolic optima (Michaletz et al., 2015, 2016), while small time constants result in stronger atmospheric coupling. The thermal time constant thus plays a fundamental role in water relations and net carbon gain of a leaf. It governs temporal variation of leaf temperature, which in turn influences instantaneous carbon assimilation rates (Berry & Bjorkman, 1980; Yamori et al., 2014) and ultimately time-integrated net carbon gain (Michaletz et al., 2015, 2016) and ecosystem carbon fluxes.

Many Earth system models make use of air temperatures, even though air and leaf temperatures may strongly differ. If models fail to correctly derive tissue temperatures, this may lead to significant error in outputs. For example, while models simulating heat impacts on rice production have accounted for heat dissipation through transpiration (van Oort et al., 2014), models widely applied for wheat have used simpler approaches such as air temperature thresholds (Alderman et al., 2014; Neukam et al., 2016). Moreover, most models are highly sensitive to input temperatures (Bassu et al., 2014; Neukam et al., 2016), meaning that more accurate consideration of leaf and canopy temperatures is of prime importance in correctly predicting climate-change impacts on plant functioning. Direct use of leaf temperatures in addition to air temperatures is likely to improve such predictions and can elucidate the exact role of temperature (Levis, 2014; Eyshi Rezaei et al., 2015). To that end, model routines need to be systematically evaluated and adapted (Webber et al., 2017) as these are currently often based on empirical data relating to air temperatures, while they lack information on how these translate into leaf and tissue temperatures (Neukam et al., 2016). More widespread monitoring of leaf temperatures, spurred by improvements in measurement technology and lowering of prices, will likely help move the focus from air to leaf temperatures in modelling.

## 5.5.5 References

### Theory, significance, and large datasets

Aubrecht et al. (2016), Gessler et al. (2014), Helliker & Richter (2008), Michaletz et al. (2016)

### More on methods and existing protocols

Costa et al. (2013), Doughty et al. (2011), Ehleringer (1981), Leigh et al. (2012), Pérez-Harguindeguy et al. (2013), Shiklomanov et al. (2016)

### All references

- Alderman, P., Quilligan, E., Asseng, S., Ewert, F., & Reynolds, M. (2014). *Proceedings of the Workshop on Modeling Wheat Response to High Temperature; El Batán, Texcoco, Mexico; 19-21 Jun 2013*. CIMMYT - International Maize and Wheat Improvement Centre.
- Aubrecht, D. M., Helliker, B. R., Goulden, M. L., Roberts, D. A., Still, C. J., & Richardson, A. D. (2016). Continuous, long-term, high-frequency thermal imaging of vegetation: Uncertainties and recommended best practices. *Agricultural and Forest Meteorology*, 228-229, 315-326.
- Barbour, M. M., & Farquhar, G. D. (2000). Relative humidity- and ABA-induced variation in carbon and oxygen isotope ratios of cotton leaves. *Plant, Cell & Environment*, 23(5), 473-485.
- Bassu, S., Brisson, N., Durand, J. L., Boote, K., Lizaso, J., Jones, J. W., ... Waha, K. (2014). How do various maize crop models vary in their responses to climate change factors? *Global Change Biology*, 20(7), 2301-2320.
- Berry, J., & Bjorkman, O. (1980). Photosynthetic response and adaptation to temperature in higher plants. *Annual Review of Plant Physiology*, 31(1), 491-543.
- Bögelein, R., Thomas, F. M., & Kahmen, A. (2017). Leaf water  $^{18}\text{O}$  and  $^2\text{H}$  enrichment along vertical canopy profiles in a broadleaved and a conifer forest tree. *Plant, Cell & Environment*, 40(7), 1086-1103.
- Bowen, G. J., West, J. B., Miller, C. C., Zhao, L., & Zhang, T. (2017). IsoMAP: Isoscapes Modeling, Analysis, and Prediction (version 1.0). The IsoMAP Project. <http://isomap.org>.
- Caillet, R., Suppo, C., Casas, J., Arthur Woods, H., & Pincebourde, S. (2014). Warming decreases thermal heterogeneity of leaf surfaces: implications for behavioural thermoregulation by arthropods. *Functional Ecology*, 28(6), 1449-1458.
- Chærle, L., Hagenbeek, D., De Bruyne, E., Valcke, R., & van der Straeten, D. (2004). Thermal and chlorophyll-fluorescence imaging distinguish plant-pathogen interactions at an early stage. *Plant and Cell Physiology*, 45(7), 887-896.
- Chelle, M. (2005). Phylloclimate or the climate perceived by individual plant organs: What is it? How to model it? What for? *New Phytologist*, 166(3), 781-790.
- Costa, J. M., Grant, O. M., & Chaves, M. M. (2013). Thermography to explore plant–environment interactions. *Journal of Experimental Botany*, 64(13), 3937-3949.
- De Boeck, H. J., van de Velde, H., de Groote, T., & Nijs, I. (2016). Ideas and perspectives: Heat stress: more than hot air. *Biogeosciences*, 13(20), 5821-5825.

- De Boeck, H. J., Kockelbergh, F., & Nijs, I. (2017). More realistic warming by including plant feedbacks: A new field-tested control method for infrared heating. *Agricultural and Forest Meteorology*, 237-238, 355-361.
- Doughty, C. E., Field, C. B., & McMillan, A. M. S. (2011). Can crop albedo be increased through the modification of leaf trichomes, and could this cool regional climate? *Climatic Change*, 104(2), 379-387.
- Ehleringer, J. R. (1981). Leaf absorptances of Mohave and Sonoran desert plants. *Oecologia*, 49(3), 366-370.
- Eyshi Rezaei, E., Webber, H., Gaiser, T., Naab, J., & Ewert, F. (2015). Heat stress in cereals: Mechanisms and modelling. *European Journal of Agronomy*, 64, 98-113.
- Faye, E., Dangles, O., & Pincebourde, S. (2016). Distance makes the difference in thermography for ecological studies. *Journal of Thermal Biology*, 56, 1-9.
- Flanagan, L. B., & Farquhar, G. D. (2014). Variation in the carbon and oxygen isotope composition of plant biomass and its relationship to water-use efficiency at the leaf- and ecosystem-scales in a northern Great Plains grassland. *Plant, Cell & Environment*, 37(2), 425-438.
- Gerhards, M., Rock, G., Schlerf, M., & Udelhoven, T. (2016). Water stress detection in potato plants using leaf temperature, emissivity, and reflectance. *International Journal of Applied Earth Observation and Geoinformation*, 53, 27-39.
- Gessler, A., Ferrio, J. P., Hommel, R., Treydte, K., Werner, R. A., & Monson, R. K. (2014). Stable isotopes in tree rings: towards a mechanistic understanding of isotope fractionation and mixing processes from the leaves to the wood. *Tree Physiology*, 34(8), 796-818.
- Hall, T. D., Chastain, D. R., Horn, P. J., Chapman, K. D., & Choinski, J. S. (2014). Changes during leaf expansion of  $\Phi_{PSII}$  temperature optima in *Gossypium hirsutum* are associated with the degree of fatty acid lipid saturation. *Journal of Plant Physiology*, 171(6), 411-420.
- Hanson, D. T., & Sharkey, T. D. (2001). Effect of growth conditions on isoprene emission and other thermotolerance-enhancing compounds. *Plant, Cell & Environment*, 24(9), 929-936.
- Helliker, B. R., & Richter, S. L. (2008). Subtropical to boreal convergence of tree-leaf temperatures. *Nature*, 454(7203), 511-514.
- Jerbi, T., Wuyts, N., Cane, M. A., Faux, P.-F., & Draye, X. (2015). High resolution imaging of maize (*Zea mays*) leaf temperature in the field: the key role of the regions of interest. *Functional Plant Biology*, 42(9), 858-864.
- Jia, L., Li, Z. I., Menenti, M., Su, Z., Verhoef, W., & Wan, Z. (2003). A practical algorithm to infer soil and foliage component temperatures from bi-angular ATSR-2 data. *International Journal of Remote Sensing*, 24(23), 4739-4760.
- Jones, H. G. (2014). *Plants and Microclimate: A Quantitative Approach to Environmental Plant Physiology*. Cambridge: Cambridge University Press.
- Jones, H. G., & Vaughan, R. A. (2010). *Remote Sensing of Vegetation: Principles, Techniques, and Applications*. Oxford: Oxford University Press.
- Jones, H. G., Serraj, R., Loveys, B. R., Xiong, L., Wheaton, A., & Price, A. H. (2009). Thermal infrared imaging of crop canopies for the remote diagnosis and quantification of plant responses to water stress in the field. *Functional Plant Biology*, 36(11), 978-989.
- Kahmen, A., Sachse, D., Arndt, S. K., Tu, K. P., Farrington, H., Vitousek, P. M., & Dawson, T. E. (2011). Cellulose  $\delta^{18}\text{O}$  is an index of leaf-to-air vapor pressure difference (VPD) in tropical plants. *Proceedings of the National Academy of Sciences USA*, 108(5), 1981-1986.

- Leigh, A., Sevanto, S., Ball, M. C., Close, J. D., Ellsworth, D. S., Knight, C. A., ... Vogel, S. (2012). Do thick leaves avoid thermal damage in critically low wind speeds? *New Phytologist*, 194(2), 477-487.
- Leuzinger, S., & Körner, C. (2007). Tree species diversity affects canopy leaf temperatures in a mature temperate forest. *Agricultural and Forest Meteorology*, 146(1–2), 29–37.
- Levis, S. (2014). Crop heat stress in the context of Earth System modeling. *Environmental Research Letters*, 9(6), 061002.
- Liang, S. (2005). *Quantitative Remote Sensing of Land Surfaces*. Chichester: John Wiley & Sons.
- Marchand, F. L., Mertens, S., Kockelbergh, F., Beyens, L., & Nijs, I. (2005). Performance of High Arctic tundra plants improved during, but deteriorated after, exposure to a simulated extreme temperature event. *Global Change Biology*, 11(12), 2078-2089.
- Martínez, J., Egea, G., Agüera, J., & Pérez-Ruiz, M. (2017). A cost-effective canopy temperature measurement system for precision agriculture: a case study on sugar beet. *Precision Agriculture*, 18(1), 95-110.
- Michaletz, S. T. (2018). Evaluating the kinetic basis of plant growth from organs to ecosystems. *New Phytologist*, 219(1), 37-44.
- Michaletz, S. T., Weiser, M. D., Zhou, J., Kaspari, M., Helliker, B. R., & Enquist, B. J. (2015). Plant thermoregulation: Energetics, trait-environment interactions, and carbon economics. *Trends in Ecology & Evolution*, 30(12).
- Michaletz, S. T., Weiser, M. D., McDowell, N. G., Zhou, J., Kaspari, M., Helliker, B. R., & Enquist, B. J. (2016). The energetic and carbon economic origins of leaf thermoregulation. *Nature Plants*, 2, 16129.
- Morecroft, M. D., & Roberts, J. M. (1999). Photosynthesis and stomatal conductance of mature canopy Oak (*Quercus robur*) and Sycamore (*Acer pseudoplatanus*) trees throughout the growing season. *Functional Ecology*, 13(3), 332-342.
- Neukam, D., Ahrends, H., Luig, A., Manderscheid, R., & Kage, H. (2016). Integrating wheat canopy temperatures in crop system models. *Agronomy*, 6(1), 7.
- Neuner, G., & Buchner, O. (2012). Dynamics of tissue heat tolerance and thermotolerance of PS II in alpine plants. In C. Lütz (Ed.), *Plants in Alpine Regions: Cell Physiology of Adaption and Survival Strategies* (pp. 61-74). Vienna: Springer.
- Oerke, E.-C., Fröhling, P., & Steiner, U. (2011). Thermographic assessment of scab disease on apple leaves. *Precision Agriculture*, 12(5), 699-715.
- Padhi, J., Misra, R. K., & Payero, J. O. (2012). Estimation of soil water deficit in an irrigated cotton field with infrared thermography. *Field Crops Research*, 126, 45-55.
- Pérez-Harguindeguy, N., Díaz, S., Garnier, E., Lavorel, S., Poorter, H., Jaureguiberry, P., ... Cornelissen, J. H. C. (2013). New handbook for standardised measurement of plant functional traits worldwide. *Australian Journal of Botany*, 61(3), 167-234.
- Shiklomanov, A. N., Dietze, M. C., Viskari, T., Townsend, P. A., & Serbin, S. P. (2016). Quantifying the influences of spectral resolution on uncertainty in leaf trait estimates through a Bayesian approach to RTM inversion. *Remote Sensing of Environment*, 183, 226-238.
- Slot, M., Garcia, M. N., & Winter, K. (2016). Temperature response of CO<sub>2</sub> exchange in three tropical tree species. *Functional Plant Biology*, 43(5), 468-478.

- Song, X., Barbour, M. M., Saurer, M., & Helliker, B. R. (2011). Examining the large-scale convergence of photosynthesis-weighted tree leaf temperatures through stable oxygen isotope analysis of multiple data sets. *New Phytologist*, 192(4), 912-924.
- van Oort, P. A. J., Saito, K., Zwart, S. J., & Shrestha, S. (2014). A simple model for simulating heat induced sterility in rice as a function of flowering time and transpirational cooling. *Field Crops Research*, 156, 303-312.
- Webber, H., Martre, P., Asseng, S., Kimball, B., White, J., Ottman, M., ... Ewert, F. (2017). Canopy temperature for simulation of heat stress in irrigated wheat in a semi-arid environment: A multi-model comparison. *Field Crops Research*, 202, 21-35.
- Yamori, W., Hikosaka, K., & Way, D. A. (2014). Temperature response of photosynthesis in C<sub>3</sub>, C<sub>4</sub>, and CAM plants: temperature acclimation and temperature adaptation. *Photosynthesis Research*, 119(1), 101-117.

**Authors:** Michaletz ST<sup>1,2,3</sup>, Blonder B<sup>4,5</sup>, De Boeck HJ<sup>6</sup>

**Reviewer:** Goldsmith GR<sup>7</sup>

## Affiliations

<sup>1</sup> Earth and Environmental Sciences Division, Los Alamos National Laboratory, Los Alamos, USA

<sup>2</sup> Biosphere 2 and Department of Ecology & Evolutionary Biology, University of Arizona, Tucson, USA

<sup>3</sup> Department of Botany and Biodiversity Research Centre, University of British Columbia, Vancouver, Canada

<sup>4</sup> Environmental Change Institute, School of Geography and the Environment, University of Oxford, Oxford, UK

<sup>5</sup> School of Life Sciences, Arizona State University, Tempe, USA

<sup>6</sup> Centre of Excellence PLECO (Plants and Ecosystems), Department of Biology, Universiteit Antwerpen, Wilrijk, Belgium

<sup>7</sup> Schmid College of Science and Technology, Chapman University, Orange, USA

## 5.6 Leaf thermal traits

**Authors:** Michaletz ST<sup>1,2,3</sup>, Blonder B<sup>4,5</sup>

**Reviewer:** Prentice IC<sup>6</sup>

**Measurement unit:** various (see below); **Measurement scale:** leaf; **Equipment costs:** €€-€€€; **Running costs:** €-€€€; **Installation effort:** medium to high; **Maintenance effort:** -; **Knowledge need:** medium; **Measurement mode:** manual

Leaf thermal traits determine the exchanges of energy between leaves and their environment (Gates, 1980; Campbell & Norman, 1998; Monteith & Unsworth, 2013; Jones, 2014). As such, they are closely linked to leaf temperature, water loss, and carbon gain. Thermal properties that influence leaf energy fluxes include absorptance, angle, area (projected and total), emissivity, stomatal conductance, and width. Others are implicated in energy storage, and include mass, specific heat capacity, thickness, and water content (1-LDMC, leaf dry matter content; g g<sup>-1</sup>). Finally, composite leaf properties may influence both fluxes and storage, and include the leaf mass per area (LMA; kg m<sup>-2</sup>) and the thermal time constant. Together these properties interact with microclimate variables to determine the energy balance and temperature of the leaf, with implications for physiological rates and plant-environment fluxes.

Each leaf trait plays a role in regulating leaf-environment energy fluxes. Absorptance quantifies the fraction of incident radiation that is not reflected or transmitted by the leaf. Angle determines how a leaf interchanges radiation with its environment. Area determines the amount of leaf surface that contributes to radiation, convection, and latent heat (transpiration) fluxes. Emissivity quantifies the leaf's ability to emit thermal radiation. Stomatal conductance determines the instantaneous rate of evaporation of water through stomatal pores, which influences latent heat fluxes. Width partially determines the depth of the leaf boundary layer, which in turn influences rates of transpiration and convection. Mass, specific heat capacity, thickness, and water content determine how much thermal energy a leaf can store. LMA relates the amount of mass that can store thermal energy to the surface area over which energy can flow between the leaf and environment. The thermal time constant quantifies how rapidly leaf temperature responds to temporal variations in microclimate; small thermal time constants correspond to leaves that respond rapidly to changes in environmental temperature, while large thermal time constants correspond to leaves that respond slowly to changes in environmental temperature. Because each thermal trait helps regulate leaf energetics, metabolism, and physiology, they all play critical roles in linking environmental variation to plant function.

Leaf thermal traits are key variables for understanding and predicting the effects of climate and global change on vegetation. They vary across environmental gradients, which may reflect acclimation and local adaptation that maximise plant performance and ultimately fitness. For example, leaf thermal traits can decouple leaf temperature from ambient air temperature, resulting in a relative homeostasis that helps maintain leaf temperatures near metabolic optima (Michaletz et al., 2015, 2016; Dong et al., 2017). Thermal traits such as leaf angle and absorptance have been shown to vary directionally across elevational temperature gradients (Ehleringer, 1988). Variation in these and other traits may underlie the relative invariance of carbon gain across environmental

gradients that has been observed in many studies (Körner & Diemer, 1987; Diemer & Körner, 1996; Enquist et al., 2017; Malhi et al., 2017; Wang et al., 2017; Michaletz, 2018).

Leaf thermal traits may also minimise temporal variation in leaf temperatures and physiological rates. For example, the thermal time constant controls temporal variation in leaf temperature, which in turn influences instantaneous and time-integrated leaf carbon gain (Berry & Bjorkman, 1980; Yamori et al., 2014; Michaletz et al., 2015, 2016) and, ultimately, ecosystem carbon fluxes. Large time constants may dampen leaf temperature variation relative to ambient levels and help maintain leaves near metabolic optima (Michaletz et al., 2015, 2016), while small time constants may allow stronger atmospheric coupling and dissipation of heat. Leaf thermal traits thus play an important role in how ecosystem fluxes of water, gases, and energy vary across climate gradients and respond to global change.

Although the importance of leaf thermal traits in controlling leaf temperatures and physiological rates is well established, variation of leaf thermal traits in response to environmental variation has been understudied relative to leaf economic traits. Characterising variation in leaf thermal traits across climate gradients and in response to climate change, and understanding the implications of this variation for leaf energetics and metabolism, is a frontier research area in global change biology.

### 5.6.1 What and how to measure?

Leaf thermal traits vary substantially in both time and space. Studies have characterised variation through leaf ontogeny and season (Wu et al., 2016, 2017) or within individual plant crowns (Sack et al., 2006; Hulshof & Swenson, 2010). Other studies aim to minimise this variation by preferentially targeting young, fully-expanded leaves from sunlit areas of the canopy (Pérez-Harguindeguy et al., 2013). Thus, sampling schemes used to address multiple scales of variation in leaf properties are recommended. For example, sampling should generally aim for at least 5 leaves (leaflets) per individual, from 5 individuals per species, in order to have robust estimates of the mean (Baraloto et al., 2010; Hulshof & Swenson, 2010). Measurements should be paired at the leaf scale when estimating composite traits such as LMA, LDMC, or the thermal time constant (Knight & Ackerly, 2003; Keenan & Niinemets, 2016; Michaletz et al., 2016). We refer readers to Baraloto et al. (2010) and Hulshof & Swenson (2010) for further information on leaf trait sampling design.

Some thermal traits (e.g. angle and stomatal conductance) require *in situ* measurement on the intact live plant, while other thermal traits require destructive sampling and laboratory measurement. Thus, traits should be measured in a specific sequence: angle, stomatal conductance, absorptance, emissivity, fresh mass, area and width, dry mass, and specific heat capacity. Destructively sampled leaves should be stored in plastic zipper bags in a refrigerator or under ice until all measurements have been obtained. Measurements can then be used to calculate composite traits such as LMA, LDMC, and the thermal time constant. These recommendations are intended to help minimise the effects of sampling and measurement protocols on the measured variables (e.g. resulting from xylem embolism, evaporation, leaf shrinkage, etc.)

The **angle** (rad) of an individual leaf can be measured using a clinometer. The leaf angle is measured as the angle between the horizontal plane (ground) and a plane parallel to the leaf blade. Design of

leaf angle measurements should consider that angle can vary diurnally or seasonally in response to plant water status and leaf turgor.

**Stomatal conductance** ( $\text{mol m}^{-2} \text{s}^{-1}$ ) can be measured using a leaf porometer or a gas exchange system (see [protocol 5.7 Stomatal conductance](#)). Many studies measure the maximum stomatal conductance of well-watered plants under *in situ* light and growth conditions (e.g. mid-morning measurements), although stomatal conductance varies widely through time and thus measurement strategies will vary depending on the research question. Stomatal conductance is generally measured in molar units, but energy balance analyses sometimes require velocity units; velocity units can be calculated from molar units as  $g_{s,v} = g_{s,m}(RT/P)$ , where  $g_{s,v}$  ( $\text{m s}^{-1}$ ) is stomatal conductance in velocity units,  $g_{s,m}$  ( $\text{mol m}^{-2} \text{s}^{-1}$ ) is stomatal conductance in molar units,  $R$  ( $8.3145 \text{ Pa m}^{-3} \text{ mol}^{-1} \text{ K}^{-1}$ ) is the gas constant,  $T$  (K) is air temperature, and  $P$  (Pa) is air pressure (Jones, 2014).

**Absorptance** (dimensionless) is measured using a spectroradiometer with an integrating sphere (Ehleringer, 1981; Shiklomanov et al., 2016). Absorptance should be measured across the total solar wavelengths 400–3000 nm, as the full spectrum is relevant for leaf radiation fluxes (Ehleringer, 2000). Absorptance can alternatively be measured across a smaller range of wavelengths (e.g. 400–700 nm) and corrected to the 400–3000 nm region using calibration relationships established for the region and taxa of interest (Ehleringer, 1981). If an integrating sphere is not available, absorptance can be estimated from spectroradiometer reflectance spectra and inversion of the PROSPECT-5B leaf radiative transfer model (Shiklomanov et al., 2016; Wu et al., 2018).

**Emissivity** (dimensionless) can be measured using a thermocouple and infrared temperature sensor with an adjustable emissivity setting. The infrared sensor emissivity is adjusted and taken as the value where the temperature estimated from the infrared sensor agrees with that of a fine thermocouple affixed to the leaf surface (see [protocol 5.5 Leaf temperature](#); ASTM Standard E1933-14, 2014).

Measurement protocols for **leaf area** ( $\text{m}^2$ ), **leaf width** (m), **water-saturated fresh mass** (kg), **dry mass** (kg), **LDMC** (dimensionless), and **LMA** ( $\text{kg m}^{-3}$ ) are described in Pérez-Harguindeguy et al. (2013) (see also [protocol 4.16 Functional traits](#)). The **specific heat capacity**  $c$  ( $\text{J kg}^{-1} \text{ K}^{-1}$ ) varies with leaf water content ( $1 - \text{LDMC}$ ) and can be calculated using the rule of simple mixtures (Michaletz et al., 2015):

$$c = \text{LDMC} \cdot c_{LDM} + (1 - \text{LDMC}) \cdot c_w \quad (1)$$

where  $c_w$  ( $4180 \text{ J kg}^{-1} \text{ K}^{-1}$ ) is the specific heat capacity of water. The specific heat capacity of leaf dry matter  $c_{LDM}$  ( $\text{J kg}^{-1} \text{ K}^{-1}$ ) can be measured on oven-dried leaf samples using differential scanning calorimetry (DSC; ASTM Standard E1269-11, 2011). If a thermogravimetric analyser is unavailable for DSC, a value of  $c_{LDM} = 1500 \text{ J kg}^{-1} \text{ K}^{-1}$  can be assumed (Ahn et al., 2009; Zanoelo et al., 2011; Dupont et al., 2014).

The **leaf thermal time constant**  $\tau$  (s) can be quantified in two ways. First, it can be quantified via measurement of leaf temperature time series data (see [protocol 5.5 Leaf temperature](#)). In this approach, the time constant can be estimated by imposing periodic thermal forcing or a step change in temperature and fitting the resultant time series of leaf temperatures (Leigh et al., 2006; Vogel, 2009; Jones, 2014). Second, it can be calculated as a composite leaf trait comprising mass, specific heat capacity, total area, size, geometry, stomatal conductance, LMA, and LDMC (Michaletz et al., 2015, 2016):

$$\tau = \varphi LMA \left[ \frac{c_{p,w}}{LDMC \cdot h} + \frac{c_{p,d} - c_{p,w}}{h} \right] \quad (2)$$

where  $\varphi$  (dimensionless) is the ratio of projected to total leaf area, LMA is the leaf mass per area, LDMC is the leaf dry matter content,  $c_{p,d}$  ( $\text{J kg}^{-1} \text{K}^{-1}$ ) is the specific heat capacity of dry leaf matter, and  $c_{p,w}$  ( $\text{J kg}^{-1} \text{K}^{-1}$ ) is the specific heat capacity of water. A heat transfer coefficient  $h$  ( $\text{W m}^{-2} \text{K}^{-1}$ ) that considers convection, radiation, and transpiration can be calculated as:

$$h = \rho_a c_{p,a} [g_h + g_r + g_w s / \gamma] \quad (\text{simpler forms are given in the supplement of Michaletz et al. 2015}).$$

Here,  $\rho_a$  ( $\text{kg m}^{-3}$ ) is air density,  $c_{p,a}$  ( $\text{J kg}^{-1} \text{K}^{-1}$ ) is the specific heat capacity of air at a constant pressure, and  $g_h$ ,  $g_r$ , and  $g_w$  are conductances to heat, radiation, and water vapour, respectively. These conductances vary with properties of the air (velocity, temperature, density) and leaf (type, size, stomatal conductance, emissivity) as described in (Michaletz et al., 2015). Finally, the psychrometric “constant”  $\gamma$  ( $\text{Pa K}^{-1}$ ) is given by  $\gamma = P c_p / 0.622 \lambda$ , where  $P$  ( $\text{Pa}$ ) is the air pressure and  $\lambda$  ( $\text{J kg}^{-1}$ ) is the latent heat of vaporisation of water.

Measurement of leaf thermal traits is generally accomplished via manual measurement of *in situ* or destructively sampled leaves. This can occur at a fixed point in time (such as the peak of the growing season) or fixed intervals through time (e.g. to characterise temporal variation in thermal traits). For cases where the thermal time constant is estimated from temperature time series data, this may be accomplished via deployment of leaf thermocouples, infrared thermometers, or infrared cameras as described in [protocol 5.5 Leaf temperature](#).

### **Where to start**

Baraloto et al. (2010), Hulshof & Swenson (2010), Jones (2014), Pérez-Harguindeguy et al. (2013)

### **5.6.2 Special cases, emerging issues, and challenges**

Efforts are underway to improve the land component of Earth system models (ESMs) by replacing plant functional types (which are conventionally prescribed to have fixed values of traits) with more realistic, continuous variation in functional traits (Kattge et al., 2011; Scheiter et al., 2013; Fyllas et al., 2014; van Bodegom et al., 2014; Wullschleger et al., 2014; Fisher et al., 2015; Sakschewski et al., 2015; Christoffersen et al., 2016). Temperature is a key driver of rates of plant metabolism, but ESMs may not accurately estimate the operating temperatures of plants because even though they include surface energy balance calculations, they generally do not accurately represent the spatial and temporal variation of leaf thermal traits (Dong et al., 2017). In offline dynamic global vegetation models (DGVMs) leaf temperature is normally assumed to equal ambient air temperature; but in reality leaf temperatures can differ from ambient air temperature (commonly by 3 to 6 °C and sometimes by up to 29 °C (Michaletz et al., 2016), suggesting that this approximation is unsatisfactory.

### **5.6.3 References**

### **Theory, significance, and large datasets**

BIEN: The Botanical Information and Ecology Network (<http://bien.nceas.ucsb.edu/bien/>); Jones (2014), Kattge et al. (2011), Michaletz et al. (2016)

### **More on methods and existing protocols**

Campbell & Norman (1998), Ehleringer (1981), Gates (1980), Monteith & Unsworth (2013), Pérez-Harguindeguy et al. (2013)

### **All references**

- Ahn, H. K., Sauer, T. J., Richard, T. L., & Glanville, T. D. (2009). Determination of thermal properties of composting bulking materials. *Bioresource Technology*, 100(17), 3974-3981.
- ASTM Standard E1269-11. (2011). Standard Test Method for Determining Specific Heat Capacity by Differential Scanning Calorimetry.
- ASTM Standard E1933-14. (2014). Standard Practice for Measuring and Compensating for Emissivity Using Infrared Imaging Radiometers. *ASTM International, West Conshohocken*.
- Baraloto, C., Paine, C. E. T., Patiño, S., Bonal, D., Héault, B., & Chave, J. (2010). Functional trait variation and sampling strategies in species-rich plant communities. *Functional Ecology*, 24(1), 208-216.
- Berry, J., & Bjorkman, O. (1980). Photosynthetic response and adaptation to temperature in higher plants. *Annual Review of Plant Physiology*, 31(1), 491-543.
- Campbell, G. S., & Norman, J. M. (1998). *An Introduction to Environmental Biophysics*. New York: Springer Science+Business Media.
- Christoffersen, B. O., Gloor, M., Fauset, S., Fyllas, N. M., Galbraith, D. R., Baker, T. R., ... Meir, P. (2016). Linking hydraulic traits to tropical forest function in a size-structured and trait-driven model (TFS v.1-Hydro). *Geoscientific Model Development*, 9(11), 4227-4255.
- Diemer, M., & Körner, C. (1996). Lifetime leaf carbon balances of herbaceous perennial plants from low and high altitudes in the Central Alps. *Functional Ecology*, 10(1), 33-43.
- Dong, N., Prentice, I. C., Harrison, S. P., Song, Q. H., & Zhang, Y. P. (2017). Biophysical homoeostasis of leaf temperature: A neglected process for vegetation and land-surface modelling. *Global Ecology and Biogeography*, 26(9), 998-1007.
- Dupont, C., Chiriac, R., Gauthier, G., & Toche, F. (2014). Heat capacity measurements of various biomass types and pyrolysis residues. *Fuel*, 115, 644-651.
- Ehleringer, J. R. (1981). Leaf absorptances of Mohave and Sonoran desert plants. *Oecologia*, 49(3), 366-370.
- Ehleringer, J. R. (1988). Changes in leaf characteristics of species along elevational gradients in the Wasatch Front, Utah. *American Journal of Botany*, 680-689.
- Ehleringer, J. R. (2000). Temperature and energy budgets. In R. W. Pearcy, J. R. Ehleringer, H. A. Mooney, & P. W. Rundel (Eds.), *Plant Physiological Ecology: Field methods and instrumentation* (pp. 117-135). Dordrecht: Springer.

- Enquist, B. J., Patrick Bentley, L., Shenkin, A., Maitner, B., Savage, V., Michaletz, S. T., ... Malhi, Y. (2017). Assessing trait-based scaling theory in tropical forests spanning a broad temperature gradient. *Global Ecology and Biogeography*, 26, 1357-1373.
- Fisher, R. A., Muszala, S., Verteinstein, M., Lawrence, P., Xu, C., McDowell, N. G., ... Bonan, G. (2015). Taking off the training wheels: the properties of a dynamic vegetation model without climate envelopes. *Geoscientific Model Development Discussions*, 8(4), 3293-3357.
- Fyllas, N. M., Gloor, E., Mercado, L. M., Sitch, S., Quesada, C. A., Domingues, T. F., ... Lloyd, J. (2014). Analysing Amazonian forest productivity using a new individual and trait-based model (TFS v.1). *Geoscientific Model Development*, 7(4), 1251-1269.
- Gates, D. M. (1980). *Biophysical Ecology*. New York: Springer-Verlag.
- Hulshof, C. M., & Swenson, N. G. (2010). Variation in leaf functional trait values within and across individuals and species: an example from a Costa Rican dry forest. *Functional Ecology*, 24(1), 217-223.
- Jones, H. G. (2014). *Plants and Microclimate: A Quantitative Approach to Environmental Plant Physiology*. Cambridge: Cambridge University Press.
- Kattge, J., Diaz, S., Lavorel, S., Prentice, I. C., Leadley, P., Bonisch, G., ... Wirth, C. (2011). TRY – a global database of plant traits. *Global Change Biology*, 17(9), 2905-2935.
- Keenan, T. F., & Niinemets, Ü. (2016). Global leaf trait estimates biased due to plasticity in the shade. *Nature Plants*, 3, 16201.
- Knight, C. A., & Ackerly, D. D. (2003). Evolution and plasticity of photosynthetic thermal tolerance, specific leaf area and leaf size: congeneric species from desert and coastal environments. *New Phytologist*, 160(2), 337-347.
- Körner, C., & Diemer, M. (1987). In situ photosynthetic responses to light, temperature and carbon dioxide in herbaceous plants from low and high altitude. *Functional Ecology*, 1(3), 179-194.
- Leigh, A., Close, J. D., Ball, M. C., Siebke, K., & Nicotra, A. B. (2006). Leaf cooling curves: measuring leaf temperature in sunlight. *Functional Plant Biology*, 33(5), 515-519.
- Malhi, Y., Girardin, C. A. J., Goldsmith, G. R., Doughty, C. E., Salinas, N., Metcalfe, D. B., ... Silman, M. (2017). The variation of productivity and its allocation along a tropical elevation gradient: a whole carbon budget perspective. *New Phytologist*, 214(3), 1019-1032.
- Michaletz, S. T. (2018). Evaluating the kinetic basis of plant growth from organs to ecosystems. *New Phytologist*, 219(1), 37-44.
- Michaletz, S. T., Weiser, M. D., Zhou, J., Kaspari, M., Helliker, B. R., & Enquist, B. J. (2015). Plant thermoregulation: Energetics, trait-environment interactions, and carbon economics. *Trends in Ecology & Evolution*, 30(12), 714-724.
- Michaletz, S. T., Weiser, M. D., McDowell, N. G., Zhou, J., Kaspari, M., Helliker, B. R., & Enquist, B. J. (2016). The energetic and carbon economic origins of leaf thermoregulation. *Nature Plants*, 2, 16129.
- Monteith, J. L., & Unsworth, M. (2013). *Principles of Environmental Physics: Plants, Animals, and the Atmosphere*. New York: Academic Press.
- Pérez-Harguindeguy, N., Díaz, S., Garnier, E., Lavorel, S., Poorter, H., Jaureguiberry, P., ... Cornelissen, J. H. C. (2013). New handbook for standardised measurement of plant functional traits worldwide. *Australian Journal of Botany*, 61(3), 167-234.
- Sack, L., Melcher, P. J., Liu, W. H., Middleton, E., & Pardee, T. (2006). How strong is intracanopy leaf plasticity in temperate deciduous trees? *American Journal of Botany*, 93(6), 829-839.

- Sakschewski, B., von Bloh, W., Boit, A., Rammig, A., Kattge, J., Poorter, L., ... Thonicke, K. (2015). Leaf and stem economics spectra drive diversity of functional plant traits in a dynamic global vegetation model. *Global Change Biology*, 21(7), 2711-2725.
- Scheiter, S., Langan, L., & Higgins, S. I. (2013). Next-generation dynamic global vegetation models: learning from community ecology. *New Phytologist*, 198(3), 957-969.
- Shiklomanov, A. N., Dietze, M. C., Viskari, T., Townsend, P. A., & Serbin, S. P. (2016). Quantifying the influences of spectral resolution on uncertainty in leaf trait estimates through a Bayesian approach to RTM inversion. *Remote Sensing of Environment*, 183, 226-238.
- van Bodegom, P. M., Douma, J. C., & Verheijen, L. M. (2014). A fully traits-based approach to modeling global vegetation distribution. *Proceedings of the National Academy of Sciences USA*, 111(38), 13733-13738.
- Vogel, S. (2009). Leaves in the lowest and highest winds: temperature, force and shape. *New Phytologist*, 183(1), 13-26.
- Wang, H., Prentice, I. C., Davis, T. W., Keenan, T. F., Wright, I. J., & Peng, C. (2017). Photosynthetic responses to altitude: an explanation based on optimality principles. *New Phytologist*, 213(3), 976-982.
- Wu, J., Albert, L. P., Lopes, A. P., Restrepo-Coupe, N., Hayek, M., Wiedemann, K. T., ... Saleska, S. R. (2016). Leaf development and demography explain photosynthetic seasonality in Amazon evergreen forests. *Science*, 351(6276), 972-976.
- Wu, J., Chavana-Bryant, C., Prohaska, N., Serbin, S. P., Guan, K., Albert, L. P., ... Saleska, S. R. (2017). Convergence in relationships between leaf traits, spectra and age across diverse canopy environments and two contrasting tropical forests. *New Phytologist*, 214(3), 1033-1048.
- Wu, J., Kobayashi, H., Stark, S. C., Meng, R., Guan, K., Tran, N. N., ... Saleska, S. R. (2018). Biological processes dominate seasonality of remotely sensed canopy greenness in an Amazon evergreen forest. *New Phytologist*, 217(4), 1507-1520.
- Wullschleger, S. D., Epstein, H. E., Box, E. O., Euskirchen, E. S., Goswami, S., Iversen, C. M., ... Xu, X. (2014). Plant functional types in Earth system models: past experiences and future directions for application of dynamic vegetation models in high-latitude ecosystems. *Annals of Botany*, 114(1), 1-16.
- Yamori, W., Hikosaka, K., & Way, D. A. (2014). Temperature response of photosynthesis in C<sub>3</sub>, C<sub>4</sub>, and CAM plants: temperature acclimation and temperature adaptation. *Photosynthesis Research*, 119(1), 101-117.
- Zanoelo, E. F., Beninca, C., & Ribeiro, E. (2011). Thermophysical properties of Mate leaves: Experimental determination and theoretical effect of moisture content. *Journal of Food Process Engineering*, 34(6), 2124-2136.

**Authors:** Michaletz ST<sup>1,2,3</sup>, Blonder B<sup>4,5</sup>

**Reviewer:** Prentice IC<sup>6</sup>

## Affiliations

<sup>1</sup> Earth and Environmental Sciences Division, Los Alamos National Laboratory, Los Alamos, USA

<sup>2</sup> Biosphere 2 and Department of Ecology & Evolutionary Biology, University of Arizona, Tucson, USA

<sup>3</sup> Department of Botany and Biodiversity Research Centre, University of British Columbia, Vancouver, Canada

<sup>4</sup> Environmental Change Institute, School of Geography and the Environment, University of Oxford, Oxford, UK

<sup>5</sup> School of Life Sciences, Arizona State University, Tempe, USA

<sup>6</sup> AXA Chair Programme in Biosphere and Climate Impacts, Department of Life Sciences, Imperial College London, Ascot, UK

## 5.7 Stomatal conductance

**Authors:** Zinnert J<sup>1</sup>, Estiarte M<sup>2,3</sup>, Johnson DM<sup>4</sup>

**Reviewer:** Dickman LT<sup>5</sup>

**Measurement unit:** Mol H<sub>2</sub>O m<sup>-2</sup> s<sup>-1</sup>; **Measurement scale:** leaf; **Equipment costs:** €€–€€€; **Running costs:** €; **Installation effort:** low; **Maintenance effort:** low; **Knowledge need:** medium; **Measurement mode:** manual or data logger

Stomatal conductance is a calculation of the influence of stomatal opening on rate of diffusion of CO<sub>2</sub> entering or water vapour exiting through the stomata of a leaf. Stomata are an important regulatory point for water movement through the soil–plant–air-continuum (van den Honert, 1948) through varying the diffusion resistance. The conductance of water vapour (i.e. inverse of the diffusion resistance) expresses the regulatory control exerted by stomata through the degree of stomatal opening (Pearcy et al., 1989). Environmental signals such as incident light intensity, CO<sub>2</sub> concentration, water availability, vapour pressure deficit (VPD), and leaf temperature affect stomatal aperture (Farquhar et al., 1980). Under favourable conditions of low evaporative demand and high light, maximum stomatal conductance determines the upper limit of CO<sub>2</sub> assimilation in a leaf. The ability of a plant to regulate stomatal opening in response to environmental conditions enables it to modulate the rate of transpiration while maintaining carbon uptake (Cowan 1977, Farquhar et al. 1980). Stomatal closure is considered to be the earliest response to drought (Flexas & Medrano, 2002) and other environmental stressors, and is a limitation to photosynthesis. However, dependence of leaf temperature on stomatal conductance occurs through leaf transpiration. Plants must balance lowering stomatal conductance to conserve water with preventing extreme leaf temperatures which affect metabolic rates and physiological processes (De Boeck et al., 2016). As such, stomatal conductance is an important parameter especially in climate-change studies and in process-based models that can be used to predict species responses to climate change (Sperry & Love, 2015; Tai et al., 2018). Stomatal conductance influences both photosynthesis and transpiration, exerting major control on carbon and water cycling, and energy exchange from leaf to landscape level as well as between the Earth's surface and atmosphere. Because stomata control the rate of water loss in vegetated areas, they affect atmospheric moisture levels and surface temperature. Stomatal conductance is a clearly defined variable that is easily measured for model parameterisation and has substantial biological relevance (Buckley & Mott, 2013). Maximum stomatal conductance is also a function of stomatal density and size (Drake et al., 2013), which vary due to genetic factors or environmental conditions during growth (Bertolino et al., 2019). Stomatal density measurements may, thus, complement conductance measurements to compare species and when treatments can affect leaf development.

### 5.7.1 What and how to measure?

Diffusion porometers and infrared gas analysers (IRGAs) are the most widely used instruments for quantitatively measuring stomatal conductance and can be used either in the field or laboratory (Bell & Squire, 1981; Kirkham, 2005). These measure the diffusion of water vapour from inside the leaf through the stomata.

### ***Gold standard***

Recent IRGAs measure the difference in water vapour concentration between a reference IRGA and sample IRGA as air flows through a chamber that is clamped to the leaf surface. Leaf temperature is measured with a thermocouple held in the bottom of the chamber, minimising error in temperature measurements. To calculate stomatal conductance, transpiration and total conductance are used. Transpiration is a function of the air flow rate, reference and sample water vapour, and leaf area. The total conductance to water vapour includes both stomatal conductance and the boundary layer. The boundary layer is negligible due to air flow through the chamber, thus caution should be used when reporting transpiration, especially in species with large leaves (Meinzer et al., 1995). Total conductance is a function of transpiration and water vapour concentration within the leaf. Temperature is used to estimate the water vapour concentration within the leaf. Stomatal conductance is calculated from total conductance by removing the contribution of the boundary layer. The boundary layer conductance depends on whether the leaf has stomata on one or both sides, thus it is important to accurately input the stomatal ratio (i.e. fraction of stomata on one side of the leaf to the other) before taking measurements (see below *Installation, field operation, maintenance and interpretation*).

### ***Bronze standard***

Steady-state porometers are typically less expensive and even more lightweight and portable than most IRGAs. They measure the water vapour flux and gradient near a leaf. A chamber is clamped to the leaf surface and the vapour pressure at two different fixed locations in the diffusion path is measured. Leaf temperature is measured with infrared thermometers or a thermocouple held in the bottom of the leaf chamber. Stomatal conductance is calculated from the vapour pressure measurements, the known conductance of the diffusion path, and temperature. Steady-state diffusion porometers are calibrated directly against relative humidity. However, any error in the humidity sensor will result in stomatal conductance calculation errors. At relative humidity of 50%, these errors are low, but rise dramatically above 80% relative humidity (Pearcy et al., 1989).

### ***Installation, field operation, maintenance, interpretation***

Instructions are provided for taking measurements with an IRGA. Set-up and calibration may differ based on the instrument used and should follow the manual. These instructions assume the IRGA has been properly calibrated. Once the system is ready, the basic procedure for taking measurements is simple. Set the desired environmental conditions within the chamber. Depending on the question, these may follow ambient conditions or may have pre-determined values. Flow rate is typically fixed to 500  $\mu\text{mol s}^{-1}$  but may be adjusted if desired. Light level may be modified if using an LED source attached to the chamber (ambient is a good value to start with as it will not be an abrupt change for the leaf). If an LED source is not used, orientate the chamber so that shading of the leaf by the chamber walls does not occur. In direct sun, the leaf fan can be used to control the temperature. Humidity and  $\text{CO}_2$  interact with the sample cell  $\text{CO}_2$ . Due to the relationship between stomatal conductance and  $\text{CO}_2$  assimilation, having stable values of  $\text{H}_2\text{O}$  and  $\text{CO}_2$  are important in obtaining

reliable measurements. The desiccant setting controls the humidity within the chamber from ambient down to zero. Drierite (drying agent) is used as the desiccant and should be adjusted according to required conditions. Humidity within the chamber is a balance between water vapour coming from the leaf and air flow rate. Desiccant set to zero will result in a large vapour pressure deficit at the leaf surface and may affect stomatal conductance. Controlling CO<sub>2</sub> with a CO<sub>2</sub> mixer provides more accurate and easily obtained measurements. CO<sub>2</sub> is typically adjusted to ambient levels and soda lime is used to scrub ambient CO<sub>2</sub>. The soda lime-scrub setting controls reference CO<sub>2</sub> from ambient down to zero and can be adjusted accordingly if not using a CO<sub>2</sub> mixer. Insert the leaf into the chamber and close it. Check the latch to ensure a good seal. Check to ensure that the proper leaf area has been set based on the area exposed inside the chamber. On some IRGAs you may be able to adjust stomatal ratio (i.e. estimate of the ratio of stomata on one side of the leaf to the other). Use 1 if stomatal density on the top and bottom are equal, use 0 if stomata are only present on one side, and use 0.5 if you are not sure. Because the calculation of stomatal conductance includes stomatal ratio, incorrect values will yield measurement errors. Observe the CO<sub>2</sub> and H<sub>2</sub>O concentrations for the reference and the sample and ensure that they have stabilised. CO<sub>2</sub> concentrations of the sample should stabilise within 30 seconds of clamping onto the leaf and should be lower than the reference CO<sub>2</sub> under conditions where photosynthesis exceeds respiration. Record the value for stomatal conductance and depending on your experiment, proceed to the next leaf.

### **Where to start**

Bell & Squire (1981), Drake et al. (2013), Flexas & Medrano (2002), Kirkham (2005), Pearcy et al. (1989)

### **5.7.2 Special cases, emerging issues, and challenges**

#### **Timing**

Stomatal conductance is highly dynamic on a diurnal basis as well as throughout the growing season requiring frequent measurements in time and space to thoroughly assess conductance relative to temporal shifts in environmental parameters. Minimum steady-state stomatal conductance ( $g_{min}$ ) occurs in the morning prior to light exposure (Drake et al., 2013). Maximum stomatal opening generally occurs in the early portion of the day, so measurements comparing stomatal conductance of different species or under different treatment conditions are typically taken mid to late morning (~8:00 to 10:00 a.m. depending on species and site). Timing may differ based on site location and environmental conditions such as temperature, vapour pressure, soil water availability, and so on.

#### **Selection of leaves**

Measurements are most commonly made on fully exposed sun leaves of whole plants. Because stomatal development depends on leaf age, care should be taken to standardise measurements across species and treatments, typically on mature leaves. With diffusion and steady-state porometers, ambient light conditions should also be standardised, preferably using light-saturated canopy leaves. Measurements with IRGAs allow for adjustment of PAR, and are commonly set with

either ambient PAR values or saturating PAR ( $\geq 1500 \mu\text{mol m}^{-2} \text{s}^{-1}$  for most species) depending on the question of interest. With porometers that do not enclose the whole leaf, measurements are most commonly taken from the abaxial leaf surface where stomatal density is highest (Meidner & Mansfield, 1968), but stomata may occur on both sides of the leaf, depending on species (Smith et al., 1997) and this should be taken into consideration when taking measurements. It is not recommended to detach leaves for stomatal conductance measurements on angiosperms as this can cause stomata to close; however, conifers can be detached and measured within 20 mins. In the lab, it is ideal to take stomatal conductance measurements under saturating light conditions.

### ***Measurement conditions***

The boundary layer is a thin layer of still air around all surfaces. The thickness of the boundary layer above and below the leaf surface affects diffusion of gas and water vapour through the stomata and is determined by surface roughness, leaf characteristic dimension (i.e. leaf thickness in the direction of the wind), and wind speed. A leaf with high pubescence is rougher than one with a smooth waxy cuticle and will have a thicker boundary layer. Increased wind speed results in a thinner boundary layer. Most instruments for calculating stomatal conductance pass air through the chamber, thus removing any resistance from the boundary layer. Measurements should not be taken on windy days when the boundary air layer is thinner as evaporative demand is higher, potentially reducing stomatal conductance. Likewise, since the calculation for stomatal conductance uses a water vapour gradient, measurements should not be taken on wet leaves. Instead, wet leaves should be gently blotted with tissue paper to remove any surface moisture prior to measurement.

Stomatal response curves are becoming more common in the literature, particularly the response of stomata to increasing VPD (Woodruff et al., 2010; Ocheltree et al., 2014). This requires an instrument that allows for precise control over VPD in the sample chamber (e.g. LI-COR LI-6800, PP Systems CIRAS-3).

Stomata play a critical role in controlling both water loss and CO<sub>2</sub> uptake, thus modelling stomatal conductance under various environmental conditions is of interest in many disciplines. Damour et al. (2010), Buckley & Mott (2013), and Buckley (2017) review in depth many of the available stomatal conductance models. Models of stomatal conductance occur at multiple spatial levels, from subcellular to Earth system processes. Empirical models were the first developed and were used to account for stomatal responses to light intensity, VPD, air temperature, CO<sub>2</sub> concentration, and leaf water potential (e.g. Jarvis, 1976; more models reviewed in Damour et al., 2010). Numerous models have been developed based on the relationship between stomatal conductance (gs) and net photosynthetic rate (A<sub>net</sub>). The empirical Ball-Berry stomatal conductance model (Ball et al., 1987) is one of the most commonly used models and is often used in land surface climate models to simulate regulation of evapotranspiration (Bonan et al., 2014). Empirical models are often simpler and used in larger canopy or global level processes (Buckley & Mott, 2013). With a better understanding of plant physiology, mechanistic or process-based models have been proposed. Mechanistic models tend to be mathematically complex and are often used in investigating cellular and subcellular processes in environmental sensing (Buckley & Mott, 2013). Mechanistic models include stomatal response to abscisic acid (ABA; e.g. Davies & Zhang, 1991; Tardieu & Simonneau, 1998), transpiration that includes hydraulic architecture (e.g. Tyree & Sperry, 1988), and predictions of photosynthesis under

fluctuating conditions (reviewed in Buckley & Mott, 2013). Currently, most stomatal conductance models are adapted for well-watered conditions and do not sufficiently account for multiple environmental influences, especially drought conditions (Damour et al., 2010; Bonan et al., 2014).

### **Stomatal density**

Stomatal density refers to the number of stomata per area of leaf and is related to stomatal conductance and thus the CO<sub>2</sub> and water fluxes through plants. Stomatal density can provide additional information as to differences in conductance among plants. Stomatal density can be made through impressions of adaxial and/or abaxial epidermis of a leaf using cyanoacrylate adhesive (Wilson, Pusey and Otto, 1981). A microscope slide is immediately pressed against the glue and held firmly for 90 sec. The slide is then gently peeled away from the skin. With this technique, a sheet of the outermost two to three layers of cells adheres to the slide. Clear nailpolish can also be used by painting onto the leaf surface and peeling away after it has dried. Features of the epidermis, including individual cells, stomata and trichomes are visible at most magnifications with these methods. Impressions can be examined with a light microscope. Stomata are counted in a known field of view to calculate stomatal density. Epidermal cells can also be calculated and used with stomata to calculate a stomatal index as  $[s/(e+s)] \times 100$ , where s is number of stomata and e is number of epidermal cells (Salisbury, 1928).

### **5.7.3 References**

#### **Theory, significance, and large datasets**

Buckley & Mott (2013), Cowan (1977), Farquhar et al. (1980), Pearcy et al. (1989), van den Honert (1948)

#### **More on methods and existing protocols**

Buckley (2017), Buckley & Mott (2013), Kirkham (2005), Pearcy et al. (1989), Tardieu & Simonneau (1998)

#### **All references**

Ball J. T., Woodrow, I. E., & Berry, J. A. (1987). A model predicting stomatal conductance and its contribution to the control of photosynthesis under different environmental conditions. In J. Biggens (Ed.), *Progress in Photosynthesis Research* (pp. 221-224). Netherlands: Martinus Nijhoff Publishers.

Bell, C. J., & Squire, G. R. (1981). Comparative measurements with two water vapour diffusion porometers (dynamic and steady-state). *Journal of Experimental Botany*, 32(131), 1143-1156.

Bertolini, L.T., Caine, R. S., & Gray, J.E. (2019). Impact of stomatal density and morphology on water-use efficiency in a changing world. *Frontiers in Plant Science*, 10, 225.

- Bonan, G. B., Wiliams, M., Fisher, R. A., & Oleson, K. W. (2014). Modeling stomatal conductance in the earth system: linking leaf water-use efficiency and water transport along the soil–plant–atmosphere continuum. *Geoscientific Model Development*, 7, 2193-2222.
- Buckley, T. N. (2017). Modeling stomatal conductance. *Plant Physiology*, 174, 572-582.
- Buckley, T. N., & Mott, K. A. (2013). Modelling stomatal conductance in response to environmental factors. *Plant, Cell, & Environment*, 36(9), 1691-1699.
- Cowan, I. R. (1977). Stomatal behavior and environment. *Advances in Botanical Research*, 4, 117-228.
- Damour, G., Simonneau, T., Cochard, H., & Urban, L. (2010). An overview of models of stomatal conductance at the leaf level. *Plant, Cell, & Environment*, 33, 1419-1438.
- Davies, W. J., & Zhang, J. H. (1991). Root signals and the regulation of growth and development of plants in drying soil. *Annual Review of Plant Physiology and Plant Molecular Biology*, 42, 55-76.
- De Boeck, H. J., van de Velde, H., de Groote, T., & Nijs, I. (2016). Ideas and perspectives: heat stress: more than hot air. *Biogeosciences*, 13(20), 5821-5825.
- Drake, P. L., Froend, R. H., & Franks, P. J. (2013). Smaller, faster stomata: scaling of stomatal size, rate of response, and stomatal conductance. *Journal of Experimental Botany*, 64(2), 495-505.
- Farquhar, G.D., von Caemmerer, S., & Berry, J.A. (1980). A biochemical model of photosynthetic CO<sub>2</sub> assimilation in leaves of C<sub>3</sub> species. *Planta*, 149(1), 78-90.
- Flexas, J., & Medrano, H. (2002). Drought-inhibition of photosynthesis in C<sub>3</sub> plant: stomatal and non-stomatal limitations revisited. *Annals of Botany*, 89(2), 183-189.
- Jarvis, P. G. (1976). The interpretation of the variations in leaf water potential and stomatal conductance found in canopies in the field. *Philosophical Transactions of the Royal Society of London Series B*, 273, 593-610.
- Kirkham, M. B. (2005). Stomata and measurement of stomatal resistance In *Principles of Soil and Plant Water Relations*. (pp. 379-401). Cambridge, MA: Academic Press.
- Meidner, H., & Mansfield, T. A. (1968). *Physiology of Stomata*. New York: McGraw-Hill.
- Meinzer, F. C., Goldstein, G., Jackson, P., Holbrook, N. M., Gutierrez, M. V., & Cavelier, J. (1995). Environmental and physiological regulation of transpiration in tropical forest gap species: the influence of boundary layer and hydraulic properties. *Oecologia*, 101(4), 514-522.
- Ocheltree, T. W., Nippert, J. B., & Prasad, P. V. V. (2014). Stomatal responses to changes in vapor pressure deficit reflect tissue-specific differences in hydraulic conductance. *Plant, Cell & Environment*, 37(1), 132-139.
- Pearcy, R. W., Schulze, E.-D., & Zimmerman, R. (1989). Measurement of transpiration and leaf conductance. In R. W. Pearcy, J. Ehleringer, H. A. Mooney, & P. W. Rundel (Eds.), *Plant Physiological Ecology: Field Methods and Instrumentation* (pp. 137-160). New York: Chapman and Hall.
- Salisbury, E. J. (1928). On the causes and ecological significance of stomatal frequency, with special reference to the woodland flora. *Philosophical Transactions of the Royal Society of London*, B216(431-439), 1-65.

- Smith, W. K., Vogelmann, T. C., DeLucia, E. H., Bell, D. T., & Shepherd, K. A. (1997). Leaf form and photosynthesis. *Bioscience*, 47(11), 785-793.
- Sperry, J. S. & Love, D. M. (2015). What plant hydraulics can tell us about responses to climate-change droughts. *New Phytologist*, 207(1), 14-27.
- Tai, X., Mackay, D. S., Sperry, J. S., Brooks, P., Anderegg, W. R., Flanagan, L. B., ... Hopkinson, C. (2018). Distributed plant hydraulic and hydrological modeling to understand the susceptibility of riparian woodland trees to drought-induced mortality. *Water Resources Research*, 54(7), 4901-4915.
- Tardieu, F. & Simonneau, T. (1998). Variability among species of stomatal control under fluctuating soil water status and evaporative demand: modelling isohydric and anisohydric behaviours. *Journal of Experimental Botany*, 49, 419-432.
- Tyree, M. T. & Sperry, J. S. (1988). Do woody plants operate near the point of catastrophic xylem dysfunction caused by dynamic water stress? *Plant Physiology*, 88, 574-580.
- van der Honert, T. H. (1948). Water transport in plants as a catenary process. *Discussions of the Faraday Society*, 3, 146-153.
- Wilson, C. K. L., Pusey, P. L. & Otto, B. E. (1981). Plant epidermal sections and imprints using cyanoacrylate adhesives. *Canadian Journal of Plant Science*, 61(3), 781-783.
- Woodruff, D. R., Meinzer, F. C., & McCulloh, K. A. (2010). Height-related trends in stomatal sensitivity to leaf-to-air vapour pressure deficit in a tall conifer. *Journal of Experimental Botany*, 61(1), 203-210.

**Authors:** Zinnert J<sup>1</sup>, Estiarte M<sup>2,3</sup>, Johnson DM<sup>4</sup>

**Reviewer:** Dickman LT<sup>5</sup>

## Affiliations

<sup>1</sup> Department of Biology, Virginia Commonwealth University, Richmond, USA

<sup>2</sup> CSIC, Global Ecology Unit CREAF-CSIC-UAB, Bellaterra, Spain

<sup>3</sup> CREAF, Cerdanyola del Vallès, Spain

<sup>4</sup> Warnell School of Forestry and Natural Resources, University of Georgia, Athens, USA

<sup>5</sup> Earth and Environmental Sciences Division, Los Alamos National Laboratory, Los Alamos, USA

## 5.8 Psychrometry for water potential measurements

**Authors:** Miller ML<sup>1</sup>, Estiarte E<sup>2,3</sup>, Johnson DM<sup>4</sup>, Zinnert J<sup>5</sup>

**Reviewer:** Meinzer F<sup>6</sup>

**Measurement unit:** MPa; **Measurement scale:** single leaf or stem segment, soil sample; **Equipment costs:** €€; **Running costs:** €; **Installation effort:** medium; **Maintenance effort:** medium; **Knowledge need:** medium; **Measurement mode:** data logger

Water potential, at its most basic, is a measure of the chemical potential of water within a system as compared to that of pure water (assumed to be 0 MPa at ~ 25 °C) (Tyree & Zimmermann, 2002; Lambers et al., 2008). Plant water potential ( $\Psi_w$ ) has four components: osmotic ( $\Psi_\pi$ ), matric ( $\Psi_m$ ), hydrostatic pressure ( $\Psi_p$ ), and gravitational ( $\Psi_g$ ) potential (Campbell & Norman, 1998). Matric potential is typically the major component of soil water potential, but it is often ignored in relation to plant material. Likewise, the gravitational component (0.01 MPa m<sup>-1</sup>) is only significant in very tall plant species. Thus, overall plant water potential is generally considered to be  $\Psi_w = \Psi_\pi + \Psi_p$  (Tyree & Zimmermann, 2002; Lambers et al., 2008). Water movement along the soil–plant–atmosphere continuum occurs from compartments of higher to lower  $\Psi_w$  (less negative to more negative). In living plant tissues,  $\Psi_p$  is the turgor pressure, whereas in the xylem conduits  $\Psi_\pi$  is usually negligible and  $\Psi_p$  is zero or negative. The ability to accurately measure plant tissue-specific  $\Psi_w$  in conjunction with other plant physiological properties such as gas exchange or hydraulic conductivity, allows for the evaluation of species' capacities to function across different ecotones, extreme climate events, and even permits predictions of drought tolerance. Measurements of water potential can prove useful whenever the cycling of water is affected. This is the case in most climate-change studies, but also in studies into effects of other global changes that could alter the water balance, including biodiversity loss or eutrophication.

### 5.8.1 What and how to measure?

The Scholander-style pressure chamber (PMS Instrument Company) or “pressure bomb” is a standard water potential measurement tool used extensively in plant research (Scholander et al., 1965). However, this approach is limited by the type and size of the plant sample. Water potential measurements on blocks or sections of wood, small tissue samples, or non-woody tissues (i.e. individual small leaves) require an alternative methodology. Thermocouple psychrometry provides a reliable alternative to the pressure bomb.

For thermocouple psychrometry-based water potential measurements of plant tissue, a sample is typically encased in a sealable chamber containing a sample and a reference thermocouple junction. The most common type of thermocouple psychrometer relies on the Peltier effect, whereby an electrical current is briefly passed through the sample thermocouple junction, cooling it below the dew-point temperature of the air in the chamber, causing condensation on the junction (Spanner, 1951). Evaporation of the condensed water upon cessation of cooling creates a temperature depression of the sample junction in comparison to the dry reference junction. This temperature depression and the resulting voltage output (μV) are primarily dependent on the relative humidity

inside the chamber. The voltage output can be converted to water potential (MPa) based on the known relationship between vapour pressure (i.e. relative humidity) and water potential in a closed system at a stable temperature. Thus, the water potential of the plant or soil sample is inferred from vapour pressure that is at equilibrium with the sample (Boyer, 1995; Andraski & Scanlon, 2002). Psychrometer chambers are typically connected to a datalogger programmed to provide a specific magnitude and duration of cooling current and to record subsequent microvolt outputs after cooling. A stable thermal environment during psychrometric measurements is crucial because of the exceptionally small temperature differentials and output voltages generated during measurements. Psychrometers have been used for decades to monitor plant and soil water status and the theory behind their operation is discussed extensively in the literature (e.g. Brown & Haveren, 1972; Brown & Bartos, 1982; Boyer, 1995; Marigo & Peltier, 1996; Andraski & Scanlon, 2002; Nobel 2009; Kirkham, 2014).

Prior to use, each thermocouple psychrometer is calibrated against a known set of salt solutions (see below *5.8.2 Special cases, emerging issues, and challenges*). The thermocouple psychrometers, such as those provided by JRD Merrill Specialty Equipment, are enclosed along with a plant or soil sample, in a stainless-steel chamber (e.g. part 81-500) and then placed into an isothermal environment for equilibration. During equilibration, the datalogger, programmed to convert  $\mu\text{V}$  to MPa, takes subsequent measurements at regular intervals (30 minutes to one hour) until the vapour pressure in the chamber equilibrates to the enclosed plant sample. Equilibration can be somewhat arbitrary, but can often take four or more hours and can generally be assumed when two to three subsequent measurements indicate unchanging MPa. The psychrometer-specific calibration factor (see below) is then applied to the datalogger output by the user for a final water potential. Depending on the datalogger manufacturer (see below), calculation of the output water potential from the raw data may be customisable or proprietary. Discussions regarding interpretation can be found in Brown & Bartos (1982) and Andraski & Scanlon (2002).

### **Where to start**

Amado & Blanco (2004), Andraski & Scanlon (2002), Brown & Bartos (1982), Brown & Haveren (1972), Bulut & Leong (2008)

## **5.8.2 Special cases, emerging issues, and challenges**

### **System variants**

Currently, Campbell Scientific CR6 and CR7 (legacy) dataloggers are commonly used instruments for use with the barrel-style, screen-caged, or end-screen style Peltier psychrometers. The CR6 combined with a multiplexer can support up to 32 individual sensors. The program used with the CR6 is highly modifiable to suit individual needs and the conversion from microvolt ( $\mu\text{V}$ ) output to water potential ( $\Psi_w$ ), based on Brown & Bartos (1982), is included in the programming. An alternative system, the PsyPro, provides a more user-friendly interface, but is limited in the number of simultaneous measurements (8 sensors) and is not as customisable (see Bulut & Leong 2008, for a more thorough discussion of the pros and cons of the PsyPro and the CR7). Additionally, the PsyPro's conversion from  $\mu\text{V}$  to  $\Psi_w$  is proprietary. Regardless of datalogger used, sensors need to be

calibrated by the user due to minute differences during thermocouple construction, differences between manufacturers, and sensor drift. Brown & Bartos (1982) and Reece (1996) suggest that sensors can be calibrated in batches, where one calibration factor is applied to a subset of all psychrometers. In this configuration, thermocouple psychrometer sensors can be purchased with either a Viking-style connector for easy plug and play connections to dataloggers such as the PsyPro, or without connectors (four-wired) for wiring into Campbell Scientific-style dataloggers. If the psychrometers need to be used with both styles of systems, pigtails can be purchased with the Viking-style connector on one end and 4-wires on the other end, allowing psychrometers purchased with Viking connectors to be used in Campbell Scientific dataloggers.

*In situ* psychrometric measurements are also possible. For example, ICT International manufactures stem and leaf specific psychrometers and associated dataloggers are designed for application on live (unexcised) plant tissue in field conditions. Additionally, psychrometry can be used for long-term soil monitoring (Andraski & Scanlon, 2002). For soil monitoring, caged-screen or ceramic-bulb sensors are typically inserted directly into the soil rather than enclosing a disturbed soil sample with the thermocouple in a chamber as previously described.

### **Calibration**

Prior to use, psychrometers, regardless of type or manufacturer, must be calibrated for maximum accuracy. Calibration for the psychrometers is typically performed with a range of known concentrations of salt solutions (KCl or NaCl) with known osmotic potentials ( $\Psi_\pi$ ) at a given temperature, though care must be taken when mixing solutions regarding molality or osmolality (Tyree & Zimmermann, 2002; Nobel, 2009). While there is no specific recommended number of solutions used or the frequency of calibration, 4–6 solutions are commonly used (Brown & Bartos, 1982; Andraski & Scanlon 2002; Bulut & Leong, 2008). More variability in output has been shown for more negative water potentials and decreased resolution has been illustrated at very high water potentials (near zero), so solutions can be tailored to the expected range of use: a reliable range of psychrometric readings is generally considered to be -0.3 to -7.0 or -8.0 MPa (Andraski & Scanlon 2002; Scanlon et al., 2002; Bulut & Leong 2008). Water potential equivalents for KCl and NaCl can be found throughout the literature including Lang (1967), Brown & Bartos (1982), Bulut & Leong (2008). Water potential can also be calculated based on van't Hoff's equation and empirical measurements of the activity coefficients of the respective solution (e.g. Amado & Blanco, 2004). Results of the calibration solutions can be plotted as estimated  $\Psi_w$  (based on published values per salt solution) as a function of either  $\mu V$  or measured  $\Psi_w$ , although using  $\mu V$  can be confusing and is best used for troubleshooting purposes only. The resulting linear regression is the psychrometer-specific calibration factor (see Andraski & Scanlon, 2002 for discussion).

The general procedure for calibration is to place a disc of filter paper inside the psychrometer chamber lid or a strip of filter paper around the internal chamber and saturate the disc with a constant volume of salt solution. The psychrometer is then sealed, double bagged in large "ziploc" style 3.75 or 7.5 L bags and placed into a water bath. The sensors are then allowed to equilibrate, where the water potential of the vapour in the chamber equals the water potential (osmotic potential) of the salt solution – generally 30 minutes to 4–6 h is required depending on the

concentration of the salt solution and the chamber size. Equilibration is assumed with at least three subsequent consistent measurements.

Psychrometry chambers require regular calibration at a set temperature, and whatever temperature is used for calibration must also be used for sample measurements. The temperature of the water bath is up to the end user, but some practical considerations are advised. For instance, if the water bath is 21 °C, then the temperature control will need to be wired for both heating and cooling. However, if 25 °C is selected, then only the immersion heater will likely be necessary if operated indoors. Additionally, Brown & Bartos (1982) found that 25 °C provided the lowest variability (as compared to 15 and 35 °C) and many of the above references published water potential equivalents of the calibration solutions at 25 °C.

### ***Environments***

While, traditionally, calibration occurs in a temperature-controlled water bath (Brown & Bartos, 1982), an adequate thermal environment can be created in myriad ways. An insulated, non-temperature controlled water bath in a lab environment with relatively stable temperatures provides an adequate psychrometer environment (Andraski & Scanlon, 2002). Lacking ideal thermally-controlled lab settings, an isothermal environment can be created with a modified cooler or high-density Styrofoam with heating and/or cooling and circulation capabilities (e.g. see description in ICT International's Stem Psychrometer Manual, Ch. 16, <http://www.ictinternational.com/support/product-manuals/>). Isothermal conditions cannot be achieved for aboveground and shallow soil *in situ* sensors, but rapid temperature fluctuations can be minimised by insulating foam and reflective covering for aboveground sensors, and orientation of sensors in shallow soils may minimise temperature gradients (Andraski & Scanlon, 2002). Rawlins & Dalton (1967) have illustrated that major impacts of temperature fluctuations in soil can be largely eliminated.

### ***Comparing psychrometry results to pressure bomb results***

Caution should be exercised in comparing measurements of plant water potential made with psychrometers and the pressure chamber. Although measurements made with the two techniques are often in good agreement, notable discrepancies can occur under certain conditions (e.g. Boyer, 1967; Turner et al., 1984). The presence of native apoplastic solutes is undetectable in pressure chamber measurements, but the influence of these solutes on tissue water potential would be detected in psychrometric measurements. Other sources of discrepancies between the two techniques include an increase in sample turgor, and therefore water potential in the psychrometer chamber resulting from cellular uptake of solutes released from damaged cells, and production of respiratory water during equilibration of tissue in the psychrometer chamber.

### ***Challenges***

Contaminants, including skin oils and residue from evaporated liquids can render measurements unusable. When changing salt solutions or plant samples, all surfaces within the chamber must be cleaned thoroughly to remove contaminates such as particles, plant residues (i.e. sap), and

evaporative residues. Additionally, the thermocouple junctions need to be cleaned regularly according to manufacturer's specifications and subsequently recalibrated. In practice, accurate sensor calibrations and a stable temperature environment are key to accurate psychrometric measurements because the sensor outputs can be highly influenced by temperature gradients.

### 5.8.3 References

#### ***Theory, significance, and large datasets***

Campbell & Gardner (1971), Kirkham (2014), Nobel (2009), Scanlon et al. (2002), Spanner (1951)

#### ***More on methods and existing protocols***

Lang (1967), Lüttege & Nobel (1984), Marigo & Peltier (1996), Schaefer et al. (1986), Touchette (2006)

#### ***All references***

- Amado, E., & Blanco, L. H. (2004). Osmotic and activity coefficients of aqueous solutions of KCl at temperatures of 283.15, 288.15, 293.15 and 298.15 K: A new isopiestic apparatus. *Fluid Phase Equilibria*, 226, 261-265.
- Andraski, B. J., & Scanlon, B. R. (2002). Thermocouple psychrometry. In J. H. Dan, & C. G. Topp (Eds.), *Methods of Soil Analysis: Part 4*. Madison: Soil Science Society of America.
- Boyer, J. S. (1967). Leaf water potentials measured with a pressure chamber. *Plant Physiology*, 42(1), 133-137.
- Boyer, J. S. (1995). *Measuring the Water Status of Plants and Soils*. San Diego: Academic Press.
- Brown R. W., & Bartos D. L. (1982). A calibration model for screen-caged Peltier thermocouple psychrometers. Research Paper INT-293 USDA Forest Service Intermountain Forest and Range Experiment Station.
- Brown, R. W., & Haveren, B. P. V. (1972). Psychrometry in water relations research. In Symposium on Thermocouple Psychrometers (1971: Utah State University). Agricultural Experiment Station.
- Bulut R., & Leong E. C. (2008). Indirect measurement of suction. *Geotechnical and Geological Engineering*, 26, 633-644.
- Campbell, G. S., & Gardner, W. H. (1971). Psychrometric measurements of soil water potential: temperature and bulk density effects. *Soil Science Society of America Proceedings*, 35, 8-12.
- Campbell, G. S., & Norman, J. M. (1998). *An Introduction to Environmental Biophysics* (2nd ed.). New York: Springer Science & Business Media.
- Kirkham, M. B. (2014). Thermocouple psychrometers. In *Principles of Soil and Plant Water Relations* (2<sup>nd</sup> ed., pp. 311-332). Waltham: Elsevier.
- Lambers, H., Chapin, F. S., & Pons, T. L. (2008). *Plant Physiological Ecology* (2<sup>nd</sup> ed.) New York: Springer.

- Lang, A. R. G. (1967). Osmotic coefficients and water potentials of sodium chloride solutions from 0 to 40°C. *Australian Journal of Chemistry*, 20(9), 2017-2023.
- Lüttge, U., & Nobel, P. S. (1984). Day-night variations in malate concentration, osmotic pressure, and hydrostatic pressure in *Cereus validus*. *Plant Physiology*, 75(3), 804-807.
- Marigo G., & Peltier J. P. (1996). Analysis of the diurnal change in osmotic potential in leaves of *Fraxinus excelsior* L. *Journal of Experimental Botany*, 47(299), 763-769.
- Nobel, P. S. (2009). *Physicochemical and Environmental Plant Physiology* (4<sup>th</sup> ed.). Oxford: Academic Press.
- Rawlins, S. L., & Dalton, F. N. (1967). Psychrometric measurement of soil water potential without precise temperature control. *Soil Science Society of America Journal*, 31(3), 297-301.
- Reece, C. F. (1996). Evaluation of a line heat dissipation sensor for measuring soil matric potential. *Soil Science Society of America Journal*, 60(4), 1022-1028.
- Scanlon, B. R., Andraski, B. J., & Bilskie J. (2002). Miscellaneous methods for measuring matric or water potential. In J. H. Dane, & C. G. Topp (Eds.), *Methods of Soil Analysis: Part 4* (pp. 643-670). Madison: Soil Science Society of America.
- Schaefer, N. L., Trickett, E. S., Ceresa, A., & Barrs, H. D. (1986). Continuous monitoring of plant water potential. *Plant Physiology*, 81(1), 45-49.
- Scholander, P. F., Bradstreet, E. D., Hemmingsen, E. A., & Hammel, H. T. (1965). Sap pressure in vascular plants: negative hydrostatic pressure can be measured in plants. *Science*, 148(3668), 339-346.
- Spanner, D. C. (1951). The Peltier effect and its use in the measurement of suction pressure. *Journal of Experimental Botany*, 2(5), 145-168.
- Touchette, B. W. (2006). Salt tolerance in a *Juncus roemerianus* brackish marsh: spatial variations in plant water relations. *Journal of Experimental Marine Biology and Ecology*, 337(1), 1-12.
- Turner, N. C., Spurway, R. A., & Schulze, E. D. (1984). Comparison of water potentials measured by in situ psychrometry and pressure chamber in morphologically different species. *Plant Physiology*, 74(2), 316-319.
- Tyree, M. T., & Zimmermann, M. H. (2002). *Xylem Structure and the Ascent of Sap* (2<sup>nd</sup> ed.). Berlin: Springer

**Authors:** Miller ML<sup>1</sup>, Estiarte E<sup>2,3</sup>, Johnson DM<sup>4</sup>, Zinnert J<sup>5</sup>

**Reviewer:** Meinzer F<sup>6</sup>

## Affiliations

<sup>1</sup> University of Idaho, College of Natural Resources, Moscow, USA

<sup>2</sup> CSIC, Global Ecology Unit CREAF-CSIC-UAB, Bellaterra, Spain

<sup>3</sup> CREAF, Cerdanyola del Vallès, Spain

<sup>4</sup> Warnell School of Forestry and Natural Resources, University of Georgia, Athens, USA

<sup>5</sup> Department of Biology, Virginia Commonwealth University, Richmond, USA

<sup>6</sup> Pacific Northwest Research Station, USDA Forest Service, Corvallis, USA

## 5.9 Pressure-volume curve – TLP, $\epsilon$ , $\Psi_0$

**Authors:** Zinnert J<sup>1</sup>, Wood LK<sup>1</sup>, Johnson DM<sup>2</sup>, Estiarte<sup>3,4</sup>

**Reviewer:** Dickman LT<sup>5</sup>

**Measurement unit: MPa; Measurement scale: leaf or stem; Equipment costs: €€; Running costs: €;**  
**Installation effort: medium; Maintenance effort: low; Knowledge need: medium; Measurement mode: manual**

Plant water relations are important in the maintenance of turgor and control the hydration of cells for proper physiological functioning, especially during periods of drought. As plants lose turgor, there is a decline in critical physiological functions such as cell expansion and photosynthesis. Water potential is an indicator of plant water status and is made up of both osmotic and turgor potential. Pressure volume curves describe the relationship between bulk water potential ( $\Psi_w$ , movement driven by a pressure gradient) and relative water content (RWC) through iterative measurements of a drying leaf. From the mass and water potential measurements several important parameters can be derived: turgor loss point (TLP), bulk modulus of elasticity ( $\epsilon$ ), and osmotic potential ( $\Psi_0$ ). TLP indicates the point at which the turgor pressure in cells is zero and can be used as an indicator of tolerance of leaves to drought stress.  $\epsilon$  indicates plant cell-wall elasticity (for more detail on  $\epsilon$  see Brattlett et al. 2012).  $\Psi_0$  is the pressure due to solutes in living cells within the leaves. Pressure-volume curves can be used in coordination with stomatal conductance ( $gs$ ), stem- or leaf-specific hydraulic conductivity ( $KS$ ,  $KL$ ), or vulnerability to embolism (described in Pérez-Harguindeguy et al. 2013) to gain further insight into hydraulic functioning within the plant.

Across plant species, there is a continuum of responses to drought that result in different ranges of water potentials. The most conservative end of the spectrum, isohydry, is characterised by stomatal closure at “set-point” water potentials, or potentially by having constant access to water (i.e. deep roots). Isohydric species prevent the plant from experiencing embolism-inducing xylem pressures and reducing the need for solute accumulation/osmotic adjustment to maintain turgor as soil dries (Meinzer et al., 2014). The opposite end of the spectrum, anisohydry, encompasses plants that do not regulate water potential to a set value or those that may experience dry soils in their rooting areas. Water potentials decline in more anisohydric species as the soil dries. (Tardieu & Simonneau, 1998; McDowell et al., 2008; Meinzer et al., 2014). TLP and  $\Psi_0$  derived from pressure-volume curves provide insight on the isohydric and anisohydric response to water stress (Tyree & Hammel, 1972; Meinzer et al., 2016). TLP,  $\epsilon$  and  $\Psi_0$  are traits that are mechanistically linked to drought tolerance and can be used to determine the degree to which plants resist or adapt to temporary or prolonged water stress, enhancing our ability to make predictions about how climate change will affect plant success and thus a useful measurement in climate-change studies.

### 5.9.1 What and how to measure?

Pressure volume curves (Figure 5.9.1) are generated by plotting the inverse of the negative  $\Psi_w$  against the relative water deficit ( $100 - RWC$ ) obtained using a balance and a Scholander pressure chamber (described below). The resulting figure has two distinct parts: the non-linear portion and

the linear portion of the plot ([Figure 5.9.1](#)). Leaves or distal ends of shoots from whole plants should be excised pre-dawn or from well-irrigated plants to ensure starting the measurements at the highest  $\Psi_w$  or turgid weight (Tyree & Hammel, 1972). It is best to limit stomatal water loss from samples between collection and processing. This can be done by wrapping the sample in plastic wrap, inserting the sample in a sealed plastic bag with a damp paper towel, and placing the bag in a cooler to decrease respiration and water loss. For optimal measurements, samples should be processed as close to collection as possible. Each sample is weighed before and after obtaining the water potential using a Scholander pressure chamber which is described in detail in Pérez-Harguindeguy et al. (2013). It should be noted that samples should be bagged when not bench dehydrating and should be kept in plastic bags for 20 minutes before making any water potential measurements (i.e. after drying on the bench, place samples in plastic bags prior to making water potential measurements). The sample is placed in the gasket with the stem pointing upward and a positive pressure is applied gradually until water appears on the cut end of the sample. The positive pressure applied is equal to the negative pressure within the stem (Pérez-Harguindeguy et al., 2013). The sample is laid on the bench to desiccate and the measurements are repeated. Subsequent measurements are taken every 2–5 minutes initially, depending on the humidity of the room and the speed with which the sample loses water. After the sample has lost some water (differs depending on species), sample intervals can be increased to 15 minutes to 2 hours. Measurements are taken until 6–8 points have been collected along the linear portion of the pressure volume curve. It may take some experimentation to determine how long it takes to reach this point. Relative water content is calculated as:

$$\frac{(\text{fresh weight (g)} - \text{dry weight(g)}) * 100}{\text{turgid weight (g)} - \text{dry weight (g)}}$$

where the fresh weight is the mean of the weights taken before and after each  $\Psi_w$  iterative measurement, the turgid weight is the weight of the sample taken before the first measurement, and the dry weight is the weight of the dried sample taken after all measurements are completed. Leaves should be dried at a maximum of 70 °C for 72 h to constant weight (Pérez-Harguindeguy et al., 2013) to determine dry weight. The temperature and time for drying depend on the study question, how many samples are dried, the size, thickness and type of the plant material (e.g. large, fleshy or succulent leaves need more time) see [protocol 2.1.1 Aboveground plant biomass](#) for more details on the drying. The x-axis of the plotted data is 100 – RWC and the y-axis is the 1 /  $-\Psi_w$  at each weight ([Figure 5.9.1](#)). From this graph, TLP and  $\Psi_o$  at TLP can be estimated from the inflection point where the curved portion of the line meets the linear portion. The linear portion can be extrapolated to the y-intercept, which will give the  $\Psi_o$  at full turgor pressure.

The extrapolated linear portion of the line can be subtracted from the curve to get the turgor potential ( $\Psi_p$ ) using the equation  $\Psi_w = \Psi_o + \Psi_p$ . To calculate  $\varepsilon$ ,  $\Psi_p$  can be plotted separately with RWC on the x-axis and a non-linear curve fitted to the line, where  $\varepsilon$  is the derivative of that curve:

$$\frac{d\Psi_p}{dRWC} * \frac{1}{RWC}$$

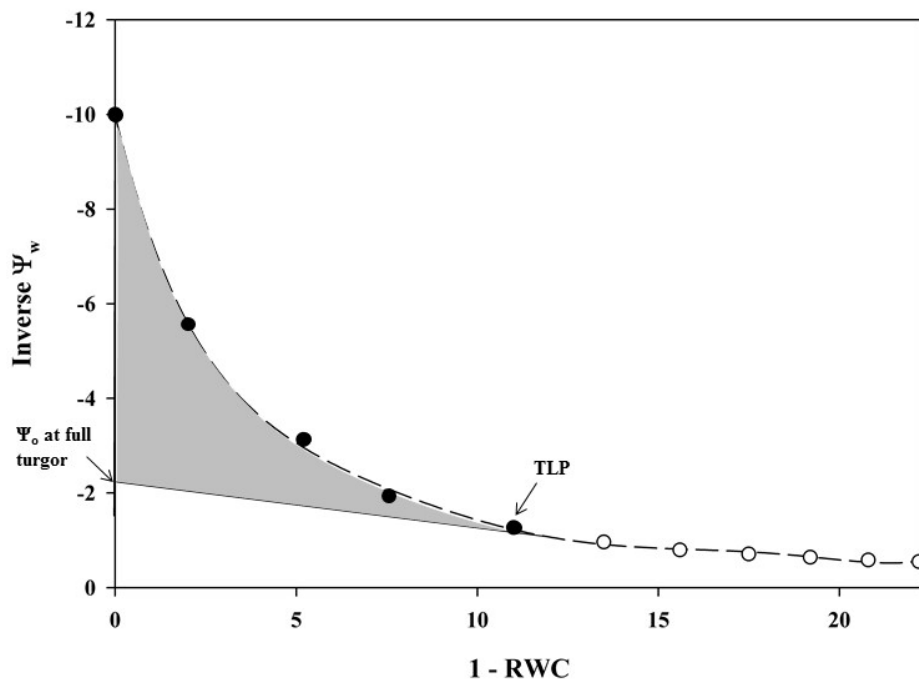


**Figure 5.9.1** Example of a pressure-volume curve. The filled circles are the first 5 iterative measurements: the open circles are the last 6 measurements. The linear portion (solid line) shows the osmotic potential ( $\Psi_o$ ), the curved portion (dashed line) is the water potential before the turgor loss point (TLP), and the shaded area is the turgor potential ( $\Psi_p$ ). Bulk modulus ( $\epsilon$ ) can be obtained by plotting  $\Psi_p$  against relative water content (RWC) and calculating the derivative of the non-linear curve.

The Scholander pressure chamber is a useful instrument for investigating plant water status by applying positive pressure to equal the tension of the water within the xylem. To operate, a compressed nitrogen tank needs to be connected to the intake valve on the pressure chamber. While acquiring samples, the control valve on the chamber should be set to “off”. Slowly open the valve on the nitrogen tank. For the initial measurement, a fresh excised sample is cut with a sharp blade to ensure a clean surface. The sample is placed through the rubber gasket on the lid of the chamber with the cut edge facing upward. Put the lid back on the chamber by pushing down and turning clockwise to stop. This seals the chamber with fresh foliage inside. Turn the control valve to “chamber” to pressurise the chamber. The rate valve should be set so that the pressure increases at the desired rate (this should be no more than 0.1 bar per second). Once the rate valve is set for the desired pressure increase per time, it should not be adjusted. Using the rate valve as an on/off valve will result in valve failure. As the positive pressure approaches the negative pressure within the plant sample, a droplet of water will appear on the cut edge of the sample and the gas should be cut off without venting the chamber. The pressure (in bars or MPa) can be read on the pressure gauge. Once the pressure is recorded, turn the control valve to “exhaust” to release pressure from the chamber. Remove the lid, rubber gasket, and sample. For more detailed information see Pérez-Harguindeguy et al. (2013).

### **Where to start**

Barlett et al. (2012), Meinzer et al. (2014, 2016), Pérez-Harguindeguy et al. (2013), Tardieu & Simonneau (1998), Tyree & Hammel (1972)

### **5.9.2 Special cases, emerging issues, and challenges**

Time of drying depends on cuticular resistance, specific leaf area of sample, and relative humidity of the room in which the measurements are being performed. Pressure-volume curves of similar species can be acquired from previous publications or multiple trials can be done to look at speed of water loss and associated  $\Psi_w$ .

Bulk modulus of elasticity and  $\Psi_o$  at TLP may be underestimated by pressure volume curves constructed as above (Cheung et al., 1976). There can be accuracy issues with artificial rehydration of samples in the lab: rehydration can result in rapid changes in  $\Psi_o$  and TLP leading to values that are not representative of the actual status of plants under study (Meinzer et al., 2014). This presents issues when assessing samples in drought treatments and comparisons should be limited to sample differences relative to each other within that experiment rather than values obtained in other studies.

### **5.9.3 References**

#### **Theory, significance, and large datasets**

Barlett et al. (2012), Cheung et al. (1976), Meinzer et al. (2016), Tardieu & Simonneau (1998), Tyree & Hammel (1972)

#### **More on methods and existing protocols**

Meinzer et al. (2014), Pérez-Harguindeguy et al. (2013)

### **All references**

- Bartlett, M.K., Scoffoni, C. & Sack, L. (2012). The determinants of leaf turgor loss point and prediction of drought tolerance of species and biomes: a global meta-analysis. *Ecology Letters*, 15(5), 393-405.
- Cheung, Y.N.S., Tyree, M.T., & Dainty, J. (1976). Some possible sources of error in determining bulk elastic moduli. *Journal of Experimental Botany*, 23(74), 267-282.
- McDowell, N., Pockman, W. T. Allen, C. D., Breshears, D. D., Cobb, N., Kolb, T., ... Yepez, E. A. (2008). Mechanisms of plant survival and mortality during drought: why do some plants survive while others succumb to drought? *New Phytologist*, 178, 719-739.
- Meinzer, F. C., Woodruff, D. R., Marias, D. E., McCulloh, K. A., & Sevanto, S. (2014). Dynamics of leaf water relations components in co-occurring iso- and anisohydric conifer species. *Plant, Cell & Environment*, 37(11), 2577-2586.

- Meinzer, F. C., Woodruff, D. R., Marias, D. E., Smith, D. D., McCulloh, K. A., Howard, A. R., & Magedman, A. L. (2016). Mapping 'hydroscapes' along iso- to anisohydric continuum of stomatal regulation of plant water status. *Ecology Letters*, 19, 1343-1352.
- Pérez-Harguindeguy, N., Díaz S., Garnier, E., Lavorel, S., Poorter, H., Jaureguiberry, P., ... Cornelissen, J. H. C. (2013). New handbook for standardized measurement of plant functional traits worldwide. *Australian Journal of Botany*, 61, 167-234.
- Tardieu, F. & Simonneau, T. (1998). Variability among species of stomatal control under fluctuating soil water status and evaporative demand: modelling isohydric and anisohydric behaviours. *Journal of Experimental Botany*, 49(Special Issue), 419-432.
- Tyree, M.T. & Hammel, H.T. (1972). The measurement of turgor pressure and water relations of plants by the pressure-bomb technique. *Journal of Experimental Botany*, 23(74), 267-282.

**Authors:** Zinnert J<sup>1</sup>, Wood LK<sup>1</sup>, Johnson DM<sup>2</sup>, Estiarte<sup>3,4</sup>

**Reviewer:** Dickman T<sup>5</sup>

## Affiliations

<sup>1</sup> Department of Biology, Virginia Commonwealth University, Richmond, USA

<sup>2</sup> Warnell School of Forestry and Natural Resources, University of Georgia, Athens, USA

<sup>3</sup> CSIC, Global Ecology Unit CREAF-CSIC-UAB, Bellaterra, Spain

<sup>4</sup> CREAF, Cerdanyola del Vallès, Spain

<sup>5</sup> Earth and Environmental Sciences Division, Los Alamos National Laboratory, Los Alamos, USA

## 5.10 Maximum leaf hydraulic conductance

**Authors:** Scoffoni C<sup>1</sup>, Sack L<sup>2</sup>

**Reviewer:** Dickmann LT<sup>3</sup>, Estiarte M<sup>4,5</sup>

**Measurement unit:**  $K_{leaf}$  in  $\text{mmol m}^{-2} \text{ s}^{-1} \text{ MPa}^{-1}$ ; **Measurement scale:** leaf; **Equipment costs:** €€€; **Running costs:** €; **Installation effort:** low; **Maintenance effort:** low; **Knowledge need:** medium; **Measurement mode:** data logger

The leaf hydraulic conductance ( $K_{leaf}$ ) quantifies the efficiency of water movement through the leaf, from the petiole to evaporation sites. Thus,  $K_{leaf}$  is influenced by liquid flow through the leaf vein xylem and across the leaf bundle sheath and through the mesophyll, including vapour movement through the airspaces (Sack & Tyree, 2005; Sack & Holbrook, 2006; Buckley et al., 2015, 2017).  $K_{leaf}$  is calculated as the flow rate of water through the leaf (typically normalised by leaf area) for a given water potential driving force. To capture CO<sub>2</sub> for photosynthesis, stomata open, exposing the vapour-saturated intercellular airspaces to the dry atmosphere. The higher the  $K_{leaf}$ , the more efficiently leaves can replace water lost via diffusion to the dry atmosphere, allowing stomata to remain open. The maximum leaf hydraulic conductance (i.e. that of a fully hydrated plant;  $K_{max}$ ) varies more than 65-fold across species (Sack & Holbrook, 2006) and constrains both light-saturated photosynthesis and stomatal conductance across diverse and closely related species (Brodribb et al., 2007; Scoffoni et al., 2016). The  $K_{leaf}$  can also be extremely sensitive to internal and environmental factors, such as light (Sack et al., 2002; Cochard et al., 2007; Scoffoni et al., 2008; Guyot et al., 2012) and soil and atmospheric drought (Scoffoni & Sack, 2017).  $K_{leaf}$  is thus an important trait playing a role in determining species plasticity, evolution and distribution across habitats (Blackman et al., 2012, 2014; Scoffoni et al., 2015).

### 5.10.1 What and how to measure?

While there are several methods currently in use to measure  $K_{leaf}$ , the evaporative flux method (EFM; Sack et al., 2002; Sack & Scoffoni, 2012) has the advantage of mimicking the natural transpirational pathways of water movement in the leaf. The rate of transpiratory water flow is measured via either a 5-decimal analytical balance or a flow meter (for construction details, see Sack et al., 2011). While the flow meter is relatively inexpensive, easily transportable, and completely field deployable, it does require more preparation and knowledge than the balance method. In the EFM, an excised leaf is connected by tubing to a water source on a balance (or to a flowmeter). The leaf is placed under a light source and over a box fan to ensure stomata are open. The loss of water from the balance is recorded at regular intervals (5 to 30 s) to calculate the flow rate through the leaf. When a steady-state is reached (and after a period of > 20 min to ensure leaves are acclimated to light), the leaf is taken off the system, petiole dabbed dry, and placed in a sealable plastic bag previously exhaled into (to create a high humidity and CO<sub>2</sub> atmosphere to suppress transpiration) and equilibrated in the dark for > 20 min. The water potential driving force of the flow is then measured using a pressure chamber.  $K_{leaf}$  is calculated by dividing the flow rate by the water potential driving force, and normalising by leaf area and measurement temperature (for step by step protocols and videos, see Sack & Scoffoni, 2012), and therefore highly relevant in a climate-change context.

Branches can be collected in the field the day prior to measurements and placed in large dark plastic bags filled with wet paper towels. Plant material can be transported to the lab in a cooler. In the lab, at least two nodes should be cut under water to ensure the removal of any embolized conduits (as a result of cutting shoots off individuals in air in the field), and the shoots should be left to rehydrate in pure water overnight, with two dark plastic bags filled with wet paper towels covering them, ensuring high atmospheric humidity around the rehydrating samples. Alternatively, if working with greenhouse plants, whole pots can be transported to the lab the evening prior to measurements, watered to saturation and covered in two dark plastic bags filled with wet paper towers.

#### ***Measuring $K_{leaf}$ using the EFM with a balance***

A custom-built top is needed for the balance that will stably secure a metal or glass tube inside a container of water on the balance. Water will then flow from the container, up through the tube, and then into plastic tubing to the leaf. Prior to measurements, beakers filled with wet paper towels should be placed inside the balance, and the balance sealed, such that high humidity within the balance prevents evaporation from the container of water: verify no drift in the mass value on the balance. Next, under pure water, cut a leaf off a fully hydrated branch and rapidly wrap parafilm around its petiole. Recut the tip of the petiole under pure water using a fresh razor blade and connect it (while under water) to tubing that runs to the water source on the balance (after making sure no air bubbles are trapped anywhere in the system). You can gently lift the connection out of water to check for leaks by raising the sample above the pressure head. If no air bubble appears in the tubing, then the seal is good. Place the leaf adaxial surface upwards in wooden frames strung with fishing line to stabilise the leaf, above a large box fan, and under at least  $1000 \mu\text{mol m}^{-2} \text{s}^{-1}$  photosynthetically active radiation. Maintain leaf temperature around  $25^\circ\text{C}$  throughout the experiment. Allow leaves to transpire on the apparatus for at least 30 min (to allow leaves sufficient time to acclimate to high irradiance) and until flow rate has stabilised – no upward or downward trend – and with a coefficient of variation < 5% for at least five measurements made at 30 sec flow intervals. Discard measurements if the flow suddenly changes, either due to apparent leakage from the seal or blockage in the system by particles or air bubbles. When flow stabilises, record leaf temperature with a thermocouple and quickly remove the leaf from the tubing. Dab dry the petiole and place the leaf into a sealable bag which has been previously exhaled into to halt transpiration. Let the leaf sit for at least 30 min to equilibrate. Measure the final leaf water potential on the equilibrated leaf using a pressure chamber, and the leaf area with a scanner and image analysis, or a leaf area meter.

#### ***Measuring $K_{leaf}$ using a flowmeter***

A pressure-drop flowmeter can be built following detailed steps available online (Sack et al., 2011). Every morning prior to measurements, calibrate the transducers of the flowmeter by plotting the voltage against known positive pressures, obtained by placing the water source connected to the flowmeter at different heights. The slope and intercept are used to convert the voltage into pressure units. To check accuracy, move the water source to an intermediate height and ensure transducers values are comparable and are the same as the pressure generated from the height. If one or both transducers are not responding to applied pressure, first check for a loose connection, for example

ensure wires are making contact with the data acquisition board transmitting transducer input to the computer. Tighten if necessary. If there is still no response, check for air bubbles in the system and flush, and check for air bubbles in the transducers themselves. Connect the leaf following the same recommendations as for the balance method. At the end of the measurement, in addition to measuring leaf temperature, measure the water temperature before and after the resistor of the flowmeter. You will need this to adjust the resistance value for differences in water viscosity. The flow rate is calculated by the difference in pressure between the two transducers divided by the resistor (which you can measure using either a balance or a pipette, measuring the flow rate through the resistor at different heights). The  $K_{leaf}$  ( $\text{mmol m}^{-2} \text{s}^{-1} \text{MPa}^{-1}$ ) is calculated by dividing the flow rate (normalised by leaf temperature and size) by the final leaf water potential driving force (measured at the end of the experiment using a pressure chamber).

### **Where to start**

Brodribb et al. (2007), Sack & Holbrook (2006), Sack & Scoffoni (2012), Sack et al. (2002, 2011), Scoffoni et al. (2016)

### **5.10.2 Special cases, emerging issues, and challenges**

The EFM can also be used to measure stomatal conductance, by recording the air temperature and relative humidity around the leaf during steady-state flow at the end of the measurement. These parameters can be used to measure the vapour pressure difference driving diffusion of water vapour out of the leaf through stomata. Stomatal conductance ( $g_s$ ;  $\text{mmol m}^{-2} \text{s}^{-1}$ ) is then calculated by dividing the flow rate through the leaf by the vapour pressure difference expressed as a mole fraction. The ratio of hydraulic supply over demand ( $K_{leaf} / g_s$ ) can then also be calculated (Sack & Scoffoni, 2012); a higher supply over demand would enable species to maintain stomata open during rapid changes in vapor pressure differences (VPD) during the day (Carins Murphy et al., 2012; Scoffoni et al., 2015, 2016). The system can also be modified to measure  $K_{leaf}$  under varying environmental factors, such as light (Scoffoni et al., 2008). Some species can rapidly enhance their  $K_{leaf}$  values by substantial amounts under high light (Sack et al., 2002; Cochard et al., 2007; Scoffoni et al., 2008; Voicu et al., 2008; Guyot et al., 2012) and under shifts that are associated with changes in the expression and activation of aquaporins (Cochard et al., 2007; Shatil-Cohen et al., 2011; Shatil-Cohen & Moshelion, 2012; Laur & Hacke, 2014a, 2014b; Sade et al., 2014).

The use of a digital pressure chamber and stereoscope is highly recommended for more accurate water potential measurement, especially at high water potentials.

A number of additional methods exist for the determination of  $K_{leaf}$ . A version of the evaporative flux method can be applied with leaves still attached, by determining transpiration rate using a gas exchange or sapflow system, and dividing by the driving force estimated from the difference in water potentials between transpiring and non-transpiring (bagged) leaves (Sack & Tyree, 2005). The vacuum pump method involves measuring the flow rate of water through a leaf under varying levels of subatmospheric pressures (partial vacuum), and  $K_{leaf}$  is calculated from the slope of flow against pressure. The high-pressure flow method calculates  $K_{leaf}$  from the flow rate of water delivered through a leaf at a known pressure. Finally, the rehydration kinetics method estimates  $K_{leaf}$  as the

inverse of the resistance in series with a charging capacitor as a leaf recovers from rehydration (Brodribb & Holbrook, 2003; Blackman & Brodribb, 2011). However, with that method, it is not easy to light acclimate the samples prior to measurements, which would underestimate  $K_{leaf}$  for many species (Scoffoni et al., 2008). Obtaining  $K_{leaf}$  values above -0.5 MPa is difficult (Scoffoni et al., 2008), and most importantly, the pathways of water movement in rehydrating leaves could be very distinct from those of a transpiring leaf (Zwieniecki et al., 2007). While all these various methods have yielded comparable maximum  $K_{leaf}$  values to the EFM in several species it remains unclear whether the pathways for water movement are equivalent across methods (e.g. Tsuda & Tyree, 2000; Nardini et al., 2001, 2010; Sack et al., 2002; Scoffoni et al., 2008; Blackman & Brodribb, 2011; Hernandez-Santana et al., 2016).

### 5.10.3 References

#### Theory, significance, and large datasets

Carins Murphy et al. (2012), Laur & Hacke (2014b), Nardini et al. (2010), Sack & Scoffoni (2012), Sack & Tyree (2005), Sack et al. (2002)

#### More on methods and existing protocols

Guyot et al. (2012), Sack & Scoffoni (2012), Scoffoni et al. (2008)

#### All references

- Blackman, C. J., & Brodribb, T. J. (2011). Two measures of leaf capacitance: insights into the water transport pathway and hydraulic conductance in leaves. *Functional Plant Biology*, 38(2), 118-126.
- Blackman, C. J., Brodribb, T. J., & Jordan, G. J. (2012). Leaf hydraulic vulnerability influences species' bioclimatic limits in a diverse group of woody angiosperms. *Oecologia*, 168(1), 1-10.
- Blackman, C. J., Gleason, S. M., Chang, Y., Cook, A. M., Laws, C., & Westoby, M. (2014). Leaf hydraulic vulnerability to drought is linked to site water availability across a broad range of species and climates. *Annals of Botany*, 114(3), 435-440.
- Brodribb, T. J., & Holbrook, N. M. (2003). Stomatal closure during leaf dehydration, correlation with other leaf physiological traits. *Plant Physiology*, 132(4), 2166-2173.
- Brodribb, T. J., Field, T. S., & Jordan, G. J. (2007). Leaf maximum photosynthetic rate and venation are linked by hydraulics. *Plant Physiology*, 144(4), 1890-1898.
- Buckley, T. N., John, G. P., Scoffoni, C., & Sack, L. (2015). How does leaf anatomy influence water transport outside the xylem? *Plant Physiology*, 168(4), 1616-1635.
- Buckley, T. N., John, G. P., Scoffoni, C., & Sack, L. (2017). The sites of evaporation within leaves. *Plant Physiology*, 173, 1763-1782.
- Carins Murphy, M. R., Jordan, G. J., & Brodribb, T. J. (2012). Differential leaf expansion can enable hydraulic acclimation to sun and shade. *Plant, Cell & Environment*, 35(8), 1407-1418.

- Cochard, H., Venisse, J. S., Barigah, T. S., Brunel, N., Herbette, S., Guillot, A., ... Sakr, S. (2007). Putative role of aquaporins in variable hydraulic conductance of leaves in response to light. *Plant Physiology*, 143(1), 122-133.
- Guyot, G., Scoffoni, C., & Sack, L. (2012). Combined impacts of irradiance and dehydration on leaf hydraulic conductance: insights into vulnerability and stomatal control. *Plant, Cell & Environment*, 35, 857-871.
- Hernandez-Santana, V., Rodriguez-Dominguez, C. M., Fernandez, J. E., & Diaz-Espejo, A. (2016). Role of leaf hydraulic conductance in the regulation of stomatal conductance in almond and olive in response to water stress. *Tree Physiology*, 36(6): 725-735.
- Laur, J., & Hacke, U. G. (2014a). Exploring *Picea glauca* aquaporins in the context of needle water uptake and xylem refilling. *New Phytologist*, 203(2), 388-400.
- Laur, J., & Hacke, U. G. (2014b). The role of water channel proteins in facilitating recovery of leaf hydraulic conductance from water stress in *Populus trichocarpa*. *PLoS One*, 9(11), e111751.
- Nardini, A., Tyree, M. T., & Salleo, S. (2001). Xylem cavitation in the leaf of *Prunus laurocerasus* and its impact on leaf hydraulics. *Plant Physiology*, 125(4), 1700-1709.
- Nardini, A., Raimondo, F., Lo Gullo, M. A., & Salleo, S. (2010). Leafminers help us understand leaf hydraulic design. *Plant, Cell & Environment*, 33(7), 1091-1100.
- Sack, L., & Holbrook, N. M. (2006). Leaf hydraulics. *Annual Review of Plant Biology*, 57, 361-381.
- Sack, L., & Scoffoni, C. (2012). Measurement of leaf hydraulic conductance and stomatal conductance and their responses to irradiance and dehydration using the evaporative flux methods (EFM). *Journal of Visualized Experiments*, (70), e4179.
- Sack, L., & Tyree, M. T. (2005). Leaf hydraulics and its implications in plant structure and function. In N. M. Holbrook, & M. A. Zwieniecki (Eds.), *Vascular Transport in Plants* (pp. 93-114). Oxford: Elsevier/Academic Press.
- Sack, L., Melcher, P. J., Zwieniecki, M. A., & Holbrook, N. M. (2002). The hydraulic conductance of the angiosperm leaf lamina: a comparison of three measurement methods. *Journal of Experimental Botany*, 53(378), 2177-2184.
- Sack, L., Bartlett, M., Creese, C., Guyot, G., & Scoffoni, C. (2011). Constructing and operating a hydraulics flow meter. <http://prometheuswiki.org/tiki-index.php?page=Constructing+and+operating+a+hydraulics+flow+meter>: Prometheus Wiki.
- Sade, N., Shatil-Cohen, A., Attia, Z., Maurel, C., Boursiac, Y., Kelly, G., ... Moshelion, M. (2014). The role of plasma membrane aquaporins in regulating the bundle sheath-mesophyll continuum and leaf hydraulics. *Plant Physiology*, 166(3), 1609-1620.
- Scoffoni, C., & Sack, L. (2017). The causes and consequences of leaf hydraulic decline with dehydration. *Journal of Experimental Botany*, 68(16), 4479-4496.
- Scoffoni, C., Pou, A., Aasamaa, K., & Sack, L. (2008). The rapid light response of leaf hydraulic conductance: new evidence from two experimental methods. *Plant, Cell & Environment*, 31(12), 1803-1812.

- Scoffoni, C., Kunkle, J., Pasquet-Kok, J., Vuong, C., Patel, A. J., Montgomery, R. A., ... Sack, L. (2015). Light-induced plasticity in leaf hydraulics, venation, anatomy and gas exchange in ecologically diverse Hawaiian lobeliads. *New Phytologist*, 207, 43-58.
- Scoffoni, C., Chatelet, D. S., Pasquet-Kok, J., Rawls, M., Donoghue, M. J., Edwards, E. J., & Sack, L. (2016). Hydraulic basis for the evolution of photosynthetic productivity. *Nature Plants*, 2, a16072.
- Shatil-Cohen, A., & Moshelion, M. (2012). Smart pipes: the bundle sheath role as xylem-mesophyll barrier. *Plant Signaling & Behavior*, 7(9), 1088-1091.
- Shatil-Cohen, A., Attia, Z., & Moshelion, M. (2011). Bundle-sheath cell regulation of xylem-mesophyll water transport via aquaporins under drought stress: a target of xylem-borne ABA? *Plant Journal*, 67(1), 72-80.
- Tsuda, M., & Tyree, M. T. (2000). Plant hydraulic conductance measured by the high pressure flow meter in crop plants. *Journal of Experimental Botany*, 51(345), 823-828.
- Voicu, M. C., Zwiazek, J. J., & Tyree, M. T. (2008). Light response of hydraulic conductance in bur oak (*Quercus macrocarpa*) leaves. *Tree Physiology*, 28(7), 1007-1015.
- Zwieniecki, M. A., Brodribb, T. J., & Holbrook, N. M. (2007). Hydraulic design of leaves: insights from rehydration kinetics. *Plant, Cell & Environment*, 30(8), 910-921.

**Authors:** Scoffoni C<sup>1</sup>, Sack L<sup>2</sup>

**Reviewer:** Dickmann LT<sup>3</sup>, Estiarte M<sup>4,5</sup>

## Affiliations

<sup>1</sup> Department of Biological Sciences, California State University, Los Angeles, USA

<sup>2</sup> Department of Ecology and Evolutionary Biology, University of California Los Angeles, Los Angeles, USA

<sup>3</sup> Earth and Environmental Sciences Division, Los Alamos National Laboratory, Los Alamos, USA

<sup>4</sup> CSIC, Global Ecology Unit CREAF-CSIC-UAB, Bellaterra, Spain

<sup>5</sup> CREAF, Cerdanyola del Vallès, Spain

## 5.11 Metabolomic profiling in plants using mass-spectrometry

**Authors:** Oravec M<sup>1</sup>, Večeřová K<sup>1</sup>, Gargallo-Garriga A<sup>1,2,3</sup>, Sardans J<sup>2,3</sup>, Urban O<sup>1</sup>

**Reviewers:** Holub P<sup>1</sup>, Klem K<sup>4</sup>, Peñuelas J<sup>2,3</sup>

**Measurement unit: molecules/ions (m/z); Measurement scale: leaf, branch, tissue, exudates, soil and air samples; Equipment costs: €€€; Running costs: €€; Installation effort: high; Maintenance effort: medium (services of instruments); Knowledge need: high; Measurement mode: manual**

Metabolomics is an “omics” approach that aims to analyse all low molecular-weight metabolites in biological samples. Metabolomic profiling represents a new tool to assess a plant’s response to biotic or abiotic stresses. In ecological studies, ecometabolomics aims to study the metabolome structure of organisms and media (water, soil, air, etc.) in field conditions (Peñuelas & Sardans, 2009; Sardans et al., 2011). Metabolome analyses provide the metabolism structure (the metabolites and their concentrations), thus informing on the functional state of the organisms, media, or overall ecosystem. The metabolome can be considered as the chemical phenotype of organisms (Fiehn, 2002). Because the chemical phenotypes are not fixed, metabolomics has been used to understand how organisms function under different environmental conditions (Yuan et al., 2009; Rivas-Ubach et al., 2012; Yoshikawa et al., 2013; Gargallo-Garriga et al., 2014). Target and non-target metabolomic profiling has been used to identify changes in plant metabolome and metabolic pathways enabling the investigation of plant-specific responses to biotic (e.g. pests) (Rivas-Ubach et al., 2016) or abiotic stress factors, such as increase of UV radiation (Oravec et al., 2015), drought (Rivas-Ubach et al., 2012; Gargallo-Garriga et al., 2014), temperature (Gargallo-Garriga et al., 2015), nutrient deficiency (Gargallo-Garriga et al., 2017), and/or air pollution (Večeřová et al., 2016). Metabolomics can thus substantially contribute to studies predicting acclimation of plants to environmental perturbances related to climate-change and other global-change drivers. Metabolomics has already shown great potential to provide in-depth understanding of biological systems, pathways, and their functionally dynamic interactions. Moreover, metabolomic profiling provides an understanding at the molecular level of how plants respond to changes in the growth environment and whether and how they acclimate and resist. Metabolomics can thus contribute to the understanding of the impact of climate and global change and also to answer basic ecological questions regarding the impacts of competition or trophic relationships on organisms.

### 5.11.1 What and how to measure?

Tandem analytical techniques and basic analytical techniques are used for the analysis of the metabolome. These are a combination of separation techniques: high performance liquid chromatography (HPLC) and gas chromatograph (GC) with mass spectrometer (MS) detection techniques. HPLC-MS systems are used in particular for target and non-target analyses of polar and semi-polar primary and secondary metabolites (polyphenols, amino acids, saccharides, phytohormones, etc.), while GC-MS is especially suitable for target analyses of non-polar metabolites or polar metabolites that can be easily derived (fatty acids, volatile compounds, etc.). A combination of HPLC and GC techniques may thus lead to a comprehensive description of plant metabolome and its changes. Proton-based nuclear magnetic resonance (<sup>1</sup>H NMR) coupled or not with <sup>13</sup>C NMR is also

a frequently used metabolomic platform that does not rely on previous separation methods for untargeted metabolomics profiling analysis (Rivas-Ubach et al., 2013). However, the low sensitivity of this method currently precludes its more extended use (Sardans et al., 2011). Basic analytical techniques such as Fourier transformed infrared spectroscopy, Raman spectroscopy, spectrofluorometry, and/or classical spectrophotometers can be used as complementary analytical techniques for investigation of other groups of metabolites including photosynthetic and photoprotective pigments (chlorophylls, carotenoids, xanthophylls). Determination of nitrogen and carbon contents in biological samples using an elemental analyser with a thermal conductivity detector yields important supplementary information about the stoichiometry of tissues, organs, and/or whole plants. This coupling of metabolomics with elemental analyses allows one to relate changes in plant function with changes in plant use of different elements, constituting a notable advantage for integrative ecological studies. The C/N/P stoichiometry plays an important role in the metabolism, as does the stoichiometry of other nutrients such as calcium, magnesium, and potassium. P, K, Ca, Mg, and many other elements are analysed with inductively coupled plasma - mass spectrometry (ICP-MS) techniques.

The measurement results are subsequently processed by statistical software (modified MatLab, R, or Sieve). For identification of metabolites, available commercial databases and mass libraries built by each lab are used. KEGG (Kyoto Encyclopaedia of Genes and Genomes) is thereafter generally used for description of affected metabolic pathways, i.e. which ones are up- and which ones are down-regulated in the different organs of the plants (Gargallo-Garriga et al., 2014). Information from non-target analyses is further used for target analysis. The overall results from metabolomic profiling are combined with results from physiological measurements. The main aim is to find relationships between the changes of metabolome and stress-induced changes in physiology.

### ***Sampling, sample storage, and measuring protocols***

The samples (ideally approximately 300 mg dry weight) have to be frozen in liquid nitrogen immediately after sampling and kept at  $-80^{\circ}\text{C}$  (max. 2 months), and stored dry-frozen at  $\leq -20^{\circ}\text{C}$  until further processing. The effects of long-term storage and storage temperature have been investigated so that studies can be planned without possible degradation of chemical compounds. It is crucial to protect samples against contamination and water during all steps of the process, and therefore it is necessary to adhere to “good laboratory practices”. Since the metabolomics profiles may have substantial daily courses, it is recommended to respect such daily dynamics and to collect all samples within narrow time intervals depending on the experimental goal. Local microclimatic and radiation conditions also have to be considered. Accordingly, leaves/branches with the same cardinal orientation should be sampled within dense ecosystems to reduce the variability among samples. Moreover, plant age, geographical origin of plant species (Meijon et al., 2016), and/or elevation where the plants grow (Rajsnerová et al., 2015; Rivas-Ubach et al., 2017) have been shown to potentially influence the metabolome of plant tissues. Sampling campaigns thus have to respect these factors to reduce variability of plant metabolome, to minimise artefacts, and to increase reproducibility of metabolomic data.

The following protocols are based on the protocols for metabolite profiling in plants developed by Fiehn et al. (2000) and include further modifications with respect to analytical instruments used.

Before chromatographic analyses, the frozen samples are homogenised using a pestle and mortar with the addition of liquid nitrogen. Leaf tissues, for example, can be ground under liquid nitrogen with a pestle and mortar, or using a ball mill with pre-chilled holders (summarised in Fiehn, 2002). Other plant organs such as roots and grains, however, may be sometimes too hard to use in ball mills. After homogenisation, different methods of metabolite extraction could be used but, again, no systematic study comparing extraction techniques is available. Some groups of metabolites, including fatty acids among others (Folch et al., 1957; Večeřová et al., 2016), require specific extraction procedures that have to be even further modified depending on the type of sample (soil, plant, thylakoid membrane, etc.). Most frequently, homogenised samples are extracted using a methanol:H<sub>2</sub>O solution (1:2) that has been demonstrated to be optimal to extract most polar and semi-polar metabolites. For a-polar metabolites a solution of methanol:chloroform:H<sub>2</sub>O (1:2:2) can be used. In this case, an aliquot of the upper (polar) phase is used to analyse saccharides, phenolic compounds, amino acids, and Krebs cycle acids employing an UltiMate 3000 HPLC coupled with an LTQ Orbitrap XL high resolution mass spectrometer (HRMS) (ThermoFisher Scientific).

For the polar and semi-polar extraction a Hypersil GOLD column (150 × 2.1 mm, 3 µm; ThermoFisher Scientific) is used for separation of metabolites. The flow rate of the mobile phase is 0.3 mL min<sup>-1</sup> and column temperature is set to 30 °C. The mobile phase consists of (A) acetonitrile and (B) water containing 0.1% acetic acid. Both mobile phases (A) and (B) are filtrated and degassed for 10 min in an ultrasonic bath prior to use. Gradient elution chromatography is started with 10% acetonitrile (A) and 90% water (0.1% acetic acid) (B) and is held for 5 min. Within a time interval of 5–20 min, the mobile phase (A) composition is increased to 90 %. This composition is then maintained for 5 min, after which the system is equilibrated to initial conditions (10% acetonitrile (A) and 90% water (0.1% acetic acid)) over a period of 5 min. The 254, 272, 274, and 331 nm wavelengths are monitored.

The HRMS is equipped with a HESI II heated electrospray ionization source (ThermoFisher Scientific), operated in full scan mode with a mass resolution of 60,000, when the minimum peak separation is represented by a full width of the peak at half maximum (FWHM). Full scan spectra are acquired over the mass range 50–1000 m/z in positive polarity mode and 65–1000 m/z in negative polarity mode. The mass resolution and sensitivity of the HRMS are regularly controlled by injecting a mixture of phenolic compounds. As a control, phthalate is taken as an internal control mass. The compounds are assigned on the basis of public or private mass libraries created using standards measured in MS and MS<sup>n</sup> modes.

Gas chromatography coupled with mass spectrometry (GC-MS) is used to analyse a spectrum of fatty acids. Homogenised samples are transferred into vials and 1.5 mL of a chloroform:methanol solution (2:1) is added. The vials are placed in a thermoblock at 60 °C for 30 min. The lower phase (chloroform) is collected and the process is repeated. In case of insufficient phase separation, 1 mL of 0.88% potassium chloride should be added. After collection of lower phases and the addition of an internal standard (nonadecanoic acid), extracts are dried using nitrogen flow. The methyl esters derivatives of fatty acids are prepared using 1 mL of 3 N methanolic HCl, which is added to the dried extract and then heated for 90 min at 60 °C. Subsequently, the samples are extracted three times with 2.5 mL of *n*-hexane and dried using nitrogen flow. Finally, extracts are dissolved in 1 mL of *n*-hexane.

The analysis of fatty acids methyl esters is performed with a TSQ Quantum XLS triple Quadrupole (ThermoFischer Scientific) on a 30 m, 0.25 mm (inside diameter), 0.25 µm column (ZB-5MS;

Phenomenex). Samples ( $1 \mu\text{L}$ ) are injected in splitless mode. The inlet pressure of the carrier gas (helium) is 100 kPa at the initial oven temperature and its flow rate is  $1.2 \text{ mL min}^{-1}$ . Meanwhile the injection temperature is  $250^\circ\text{C}$ . The temperature gradient of the oven begins at  $100^\circ\text{C}$  and is increased to  $150^\circ\text{C}$  at the rate of  $10^\circ\text{C min}^{-1}$ , followed by a temperature increase to  $260^\circ\text{C}$  at the rate of  $2.5^\circ\text{C min}^{-1}$ . The interface temperature is maintained at  $250^\circ\text{C}$ . GC-MS (electrospray ionization 50 eV, ion source temperature  $200^\circ\text{C}$ ) is performed at full scan in the  $50\text{--}450 \text{ m/z}$  range (scan time 0.15 s). The fatty acids' methyl esters are searched in the public and private mass libraries created from measurement of standards using GC-MS in full scan mode.

### **Where to start**

Fiehn (2002), Fiehn et al. (2000), Folch et al. (1957), Gargallo-Garriga et al. (2015), Meijon et al. (2016), Peñuelas & Sardans (2009), Rivas-Ubach et al. (2017), Večeřová et al. (2016), Weckwerth & Kahl (2013)

### **5.11.2 Special cases, emerging issues, and challenges**

Metabolomic profiling can be used, among others, to identify biomarkers of early-stress detection (Kaplan et al., 2004; Boudonck et al., 2009). Metabolomics could also represent, in conjunction with physiological and morphological traits, an important additive method of plant phenotyping, the breeding and selection of genotypes with the highest resistance to biotic and abiotic stresses. Metabolomics techniques could be also used to explore root exudates and thus to investigate plant-soil interactions (Sardans & Peñuelas, 2013). An overview of current developments and future challenges in ecological metabolomics can be found in Sardans et al. (2011).

A number of metabolomics applications could be extended by the application of other ionisation techniques such as DART (Direct Analysis in Real Time). This ambient ionisation technique does not require sample preparation, so solid and liquid materials can be analysed by mass spectrometry in their native state (Zhou et al., 2010; Lesiak et al., 2014; Armitage et al., 2015).

Desorption electrospray ionisation (DESI) is another ambient ionisation technique compliant with high-resolution mass spectrometry. DESI can be used for imaging metabolite distribution (localisation) in plant tissues or surfaces of biological systems. Visualisation of metabolite heterogeneity can be potentially used for the detection of pathogen infections on plant leaves (Takats et al., 2005; Chernetsova & Morlock, 2011).

Other ionisation techniques such as APCI (atmospheric pressure chemical ionisation) are suitable for investigating thermally stable samples with low to medium (less than 1500 Da) molecular weight, and medium to high polarity including non-polar lipids (Byrdwell, 2001), pesticides (Jansson et al., 2004), and/or various natural organic compounds (amino acids, saponins, phenyl propanoids, etc.). In contrast, electrospray ionisation (ESI) is especially useful in producing ions from macromolecules (Whitehouse et al., 1989).

### **Where to start**

Jansson et al. (2004); Kaplan et al. (2004); Sardans et al. (2011); Takats et al. (2005); Whitehouse et al. (1989)

#### 5.11.4 References

##### ***Theory, significance, and large datasets***

Fiehn (2002); Gargallo-Garriga et al. (2014); Peñuelas & Sardans (2009); Sardans & Peñuelas (2013); Weckwerth & Kahl (2013)

##### ***More on methods and existing protocols***

Fiehn et al. (2000); Jansson et al. (2004); Rivas-Ubach et al. (2012); Večeřová et al. (2016); Zhou et al. (2010)

##### ***All references***

- Armitage, R. A., Jakes, K., & Day, C. (2015). Direct analysis in real time-mass spectroscopy for identification of red dye colourants in Paracas Necropolis Textiles. *STAR: Science & Technology of Archaeological Research*, 1(2), 60-69.
- Boudonck, K. J., Mitchell, M. W., Német, L., Keresztes, L., Nyska, A., Shinar, D., & Rosenstock, M. (2009). Discovery of metabolomics biomarkers for early detection of nephrotoxicity. *Toxicologic Pathology*, 37(3), 280-292.
- Byrdwell, W. C. (2001). Atmospheric pressure chemical ionization mass spectrometry for analysis of lipids. *Lipids*, 36(4), 327-346.
- Chernetsova, E. S., & Morlock, G. E. (2011). Ambient desorption ionization mass spectrometry (DART, DESI) and its bioanalytical applications. *Bioanalytical Reviews*, 3(1), 1-9.
- Fiehn, O. (2002). Metabolomics—the link between genotypes and phenotypes. *Plant Molecular Biology*, 48, 155-171.
- Fiehn, O., Kopka, J., Dörmann, P., Altmann, T., Trethewey, R. N., & Willmitzer, L. (2000). Metabolite profiling for plant functional genomics. *Nature Biotechnology*, 18(11), 1157-1161.
- Folch, J., Lees, M., & Sloane-Stanley, G. H. (1957). A simple method for the isolation and purification of total lipids from animal tissues. *Journal of Biological Chemistry*, 226(1), 497-509.
- Gargallo-Garriga, A., Sardans, J., Pérez-Trujillo, M., Rivas-Ubach, A., Oravec, M., Vecerova, K., ... Parella, T. (2014). Opposite metabolic responses of shoots and roots to drought. *Scientific Reports*, 4, a6829.
- Gargallo-Garriga, A., Sardans, J., Pérez-Trujillo, M., Oravec, M., Urban, O., Jentsch, A., ... Peñuelas, J. (2015). Warming differentially influences the effects of drought on stoichiometry and metabolomics in shoots and roots. *New Phytologist*, 207(3), 591-603.
- Gargallo-Garriga, A., Wright, S. J., Sardans, J., Pérez-Trujillo, M., Oravec, M., Večeřová, K., ... Peñuelas, J. (2017). Long-term fertilization determines different metabolomic profiles and responses in

- saplings of three rainforest tree species with different adult canopy position. *PLoS One*, 12(5), e0177030.
- Jansson, C., Pihlström, T., Österdahl, B. G., & Markides, K. E. (2004). A new multi-residue method for analysis of pesticide residues in fruit and vegetables using liquid chromatography with tandem mass spectrometric detection. *Journal of Chromatography A*, 1023(1), 93-104.
- Kaplan, F., Kopka, J., Haskell, D. W., Zhao, W., Schiller, K. C., Gatzke, N., ... Guy, C. L. (2004). Exploring the temperature-stress metabolome of *Arabidopsis*. *Plant Physiology*, 136(4), 4159-4168.
- Lesiak, A. D., Cody, R. B., Dane, A. J., & Musah, R. A. (2014). Rapid detection by direct analysis in real time-mass spectrometry (DART-MS) of psychoactive plant drugs of abuse: The case of *Mitragyna speciosa* aka "Kratom". *Forensic Science International*, 242, 210-218.
- Meijón, M., Feito, I., Oravec, M., Delatorre, C., Weckwerth, W., Majada, J., & Valledor, L. (2016). Exploring natural variation of *Pinus pinaster* Aiton using metabolomics: is it possible to identify the region of origin of a pine from its metabolites? *Molecular Ecology*, 25(4), 959-976.
- Oravec, M., Novotná, K., Rajsnerová, P., et al. (2015). Target and non-target metabolomics profiling of different barley varieties affected by enhanced ultraviolet radiation and various C:N stoichiometry. *FASEB Journal* 29(1 Supplement), Abstract 887.7.
- Peñuelas, J., & Sardans, J. (2009). Ecological metabolomics. *Chemistry and Ecology*, 25(4), 305-309.
- Rajsnerová, P., Klem, K., Holub, P., Novotná, K., Večeřová, K., Kozáčiková, M., ... Urban, O. (2015). Morphological, biochemical and physiological traits of upper and lower canopy leaves of European beech tend to converge with increasing altitude. *Tree Physiology*, 35(1), 47-60.
- Rivas-Ubach, A., Sardans, J., Pérez-Trujillo, M., Estiarte, M., & Peñuelas, J. (2012). Strong relationship between elemental stoichiometry and metabolome in plants. *Proceedings of the National Academy of Sciences*, 109(11), 4181-4186.
- Rivas-Ubach, A., Pérez-Trujillo, M., Sardans, J., Gargallo-Garriga, A., Parella, T., & Peñuelas, J. (2013). Ecometabolomics: optimized NMR-based method. *Methods in Ecology and Evolution*, 4(5), 464-473.
- Rivas-Ubach, A., Sardans, J., Hódar, J. A., García-Porta, J., Guenther, A., Oravec, M., ... Peñuelas, J. (2016). Similar local, but different systemic, metabolomic responses of closely related pine subspecies to folivory by caterpillars of the processionary moth. *Plant Biology*, 18(3), 484-494.
- Rivas-Ubach, A., Sardans, J., Hódar, J. A., García-Porta, J., Guenther, A., Paša-Tolić, L., ... Peñuelas, J. (2017). Close and distant: Contrasting the metabolism of two closely related subspecies of Scots pine under the effects of folivory and summer drought. *Ecology and Evolution*, 7(21), 8976-8988.
- Sardans, J., & Peñuelas, J. (2013). Plant-soil interactions in Mediterranean forest and shrublands: impacts of climatic change. *Plant and Soil*, 365(1-2), 1-33.
- Sardans, J., Peñuelas, J., & Rivas-Ubach, A. (2011). Ecological metabolomics: overview of current developments and future challenges. *Chemoecology*, 21(4), 191-225.

- Takats, Z., Wiseman, J. M., & Cooks, R. G. (2005). Ambient mass spectrometry using desorption electrospray ionization (DESI): instrumentation, mechanisms and applications in forensics, chemistry, and biology. *Journal of Mass Spectrometry*, 40(10), 1261-1275.
- Večeřová, K., Večeřa, Z., Dočekal, B., Oravec, M., Pompeiano, A., Tříska, J., & Urban, O. (2016). Changes of primary and secondary metabolites in barley plants exposed to CdO nanoparticles. *Environmental Pollution*, 218, 207-218.
- Weckwerth, W., & Kahl, G. (Eds.). (2013). *The Handbook of Plant Metabolomics*. Chichester: John Wiley & Sons.
- Whitehouse, C. M., Dreyer, R. N., Yamashita, M., & Fenn, J. B. (1989). Electrospray ionization for mass-spectrometry of large biomolecules. *Science*, 246(4926), 64-71.
- Yoshikawa, K., Hirasawa, T., Ogawa, K., Hidaka, Y., Nakajima, T., Furusawa, C., & Shimizu, H. (2013). Integrated transcriptomic and metabolomic analysis of the central metabolism of *Synechocystis* sp. PCC 6803 under different trophic conditions. *Biotechnology Journal*, 8(5), 571-580.
- Yuan, J., Doucette, C. D., Fowler, W. U., Feng, X. J., Piazza, M., Rabitz, H. A., ... Rabinowitz, J. D. (2009). Metabolomics-driven quantitative analysis of ammonia assimilation in *E. coli*. *Molecular Systems Biology*, 5(1), 302.
- Zhou, M., McDonald, J. F., & Fernández, F. M. (2010). Optimization of a direct analysis in real time/time-of-flight mass spectrometry method for rapid serum metabolomic fingerprinting. *Journal of the American Society for Mass Spectrometry*, 21(1), 68-75.

**Authors:** Oravec M<sup>1</sup>, Večeřová K<sup>1</sup>, Gargallo-Garriga A<sup>1,2,3</sup>, Sardans J<sup>2,3</sup>, Urban O<sup>1</sup>

**Reviewers:** Holub P<sup>1</sup>, Klem K<sup>4</sup>, Peñuelas J<sup>2,3</sup>

## Affiliations

<sup>1</sup> Global Change Research Institute, The Czech Academy of Sciences, Brno, Czech Republic

<sup>2</sup> CSIC, Global Ecology Unit CREAF-CSIC-UAB, Bellaterra, Spain

<sup>3</sup> CREAF, Cerdanyola del Vallès, Spain

<sup>4</sup> Mendel University in Brno, Faculty of AgriSciences, Brno, Czech Republic

## 5.12 Reflectance assessment of plant physiological status

**Author:** Filella I<sup>1,2</sup>, Bjerke J W<sup>3</sup> and Macias-Fauria M<sup>4</sup>

**Reviewer:** Peñuelas J<sup>1,2</sup>

**Measurement unit:** unitless; **Measurement scale:** leaf - canopy; **Equipment costs:** €€–€€€; **Running costs:** €; **Installation effort:** low; **Maintenance effort:** low; **Knowledge need:** medium; **Measurement mode:** manual and data logger

Measurements of reflectance can be used not only to assess the biomass of vegetation but also its physiological status. The light reflected by a leaf towards the observer is governed by the concentration of biochemical compounds in the leaf and by the foliar surface and internal structure. Chlorophyll mainly absorbs in the red visible region of the spectrum and partially in the blue and green regions that are also generally absorbed by other pigments such as xanthophylls and carotenoids (Jackson, 1986; Peñuelas & Filella, 1998; Carter & Knapp, 2001; Gitelson et al., 2003). Foliar absorption/reflection in the near-infrared region depends mainly on the structural discontinuities and water content of foliar cells (Peñuelas & Filella, 1998). The analysis of remotely measured reflected light can thus be used to extract information about plant-stress conditions and photosynthetic status for both natural vegetation and crops (Jackson, 1986; Peñuelas & Filella, 1998; Carter & Knapp, 2001; Ustin et al., 2009). More specifically, reflectance could provide a rapid and easy alternative for assessing pigment composition to estimate nutrient status (by assessment of chlorophyll), phenology, and general stress (by assessment of carotenoids and chlorophylls) or photosynthetic efficiency (by assessment of xanthophylls at a daily scale and the chlorophyll/carotenoid ratio at a seasonal scale). Reflectance can also be used to assess the water content of plants (by measuring in the water-absorption band). All these possibilities make reflectance a useful and increasingly used tool for the assessment of plant stress, applicable in most studies that focus on global-change impacts (e.g. drought, water logging, eutrophication).

While the use of reflectance values can provide valuable information about many aspects of plant physiological status, this is acquired indirectly, requiring a correlative dataset between destructively-obtained compound concentrations and reflectance values or indices (combinations of values at certain wavelengths). Thus, reflectance values will not normally represent a “Gold standard” in terms of accuracy (these will be the destructive methods discussed in other protocols in this chapter), but are highly practical since they can generate non-destructive, rapid, and scalable information.

### 5.12.1 What and how to measure?

Reflectance can be detected using narrow-bandwidth spectroradiometers that measure in the visible and near-infrared regions of the spectrum. In addition to reflectance at particular wavelengths, many high spectral resolution reflectance vegetation indices (which partly remove disturbances caused by external factors) have been proposed (Peñuelas & Filella, 1998). The entire spectrum can also be used to extract the most integrated information (Ustin et al., 2009). Reflectance measured at a close range (< 1 m) has traditionally been undertaken using narrow-bandwidth spectroradiometers that measure in the visible and near-infrared regions of the spectrum (Filella and Peñuelas, 1994). More

recently, hand-held optical sensors have been developed to provide instant readings of different indices, such as PRI (Shrestha et al. 2012) or most frequently of the normalized difference vegetation index (NDVI) (Kitić et al., 2019), which is based on the leaf reflectance in the NIR and red bandwidths (also see protocol 5.2). Some sensors are built into digital cameras so that single NDVI values can be retrieved at pixel scale. Such readings can be used for upscaling, by comparing with NDVI data measured from Unmanned Aerial Vehicles (UAVs) or satellites (Bokhorst et al., 2012). (see [protocol 5.2. Chlorophyll and carotenoid content](#)).

### ***Chlorophyll concentration: nitrogen status***

Several studies have reported that indices based on reflectance in the far-red region can precisely estimate foliar chlorophyll concentration (Filella & Peñuelas, 1994; Gitelson & Merzlyak, 1997; Datt, 1999). Foliar optical properties within a relatively narrow spectral band near 700 nm are thus crucial for the detection of plant stress and the estimation of foliar chlorophyll concentration. Chlorophyll concentration can also be derived using reflectances at 675 and 550 nm. Indices of chlorophyll concentration have been developed that include several of these waveband reflectances (Filella et al., 1995; Gitelson & Merzlyak, 1997). Foliar chlorophyll concentration and nitrogen availability are closely correlated, so the assessment of chlorophyll content by reflectance can also be used to characterise the nitrogen status of natural vegetation and crops (Filella et al., 1995; Wang et al., 2016).

### ***Stress: carotenoid/chlorophyll ratio***

Ratios of reflectances in the blue region (where carotenoids and chlorophylls absorb) and the red region (where only chlorophylls absorb) are highly correlated with the carotenoid/chlorophyll ratio in various plant species, both at the foliar and canopy levels (Peñuelas et al., 1994, 1995; Blackburn, 1998; Merzlyak et al., 1999; Sims & Gamon, 2002). (see [protocol 5.2. Chlorophyll and carotenoid content](#)).

### ***Photosynthetic efficiency***

Some of the light energy absorbed by chlorophyll for photosynthesis is lost as heat or fluorescence, and changes in the photosynthetic rate cause complementary changes in fluorescence emission (see [protocol 5.1 Chlorophyll fluorescence](#)) or heat dissipation. Heat dissipation is linked to the xanthophyll de-epoxidation cycle, which has been correlated with reflectance at 531 nm. The photochemical reflectance index (PRI), based on reflectance at 531 nm, measures changes in reflectance caused by the interconversion and dissipation of xanthophylls (Gamon et al., 1992; Peñuelas et al., 1995) and has already been widely tested as a good estimator of light use efficiency (LUE) at the foliar, canopy, and ecosystem levels and various temporal scales (Zhang et al., 2016).

### ***Water content***

Water absorbs in the near-infrared region at 950–970 nm. A reflectance water index has been defined as the ratio R900:R970. This water index has been highly correlated with plant-water content in several species of trees, shrubs, crops, and grasses (Peñuelas et al., 1993, 1997; Serrano et al., 2000).

### ***Canopy measurements***

A detailed description of the methods involved in field spectroradiometric measurements can be found in Milton et al. (2009). Measurements can be made by pointing the sensor (spectroradiometer or optical fibre, depending on the model) at the canopy (either with single measurements or installing the spectroradiometer in fixed measuring structures for continuous measurements). The measured area is a function of the field of view of the instrument and the measuring height. The footprint area should be 100% of the target when measuring a point on a surface. Several readings should be made covering the entire object area to obtain a representative measurement of the object. Radiance reflected from the target must be calibrated against a levelled “white” (~100% reflectance) standard to validate reflectance retrieval (e.g. using a Spectralon panel; Labsphere).

Spectral reflectance at the canopy level is a combination of soil and vegetation reflectance, and the weighting for either of these factors depends on external parameters such as illumination or canopy structure. The source of illumination for field measurements is usually the sun, and the quality of the spectra measured is affected by changes in irradiance and by the position of the sun. Some recommendations to minimise these disturbances have been suggested:

- Illumination conditions must be constant throughout the measurement (clear sky conditions and no changes in cloud cover).
- Measurements should be made around solar midday, when the sun is at its highest position, and the sensor should be pointed vertically downward (nadir) to the measuring surface.
- Reference measurements must be made simultaneously or at least immediately before or after the reflectance measurement.
- The measured surface should not be shaded by the operator or measuring structures.

### ***Foliar measurements***

A leaf clip using either its own light source or natural light can be used for foliar measurements. The illumination conditions and other factors disturbing foliar information are controlled when using clips with their own light sources. Foliar properties can also be measured by pointing an optical fibre or sensor near enough to a horizontal leaf to ensure that the footprint area is the leaf, while avoiding shading the target.

The instruments and calibration panels must be calibrated and in good condition for all types of measurements.

### ***Where to start***

Blackburn (1998), Filella & Peñuelas (1994), Gamon et al. (1992), Gitelson et al. (2003), Peñuelas & Filella (1998), Ustin et al. (2009)

### 5.12.2 Special cases, emerging issues, and challenges

As explained above, some of the energy absorbed by chlorophyll that is not used for photosynthesis is dissipated as heat (and can be estimated by the photochemical reflectance index; PRI), and some is dissipated as fluorescence (see [protocol 5.1 Chlorophyll fluorescence](#)). In addition to the methods for measuring actively induced fluorescence described in [protocol 5.1 Chlorophyll fluorescence](#), emitted fluorescence (sun-induced fluorescence; SIF) can be passively and remotely estimated using spectroradiometers with high spectral resolution (Meroni et al., 2009; Porcar-Castell et al., 2014). The combination of PRI and SIF has greatly improved remote estimates of LUE and GPP in a cornfield (Cheng et al., 2013).

UAVs mounted with various multispectral cameras are increasingly providing exciting opportunities for obtaining indices of canopy reflectance and SIF at desired spatiotemporal resolutions (Zarco-Tejada et al., 2013; Gago et al., 2015), which could provide very specialised information of the physiological status of vegetation at the canopy level. Remote sensing of the physiological characteristics of vegetation canopies is an emerging and rapidly evolving field: only UAV remote sensing will be briefly introduced in this protocol, since spaceborne and airplane-based airborne remote sensing can be used to inform and upscale field measurements but represent techniques that do not fall within field-based ecology protocols and are hence out of the scope of this chapter. The use of UAVs offers the possibility to scale-up measurements, enabling the study of spatial and temporal ranges and resolutions in the dynamics of plant physiology not available with hand-held methodologies alone. Nevertheless, it also adds more complexity to the interpretation of reflectance values. Disturbances in canopy measurements caused by factors such as the position of the sun, the canopy structure, and the heterogeneity of the target represent an additional challenge to data interpretation.

We strongly encourage the reader interested in inferring physiological characteristics of vegetation canopies through the use of UAVs to refer to UAV-specific methodological material. Nevertheless, we briefly mention in here basic UAV *best-practice* advice based on Assmann et al. (2019), who provide a hands-on and detailed protocol of UAV vegetation monitoring using multispectral cameras. Recommendations provided under *Canopy measurements* also apply in here. The following general guidelines, addressed at increasing the replicability and quality of UAV-acquired reflectance data, will apply to hyperspectral cameras mounted on UAVs as well, although at present these are very specialised, expensive, and only used by highly-skilled pilots:

1. *Define the spatial and temporal scales adequate to the research question:* this will determine field planning and technical aspects of the operation, such as flight elevation, speed, and duration, which might be constrained by mechanical limitations of the UAV.
2. *Flight planning:* consider image overlap (it will impact on the mosaicking of the individual images, influencing the number of pixels captured near to nadir – 90° over the target surface, and on overall data size) and flight conditions (e.g. weather and sun angle will impact radiometric calibration).

3. *Ground control points*: to be determined with high-accuracy global navigation systems (e.g. differential GPS). This step is essential for repeatability or for combination with other images.
4. *Radiometric calibration*: commonly used commercial cameras come with images of known spectral characteristics that can be used before and after the flight to calibrate the sensor of the camera.
5. *Flight*: it can be challenging due to sudden changes in weather conditions, or in mechanical failure, especially in respect to the UAVs internal compass.
6. *Data transfer*: frequent back-ups are advised, ideally after every flight.
7. *Image processing*: performed by specialised software, which takes into account the ground control points, the calibration information, and incident light sensor data to account for changes in irradiation during the flight.
8. After point (7), the digital numbers obtained by the sensor have been converted to georeferenced absolute reflectance values, which can then be used in vegetation indices (e.g. NDVI, see [protocol 5.2. Chlorophyll and carotenoid content](#)).

### 5.12.3 References

#### **Theory, significance, and large datasets**

Carter and Knapp (2001), Jackson (1986), Peñuelas & Filella (1998), Ustin et al. (2009)

#### **More on methods and existing protocols**

Milton et al. (2009), Peñuelas & Filella (1998), Ustin et al. (2009)

#### **All references**

Assmann, J. J., Kerby, J. T., Cunliffe, A. M. & Myers-Smith, I. H. (2019). Vegetation monitoring using multispectral sensors — best practices and lessons learned from high latitudes. *Journal of Unmanned Vehicle Systems* 7(1), 54-75.

Blackburn, G. A. (1998). Quantifying chlorophylls and carotenoids at leaf and canopy scales: An evaluation of some hyperspectral approaches. *Remote Sensing of Environment*, 66(3), 273-285.

Bokhorst, S., Tømmervik, H., Callaghan, T. V., Phoenix, G. K. & Bjerke, J. W. (2012) Vegetation recovery following extreme winter warming events in the sub-Arctic estimated using NDVI from remote sensing and handheld passive proximal sensors. *Environmental and Experimental Botany*, 81(1), 18-25.

Carter, G. A., & Knapp, A. K. (2001). Leaf optical properties in higher plants: linking spectral characteristics to stress and chlorophyll concentration. *American Journal of Botany*, 88(4), 677-684.

Cheng, Y. B., Middleton, E. M., Zhang, Q., Huemmrich, K. F., Campbell, P. K., Cook, B. D., ... Daughtry, C. S. (2013). Integrating solar induced fluorescence and the photochemical reflectance index for estimating gross primary production in a cornfield. *Remote Sensing*, 5(12), 6857-6879.

- Datt, B. (1999). A new reflectance index for remote sensing of chlorophyll content in higher plants: tests using *Eucalyptus* leaves. *Journal of Plant Physiology*, 154(1), 30-36.
- Filella, I., & Peñuelas, J. (1994). The red edge position and shape as indicators of plant chlorophyll content, biomass and hydric status. *International Journal of Remote Sensing*, 15(7), 1459-1470.
- Filella, I., Serrano, L., Serra, J., & Peñuelas, J. (1995). Evaluating wheat nitrogen status with canopy reflectance indices and discriminant analysis. *Crop Science*, 35(5), 1400-1405.
- Gago, J., Douthe, C., Coopman, R., Gallego, P., Ribas-Carbo, M., Flexas, J., ... Medrano, H. (2015). UAVs challenge to assess water stress for sustainable agriculture. *Agricultural Water Management*, 153, 9-19.
- Gamon, J. A., Penuelas, J., & Field, C. B. (1992). A narrow-waveband spectral index that tracks diurnal changes in photosynthetic efficiency. *Remote Sensing of Environment*, 41(1), 35-44.
- Gitelson, A. A., & Merzlyak, M. N. (1997). Remote estimation of chlorophyll content in higher plant leaves. *International Journal of Remote Sensing*, 18(12), 2691-2697.
- Gitelson, A. A., Gritz, Y., & Merzlyak, M. N. (2003). Relationships between leaf chlorophyll content and spectral reflectance and algorithms for non-destructive chlorophyll assessment in higher plant leaves. *Journal of Plant Physiology*, 160(3), 271-282.
- Jackson, R. D. (1986). Remote sensing of biotic and abiotic plant stress. *Annual Review of Pytopathology*, 24(1), 265-287.
- Kitić, G., Tagarakis, A., Cselyuszka, N., Panić, M., Birgermajer, S., Sakulski, D. & Matović, J. (2019). A new low-cost portable multispectral optical device for precise plant status assessment. *Computers and Electronics in Agriculture*, 162, 300-308.
- Meroni, M., Rossini, M., Guanter, L., Alonso, L., Rascher, U., Colombo, R., & Moreno, J. (2009). Remote sensing of solar-induced chlorophyll fluorescence: Review of methods and applications. *Remote Sensing of Environment*, 113(10), 2037-2051.
- Milton, E. J., Schaepman, M. E., Anderson, K., Kneubühler, M., & Fox, N. (2009). Progress in field spectroscopy. *Remote Sensing of Environment*, 113, S92-S109.
- Peñuelas, J., & Filella, I. (1998). Visible and near-infrared reflectance techniques for diagnosing plant physiological status. *Trends in Plant Science*, 3(4), 151-156.
- Peñuelas, J., Filella, I., Biel, C., Serrano, L., & Save, R. (1993). The reflectance at the 950–970 nm region as an indicator of plant water status. *International Journal of Remote Sensing*, 14(10), 1887-1905.
- Peñuelas, J., Gamon, J. A., Fredeen, A. L., Merino, J., & Field, C. B. (1994). Reflectance indices associated with physiological changes in nitrogen-and water-limited sunflower leaves. *Remote Sensing of Environment*, 48(2), 135-146.
- Peñuelas, J., Baret, F., & Filella, I. (1995). Semi-empirical indices to assess carotenoids/chlorophyll a ratio from leaf spectral reflectance. *Photosynthetica*, 31(2), 221-230.

- Peñuelas, J., Pinol, J., Ogaya, R., & Filella, I. (1997). Estimation of plant water concentration by the reflectance water index WI (R900/R970). *International Journal of Remote Sensing*, 18(13), 2869-2875.
- Porcar-Castell, A., Tyystjärvi, E., Atherton, J., van der Tol, C., Flexas, J., Pfundel, E. E., ... Berry, J. A. (2014). Linking chlorophyll a fluorescence to photosynthesis for remote sensing applications: mechanisms and challenges. *Journal of Experimental Botany*, 65(15), 4065-4095.
- Serrano, L., Ustin, S. L., Roberts, D. A., Gamon, J. A., & Peñuelas, J. (2000). Deriving water content of chaparral vegetation from AVIRIS data. *Remote Sensing of Environment*, 74(3), 570-581.
- Shrestha, S., Brueck, H., Asch, F. (2012). Chlorophyll index, photochemical reflectance index and chlorophyll fluorescence measurements of rice leaves supplied with different N levels. *Journal of Photochemistry and Photobiology B: Biology*. 113, 7–13.
- Sims, D. A., & Gamon, J. A. (2002). Relationships between leaf pigment content and spectral reflectance across a wide range of species, leaf structures and developmental stages. *Remote Sensing of Environment*, 81(2), 337-354.
- Ustin, S. L., Gitelson, A. A., Jacquemoud, S., Schaepman, M., Asner, G. P., Gamon, J. A., & Zarco-Tejada, P. (2009). Retrieval of foliar information about plant pigment systems from high resolution spectroscopy. *Remote Sensing of Environment*, 113, S67-S77.
- Wang, Z., Wang, T., Darvishzadeh, R., Skidmore, A. K., Jones, S., Suarez, L., ... Hearne, J. (2016). Vegetation indices for mapping canopy foliar nitrogen in a mixed temperate forest. *Remote Sensing*, 8(6), 491.
- Zarco-Tejada, P. J., Morales, A., Testi, L., & Villalobos, F. J. (2013). Spatio-temporal patterns of chlorophyll fluorescence and physiological and structural indices acquired from hyperspectral imagery as compared with carbon fluxes measured with eddy covariance. *Remote Sensing of Environment*, 133, 102-115.
- Zhang, C., Filella, I., Garbulsky, M. F., & Peñuelas, J. (2016). Affecting factors and recent improvements of the photochemical reflectance index (PRI) for remotely sensing foliar, canopy and ecosystemic radiation-use efficiencies. *Remote Sensing*, 8(9), 677.

**Author:** Filella I<sup>1,2</sup>, Bjerke J W<sup>3</sup> and Macias-Fauria M<sup>4</sup>

**Reviewer:** Peñuelas J<sup>1,2</sup>

## Affiliations

<sup>1</sup> CSIC, Global Ecology Unit CREAF-CSIC-UAB, Bellaterra, Spain

<sup>2</sup> CREAF, Cerdanyola del Vallès, Spain

<sup>3</sup> Norwegian Institute for Nature Research – NINA and FRAM – High North Research Centre for Climate and the Environment, Tromsø, Norway

<sup>4</sup> School of Geography and the Environment, University of Oxford, Oxford, UK

## 5.13 Stable isotopes of water for inferring plant function

**Authors:** Goldsmith GR<sup>1</sup>, Marshall JD<sup>2</sup>, Barbetta A<sup>3</sup>, Lehmann MM<sup>4</sup>

**Reviewer:** Cernusak LA<sup>5</sup>

**Measurable unit:** ratio of heavy to light isotope in per mil (‰) relative to standard; **Measurement scale:** precipitation, soil, and/or plant tissue; **Equipment costs:** €€€; **Running costs:** €; **Installation effort:** medium; **Maintenance effort:** medium; **Knowledge need:** high; **Measurement mode:** manual and data logger

Stable isotopes of hydrogen and oxygen in water, as well as plant organic materials formed using such water, have become an important tool for determining plant functional responses to the environment. Stable isotopes of water vary naturally as a function of both physical and biophysical processes as they move through the ecohydrological cycle (Gat, 2005). These variations depend on differences in the rate of evaporation and condensation between water molecules containing the light and heavy isotopes. The measurement of the ratio of the heavy to light isotopes of a given element present in a sample (i.e.  $^{18}\text{O}/^{16}\text{O}$  of leaf material, as interpreted relative to an international reference standard; Coplen, 2011) can be studied to trace the source and physical movement of those isotopes through plants, or as a record of the impact of plant biophysical processes on those isotopes (Dawson et al., 2002).

In particular, stable isotopes of water are powerful tools for interpreting how the sources of water taken up by roots vary across time and space among different plants (Brooks et al., 2010; Allen et al., 2019). Soil water reflects the isotopic composition of precipitation. In seasonal climates, winter precipitation generally is depleted in the heavy isotope and therefore has a more negative isotope ratio (Marshall et al., 2007). In turn, the isotopic composition of water taken up by plants into the xylem is altered when it reaches the evaporative sites within leaves through the process of leaf transpiration: these changes subsequently become recorded in plant organic matter (e.g. sugars) via photosynthesis. Given that transpiration is strongly controlled by plant water supply and demand (Cernusak et al., 2016), stable isotopes of hydrogen and oxygen in plant organic matter reflect the environmental conditions (particularly leaf-to-air vapour pressure deficit) in which metabolic processes occurred and the metabolic response to those conditions (Helliker & Richter, 2008; Kahmen et al., 2011; Song et al., 2011). Stable isotope ratios of hydrogen and oxygen recorded in leaf sugars, leaf tissue, phloem sap, and tree rings thus reflect plant biophysical responses recorded at different time scales (Roden et al., 2000; Cernusak et al., 2003; Gessler et al., 2009). In this respect, stable isotopes of hydrogen and oxygen are unique from instantaneous measurements. Moreover, because sample collection in the field can often be carried out relatively quickly, observations of hydrogen and oxygen isotopes can increase the breadth and depth of a study across time, space, and other variables of interest.

When used in combination with other measurements of stress physiology, stable isotopes represent a powerful means of understanding how environment affects water use among different plants and this is of particular interest for interpreting the effects of climate change in both experimental (e.g. Barbetta et al., 2015) and observational contexts (e.g. Treydte et al., 2007; Saurer et al., 2016; also see [protocol 5.5 Leaf temperature](#)). Similarly, the techniques described here can be applied to

understand other global-change drivers, such as soil fertilisation (Brooks & Mitchell, 2011) and invasive species (Reynolds & Cooper, 2010).

### 5.13.1 What and how to measure?

#### $\delta^{18}\text{O}$ and $\delta^2\text{H}$ of water

Stable isotopes of water are frequently used as a means of inferring the source of water taken up by plants (Brooks et al., 2010; Goldsmith et al., 2012; West et al., 2012; Barbata et al., 2015), as well as for inferring how plant water availability and demand (driven by environmental conditions) has affected the process of transpiration (Wang & Yakir, 1995; Ripullone et al., 2008; Kahmen et al., 2013). Given that water availability is frequently a limiting factor for plant function, there is considerable interest in understanding how plant water use will change given projected scenarios of global climate change.

Using water isotopes as a means of inferring plant function requires carefully constraining the different sources of water that can be used by plants. This begins with observing the isotope ratios of precipitation (e.g. rain, snow, fog, dew) at the study location. Where direct observations are not possible, data from monitoring networks (e.g. the Global Network of Isotopes in Precipitation – GNIP), or from geospatial interpolations of monitoring networks (e.g. [waterisotopes.org](http://waterisotopes.org)), can also be used, but these data may be less accurate and precise depending on the temporal and spatial resolution of measurements upon which the estimations are based. Precipitation isotopes are generally collected at an open site using a collector designed to prevent any evaporation (and thus isotopic fractionation) – see Ingraham (1998) for details. However, it is important to note that the isotopic composition of throughfall (i.e. after passage through the plant canopy) is likely to differ from that of precipitation and will thus more accurately represent the water entering soil (Allen et al., 2017). Throughfall mixes into the existing soil and groundwater pools, where it then becomes available to serve as the primary source of water for plants (but see Lehmann et al., 2017).

Soil samples can be collected using either a soil corer, or by opening a soil pit and sampling into the face of the pit where soil water has not been subject to evaporative fractionation while the pit was prepared. Both methods have drawbacks. The soil corer is prone to compaction and thus makes it difficult to estimate the depth of the soil being sampled, while soil pits are time consuming to dig. Given the heterogeneity of soils, it may be better to use a soil corer and tradeoff the accuracy of knowing soil depth in favour of better constraining the range of possible soil waters being used by the plants of interest. Experimental designs that representatively sample both vertical and horizontal space are likely to yield the most accurate results. Where possible, it is also informative to sample groundwater from a monitoring bore, a well or a tap with a local source, discarding the initial water sample to avoid evaporative fractionation. Soil water isotopic signals reflect seasonal changes in the soil-water pool and should be sampled as frequently as possible.

Finally, water can be collected from plant xylem in either roots or woody stems. Fractionation associated with root water uptake is likely to be limited (but see Vargas et al., 2017), but it has been consistently reported from particularly dry and/or saline environments (Ellsworth & Williams, 2007; Zhao et al., 2016). Tissue that is not suberised (e.g. leaves or green stems, as compared to woody and

brown stems) is subject to evaporative fractionation and thus does not represent the water being taken up by the plant (Dawson & Ehleringer, 1993; Martín-Gómez et al., 2017).

In all cases, samples must be collected in such a way as to prevent any possible evaporation (e.g. glass vial with screw-top lid), sealed immediately, and cooled (if possible) to reduce the possibility of isotopic fractionation *ex post facto*. With the exception of water from precipitation, water in matrices such as soil and plant tissue is generally extracted prior to analysis. The most common form of extraction is cryogenic vacuum distillation (West et al., 2006; Koeniger et al., 2011). In brief, the vial with the sample is connected to another empty vial. The sample is frozen under liquid nitrogen, lowering the water vapour pressure to nearly zero, and the air is then pumped away and evacuated from both connected vials. The vial with the sample is then heated while the empty vial is maintained in liquid nitrogen. The water vapour pressure rises in the heated tube and, because of the near vacuum, it diffuses rapidly to be condensed in the vial under liquid nitrogen. Ideally, the extraction continues until vacuum returns, at which point all the water has been extracted into the second vial. There are also other forms of extraction (e.g. microwave extraction; Munksgaard et al., 2014), as well as direct equilibration (Scrimgeour, 1995; Song & Barbour, 2016). Users are advised to validate their methods to improve confidence in their results.

Finally, the isotope ratios can then be measured by means of an isotope ratio mass spectrometer (IRMS). The IRMS is a specialised piece of lab equipment that requires significant resources – where instrumentation is not available locally, it is possible to identify other labs that will analyse samples at a reasonable cost. Quality control standards and data on the long-term accuracy and precision of the instrumentation are important for appropriate interpretation of the results.

### **$\delta^{18}\text{O}$ of bulk leaf organic material**

The incorporation of oxygen isotopes from water into plant organic material has emerged as an important means of tracking plant functional response to environment, particularly with respect to stomatal conductance (Barbour et al., 2000), leaf temperature (Helliker & Richter, 2008; also see protocol 5.5 Leaf temperature), and especially for understanding the ratio of leaf to air vapour pressure (Kahmen et al., 2011). This relies on the observation that the transpiration rate is coupled to the fractionation of leaf water, whereby light water isotopes are preferentially evaporated and the remaining pool of leaf water is thus enriched in heavy water isotopes. The extent of this enrichment is subsequently recorded in leaf organic materials through the incorporation of oxygen isotopes from water into photosynthetic products. The most common way to measure this is to observe the oxygen isotope ratios of bulk leaf organic material ( $\delta^{18}\text{O}_{\text{BL}}$ ).

Importantly, leaf water enrichment is often heterogeneous and sampling of leaves must account for this possibility. Enrichment can reflect a gradient from the bottom to the top of the leaf (e.g. grasses), from the veins to the margins (e.g. broad leaves), or alternatively, reflect multiple isotopically distinct pools of water within the leaf (Song et al., 2013; Roden et al., 2015; Cernusak et al., 2016). This enrichment is reflected in the leaf organic material and as such, it is critical to adapt sampling protocols for the leaf form of interest. For instance, some studies remove the primary vein(s) and only use the leaf lamina (Kimak et al., 2015). However, this can be difficult to achieve for leaf forms such as grasses or needles (Roden et al., 2015; Liu et al., 2017). Sampling is usually

confined to mature leaves that do not show signs of senescence and the location of sample collection in the canopy (with accompanying differences in microclimate) should be carefully considered.

Freshly sampled leaf material should rapidly be cooled in order to stop any metabolic activity (e.g. by using dry ice or liquid nitrogen). Subsequently, the leaf material should be kept frozen at -20 °C and freeze-dried. This procedure is particularly important for  $\delta^{18}\text{O}$  in leaf material, as some compounds, such as sugars, can continue to exchange oxygen isotopes with the remaining leaf water, altering the original isotope ratio relative to the time of original sampling (Lehmann et al., 2017). After drying, the leaf material can be milled to a fine powder by a steel ball mill, transferred into silver capsules, and the  $\delta^{18}\text{O}$  value determined by TC/EA-IRMS. While isotope analysis of  $\delta^{18}\text{O}_{\text{BL}}$  is straightforward, the analysis of  $\delta^2\text{H}$  in bulk leaf material is still problematic from a methodological perspective. Thus, most researchers studying hydrogen isotopes extract and purify individual compounds from leaves such as cellulose, fatty acids, or alkanes and determine their respective  $\delta^2\text{H}$  values.

### **$\delta^{18}\text{O}$ and $\delta^2\text{H}$ analysis of leaf cellulose**

For  $\delta^{18}\text{O}$ , soluble sugars and starch may not yet have exchanged all of their oxygen atoms with local water, as occurs during synthesis of structural compounds such as cellulose. Thus, there exists the possibility that variation in non-structural carbohydrate concentrations among leaves may introduce some variability into the  $\delta^{18}\text{O}_{\text{BL}}$ . For this reason, some authors have preferred to first extract cellulose from bulk tissue, which is then subject to  $\delta^{18}\text{O}$  analysis on the TC/EA-IRMS. In general, the difference between  $\delta^{18}\text{O}$  of bulk tissue and  $\delta^{18}\text{O}$  of cellulose extracted from it was shown to be less variable for wood than for leaves (Barbour et al., 2001; Cernusak et al., 2004). Thus, the decision as to whether or not cellulose extraction is necessary prior to  $\delta^{18}\text{O}$  analysis of organic material will likely be context-specific, depending on the tissue type (e.g. leaf v. wood), the number of different species analysed, and the treatments imposed on those species (e.g. less than a day v. years).

Leaf cellulose in particular functions as a record of the climatic conditions a plant has specifically experienced during leaf development and can be employed in an experimental context (Helliker & Ehleringer, 2002; Gamarra et al., 2016; Lehmann et al., 2017). Since leaf cellulose is a stable compound with a long lifetime and very low turnover, repeated measurements are generally not necessary (Kimak et al., 2015). More generally, the isotopic analysis of any dateable plant material, such as the cellulose of annual rings in stem tissues (i.e. tree-ring cellulose), can be valuable for reconstructing past plant physiological responses to climatic conditions or shifts in available water sources (Treydte et al., 2014; Saurer et al., 2016).

Several laboratory protocols have been established for isotope analysis of cellulose (Boettger et al., 2007). Many of them follow a similar procedure, in which small pieces of leaf or wood material are packed into small Teflon bags, then i) bleached using an acidic  $\text{NaClO}_2$  solution to remove lignin for several days, ii) purified with  $\text{NaOH}$  to remove fatty acids, oils, and hemicellulose, and iii) washed with deionized water and  $\text{HCl}$  solutions. The remaining cellulose is dried in an oven or freeze-dryer and stored in a dry place until measurement. Additionally, some protocols use an ultrasonicator to homogenise the cellulose material (Weigt et al., 2015). An alternative method has also been developed in which delignification and removal of non-cellulosic polysaccharides takes place within a single step through addition of a mixture of acetic and nitric acid to the plant material, which is located in screw-top vials with silicone O-ring seals (Brendel et al., 2000). Advantages of this method

are that it is relatively fast and that it can be applied to small samples. In either case, the purity of the cellulose extraction can be tested against standards using infrared spectroscopy (Rinne et al., 2005).

The prepared cellulose material can then be transferred to silver capsules and the  $\delta^{18}\text{O}$  value determined by TC/EA-IRMS. This procedure is different for  $\delta^2\text{H}$  values. Due to a high proportion of oxygen-bound hydrogen in cellulose that constantly exchanges with atmospheric humidity or water, accurate  $\delta^2\text{H}$  values of the non-exchangeable carbon-bound hydrogen (holding useful information on plant physiology) cannot be easily inferred from unprepared cellulose. To overcome this problem, cellulose must be chemically converted to cellulose nitrate (DeNiro, 1981), or equilibrated with water vapour of a known isotopic ratio (Wassenaar et al., 2015).

### **$\delta^{18}\text{O}$ and $\delta^2\text{H}$ analysis of non-structural carbohydrates**

Isotope analysis of non-structural carbohydrates, such as sugars or starch, have a higher turnover than cellulose and thus reflect the influence of short-term environmental effects on a daily or weekly time scale. Also, as noted above, the isotopic composition of these compounds may be more representative of the initial products of photosynthesis, as there will have been fewer opportunities for non-structural carbohydrates to have exchanged atoms with local water than the end products of biosynthetic pathways (e.g. cellulose and lignin). As such, the measurement of the isotope ratios of oxygen and hydrogen in non-structural carbohydrates may be of interest for understanding how trees respond to short-term environmental changes (Lehmann et al., 2018).

Recent methodological developments have made the measurement of  $\delta^{18}\text{O}$  and  $\delta^2\text{H}$  values of individual sugars, starches, and other compounds more readily accessible (Wassenaar et al., 2015; Lehmann et al., 2016). The water-soluble compounds can be easily extracted with water or methanol/chloroform/water (MCW) solutions for a short time with heating. This bulk fraction can then be freed from non-sugar compounds such as amino acids, organic acids, and polyphenols by ion-exchange chromatography and the neutral bulk sugars collected in water (Rinne et al., 2012; Lehmann et al., 2015). For starch extraction and purification, the water insoluble material can be washed repeatedly with water or MCW and the starch extracted enzymatically (Wanek et al., 2001; Richter et al., 2009). The breakdown of starch results in a mix of sugars (e.g. glucose and maltose). Both bulk sugars and starch-derived sugars can then be pipetted into silver capsules, frozen, freeze-dried, and the  $\delta^{18}\text{O}$  values determined by TC/EA-IRMS. Importantly, the samples should remain frozen between analyses to reduce the possibility of oxygen isotope exchange (Lehmann et al., 2017). To determine the  $\delta^2\text{H}$  values of bulk sugars and starch-derived sugars, samples should be equilibrated with water vapour of a known isotopic ratio before analysis by TC/EA-IRMS (Wassenaar et al., 2015).

### **Where to start**

Barbour (2007), Cernusak et al. (2016), Dawson & Ehleringer (1998), Gat (2005), Gessler et al. (2009), Roden et al. (2000), Werner et al. (2012)

### **Interpretation**

**$\delta^{18}\text{O}$  and  $\delta^2\text{H}$  of water.** At landscape scales, source water isotope ratios (e.g. snow and rainfall) vary as a function of a number of different factors. While the temperature at which the source water was formed is the primary control, there are additional effects imposed by latitude, continental landmasses, altitude, and storm event size (Dansgaard, 1964). On top of these are local effects of fractionation and mixing driven by canopy interception and transit into the soil, all of which can contribute to the formation of a distinct profile of soil water isotope composition as a function of depth below the surface (Sprenger et al., 2016). The variation in the isotopic composition of water available to plants in the soil is, in turn, used to interpret how the sources of water taken up by roots vary across time and space.

In particular, there are three primary methods used for inferring the relative proportion of water taken up by plants from different sources within the ground using stable isotopes. The first is graphical inference carried out by matching the isotope composition of the water in xylem with that of the soil using either one or both isotopes (Brunel et al., 1995). The second is the use of a two-source (Dawson & Pate, 1996) or multi-source mixing model (Phillips & Gregg, 2003; Parnell et al., 2013) that statistically solves the relative contributions of the different possible soil-water sources to the xylem water. The third is the use of an analytical and physically based model (Ogle et al., 2004) that incorporates additional information on the plant–soil interface. For all of these methods, the ability to resolve the sources of water observed in the plant xylem increases with the sampling resolution of the potential soil-water sources, as well as with the magnitude of differences among those soil-water sources. Rothfuss & Javaux (2017) provide a detailed review and comparison of these methods.

Finally, vertical profiles of water isotope values are sometimes flat or bimodal, which complicates inferences of depth of water uptake. In these instances, addition of isotopically labelled water to the soil surface, or below it (Beyer et al., 2016), may be of value (Koeniger et al., 2010). D<sub>2</sub>O is a common choice and relatively inexpensive. Changes in deuterium excess (D-excess =  $\delta^2\text{H}/8 - \delta^{18}\text{O}$ ) provide a high signal-to-noise ratio and can be a useful metric for interpretation (Lai & Ehleringer, 2011).

As noted above, the isotopic composition of water in leaves differs from the xylem due to the effects of transpiration. Evaporation of water from the leaf enriches the isotopic composition of the remaining leaf water due to i) an equilibrium fractionation associated with phase change from liquid to vapour and ii) a kinetic fractionation associated with diffusion through the stomata and boundary layer. The magnitude of this fractionation depends on the isotopic composition of both the source water and the atmospheric water vapour, as well as on the ratio of ambient air vapour pressure to leaf intracellular vapour pressure. This enrichment can be modelled using an approach originally developed for well-mixed surface waters and subsequently modified expressly for transpiration (Craig & Gordon, 1965; Dongmann et al., 1974). Cernusak et al. (2016) provide a detailed review of leaf water isotopes.

**$\delta^{18}\text{O}$  of organic material.** The  $\delta^{18}\text{O}$  of organic material reflects the effects of evaporative enrichment on leaf water isotopes used for photosynthesis. However, the  $\delta^{18}\text{O}$  of organic material differs from that of leaf water due to fractionation that occurs when oxygen is incorporated into organic molecules. This “biosynthetic” isotope fractionation factor ( $\varepsilon_0$ ) results in a c. 27‰ enrichment of organic material (including bulk organic matter, cellulose, and non-structural carbohydrates)

compared to the water used for synthesis. The  $\varepsilon_o$  reflects a reversible hydration reaction on carbonyl groups during photosynthetic carbohydrate biosynthesis (DeNiro & Epstein, 1981; Sternberg & DeNiro, 1983). There is evidence for a temperature dependency of  $\varepsilon_o$  (Sternberg & Ellsworth, 2011) and it may be important to account for this in some cases. For cellulose from tree rings, enrichment of 27 ‰ above source water is often observed (Saurer et al., 1997; Treydte et al., 2007). However, it has recently been observed that the  $\varepsilon_o$  of sucrose in grass and tree species can be higher than 27 ‰ (Lehmann et al., 2017).

The  $\delta^{18}\text{O}$  of organic material is further altered by oxygen isotope-exchange reactions occurring between carbohydrate carbonyl groups and water after photosynthesis (Hill et al., 1995; Lehmann et al., 2017). These isotopic exchange processes occur in leaves, but also during translocation of sugars (i.e. from leaves to the stem or roots). Such isotopic exchange dampens the leaf water signal that is imprinted on the organic material by partially incorporating the un-enriched source water signal (Farquhar et al., 1998; Barbour & Farquhar, 2000). Some studies, which use the isotopic composition of tree-ring cellulose to model environmental conditions and plant responses, have found that these post-photosynthetic isotope-exchange processes are relatively constant and that this parameter can be easily implemented into models (Roden et al., 2000; Sternberg, 2009). Other studies have found that these isotopic exchange processes are much more variable and change with tree species, soil moisture conditions, and precipitation amount (Gessler et al., 2013; Pflug et al., 2015; Cheesman & Cernusak, 2017). Recognition of these processes is critical for the accurate interpretation of oxygen isotopes in plant tissues.

**$\delta^2\text{H}$  of organic material.** The  $\delta^2\text{H}$  values in plants are influenced by several isotope fractionations that can be separated into photoautotrophic and heterotrophic processes (Yakir & DeNiro, 1990). Photoautotrophic isotope fractionations ( $\varepsilon_{\text{HA}}$ ) are assumed to cause a partial  $^2\text{H}$ -depletion in carbohydrates. The mechanism for  $\varepsilon_{\text{HA}}$  is most likely related to incorporation of  $^2\text{H}$ -depleted hydrogen derived from water photolysis processes, which is then transferred in the Calvin cycle to carbohydrates via NADPH (Estep & Hoering, 1981; Yakir & DeNiro, 1990). The triose phosphates from the Calvin cycle and their descendants experience an additional set of heterotrophic isotopic fractionations ( $\varepsilon_{\text{HH}}$ ) during hexose and sucrose biosynthesis, causing a  $^2\text{H}$ -enrichment in non-structural carbohydrates (Yakir & DeNiro, 1990; Zhang et al., 2009).  $\varepsilon_{\text{HH}}$  can occur in both photoautotrophic (leaves) and heterotrophic tissues (phloem, roots) and is able to affect carbon-bound hydrogen. Although the carbon-bound hydrogen is non-exchangeable from a chemical point of view, the mechanism for  $\varepsilon_{\text{HH}}$  can be partially explained by hydrogen isotope exchange reactions with (leaf) water in enzymatic catalysed reactions by aldolases or isomerases (Yakir, 1992; Schleucher et al., 1999; Augusti et al., 2006). In heterotrophic tissues,  $^2\text{H}$ -enriched hydrogen in carbohydrates and cellulose can also derive from NADPH originating from enzymatic reactions of the oxidative pentose phosphate pathway and tricarboxylic acid cycle (Zhang et al., 2009).

The  $\delta^2\text{H}$  values of non-structural carbohydrates and cellulose are known to be lower than those of the leaf water used for synthesis and to vary largely among tissues and species (Luo & Sternberg, 1992; Loader et al., 2014). For instance,  $\delta^2\text{H}$  values of cellulose derived from photosynthetic tissues have been found to be higher in CAM plants than those of C<sub>3</sub> plants (Sternberg et al., 1984). Also, the  $\delta^2\text{H}$  values among compounds of different functional groups (i.e. lipids, carbohydrates, proteins) show a very high variability in plants, making hydrogen isotopes an ideal tool to investigate biochemical processes within plants that cannot be inferred from oxygen or other isotopes (Schmidt

et al., 2007; Sachse et al., 2012). However, the interpretation of  $\delta^2\text{H}$  variations in plant material remains difficult and additional studies will be necessary to realise the full utility of this approach.

### 5.13.2 Special cases, emerging issues, and challenges

#### *Special cases*

The paired study of stable isotopes of oxygen and carbon in plant organic material (particularly with respect to leaves) can be a particularly powerful approach for providing insights not available from oxygen or carbon isotopes alone (Scheidegger et al., 2000). Additional details are provided in protocol 5.15 Water-use efficiency.

#### *Emerging methods*

While isotope ratio mass spectrometry has long been considered the gold standard for the measurement of hydrogen and oxygen isotope ratios of water and remains the only means of measuring organic samples, isotope ratio infrared spectroscopy (IRIS) has emerged as a rapid, economical, and low maintenance method for making measurements of both discrete liquid water samples and continuous measurements of water vapour in real time (Wen et al., 2012). It is now well established that these laser-based instruments are vulnerable to interference with the absorption spectra associated with the presence of volatile organic compounds (e.g. alpha-pinene) that are often found in water extracted from plants (West et al., 2010, 2011). Such effects appear to be more limited in the context of soil water, although they may still be present. Both pre- and post-measurement methods have been developed to mitigate these effects (Martín-Gómez et al., 2015; Chang et al., 2016; Johnson et al., 2017), but so far, these methods have not completely resolved the problem and it remains critical to validate the IRIS measurements on IRMS. Nevertheless, the development of this technology has facilitated exciting advances in our ability to understand how water moves through the soil–plant–atmosphere continuum in real time. This includes continuous *in situ* monitoring of soil and plant xylem water isotopes that is likely to provide compelling new insights into plant water use in response to changing plant water supply and demand (Volkmann & Weiler, 2014; Volkmann et al., 2016; Oerter et al., 2017).

In addition to IRIS, advances in IRMS are also opening new doors for research. Plant metabolic processes or isotopic exchange can alter the isotopic signal before it is ultimately transferred to a stable compound that is functioning as a biomarker (Lehmann et al., 2017). Identifying and understanding these hidden isotope fractionation processes and how they respond to changing climatic signals is often not straightforward, but it is necessary to improve the precision and accuracy of their application. To open this black box, compound-specific isotope analysis (CSIA) by gas chromatography/pyrolysis-IRMS (GC/Pyr-IRMS) is emerging as a useful tool for determining  $\delta^{18}\text{O}$  or  $\delta^2\text{H}$  of particular biomarkers and their precursors, including specific carbohydrates (Lehmann et al., 2016), hemicellulose (Zech & Glaser, 2009), n-alkanes (Sachse et al., 2012), and levoglucosan (Blees et al., 2017). While much of this work remains in development, CSIA holds significant promise for becoming a means of directly tracking plant functional response to environment from source to sink, as well as for improving our existing use of stable isotopes of water.

### **Challenges**

The use of stable isotopes of hydrogen and oxygen as a means of answering questions regarding plant function is currently an active field of research. This includes innovations in methods development (e.g. continuous *in situ* monitoring of water isotopes; Volkmann & Weiler, 2014), as well as cautions regarding the use of existing methods (e.g. differences among methods used for extracting water from matrices; Orlowski et al., 2016). It also includes advances in our understanding of how hydrogen and oxygen isotopes fractionate and mix in the soil (e.g. Gaj et al., 2017), upon uptake (Vargas et al., 2017), and in plants (e.g. Goldsmith et al., 2017) and, as such, there will remain a premium on the careful design, implementation, and interpretation of hydrogen and oxygen isotopes based on the latest research.

### **5.13.3 References**

#### ***Theory, significance, and large datasets***

Barbour (2007), Cernusak et al. (2016), Evaristo et al. (2015), Gat (2005), Scheiddiger et al. (2000)

#### ***More on methods and existing protocols***

Lehmann et al. (2016), Loader et al. (2014), Martín-Gómez et al. (2015), Rothfuss & Javaux (2017), West et al. (2006)

#### ***All references***

- Allen, S. T., Keim, R. F., Barnard, H. R., McDonnell, J. J., & Brooks, J. R. (2017). The role of stable isotopes in understanding rainfall interception processes: a review. *Wiley Interdisciplinary Reviews: Water*, 4(1), e1187.
- Allen, S. T., Kirchner, J. W., Braun, S., Siegwolf, R. T. W., & Goldsmith, G. R. (2019). Seasonal origins of water used by trees. *Hydrology and Earth Systems Sciences*, 23(2), 1199-1210.
- Augusti, A., Betson, T. R., & Schleucher, J. (2006). Hydrogen exchange during cellulose synthesis distinguishes climatic and biochemical isotope fractionations in tree rings. *New Phytologist*, 172(3), 490-499.
- Barbeta, A., Mejía-Chang, M., Ogaya, R., Voltas, J., Dawson, T. E., & Peñuelas, J. (2015). The combined effects of a long-term experimental drought and an extreme drought on the use of plant-water sources in a Mediterranean forest. *Global Change Biology*, 21(3), 1213-1225.
- Barbour, M. M. (2007). Stable oxygen isotope composition of plant tissue: a review. *Functional Plant Biology*, 34(2), 83-94.
- Barbour, M. M., & Farquhar, G. D. (2000). Relative humidity-and ABA-induced variation in carbon and oxygen isotope ratios of cotton leaves. *Plant, Cell & Environment*, 23(5), 473-485.
- Barbour, M. M., Fischer, R. A., Sayre, K. D., & Farquhar, G. D. (2000). Oxygen isotope ratio of leaf and grain material correlates with stomatal conductance and grain yield in irrigated wheat. *Functional Plant Biology*, 27(7), 625-637.

- Barbour, M. M., Andrews, J. T., & Farquhar, G. D. (2001). Correlations between oxygen isotope ratios of wood constituents of *Quercus* and *Pinus* samples from around the world. *Australian Journal of Plant Physiology*, 28, 335-348.
- Beyer, M., Koeniger, P., Gaj, M., Hamutoko, J. T., Wanke, H., & Himmelsbach, T. (2016). A deuterium-based labeling technique for the investigation of rooting depths, water uptake dynamics and unsaturated zone water transport in semiarid environments. *Journal of Hydrology*, 533(Supplement C), 627–643.
- Blees, J., Saurer, M., Siegwolf, R. T., Ulevicius, V., Prevôt, A. S., Dommen, J., & Lehmann, M. M. (2017). Oxygen isotope analysis of levoglucosan, a tracer of wood burning, in experimental and ambient aerosol samples. *Rapid Communications in Mass Spectrometry*, 31(24), 2101-2108.
- Boettger, T., Haupt, M., Knöller, K., Weise, S. M., Waterhouse, J. S., Rinne, K. T., ... Schleser, G. H.. (2007). Wood cellulose preparation methods and mass spectrometric analyses of  $\delta^{13}\text{C}$ ,  $\delta^{18}\text{O}$ , and nonexchangeable  $\delta^2\text{H}$  values in cellulose, sugar, and starch: an interlaboratory comparison. *Analytical Chemistry*, 79(12), 4603-4612.
- Brendel, O., Iannetta, P. P. M., & Stewart, D. (2000). A rapid and simple method to isolate pure alpha-cellulose. *Phytochemical Analysis*, 11(1), 7-10.
- Brooks, J. R. & Mitchell, A. K. (2011). Interpreting tree responses to thinning and fertilization using tree-ring stable isotopes. *New Phytologist* 190(3), 770-782.
- Brooks, J. R., Barnard, H. R., Coulombe, R., & McDonnell, J. J. (2010). Ecohydrologic separation of water between trees and streams in a Mediterranean climate. *Nature Geoscience*, 3(2), 100-104.
- Brunel, J. P., Walker, G. R., & Kennett-Smith, A. K. (1995). Field validation of isotopic procedures for determining sources of water used by plants in a semi-arid environment. *Journal of Hydrology*, 167(1-4), 351-368.
- Cernusak, L. A., Wong, S. C., & Farquhar, G. D. (2003). Oxygen isotope composition of phloem sap in relation to leaf water in *Ricinus communis*. *Functional Plant Biology*, 30(10), 1059-1070.
- Cernusak, L. A., Pate, J. S., & Farquhar, G. D. (2004). Oxygen and carbon isotope composition of parasitic plants and their hosts in southwestern Australia. *Oecologia*, 139, 199-213.
- Cernusak, L. A., Barbour, M. M., Arndt, S. K., Cheesman, A. W., English, N. B., Feild, T. S., ... McInerney, F. A. (2016). Stable isotopes in leaf water of terrestrial plants. *Plant, Cell & Environment*, 39(5), 1087-1102.
- Chang, E., Wolf, A., Gerlein-Safdi, C., & Caylor, K. K. (2016). Improved removal of volatile organic compounds for laser-based spectroscopy of water isotopes. *Rapid Communications in Mass Spectrometry*, 30(6), 784-790.
- Cheesman, A. W., & Cernusak, L. A. (2017). Infidelity in the outback: climate signal recorded in  $\Delta^{18}\text{O}$  of leaf but not branch cellulose of eucalypts across an Australian aridity gradient. *Tree Physiology*, 37(5), 554-564.

- Coplen, T. B. (2011). Guidelines and recommended terms for expression of stable-isotope-ratio and gas-ratio measurement results. *Rapid Communications in Mass Spectrometry*, 25(17), 2538-2560.
- Craig, H., & Gordon, L. I. (1965). Deuterium and oxygen 18 variations in the ocean and marine atmosphere. In E. Tongiogi (Ed.) *Proceedings of Stable Isotopes in Oceanographic Studies and Paleotemperatures* (pp. 9-130). V. Lishi e F.
- Dansgaard, W. (1964). Stable isotopes in precipitation. *Tellus*, 16(4), 436-468.
- Dawson, T. E., & Ehleringer, J. R. (1993). Isotopic enrichment of water in the “woody” tissues of plants: implications for plant water source, water uptake, and other studies which use the stable isotopic composition of cellulose. *Geochimica et Cosmochimica Acta*, 57(14), 3487-3492.
- Dawson, T. E., & Ehleringer, J. R. (1998). Plants, isotopes and water use: a catchment-scale perspective. In C. Kendall, & J. J. McDonnell (Eds.), *Isotope Tracers in Catchment Hydrology* (pp. 165-202). Amsterdam: Elsevier Science
- Dawson, T. E., & Pate, J. S. (1996). Seasonal water uptake and movement in root systems of Australian phreatophytic plants of dimorphic root morphology: a stable isotope investigation. *Oecologia*, 107(1), 13-20.
- Dawson, T. E., Mambelli, S., Plamboeck, A. H., Templer, P. H., & Tu, K. P. (2002). Stable isotopes in plant ecology. *Annual Review of Ecology and Systematics*, 33(1), 507-559.
- DeNiro, M. J. (1981). The effects of different methods of preparing cellulose nitrate on the determination of the D/H ratios of non-exchangeable hydrogen of cellulose. *Earth and Planetary Science Letters*, 54(2), 177-185.
- DeNiro, M. J., & Epstein, S. (1981). Isotopic composition of cellulose from aquatic organisms. *Geochimica et Cosmochimica Acta*, 45(10), 1885-1894.
- Dongmann, G., Nürnberg, H. W., Förstel, H., & Wagener, K. (1974). On the enrichment of  $H_2^{18}O$  in the leaves of transpiring plants. *Radiation and Environmental Biophysics*, 11(1), 41-52.
- Ellsworth, P. Z., & Williams, D. G. (2007). Hydrogen isotope fractionation during water uptake by woody xerophytes. *Plant and Soil*, 291(1-2), 93-107.
- Estep, M. F., & Hoering, T. C. (1981). Stable hydrogen isotope fractionations during autotrophic and mixotrophic growth of microalgae. *Plant Physiology*, 67(3), 474-477.
- Evaristo, J., Jasechko, S., & McDonnell, J. J. (2015). Global separation of plant transpiration from groundwater and streamflow. *Nature*, 525(7567), 91–94.
- Farquhar, G. D., Barbour, M. M., & Henry, B. K. (1998). Interpretation of oxygen isotope composition of leaf material. In H. Griffiths (Ed.), *Stable Isotopes: The Integration of Biological, Ecological and Geochemical Processes* (pp. 27-62). Oxford: BIOS Scientific.
- Gaj, M., Kaufhold, S., Koeniger, P., Beyer, M., Weiler, M., & Himmelsbach, T. (2017). Mineral mediated isotope fractionation of soil water. *Rapid Communications in Mass Spectrometry*, 31(3), 269-280.

- Gamarra, B., Sachse, D., & Kahmen, A. (2016). Effects of leaf water evaporative  $^2\text{H}$ -enrichment and biosynthetic fractionation on leaf wax n-alkane  $\delta^2\text{H}$  values in C<sub>3</sub> and C<sub>4</sub> grasses. *Plant, Cell & Environment*, 39(11), 2390-2403.
- Gat, J. R. (2005). *Isotope Hydrology: A Study of the Water Cycle*. World Scientific Publishing Company.
- Gessler, A., Brandes, E., Buchmann, N., Helle, G., Rennenberg, H., & Barnard, R. L. (2009). Tracing carbon and oxygen isotope signals from newly assimilated sugars in the leaves to the tree-ring archive. *Plant, Cell & Environment*, 32(7), 780-795.
- Gessler, A., Brandes, E., Keitel, C., Boda, S., Kayler, Z. E., Granier, A., ... Treydte, K. (2013). The oxygen isotope enrichment of leaf-exported assimilates—does it always reflect lamina leaf water enrichment? *New Phytologist*, 200(1), 144-157.
- Goldsmith, G. R., Muñoz-Villers, L. E., Holwerda, F., McDonnell, J. J., Asbjornsen, H., & Dawson, T. E. (2012). Stable isotopes reveal linkages among ecohydrological processes in a seasonally dry tropical montane cloud forest. *Ecohydrology*, 5(6), 779-790.
- Goldsmith, G. R., Lehmann, M. M., Cernusak, L. A., Arend, M., & Siegwolf, R. T. (2017). Inferring foliar water uptake using stable isotopes of water. *Oecologia*, 184(4), 763-766.
- Helliker, B. R., & Ehleringer, J. R. (2002). Grass blades as tree rings: environmentally induced changes in the oxygen isotope ratio of cellulose along the length of grass blades. *New Phytologist*, 155(3), 417-424.
- Helliker, B. R., & Richter, S. L. (2008). Subtropical to boreal convergence of tree-leaf temperatures. *Nature*, 454(7203), 511-514.
- Hill, S. A., Waterhouse, J. S., Field, E. M., Switsur, V. R., & Ap Rees, T. (1995). Rapid recycling of triose phosphates in oak stem tissue. *Plant, Cell & Environment*, 18(8), 931-936.
- Ingraham, N. L. (1998). Isotopic variations in precipitation. In C. Kendall, & J. J. McDonnell (Eds.), *Isotope Tracers in Catchment Hydrology* (pp. 87-118). Elsevier Science.
- Johnson, J. E., Hamann, L., Dettman, D. L., Kim-Hak, D., Leavitt, S. W., Monson, R. K., & Papuga, S. A. (2017). Performance of induction module cavity ring-down spectroscopy (IM-CRDS) for measuring  $\delta^{18}\text{O}$  and  $\delta^2\text{H}$  values of soil, stem, and leaf waters. *Rapid Communications in Mass Spectrometry*, 31(6), 547-560.
- Kahmen, A., Sachse, D., Arndt, S. K., Tu, K. P., Farrington, H., Vitousek, P. M., & Dawson, T. E. (2011). Cellulose  $\delta^{18}\text{O}$  is an index of leaf-to-air vapor pressure difference (VPD) in tropical plants. *Proceedings of the National Academy of Sciences USA*, 108(5), 1981-1986.
- Kahmen, A., Schefuß, E., & Sachse, D. (2013). Leaf water deuterium enrichment shapes leaf wax n-alkane  $\delta\text{D}$  values of angiosperm plants I: Experimental evidence and mechanistic insights. *Geochimica et Cosmochimica Acta*, 111, 39-49.
- Kimak, A., Kern, Z., & Leuenberger, M. (2015). Qualitative distinction of autotrophic and heterotrophic processes at the leaf level by means of triple stable isotope (C–O–H) patterns. *Frontiers in Plant Science*, 6, 1008.
- Koeniger, P., Leibundgut, C., Link, T., & Marshall, J. D. (2010). Stable isotopes applied as water tracers in column and field studies. *Organic Geochemistry*, 41(1), 31–40.

- Koeniger, P., Marshall, J. D., Link, T., & Mulch, A. (2011). An inexpensive, fast, and reliable method for vacuum extraction of soil and plant water for stable isotope analyses by mass spectrometry. *Rapid Communications in Mass Spectrometry*, 25(20), 3041-3048.
- Lai, C.-T., & Ehleringer, J. R. (2011). Deuterium excess reveals diurnal sources of water vapor in forest air. *Oecologia*, 165(1), 213–223.
- Lehmann, M. M., Rinne, K. T., Blessing, C., Siegwolf, R. T., Buchmann, N., & Werner, R. A. (2015). Malate as a key carbon source of leaf dark-respired CO<sub>2</sub> across different environmental conditions in potato plants. *Journal of Experimental Botany*, 66(19), 5769-5781.
- Lehmann, M. M., Fischer, M., Blees, J., Zech, M., Siegwolf, R. T., & Saurer, M. (2016). A novel methylation derivatization method for δ<sup>18</sup>O analysis of individual carbohydrates by gas chromatography/pyrolysis-isotope ratio mass spectrometry. *Rapid Communications in Mass Spectrometry*, 30(1), 221-229.
- Lehmann, M. M., Gamarra, B., Kahmen, A., Siegwolf, R. T., & Saurer, M. (2017). Oxygen isotope fractionations across individual leaf carbohydrates in grass and tree species. *Plant, Cell & Environment*, 40(8), 1658-1670.
- Lehmann, M. M., Goldsmith, G. R., Schmid, L., Gessler, A., Saurer, M., & Siegwolf, R. T. (2018). The effect of <sup>18</sup>O-labelled water vapour on the oxygen isotope ratio of water and assimilates in plants at high humidity. *New Phytologist*, 217(1), 105-116.
- Loader, N. J., Street-Perrott, F. A., Daley, T. J., Hughes, P. D. M., Kimak, A., Levanic, T., ... van Bellen, S. (2014). Simultaneous determination of stable carbon, oxygen, and hydrogen isotopes in cellulose. *Analytical Chemistry*, 87(1), 376-380.
- Liu, H. T., Yang, F., Gong, X. Y., Schäufele, R., & Schnyder, H. (2017). An oxygen isotope chronometer for cellulose deposition: the successive leaves formed by tillers of a C<sub>4</sub> perennial grass. *Plant, Cell & Environment*, 40(10), 2121-2132.
- Luo, Y. H., & Sternberg, L. (1992). Hydrogen and oxygen isotopic fractionation during heterotrophic cellulose synthesis. *Journal of Experimental Botany*, 43(1), 47-50.
- Marshall, J. D., Brooks, J. R., & Lajtha, K. (2007). Sources of variation in the stable isotopic composition of plants. In R. Michener, & K. Lajtha (Eds.), *Stable Isotopes in Ecology and Environmental Science* (pp. 22-60). Oxford: Blackwell.
- Martín-Gómez, P., Barbata, A., Voltas, J., Peñuelas, J., Dennis, K., Palacio, S., ... Ferrio, J. P. (2015). Isotope-ratio infrared spectroscopy: a reliable tool for the investigation of plant-water sources? *New Phytologist*, 207(3), 914-927.
- Martín-Gómez, P., Serrano, L., & Ferrio, J. P. (2017). Short-term dynamics of evaporative enrichment of xylem water in woody stems: implications for ecohydrology. *Tree Physiology*, 37(4), 511-522.
- Munksgaard, N. C., Cheesman, A. W., Wurster, C. M., Cernusak, L. A., & Bird, M. I. (2014). Microwave extraction-isotope ratio infrared spectroscopy (ME-IRIS): a novel technique for rapid extraction and in-line analysis of δ<sup>18</sup>O and δ<sup>2</sup>H values of water in plants, soils and insects. *Rapid Communications in Mass Spectrometry*, 28(20), 2151-2161.

- Oerter, E. J., Perelet, A., Pardyjak, E., & Bowen, G. (2017). Membrane inlet laser spectroscopy to measure H and O stable isotope compositions of soil and sediment pore water with high sample throughput. *Rapid Communications in Mass Spectrometry*, 31(1), 75-84.
- Ogle, K., Wolpert, R. L., & Reynolds, J. F. (2004). Reconstructing plant root area and water uptake profiles. *Ecology*, 85(7), 1967-1978.
- Orlowski, N., Breuer, L., & McDonnell, J. J. (2016). Critical issues with cryogenic extraction of soil water for stable isotope analysis. *Ecohydrology*, 9(1), 1-5.
- Parnell, A. C., Phillips, D. L., Bearhop, S., Semmens, B. X., Ward, E. J., Moore, J. W., ... Inger, R. (2013). Bayesian stable isotope mixing models. *Environmetrics*, 24(6), 387-399.
- Pflug, E. E., Siegwolf, R., Buchmann, N., Dobbertin, M., Kuster, T. M., Günthardt-Goerg, M. S., & Arend, M. (2015). Growth cessation uncouples isotopic signals in leaves and tree rings of drought-exposed oak trees. *Tree Physiology*, 35(10), 1095-1105.
- Phillips, D. L., & Gregg, J. W. (2003). Source partitioning using stable isotopes: coping with too many sources. *Oecologia*, 136(2), 261-269.
- Reynolds, L. V., & Cooper, D. J. (2010). Environmental tolerance of an invasive riparian tree and its potential for continued spread in the southwestern US. *Journal of Vegetation Science* 21(4), 733-743.
- Richter, A., Wanek, W., Werner, R. A., Ghashghaei, J., Jäggi, M., Gessler, A., ... Bathellier, C. (2009). Preparation of starch and soluble sugars of plant material for the analysis of carbon isotope composition: a comparison of methods. *Rapid Communications in Mass Spectrometry*, 23(16), 2476-2488.
- Rinne, K. T., Boettger, T., Loader, N. J., Robertson, I., Switsur, V. R., & Waterhouse, J. S. (2005). On the purification of  $\alpha$ -cellulose from resinous wood for stable isotope (H, C and O) analysis. *Chemical Geology*, 222(1), 75-82.
- Rinne, K. T., Saurer, M., Streit, K., & Siegwolf, R. T. (2012). Evaluation of a liquid chromatography method for compound-specific  $\delta^{13}\text{C}$  analysis of plant carbohydrates in alkaline media. *Rapid Communications in Mass Spectrometry*, 26(18), 2173-2185.
- Ripullone, F., Matsuo, N., Stuart-Williams, H., Wong, S. C., Borghetti, M., Tani, M., & Farquhar, G. (2008). Environmental effects on oxygen isotope enrichment of leaf water in cotton leaves. *Plant Physiology*, 146(2), 729-736.
- Roden, J. S., Lin, G., & Ehleringer, J. R. (2000). A mechanistic model for interpretation of hydrogen and oxygen isotope ratios in tree-ring cellulose. *Geochimica et Cosmochimica Acta*, 64(1), 21-35.
- Roden, J. S., Kahmen, A., Buchmann, N., & Siegwolf, R. (2015). The enigma of effective path length for  $^{18}\text{O}$  enrichment in leaf water of conifers. *Plant, Cell & Environment*, 38(12), 2551-2565.
- Rothfuss, Y., & Javaux, M. (2017). Reviews and syntheses: Isotopic approaches to quantify root water uptake: a review and comparison of methods. *Biogeosciences*, 14(8), 2199.
- Sachse, D., Billault, I., Bowen, G. J., Chikaraishi, Y., Dawson, T. E., Feakins, S. J., ... Polissar, P. (2012). Molecular paleohydrology: interpreting the hydrogen-isotopic composition of lipid biomarkers

- from photosynthesizing organisms. *Annual Review of Earth and Planetary Sciences*, 40, 221-249.
- Saurer, M., Borella, S., & Leuenberger, M. (1997).  $\delta^{18}\text{O}$  of tree rings of beech (*Fagus silvatica*) as a record of  $\delta^{18}\text{O}$  of the growing season precipitation. *Tellus B: Chemical and Physical Meteorology*, 49(1), 80-92.
- Saurer, M., Kirdyanov, A. V., Prokushkin, A. S., Rinne, K. T., & Siegwolf, R. T. (2016). The impact of an inverse climate-isotope relationship in soil water on the oxygen-isotopic composition of *Larix gmelinii* in Siberia. *New Phytologist*, 209(3), 955-964.
- Scheidegger, Y., Saurer, M., Bahn, M., & Siegwolf, R. (2000). Linking stable oxygen and carbon isotopes with stomatal conductance and photosynthetic capacity: a conceptual model. *Oecologia*, 125(3), 350-357.
- Schleucher, J., Vanderveer, P., Markley, J. L., & Sharkey, T. D. (1999). Intramolecular deuterium distributions reveal disequilibrium of chloroplast phosphoglucose isomerase. *Plant, Cell & Environment*, 22(5), 525-533.
- Schmidt, H.-L., Werner, R. A., Rossmann, A., Mosandl, A., & Schreier, P. (2007). Stable isotope ratio analysis in quality control of flavourings. In H. Ziegler (Ed.), *Flavourings: Production, Composition, Applications, Regulations* (pp. 589-663). Weinheim, Germany: Wiley-VCH.
- Scrimgeour, C. M. (1995). Measurement of plant and soil water isotope composition by direct equilibration methods. *Journal of Hydrology*, 172(1-4), 261-274.
- Song, X., & Barbour, M. M. (2016). Leaf water oxygen isotope measurement by direct equilibration. *New Phytologist*, 211(3), 1120-1128.
- Song, X., Barbour, M. M., Saurer, M., & Helliker, B. R. (2011). Examining the large-scale convergence of photosynthesis-weighted tree leaf temperatures through stable oxygen isotope analysis of multiple data sets. *New Phytologist*, 192(4), 912-924.
- Song, X., Barbour, M. M., Farquhar, G. D., Vann, D. R., & Helliker, B. R. (2013). Transpiration rate relates to within- and across-species variations in effective path length in a leaf water model of oxygen isotope enrichment. *Plant, Cell & Environment*, 36(7), 1338-1351.
- Sprenger, M., Leistert, H., Gimbel, K., & Weiler, M. (2016). Illuminating hydrological processes at the soil-vegetation-atmosphere interface with water stable isotopes. *Reviews of Geophysics*, 54(3), 674-704.
- Sternberg, L. (2009). Oxygen stable isotope ratios of tree-ring cellulose: the next phase of understanding. *New Phytologist*, 181(3), 553-562.
- Sternberg, L., & DeNiro, M. J. D. (1983). Biogeochemical implications of the isotopic equilibrium fractionation factor between the oxygen-atoms of acetone and water. *Geochimica et Cosmochimica Acta*, 47(12), 2271-2274.
- Sternberg, L., & Ellsworth, P. F. V. (2011). Divergent biochemical fractionation, not convergent temperature, explains cellulose oxygen isotope enrichment across latitudes. *PLoS One*, 6(11), e28040.

- Sternberg, L., DeNiro, M. J. D., & Ajie, H. (1984). Stable hydrogen isotope ratios of saponifiable lipids and cellulose nitrate from CAM, C<sub>3</sub> and C<sub>4</sub> plants. *Phytochemistry*, 23(11), 2475-2477.
- Treydte, K., Frank, D., Esper, J., Andreu, L., Bednarz, Z., Berninger, F., ... Grabner, M. (2007). Signal strength and climate calibration of a European tree-ring isotope network. *Geophysical Research Letters*, 34(24), GL031106.
- Treydte, K., Boda, S., Graf Pannatier, E., Fonti, P., Frank, D., Ullrich, B., ... Gessler, A. (2014). Seasonal transfer of oxygen isotopes from precipitation and soil to the tree ring: source water versus needle water enrichment. *New Phytologist*, 202(3), 772-783.
- Vargas, A. I., Schaffer, B., Yuhong, L., & Sternberg, L. (2017). Testing plant use of mobile vs. immobile soil water sources using stable isotope experiments. *New Phytologist*, 215(2), 582-594.
- Volkmann, T. H. M., & Weiler, M. (2014). Continual in situ monitoring of pore water stable isotopes in the subsurface. *Hydrology and Earth System Sciences*, 18(5), 1819.
- Volkmann, T. H., Kühnhammer, K., Herbstritt, B., Gessler, A., & Weiler, M. (2016). A method for in situ monitoring of the isotope composition of tree xylem water using laser spectroscopy. *Plant, Cell & Environment*, 39(9), 2055-2063.
- Wanek, W., Heintel, S., & Richter, A. (2001). Preparation of starch and other carbon fractions from higher plant leaves for stable carbon isotope analysis. *Rapid Communications in Mass Spectrometry*, 15(14), 1136-1140.
- Wang, X. F., & Yakir, D. (1995). Temporal and spatial variations in the oxygen-18 content of leaf water in different plant species. *Plant, Cell & Environment*, 18(12), 1377-1385.
- Wassenaar, L. I., Hobson, K. A., & Sisti, L. (2015). An online temperature-controlled vacuum-equilibration preparation system for the measurement of  $\delta^2\text{H}$  values of non-exchangeable-H and of  $\delta^{18}\text{O}$  values in organic materials by isotope-ratio mass spectrometry. *Rapid Communications in Mass Spectrometry*, 29(5), 397-407.
- Weigt, R. B., Bräunlich, S., Zimmermann, L., Saurer, M., Grams, T. E., Dietrich, H. P., ... Nikolova, P. S. (2015). Comparison of  $\delta^{18}\text{O}$  and  $\delta^{13}\text{C}$  values between tree-ring whole wood and cellulose in five species growing under two different site conditions. *Rapid Communications in Mass Spectrometry*, 29(23), 2233-2244.
- Wen, X. F., Lee, X., Sun, X. M., Wang, J. L., Tang, Y. K., Li, S. G., & Yu, G. R. (2012). Intercomparison of four commercial analyzers for water vapor isotope measurement. *Journal of Atmospheric and Ocean Technology*, 29(2), 235–247.
- Werner, C., Schnyder, H., Cuntz, M., Keitel, C., Zeeman, M. J., Dawson, T. E., ... Kayler, Z. E. (2012). Progress and challenges in using stable isotopes to trace plant carbon and water relations across scales. *Biogeosciences*, 9(8), 3083.
- West, A. G., Patrickson, S. J., & Ehleringer, J. R. (2006). Water extraction times for plant and soil materials used in stable isotope analysis. *Rapid Communications in Mass Spectrometry*, 20(8), 1317-1321.

- West, A. G., Goldsmith, G. R., Brooks, P. D., & Dawson, T. E. (2010). Discrepancies between isotope ratio infrared spectroscopy and isotope ratio mass spectrometry for the stable isotope analysis of plant and soil waters. *Rapid Communications in Mass Spectrometry*, 24(14), 1948-1954.
- West, A. G., Goldsmith, G. R., Matimati, I., & Dawson, T. E. (2011). Spectral analysis software improves confidence in plant and soil water stable isotope analyses performed by isotope ratio infrared spectroscopy (IRIS). *Rapid Communications in Mass Spectrometry*, 25(16), 2268-2274.
- West, A. G., Dawson, T. E., February, E. C., Midgley, G. F., Bond, W. J., & Aston, T. L. (2012). Diverse functional responses to drought in a Mediterranean-type shrubland in South Africa. *New Phytologist*, 195(2), 396-407.
- Yakir, D. (1992). Variations in the natural abundance of oxygen-18 and deuterium in plant carbohydrates. *Plant, Cell & Environment*, 15(9), 1005-1020.
- Yakir, D., & DeNiro, M. J. (1990). Oxygen and hydrogen isotope fractionation during cellulose metabolism in *Lemna gibba* L. *Plant Physiology*, 93(1), 325-332.
- Zech, M., & Glaser, B. (2009). Compound-specific  $\delta^{18}\text{O}$  analyses of neutral sugars in soils using gas chromatography–pyrolysis–isotope ratio mass spectrometry: problems, possible solutions and a first application. *Rapid Communications in Mass Spectrometry*, 23(22), 3522-3532.
- Zhang, X., Gillespie, A. L., & Sessions, A. L. (2009). Large D/H variations in bacterial lipids reflect central metabolic pathways. *Proceedings of the National Academy of Sciences USA*, 106(31), 12580-12586.
- Zhao, L. J., Wang, L. X., Cernusak, L. A., Liu, X. H., Xiao, H. L., Zhou, M. X., & Zhang, S. Q. (2016). Significant difference in hydrogen isotope composition between xylem and tissue water in *Populus euphratica*. *Plant, Cell & Environment*, 39(8), 1848-1857.

**Authors:** Goldsmith GR<sup>1</sup>, Marshall JD<sup>2</sup>, Barbetta A<sup>3</sup>, Lehmann MM<sup>4</sup>

**Reviewer:** Cernusak LA<sup>5</sup>

## Affiliations

<sup>1</sup> Schmid College of Science and Technology, Chapman University, Orange, USA

<sup>2</sup> Department of Forest Ecology and Management, Swedish University of Agricultural Sciences, Umeå, Sweden

<sup>3</sup> INRA, UMR ISPA, Villenave d'Ornon, France

<sup>4</sup> Forest Dynamics, Swiss Federal Institute for Forest, Snow and Landscape Research WSL, Birmensdorf, Switzerland

<sup>5</sup> College of Science and Engineering, James Cook University, Cairns, Australia

## 5.14 BVOC emissions from plants and soils

**Authors:** Llusià J<sup>1,2</sup>, Filella I<sup>1,2</sup>, Sardans J<sup>1,2</sup>

**Reviewer:** Peñuelas J<sup>1,2</sup>

**Measurement unit:**  $\mu\text{g g}^{-1}\text{dm h}^{-1}$ ,  $\text{nmol m}^{-2} \text{s}^{-1}$  or  $\mu\text{g m}^{-2} \text{h}^{-1}$  (**GC-MS, PTR-MS**); **Measurement scale:** site, plot, plant, leaf; **Equipment costs:**  $\text{€€€}$ ; **Running costs:**  $\text{€€€}$ ; **Installation effort:** high; **Maintenance effort:** high; **Knowledge need:** high; **Measurement mode:** manual

Biogenic volatile organic compounds (BVOCs) are a very large variety of molecules including isoprene, terpenes, alkanes, alkenes, alcohols, esters, carbonyls, and acids (Peñuelas & Llusià, 2003). The main producers and emitters of BVOCs are plants, which synthesise them in many different tissues by mean of different physiological processes. Among BVOCs, isoprene, monoterpenes, and sesquiterpenes are synthesised and emitted by several plant species. These volatile isoprenoid compounds have many protective and ecological functions and have important effects on the photochemistry and radiative properties of the atmosphere (Zimmerman et al., 1978; Kavouras et al., 1998; Peñuelas & Llusià, 2003; Owen & Peñuelas, 2005). Consequently, there is great interest in determining the emission capacities of the different species and how environmental factors and especially climate change affect the volatile isoprenoid emissions (Peñuelas & Llusià, 2001). Furthermore, BVOCs affect the chemical and physical properties of the atmosphere and therefore they are considered promoters of climate change (Fehsenfeld et al., 1992; Singh & Zimmerman, 1992; Kesselmeier & Staudt, 1999; Peñuelas & Llusià, 2001, 2003).

### 5.14.1 What and how to measure?

Plant **BVOC emissions** can be measured with different types of chambers measuring gas-exchange. Air samples are collected using an air-sampling pump that direct the air to a stainless steel tube filled with adsorbents. To measure **BVOC contents** in plant tissues, liquid nitrogen is used to maintain the terpenes unaltered and to crush the leaves. Pulverised leaves are then submerged in organic solvent to extract terpenes. Terpene content is calculated per dry weight, after drying plant material until constant weight.

After sampling, BVOC determination is generally performed by using gas chromatography-mass spectrometry (**GC-MS**) or by a proton-transfer-reaction mass spectrometer (**PTR-MS**) system. PTR-MS provides continuous monitoring of BVOCs and it is fast enough to be used in eddy covariance towers to measure BVOC exchange at the ecosystem level, but does not allow speciation of the thousands of BVOCs: for example, it does not distinguish the different monoterpenes that have the same mass. The PTR-MS system and its use in BVOC analysis have been described by Lindinger et al. (1998).

#### ***Sampling, preparation, and analysis of terpene content and emission***

A gas-exchange system is frequently used for sampling plant volatile emissions. Air exiting the cuvette is pumped through a stainless steel tube filled with adsorbents. Air samples are collected using an air-sampling pump. The flow is measured with a flowmeter. Prior to use, these tubes are

conditioned. Emission rate calculations are made on a mass balance basis and by subtracting the control samples without plants from the samples with plants (Llusia et al., 2012).

To measure BVOC contents, plant organs are submerged in liquid nitrogen immediately after sampling and transported to the laboratory. In the laboratory, samples are stored at -20 °C prior to BVOC extraction and analysis. The BVOC extractions are conducted by submerging 1–2 leaves or flowers in liquid nitrogen in a Teflon tube and crushing them with a Teflon pestle. Leaves are thereafter pulverised, and 2 ml of pentane is added to the extract. Before analysis, extracted plant material with pentane is centrifuged at 10,000 rpm for 5 min. The extracts are finally concentrated up to 200 µl with a stream of nitrogen. BVOC content is then calculated per dry weight basis, after drying plant material at a maximum of 70 °C for 72h to constant weight (Llusia et al., 2006; Pérez-Harguindeguy et al., 2013). The temperature and time for drying depend on the study question, how many samples are dried, the size, thickness and type of the plant material (e.g. large, fleshy or succulent leaves need more time) see [protocol 2.1.1 Aboveground plant biomass](#) for more details on the drying. BVOC determination is generally performed using a GC-MS system. Tubes with trapped emitted monoterpenes are inserted in the injector [and](#) desorbed into a chromatographic column. The injector is connected to a gas chromatograph with a mass spectrometer detector. A full-scan method is used in the chromatographic analyses. The desorbed samples are injected into a capillary column. The identification of monoterpenes is conducted by GC-MS and compared with standards from Fluka (Buchs, Switzerland), literature spectra, and GCD Chemstation G1074A HP. Internal standard dodecane that does not mask any terpene, together with frequent calibration with common terpene standards can be used for quantification. Blank samples of air without plants in the cuvette are necessary if clean air input is not used.

To monitor BVOC emissions continuously in time, PTR-MS can be used. The PTR-MS system and its use in BVOC analysis is described in detail by Lindinger et al. (1998). Intact leaves (or the plant organ of study) are clamped in a leaf cuvette. All tubing used is made of inert polytetrafluoroethylene (PTFE). Part of the air exiting the leaf cuvette flows through a T-system (T-shaped tube) to the PTR inlet. For volatile determination and quantification, both the air entering and exiting the leaf cuvette is analysed by PTR-MS and monitored with flow meters. The difference between the concentration of BVOCs before and after passing through the cuvette, along with the flow rates, are used to calculate the BVOC exchange (Peñuelas et al., 2007). The quantification of volatiles is based on the use of calibration standards. PTR-MS is also used in eddy covariance studies to measure BVOCs exchange at the ecosystem level.

### **Where to start**

Lindinger et al. (1998), Llusia et al. (2006, 2012), Peñuelas et al. (2007)

### **5.14.2 Special cases, emerging issues, and challenges**

#### ***Species that store BVOCs***

Some species not only produce and emit terpenes but also store them. The production of terpenoids in terpene-storing plants is highly influenced by abiotic factors (Letchamo et al., 1994; Llusia & Peñuelas, 1998, 2000). Terpene emission rates in terpene-storing plants are not necessarily

determined by terpene content, but the patterns of terpene emission from plants that store terpenes in specialised structures may be different from those of plants not having specialised structures for their storage (Lerdau et al., 1995; Seufert et al., 1995; Loreto et al., 1996; Peñuelas & Llusia, 2001).

### **BVOCs uptake**

In some cases, there are not emissions but uptake of BVOCs, posing an interesting question of impacts of those uptakes. Furthermore, several experiments can be conducted fumigating plants and soils with BVOCs to study the physiological reactions of plants, microbes, and animals.

### **Soil BVOC exchange**

Soil BVOC exchanges (Peñuelas et al., 2014) can be measured *in situ* using a flow-through chamber method. A vented soil chamber system is used with PVC collars installed permanently 3–4 cm into the soil. The collars are covered by a PVC lid with two outlets. Air samples from soil are collected using the same method as for plants described above. Soil measurements are measured *in situ* using a flow-through chamber method. Soil VOCs are sampled and the flow is regulated with a peristaltic pump. The flow adjustment is determined with a flow-meter (Asensio et al., 2008).

### **Improved continuous and fast measurements of BVOC exchange with PTR-TOF-MS**

The conventional PTR-MS (with the analyses performed with a quadrupole mass detector) offers a high temporal resolution, but does not allow the distinguishing of compounds with the same mass, which constitutes an important analytical limitation (Müller et al., 2010). PTR-“time-of-flight”-mass spectrometry (PTR-TOF-MS) couples high sensitivity with high mass resolution, for instantaneous real-time detection of multiple emitted VOCs with unambiguous identification of compounds (Brilli et al., 2014).

### **SPME in dynamic systems**

Another interesting BVOC sampling technique is the use, especially in floral studies, of spme (solid phase micro extraction) columns, i.e. a solid phase extraction sampling technique that involves the use of a fibre coated with an extracting phase (Courtois et al., 2009). Its use is very widespread to analyse mixtures of VOCs in both gaseous and liquid media (headspace), provided they are static systems. Its possible use in dynamic systems is a challenge that would greatly facilitate the study of BVOC emissions in gas-exchange systems.

### **BVOCs and climate change**

Recent data intriguingly link BVOCs with climate. BVOC emissions increase with warming and with most of the other components of the current global environmental change. This increase, apart from influencing the oxidising potential of the troposphere, might produce both negative and positive

feedbacks on warming depending on the spatial scales. Until recently, the short lifetime of BVOCs was thought to preclude them from having a significant direct influence on climate. However, there is emerging evidence that this influence might be important at different spatial scales, from local to regional and global, through aerosol formation and direct and indirect greenhouse effects (Peñuelas & Llusia, 2003; Claeys et al., 2004). BVOCs generate large quantities of organic aerosols (Laaksonen et al., 2008; Jiang et al., 2009; Spracklen et al., 2010) that could affect climate by forming cloud condensation nuclei. The result should be a net cooling of Earth's surface during the day because of radiation interception. Furthermore, the aerosols also diffuse the light received by the canopy increasing CO<sub>2</sub> fixation. However, the BVOCs also increase ozone production and the atmospheric lifetime of methane, thus enhancing the greenhouse effect of these gases. Whether increased BVOC emissions will cool or warm the climate depends on the relative weights of the negative (increased albedo and CO<sub>2</sub> fixation) and positive (increased greenhouse action) feedbacks (Claeys et al., 2004).

### 5.14.3. References

#### *Theory, significance, and large datasets*

BEMA (1997), Kesselmeier & Staudt (1999), Laothawornkitkul et al. (2009), Peñuelas et al. (1995, 2013)

#### *More on methods and existing protocols*

Hewitt et al. (2003), Ormeño et al. (2011), Watson et al. (2001)

#### *All references*

Asensio, D., Peñuelas, J., Prieto, P., Estiarte, M., Filella, I., & Llusia, J. (2008). Interannual and seasonal changes in the soil exchange rates of monoterpenes and other VOCs in a Mediterranean shrubland. *European Journal of Soil Science*, 59(5), 878-891.

BEMA, (1997). BEMA: A European Commission project on biogenic emissions in the Mediterranean area. *Atmospheric Environment*, 31, 1-256.

Brilli, F., Gioli, B., Ciccioli, P., Zona, D., Loreto, F., Janssens, I. A., & Ceulemans, R. (2014). Proton Transfer Reaction Time-of-Flight Mass Spectrometric (PTR-TOF-MS) determination of volatile organic compounds (VOCs) emitted from a biomass fire developed under stable nocturnal conditions. *Atmospheric Environment*, 97, 54-67.

Claeys, M., Graham, B., Vas, G., Wang, W., Vermeylen, R., Pashynska, V., ... Maenhaut, W. (2004). Formation of secondary organic aerosols through photo-oxidation of isoprene. *Science*, 303(5661), 1173-1176.

Courtois, E. A., Paine, C. T., Blandinieres, P. A., Stien, D., Bessiere, J. M., Houel, E., ... Chave, J. (2009). Diversity of the volatile organic compounds emitted by 55 species of tropical trees: a survey in French Guiana. *Journal of Chemical Ecology*, 35(11), 1349.

- Fehsenfeld, F. C., Calvert, J., Fall, R., Goldan, P., Guenther, A. B., Hewitt, N., ... Zimmerman, P. (1992) Emissions of volatile organic compounds from vegetation and the implications for atmospheric chemistry. *Global Biogeochemical Cycles*, 6, 389-430.
- Hewitt, C. N., Hayward, S., & Tani, A. (2003). The application of proton transfer reaction-mass spectrometry (PTR-MS) to the monitoring and analysis of volatile organic compounds in the atmosphere. *Journal of Environmental Monitoring*, 5(1), 1-7.
- Jiang, X., Niu, G. Y., & Yang, Z. L. (2009). Impacts of vegetation and groundwater dynamics on warm season precipitation over the central United States. *Journal of Geophysical Research: Atmospheres*, 114(D6).
- Kavouras, I. G., Mihalopoulos, N., & Stephanou, E. G. (1998). Formation of atmospheric particles from organic acids produced by forests. *Nature*, 395(6703), 683-686.
- Kesselmeier, J. & Staudt, M. (1999). Biogenic volatile organic compounds (VOC): an overview on emission, physiology and ecology. *Journal of Atmospheric Chemistry*, 33, 23-88.
- Laothawornkitkul J., Taylor J. E., Paul N. D., & Hewitt C. N. (2009) Biogenic volatile organic compounds in the Earth System. *New Phytologist*, 183, 27-51.
- Laaksonen, A., Kulmala, M., O'Dowd, C. D., Joutsensaari, J., Vaattovaara, P., Mikkonen, S., ... Petäjä, T. (2008). The role of VOC oxidation products in continental new particle formation. *Atmospheric Chemistry and Physics*, 8(10), 2657-2665.
- Lerdau, M., Matson, P., Fall, R., & Monson, R. (1995). Ecological controls over monoterpene emissions from Douglas fir (*Pseudotsuga menziesii*). *Ecology*, 76(8), 2640-2647.
- Letchamo, W., Marquard, R., Hözl, J., & Gosselin, A. (1994). Effects of water supply and light intensity on growth and essential oil of two *Thymus vulgaris* selections. *Angewandte Botanik*, 68(3-4), 83-88.
- Lindinger, W., Hansel, A., & Jordan, A. (1998). On-line monitoring of volatile organic compounds at pptv levels by means of proton-transfer-reaction mass spectrometry (PTR-MS) medical applications, food control and environmental research. *International Journal of Mass Spectrometry and Ion Processes*, 173(3), 191-241.
- Llusia, J., & Peñuelas, J. (1998). Changes in terpene content and emission in potted Mediterranean woody plants under severe drought. *Canadian Journal of Botany*, 76(8), 1366-1373.
- Llusia, J., & Peñuelas, J. (2000). Seasonal patterns of terpene content and emission from seven Mediterranean woody species in field conditions. *American Journal of Botany*, 87(1), 133-140.
- Llusia, J., Peñuelas, J., Alessio, G. A., & Estiarte, M. (2006). Seasonal contrasting changes of foliar concentrations of terpenes and other volatile organic compound in four dominant species of a Mediterranean shrubland submitted to a field experimental drought and warming. *Physiologia Plantarum*, 127(4), 632-649.
- Llusia, J., Peñuelas, J., Seco, R., & Filella, I. (2012). Seasonal changes in the daily emission rates of terpenes by *Quercus ilex* and the atmospheric concentrations of terpenes in the natural park of Montseny, NE Spain. *Journal of Atmospheric Chemistry*, 69(3), 215-230.

- Loreto, F., Ciccioli, P., Cecinato, A., Brancaleoni, E., Frattoni, M., Fabozzi, C., & Tricoli, D. (1996). Evidence of the photosynthetic origin of monoterpenes emitted by *Quercus ilex* L. leaves by <sup>13</sup>C labeling. *Plant Physiology*, 110(4), 1317-1322.
- Müller, M., Graus, M., Ruuskanen, T. M., Schnitzhofer, R., Bamberger, I., Kaser, L., ... Hansel, A. (2010). First eddy covariance flux measurements by PTR-TOF. *Atmospheric Measurement Techniques*, 3(2), 387-395.
- Ormeño E., Goldstein A. & Niinemets Ü. (2011). Extracting and trapping biogenic volatile organic compounds stored in plant species. *Trends in Analytical Chemistry*, 30(7), 978-989.
- Owen, S. M., & Peñuelas, J. (2005). Opportunistic emissions of volatile isoprenoids. *Trends in Plant Science*, 10(9), 420-426.
- Peñuelas, J., & Llusià, J. (2001). The complexity of factors driving volatile organic compound emissions by plants. *Biologia Plantarum*, 44(4), 481-487.
- Peñuelas, J. & Llusià, J. (2003). BVOCs: plant defense against climate warming?. *Trends in Plant Science*, 8(3), 105-109.
- Peñuelas, J., Llusià, J., & Estiarte, M. (1995). Terpenoids: a plant language. *Trends in Ecology and Evolution*, 10(7), 289.
- Peñuelas, J., Llusià, J., & Filella, I. (2007). Methyl salicylate fumigation increases monoterpene emission rates. *Biologia Plantarum*, 51(2), 372-376.
- Peñuelas, J., Guenther, A., Rapparini, F., Llusià, J., Filella, I., Seco, R., ... Greenberg, J. (2013). Intensive measurements of gas, water, and energy exchange between vegetation and troposphere during the MONTES campaign in a vegetation gradient from short semi-desertic shrublands to tall wet temperate forests in the NW Mediterranean Basin. *Atmospheric Environment*, 75, 348-364.
- Peñuelas, J., Asensio, D., Tholl, D., Wenke, K., Rosenkranz, M., Piechulla, B., Schnitzler, J.P. (2014). Biogenic volatile emissions from the soil. *Plant, Cell and Environment*, 37, 1866-1891.
- Pérez-Harguindeguy, N., Díaz, S., Garnier, E., Lavorel, S., Poorter, H., Jaureguiberry, P., ... Cornelissen, J. H. C. (2013). New handbook for standardised measurement of plant functional traits worldwide. *Australian Journal of Botany*, 61(3), 167-234.
- Seufert, G., Kotzias, D., Spartà, C., & Versino, B. (1995). Volatile organics in Mediterranean shrubs and their potential role in a changing environment. In J. Moreno, & W. C. Oechel (Eds.), *Global Change and Mediterranean-type Ecosystems* (pp. 343-370). New York: Springer.
- Singh, H. B., & Zimmerman, P. R. (1992) Atmospheric distribution and sources of nonmethane hydrocarbons. In J. O. Nriagu (Ed.), *Gaseous Pollutants: Characterization and Cycling* (pp. 177-235). Chichester: John Wiley and Sons.
- Spracklen, D. V., Carslaw, K. S., Merikanto, J., Mann, G. W., Reddington, C. L., Pickering, S., ... Boy, M. (2010). Explaining global surface aerosol number concentrations in terms of primary emissions and particle formation. *Atmospheric Chemistry and Physics*, 10(10), 4775-4793.
- Watson, J. G., Chow, J. C. & Fujita, E. M. (2001). Review of volatile organic compound source apportionment by chemical mass balance. *Atmospheric Environment*, 35, 1567-1584.

Zimmerman, P. R., Chatfield, R. B., Fishman, J., Crutzen, P. J., & Hanst, P. L. (1978). Estimates on the production of CO and H<sub>2</sub> from the oxidation of hydrocarbon emissions from vegetation. *Geophysical Research Letters*, 5(8), 679-682.

**Authors:** Llusia J<sup>1,2</sup>, Filella I<sup>1,2</sup>, Sardans J<sup>1,2</sup>

**Reviewer:** Peñuelas J<sup>1,2</sup>

### Affiliations

<sup>1</sup> CSIC Global Ecology Unit, CREAF-CSIC-UAB, Barcelona, Spain

<sup>2</sup> CREAF, Barcelona, Spain

## 5.15 Water-use efficiency

**Authors:** Goldsmith GR<sup>1</sup>, Berry ZC<sup>1</sup>, Lehmann MM<sup>2</sup>

**Reviewer:** Cernusak LA<sup>3</sup>

**Measurement unit:** carbon assimilation per unit water loss (e.g. mmol CO<sub>2</sub> mol-1 H<sub>2</sub>O);  
**Measurement scale:** plant tissues; **Equipment costs:** €€; **Running costs:** €; **Installation effort:** low;  
**Maintenance effort:** low to medium; **Knowledge need:** low to medium; **Measurement mode:** manual and data logger

Water-use efficiency (WUE) is a measure of the carbon gained by plants through photosynthesis relative to the water lost through transpiration, defined as

$$\frac{A}{E} \quad (1)$$

where  $A$  is net photosynthesis and  $E$  is transpiration. This is commonly referred to as instantaneous WUE (Farquhar & Richards, 1984). However, both  $A$  and  $E$  are functions of the resistance to water movement (generally quantified as stomatal conductance;  $g_s$ ) and the driving gradient for diffusion of CO<sub>2</sub> and H<sub>2</sub>O across the leaf surface, such that

$$\frac{A}{E} = \frac{c_a - c_i}{1.6v} \quad (2)$$

where  $c_a$  is the mole fraction of CO<sub>2</sub> in the ambient atmosphere,  $c_i$  is the mole fraction of CO<sub>2</sub> inside the leaf, 1.6 is the diffusion of H<sub>2</sub>O in air relative to that of CO<sub>2</sub> in air, and  $v$  is the vapour pressure difference between inside the leaf and the ambient atmosphere. Therefore, instantaneous WUE can depend on environmental conditions, as differences in the vapour pressure of water in the air can vary significantly and lead to significant differences in  $E$ . To improve the ability to compare across studies without these confounding effects, intrinsic WUE (iWUE; Osmond et al., 1980) was proposed, defined as

$$\frac{A}{g_s} \quad (3)$$

There is considerable interest in measures of WUE at the leaf, whole plant, and ecosystem scale motivated by the importance of understanding the implications of climate change for both carbon and water cycling. For instance, there is already evidence that increases in atmospheric CO<sub>2</sub> concentrations have increased WUE (Keenan et al., 2013). Long-term changes in temperature and precipitation are also likely to affect WUE by affecting the leaf-to-air vapour pressure difference and therefore altering rates of transpiration (Medrano et al., 2012). WUE provides an accessible measure of the effects of environmental stressors on the coupled processes of photosynthesis and transpiration and can thus contribute to our understanding of plant, species, and ecosystem functions in current and future climate scenarios.

### 5.15.1 What and how to measure?

Water-use efficiency is most commonly determined by measuring leaf gas exchange with an infrared gas analyser (IRGA), or by measuring whole plant biomass accumulation and water use (generally

with potted plants). WUE is also inferred through measurements of the stable isotope ratios of carbon in plant organic matter, most commonly in plants with a C<sub>3</sub> photosynthetic pathway. IRGA measurements are more direct and precise as well as instantaneous, but are difficult to scale to larger spatial and temporal scales (Medrano et al., 2015). Measurements on whole plants can be useful in particular experimental contexts, but have similar constraints (Cernusak et al., 2009). By comparison, stable isotopes of carbon integrate longer time periods, but must be interpreted very carefully in order to make inferences about WUE (Seibt et al., 2008).

### **Gas exchange**

Measurements of the concentration of CO<sub>2</sub> and H<sub>2</sub>O exchanged across a leaf surface serve as the primary means of quantifying WUE. This is done using commercially-available IRGAs that measure gas concentrations before and after air flows through a closed chamber containing a leaf or plant. These systems then calculate photosynthesis ( $A$ ), transpiration ( $E$ ), and stomatal conductance ( $g_s$ ) using equations that consider the flow rate, leaf area in the chamber, the ratio of stomata on both sides of the leaf, and the mole fractions of CO<sub>2</sub> and H<sub>2</sub>O (von Caemmerer & Farquhar, 1981). Intrinsic and instantaneous WUE can be calculated from these three variables as described in Eqs. 1-3 above.

Measurements begin by identifying the leaf or plant of interest and clamping the chamber around the leaf. Most commonly these measurements are done on small leaf areas (6–10 cm<sup>2</sup>), although other chambers can be used or constructed to integrate over the leaf size of interest for the study. Both the leaves and the instrument should be allowed to equilibrate and be held under consistent conditions, controlling for light, temperature, relative humidity, and ambient CO<sub>2</sub> for the duration of the measurement. WUE is known to vary on diurnal and seasonal cycles, as well as across light, temperature, and humidity gradients within canopies (Medrano et al., 2015). Research questions should consider this variability in their experimental design in order to ensure the ability to compare WUE across sample populations. Most commonly, WUE calculated from gas exchange is measured on fully sun-exposed and mature leaves during periods when stomatal conductance is non-limiting. This is usually during the late morning (09:00–11:00 hours) on sunny days where there are no extreme soil moisture deficits, unless studies are explicitly studying variation across one of these parameters.

### **Whole plant**

Measurements of whole plant biomass accumulation relative to water use can serve as an alternative means of measuring WUE (Morison & Gifford, 1984; Marks & Strain, 1989; Centritto et al., 1999; Cernusak et al., 2009). This destructive method is carried out on smaller potted plants observed in an experimental context. Biomass accumulation (i.e. growth) is generally measured by comparing the dry weights of individual plants harvested at the beginning and end of the experiment. Water use is estimated by repeatedly weighing the potted plants on a balance to determine water use and returning each plant to field capacity (or the desired water content) on a regular basis between measurements. Control pots with soil, but no plants, can be used to estimate soil evaporation. However, evaporation should be minimised by covering the sides of pots with reflective materials, as well as by adding a layer of gravel to the soil surface (Cernusak et al., 2009). The biomass

accumulation can then be divided by the cumulative water use (accounting for evaporation) to measure whole plant water-use efficiency.

### **$\delta^{13}\text{C}$ of bulk plant tissues**

An alternative means of inferring WUE is through the measurement of the ratio of the heavy to light carbon isotopes (i.e.  $^{13}\text{C}/^{12}\text{C}$ , as interpreted relative to an international reference standard; Coplen, 2011) in plant tissues such as leaves and wood. The carbon isotope composition ( $\delta^{13}\text{C}$ ) of plant tissue reflects the pathways for biochemical  $\text{CO}_2$  assimilation (i.e.  $\text{C}_3$  v.  $\text{C}_4/\text{CAM}$  metabolism), as well as the plant functional response to climatic conditions. In  $\text{C}_3$  plants, the enzyme RuBisCO discriminates against the  $^{13}\text{C}$  in favour of the lighter isotope ( $^{12}\text{C}$ ) during photosynthetic  $\text{CO}_2$  assimilation, causing  $\text{C}_3$  plants to be more depleted compared to  $\text{C}_4$  and CAM plants. However, as leaf internal  $\text{CO}_2$  ( $c_i$ ) becomes limited relative to that of the ambient atmosphere ( $c_a$ ), discrimination against  $^{13}\text{C}$  necessarily decreases and the assimilation of  $^{13}\text{C}$  and its incorporation into plant material increases.

The calculation of  $\Delta^{13}\text{C}$ , which controls for the  $\delta^{13}\text{C}$  of the atmospheric  $\text{CO}_2$  used for assimilation as described below, can thus provide insights into  $c_i/c_a$  that can be used to infer the relationship between photosynthetic  $\text{CO}_2$  assimilation and water loss (Farquhar et al., 1982, 1989). Measurements of  $\Delta^{13}\text{C}$  are most commonly made on bulk leaf organic matter, reflecting a mix of both structural (e.g. cellulose) and non-structural carbohydrates (e.g. sugars, starch), as well as other compounds. Thus, bulk leaf organic matter mixes the signals integrated over the course of leaf formation and the signals integrated over recent (e.g. daily)  $\text{CO}_2$  assimilation. As such, the time scale reflected in  $\Delta^{13}\text{C}$  measurements differs from that of gas exchange.

The leaf material of interest should be excised and transferred to sampling bags or vials. Given that metabolic processes can continue even after the leaf is sampled, it is advisable (where possible) to quickly inactivate metabolic processes by using a microwave, submersion in liquid nitrogen, or storage on dry ice. Samples should subsequently be dried by oven at a maximum of 70 °C for 72h to constant weight (Pérez-Harguindeguy et al., 2013) or freeze dryer (Popp et al., 1996; Richter et al., 2009). The temperature and time for drying depend on the study question, how many samples are dried, the size, thickness and type of the plant material (e.g. large, fleshy or succulent leaves need more time) see [protocol 2.1.1 Aboveground plant biomass](#) for more details on the drying. Leaf material should be well milled and homogenised before being transferred into tin capsules. However, it is important to confirm that the material that is used during milling (e.g. reaction vials) is not causing any significant impact on the isotope ratio of a sample due to abrasion. Finally, the isotope ratios can then be measured by means of an elemental analyser coupled to an isotope ratio mass spectrometer (IRMS). Quality control standards and information on the long-term accuracy and precision of the instrumentation are important for appropriate interpretation of the results.

A similar procedure for drying and preparing samples, without the concerns of ongoing metabolic processes, can also be used to determine the  $\delta^{13}\text{C}$  of woody tissue. This type of sampling will reflect the  $\delta^{13}\text{C}$  integrated over longer time periods (e.g. in annual tree rings). However, the  $\delta^{13}\text{C}$  ratios of assimilates can be changed by post-photosynthetic isotope fractionation processes during translocation from leaves to downstream tissues and by mixing with older carbon from storage compounds such as starch. Interpreting the  $\delta^{13}\text{C}$  ratios in woody tissues thus requires additional considerations (Gessler et al., 2014).

### **$\delta^{13}\text{C}$ of cellulose and non-structural carbohydrates**

The structural and non-structural carbohydrate fractions in the leaf bulk material can be separated by different techniques, making inferences about  $\delta^{13}\text{C}$  possible at more specific time scales. For instance, the  $\delta^{13}\text{C}$  value from leaf cellulose reflects the predominant environmental conditions during leaf development, while  $\delta^{13}\text{C}$  measurements of the water soluble content (WSC), sugar, and starch reflect  $\Delta^{13}\text{C}$  values integrated over shorter time scales (Gessler et al., 2009).

For the extraction and purification of leaf cellulose for isotope analysis, leaf material is cut into small pieces and transferred into Teflon bags (Boettger et al., 2007). Lignin is first removed by submerging the bags in acidic NaClO<sub>2</sub>. The leaf material is then freed from fatty acids, oils, and hemicellulose with NaOH. Finally, it is cleaned with deionised water and HCl solutions. The remaining residue is then oven- or freeze-dried and can be used directly for analysis. However, some labs further homogenise the cellulose material by ultrasonication (Weigt et al., 2015). Infrared spectroscopy can be used to test the efficiency of the cellulose purification against standards (Rinne et al., 2005).

The WSC of bulk plant tissue (i.e. leaf or roots) can easily be extracted by mixing the tissue with water or methanol chloroform water (MCW) solutions and heating them for a short time in a water bath (Richter et al., 2009; Lehmann et al., 2015). If water is the only solvent used for extraction, the supernatant and the insoluble material can be used after centrifugation for sugar and starch purification, respectively. By contrast, if MCW is the solvent used for extraction, the chloroform phase must be removed by bench or oven drying to avoid a significant bias in isotope ratios of sugars and starch.

To measure the  $\delta^{13}\text{C}$  of bulk sugars, the WSC fraction must be isolated from non-sugar compounds such as amino acids, organic acids, and polyphenols. This can be done by ion exchange chromatography (Rinne et al., 2012; Lehmann et al., 2015). The WSC fraction is added on the top of the ion exchange material, gravimetrically passed through the columns/cartridges using deionised water, and the flow-through containing the neutral sugar fraction collected by reaction vials. In addition, starch is enzymatically isolated from the insoluble material after several washing and heating steps using heat-stable alpha amylase (Wanek et al., 2001; Richter et al., 2009), which breaks down the starch to a mix of sugars (i.e. glucose and maltose).

Aliquots of all bulk fractions, including WSC, sugars, and starch are then pipetted to tin capsules and oven-dried at 60 °C until completely dry. As above, the isotope ratios can then be measured by means of an elemental analyser coupled to an isotope ratio mass spectrometer (IRMS).

### **Where to start**

Cernusak et al. (2009, 2013), Farquahar & Richards (1984), Farquhar et al. (1989), Medrano et al. (2015)

### **Interpretation**

**Gas exchange.** Both the instantaneous WUE ( $A/E$ ) and the intrinsic WUE ( $A/g_s$ ) can be calculated from gas exchange measurements. Instantaneous WUE is a more direct quantification of the trade-off between carbon and water, but is often difficult to compare across environments due to variations in leaf-to-air vapour pressure across measurement periods. In contrast, intrinsic WUE only considers stomatal aperture and is therefore independent of atmospheric demand of moisture (Osmond et al., 1980). Values of WUE vary across species and environmental conditions. General values for instantaneous WUE range from 2 to 11 mmol CO<sub>2</sub> mol<sup>-1</sup> H<sub>2</sub>O in woody C<sub>3</sub> plants, while values tend to be higher in C<sub>4</sub> and CAM plants (as high as 20 mmol CO<sub>2</sub> mol<sup>-1</sup> H<sub>2</sub>O) (Lambers et al., 2008). This greater WUE in C<sub>4</sub> and CAM plants reflects the adaptive regulation of water loss associated with these photosynthetic pathways. There is also wide variation in intrinsic WUE values ranging from around 10 μmol mol<sup>-1</sup> to over 200 μmol mol<sup>-1</sup> (e.g. Flexas et al., 2013; Tomás et al., 2014).

Interpretation and comparison of WUE values require some consideration of the environmental conditions in which measurements were taken. Stomatal conductance plays a key role and WUE tends to increase as stomata close (Condon et al., 2002; Tomás et al., 2014). Given that drought typically reduces stomatal conductance to minimise water loss, there is evidence that WUE will continue to increase under the drier conditions associated with current and projected global warming (Pou et al., 2008; Beer et al., 2009). There is much literature considering the effects of increasing atmospheric concentrations of CO<sub>2</sub> on WUE. This research has found support for a so-called “fertilisation effect,” whereby closures in stomatal aperture maintain a consistent leaf internal CO<sub>2</sub>, but decrease water loss: this results in increased WUE (Keenan et al., 2013; Frank et al., 2015).

**Whole plant.** Measurements of whole-plant WUE require some additional considerations of potential sources of error. Rather than repeat measurements on individual plants, the destructive nature of the approach necessitates that biomass accumulation be estimated from two different sets of individuals and this may serve as a source of random error with respect to carbon gain. In addition, whole plant measurements made over days or weeks are subject to the additional influences of i) water lost through transpiration that is not associated with carbon gain (e.g. night-time transpiration; Dawson et al., 2007) and ii) the offset of carbon gain by respiratory carbon losses through stems and roots during the day, as well as through stems, roots, and leaves during the night (Cernusak et al., 2007). The magnitude of these effects on whole-plant WUE is not well studied, although research indicates that they are not likely to outweigh differences among species or between experimental treatments (Centritto et al., 2002; Cernusak et al., 2007, 2009). Notably, night-time transpiration and respiration may lead to a disconnect between leaf-level and whole plant measures of WUE (Medrano et al., 2015). If expressed in terms of the carbon content in the plant dry mass increment per unit water lost from the plant, typical values of whole-plant WUE will be about half those measured at the leaf level, mainly reflecting respiratory carbon losses.

**δ<sup>13</sup>C.** For the purposes of inferring WUE, measurements of δ<sup>13</sup>C are generally interpreted in terms of discrimination ( $Δ^{13}C$ ), defined as

$$Δ^{13}C = \frac{\delta^{13}C_{atm} - \delta^{13}C_{plant}}{1 + \delta^{13}C_{atm}} \quad (4)$$

where  $\delta^{13}C_{plant}$  is the carbon isotope composition of plant organic matter and  $\delta^{13}C_{atm}$  is the carbon isotope composition of atmospheric CO<sub>2</sub>. It should be noted that  $\Delta^{13}C$  generally results in positive values for plant organic matter, whereas  $\delta^{13}C$  is generally negative (when interpreted relative to the standard VPDB): this can cause confusion when studies differ in their presentation of results. The calculation of  $\Delta^{13}C$  has the advantage of allowing for the interpretation of carbon isotope composition in the absence of any confounding effects of differences in the  $\delta^{13}C$  of atmospheric source CO<sub>2</sub> used by the plant for photosynthesis. While the atmosphere is generally well mixed, both spatial and temporal differences can arise. For instance, there can be differences in the  $\delta^{13}C$  of CO<sub>2</sub> between the canopy and understorey, due to the influence of CO<sub>2</sub> respired from the soil. The  $\delta^{13}C$  of CO<sub>2</sub> has also changed considerably over time: the accelerated burning of fossil fuels has led to a c. 1.5 ‰ (relative to the standard VPDB) decrease in the  $\delta^{13}C$  of atmospheric CO<sub>2</sub> since the beginning of the Industrial Revolution (Rubino et al., 2013) and this is an important consideration when interpreting long-term records (e.g. tree rings or herbarium specimens).

An important benefit of  $\Delta^{13}C$  is that it can be used as a means of approximating  $c_i/c_a$ . However, doing so differs based on the photosynthetic pathway of the species under consideration. Here we focus on an approximated relationship between  $\Delta^{13}C$  and  $c_i/c_a$  in plants with a C<sub>3</sub> photosynthetic pathway, defined as

$$\Delta^{13}C = a + (b - a) \frac{c_i}{c_a} \quad (5)$$

where  $a$  is the fractionation associated with diffusion of CO<sub>2</sub> through the stomata to the sites of carboxylation (4.4 ‰),  $b$  is the fractionation associated with carboxylation (27 ‰),  $c_i$  is the mole fraction of CO<sub>2</sub> inside the leaf, and  $c_a$  is the mole fraction of CO<sub>2</sub> in the ambient atmosphere (Farquhar et al., 1982). Thus the  $\Delta^{13}C$  of plant organic matter increases with increasing  $c_i/c_a$ . In C<sub>3</sub> plants,  $\Delta^{13}C$  ranges from c. 14 to 28 ‰ (Diefendorf et al., 2010). Alternatively, when the  $\delta^{13}C$  of atmospheric CO<sub>2</sub> can be assumed to be constant, the  $\delta^{13}C$  of plant organic matter decreases with increasing  $c_i/c_a$ . In C<sub>3</sub> plants,  $\delta^{13}C$  ranges from c. -21 to -35 ‰ (Diefendorf et al., 2010).

In many observations of plants with a C<sub>3</sub> photosynthetic pathway, there is a very strong relationship between instantaneous  $c_i/c_a$  and  $\delta^{13}C$  (Cernusak et al., 2013). Given that  $c_i/c_a$  responds to the supply and demand for CO<sub>2</sub> imposed by photosynthesis and stomatal closure to prevent water loss, this relationship can provide insights into WUE. In fact, the approximation of  $c_i/c_a$  from  $\Delta^{13}C$  has also been used to mathematically solve intrinsic WUE ( $A/g_s$ ). However, it is critically important to recognise that the relationship between  $\Delta^{13}C$  and WUE can break down because i)  $\Delta^{13}C$  is related to  $g_s$  rather than  $E$  and therefore does not account for differences in vapour pressure difference that often occur in time-integrated measures and ii)  $\Delta^{13}C$ , as expressed in equation 5, is related to  $c_i/c_a$  rather than  $c_c/c_a$  (where  $c_c$  is the mole fraction of CO<sub>2</sub> in the chloroplast) and therefore does not account for the additional resistance against the diffusion of CO<sub>2</sub> from the intracellular air spaces to the actual sites of photosynthetic carbon fixation. These limitations can lead to erroneous estimates and interpretations of intrinsic WUE (Seibt et al., 2008).

Compared to the C<sub>3</sub> photosynthetic pathway, the structural and functional differences in the C<sub>4</sub> and CAM photosynthetic pathways lead to considerable additional complexity for interpreting how changes in  $\Delta^{13}C$  may relate to changes in WUE. While a detailed explanation of these relationships is not within the purview of this protocol, a number of studies have developed the mechanistic basis for these relationships (Farquhar, 1983; Farquhar et al., 1989; reviewed by Cernusak et al., 2013;

Ellsworth & Cousins, 2016), as well as gathered empirical data on the relationships as a function of different environmental conditions (Winter et al., 2005; Ellsworth et al., 2017).

### 5.15.2 Special cases, emerging issues, and challenges

#### *Special cases*

As noted above, information on the carbon isotope ratio alone cannot fully resolve the extent to which observed differences in  $c_i/c_a$  reflect changes in photosynthesis ( $A$ ) or stomatal conductance ( $g_s$ ). Here, the coupled measurement of stable isotopes of oxygen ( $\delta^{18}\text{O}$ ) and  $\delta^{13}\text{C}$  can provide additional insights (Scheidegger et al., 2000).

As described in [protocol 5.13 Stable isotopes of water for inferring plant function](#), the  $\delta^{18}\text{O}$  of plant organic matter reflects the extent of evaporative enrichment of leaf water associated with transpiration. Evaporation of water from the leaf enriches the isotopic composition of the remaining leaf water due to i) an equilibrium fractionation associated with phase change from liquid to vapour and ii) a kinetic fractionation associated with diffusion through the stomata and boundary layer. The magnitude of this fractionation depends on the isotopic composition of both the source water and the atmospheric water vapour, as well as on the ratio of ambient air vapour pressure to leaf intracellular vapour pressure (Cernusak et al., 2016). The extent of this enrichment is subsequently recorded in plant organic matter through the incorporation of oxygen isotopes from water into photosynthetic products. Critically,  $\delta^{18}\text{O}$  is not mechanistically coupled to the drawdown of  $c_i$  via photosynthesis.

The dual carbon and oxygen isotope approach relies on these established relationships between leaf gas exchange and isotopic fractionation to derive a series of model scenarios that can be used to distinguish whether a change in the  $^{13}\text{C}/^{12}\text{C}$  of plant organic matter is likely to be the result of a change in photosynthesis (inferred by  $\delta^{13}\text{C}$ ), or stomatal conductance (inferred by  $\delta^{18}\text{O}$ ). As a result, this approach is particularly important for making statements about water-use efficiency using stable isotopes. Since its introduction, the approach has been applied in a number of different experimental contexts, including nutrient availability (Cabrera-Bosquet et al., 2011),  $\text{CO}_2$  and ozone (Grams et al., 2007), tree mortality (Herrero et al., 2013), and tree species mixtures (Grossiord et al., 2013). However, the interpretation of the approach is not always straightforward and additional care must be taken to draw meaningful conclusions (Roden & Siegwolf, 2012).

#### *Emerging issues and challenges*

There is growing recognition that estimates of water-use efficiency made at different scales (e.g. leaf, whole plant, ecosystem) using different methods (e.g. gas exchange, stable isotopes, eddy covariance) are not easily compared (Medlyn et al., 2017). This problem is particularly apparent in certain plant functional types (e.g. evergreen needle leaf, deciduous broadleaf forest,  $\text{C}_3$  grasslands). As noted above, the differences in methods and where those differences may lead to discrepancies should be considered carefully in interpreting data.

### 5.15.3 References

### **Theory, significance, and large datasets**

Cernusak et al. (2013), Diefendorf et al. (2010), Farquhar et al. (1989), Siebt et al. (2008)

### **More on methods and existing protocols**

Boettger et al. (2007), Cernusak et al. (2009), Medrano et al. (2012)

### **All references**

- Beer, C., Ciais, P., Reichstein, M., Baldocchi, D., Law, B. E., Papale, D., ... Wohlfahrt, G. (2009). Temporal and among-site variability of inherent water use efficiency at the ecosystem level. *Global Biogeochemical Cycles*, 23(2), GB003233.
- Boettger, T., Haupt, M., Knöller, K., Weise, S. M., Waterhouse, J. S., Rinne, K. T., ... Schleser, G. H. (2007). Wood cellulose preparation methods and mass spectrometric analyses of  $\delta^{13}\text{C}$ ,  $\delta^{18}\text{O}$ , and nonexchangeable  $\delta^2\text{H}$  values in cellulose, sugar, and starch: an interlaboratory comparison. *Analytical Chemistry*, 79(12), 4603-4612.
- Cabrera-Bosquet, L., Albrizio, R., Nogués, S., & Araus, J. L. (2011). Dual  $\Delta^{13}\text{C}/\delta^{18}\text{O}$  response to water and nitrogen availability and its relationship with yield in field-grown durum wheat:  $\Delta^{13}\text{C}$ ,  $\delta^{18}\text{O}$  and yield responses to water and N availability. *Plant, Cell & Environment*, 34(3), 418-433.
- Centritto, M., Lee, H. S. J., & Jarvis, P. G. (1999). Interactive effects of elevated CO<sub>2</sub> and drought on cherry (*Prunus avium*) seedlings I. Growth, whole-plant water use efficiency and water loss. *New Phytologist*, 141(1), 129–140.
- Centritto, M., Lucas, M. E., & Jarvis, P. G. (2002). Gas exchange, biomass, whole-plant water-use efficiency and water uptake of peach (*Prunus persica*) seedlings in response to elevated carbon dioxide concentration and water availability. *Tree Physiology*, 22(10), 699-706.
- Cernusak, L. A., Winter, K., Aranda, J., Turner, B. L., & Marshall, J. D. (2007). Transpiration efficiency of a tropical pioneer tree (*Ficus insipida*) in relation to soil fertility. *Journal of Experimental Botany*, 58(13), 3549-3566.
- Cernusak, L. A., Winter, K., Aranda, J., Virgo, A., & Garcia, M. (2009). Transpiration efficiency over an annual cycle, leaf gas exchange and wood carbon isotope ratio of three tropical tree species. *Tree Physiology*, 29(9), 1153-1161.
- Cernusak, L. A., Ubierna, N., Winter, K., Holtum, J. A. M., Marshall, J. D., & Farquhar, G. D. (2013). Environmental and physiological determinants of carbon isotope discrimination in terrestrial plants. *New Phytologist*, 200(4), 950-965.
- Cernusak, L. A., Barbour, M. M., Arndt, S. K., Cheesman, A. W., English, N. B., Feild, T. S., ... Farquhar, G. D. (2016). Stable isotopes in leaf water of terrestrial plants: Stable isotopes in leaf water. *Plant, Cell & Environment*, 39(5), 1087-1102.
- Condon, A. G., Richards, R. A., Rebetzke, G. J., & Farquhar, G. D. (2002). Improving intrinsic water-use efficiency and crop yield. *Crop Science*, 42(1), 122-131.

- Coplen, T. B. (2011). Guidelines and recommended terms for expression of stable-isotope-ratio and gas-ratio measurement results. *Rapid Communications in Mass Spectrometry*, 25(17), 2538-2560.
- Dawson, T. E., Burgess, S. S. O., Tu, K. P., Oliveira, R. S., Santiago, L. S., Fisher, J. B., ... Ambrose, A. R. (2007). Nighttime transpiration in woody plants from contrasting ecosystems. *Tree Physiology*, 27(4), 561-575.
- Diefendorf, A. F., Mueller, K. E., Wing, S. L., Koch, P. L., & Freeman, K. H. (2010). Global patterns in leaf  $^{13}\text{C}$  discrimination and implications for studies of past and future climate. *Proceedings of the National Academy of Sciences USA*, 107(13), 5738-5743.
- Ellsworth, P. Z., & Cousins, A. B. (2016). Carbon isotopes and water use efficiency in C<sub>4</sub> plants. *Current Opinion in Plant Biology*, 31, 155-161.
- Ellsworth, P. Z., Ellsworth, P. V., & Cousins, A. B. (2017). Relationship of leaf oxygen and carbon isotopic composition with transpiration efficiency in the C<sub>4</sub> grasses *Setaria viridis* and *Setaria italica*. *Journal of Experimental Botany*, 68(13), 3513-3528.
- Farquhar, G. (1983). On the nature of carbon isotope discrimination in C<sub>4</sub> species. *Australian Journal of Plant Physiology*, 10(2), 205.
- Farquhar, G., & Richards, R. (1984). Isotopic composition of plant carbon correlates with water-use efficiency of wheat genotypes. *Australian Journal of Plant Physiology*, 11(6), 539.
- Farquhar, G. D., O'Leary, M. H., & Berry, J. A. (1982). On the relationship between carbon isotope discrimination and the intercellular carbon dioxide concentration in leaves. *Functional Plant Biology*, 9(2), 121-137.
- Farquhar, G. D., Hubick, K. T., Condon, A. G., & Richards, R. A. (1989). Carbon isotope fractionation and plant water-use efficiency. In P. W. Rundel, J. R. Ehleringer, & K. A. Nagy (Eds.), *Stable Isotopes in Ecological Research* (pp. 21-40). New York: Springer.
- Flexas, J., Niinemets, Ü., Gallé, A., Barbour, M. M., Centritto, M., Diaz-Espejo, A., ... Medrano, H. (2013). Diffusional conductances to CO<sub>2</sub> as a target for increasing photosynthesis and photosynthetic water-use efficiency. *Photosynthesis Research*, 117(1-3), 45-59.
- Frank, D. C., Poulter, B., Saurer, M., Esper, J., Huntingford, C., Helle, G., ... Weigl, M. (2015). Water-use efficiency and transpiration across European forests during the Anthropocene. *Nature Climate Change*, 5(6), 579-583.
- Gessler, A., Brandes, E., Buchmann, N., Helle, G., Rennenberg, H., & Barnard, R. L. (2009). Tracing carbon and oxygen isotope signals from newly assimilated sugars in the leaves to the tree-ring archive. *Plant, Cell & Environment*, 32(7), 780-795.
- Gessler, A., Ferrio, J. P., Hommel, R., Treydte, K., Werner, R. A., & Monson, R. K. (2014). Stable isotopes in tree rings: towards a mechanistic understanding of isotope fractionation and mixing processes from the leaves to the wood. *Tree Physiology*, 34(8), 796-818.
- Grams, T. E. E., Kozovits, A. R., HäBerle, K.-H., Matyssek, R., & Dawson, T. E. (2007). Combining  $\delta^{13}\text{C}$  and  $\delta^{18}\text{O}$  analyses to unravel competition, CO<sub>2</sub> and O<sub>3</sub> effects on the physiological performance of different-aged trees. *Plant, Cell & Environment*, 30(8), 1023-1034.

- Grossiord, C., Granier, A., Gessler, A., Pollastrini, M., & Bonal, D. (2013). The influence of tree species mixture on ecosystem-level carbon accumulation and water use in a mixed boreal plantation. *Forest Ecology and Management*, 298, 82-92.
- Herrero, A., Castro, J., Zamora, R., Delgado-Huertas, A., & Querejeta, J. I. (2013). Growth and stable isotope signals associated with drought-related mortality in saplings of two coexisting pine species. *Oecologia*, 173(4), 1613-1624.
- Keenan, T. F., Hollinger, D. Y., Bohrer, G., Dragoni, D., Munger, J. W., Schmid, H. P., & Richardson, A. D. (2013). Increase in forest water-use efficiency as atmospheric carbon dioxide concentrations rise. *Nature*, 499(7458), 324-327.
- Lambers, H., Chapin, F. S., & Pons, T. L. (2008). *Plant Physiological Ecology* (2<sup>nd</sup> ed.). New York: Springer-Verlag.
- Lehmann, M. M., Rinne, K. T., Blessing, C., Siegwolf, R. T. W., Buchmann, N., & Werner, R. A. (2015). Malate as a key carbon source of leaf dark-respired CO<sub>2</sub> across different environmental conditions in potato plants. *Journal of Experimental Botany*, 66(19), 5769-5781.
- Marks, S., & Strain, B. R. (1989). Effects of drought and CO<sub>2</sub> enrichment on competition between two old-field perennials. *New Phytologist*, 111(2), 181-186.
- Medlyn, B. E., De Kauwe, M. G., Lin, Y.-S., Knauer, J., Duursma, R. A., Williams, C. A., ... Wingate, L. (2017). How do leaf and ecosystem measures of water-use efficiency compare? *New Phytologist*, 216(3), 758-770.
- Medrano, H., Gulias, J., Chaves, M. M., Galmes, J., & Flexas, J. (2012). Terrestrial photosynthesis changing environment molecular physiological and ecological approach: Plant science. In J. Flexas, F. Loreto, & H. Medrano (Eds.), *Terrestrial Photosynthesis in a Changing Environment: A Molecular Physiological and Ecological Approach* (pp. 523-536). Cambridge: Cambridge University Press.
- Medrano, H., Tomás, M., Martorell, S., Flexas, J., Hernández, E., Rosselló, J., ... Bota, J. (2015). From leaf to whole-plant water use efficiency (WUE) in complex canopies: Limitations of leaf WUE as a selection target. *The Crop Journal*, 3(3), 220-228.
- Morison, J., & Gifford, R. (1984). Plant growth and water use with limited water supply in high CO<sub>2</sub> concentrations. II. Plant dry weight, partitioning and water use efficiency. *Australian Journal of Plant Physiology*, 11(5), 375.
- Osmond, C. B., Björkman, O., & Anderson, D. J. (1980). *Physiological Processes in Plant Ecology: Toward a Synthesis with Atriplex*. Berlin: Springer.
- Pérez-Harguindeguy, N., Díaz, S., Garnier, E., Lavorel, S., Poorter, H., Jaureguiberry, P., ... Cornelissen, J. H. C. (2013). New handbook for standardised measurement of plant functional traits worldwide. *Australian Journal of Botany*, 61(3), 167-234.
- Popp, M., Lied, W., Meyer, A. J., Richter, A., Schiller, P., & Schwitte, H. (1996). Sample preservation for determination of organic compounds: microwave versus freeze-drying. *Journal of Experimental Botany*, 47(10), 1469-1473.

- Pou, A., Flexas, J., Alsina, M. del M., Bota, J., Carambula, C., de Herralde, F., ... Medrano, H. (2008). Adjustments of water use efficiency by stomatal regulation during drought and recovery in the drought-adapted *Vitis* hybrid Richter-110 (*V. berlandieri* × *V. rupestris*). *Physiologia Plantarum*, 134(2), 313-323.
- Richter, A., Wanek, W., Werner, R. A., Ghashghaei, J., Jäggi, M., Gessler, A., ... Gleixner, G. (2009). Preparation of starch and soluble sugars of plant material for the analysis of carbon isotope composition: a comparison of methods. *Rapid Communications in Mass Spectrometry*, 23(16), 2476-2488.
- Rinne, K. T., Boettger, T., Loader, N. J., Robertson, I., Switsur, V. R., & Waterhouse, J. S. (2005). On the purification of  $\alpha$ -cellulose from resinous wood for stable isotope (H, C and O) analysis. *Chemical Geology*, 222(1-2), 75-82.
- Rinne, K. T., Saurer, M., Streit, K., & Siegwolf, R. T. W. (2012). Evaluation of a liquid chromatography method for compound-specific  $\delta^{13}\text{C}$  analysis of plant carbohydrates in alkaline media. *Rapid Communications in Mass Spectrometry*, 26(18), 2173-2185.
- Roden, J., & Siegwolf, R. (2012). Is the dual-isotope conceptual model fully operational? *Tree Physiology*, 32(10), 1179-1182.
- Rubino, M., Etheridge, D. M., Trudinger, C. M., Allison, C. E., Battle, M. O., Langenfelds, R. L., ... Francey, R. J. (2013). A revised 1000 year atmospheric  $\delta^{13}\text{C}$ -CO<sub>2</sub> record from Law Dome and South Pole, Antarctica. *Journal of Geophysical Research: Atmospheres*, 118(15), 8482-8499.
- Scheidegger, Y., Saurer, M., Bahn, M., & Siegwolf, R. (2000). Linking stable oxygen and carbon isotopes with stomatal conductance and photosynthetic capacity: a conceptual model. *Oecologia*, 125(3), 350-357.
- Seibt, U., Rajabi, A., Griffiths, H., & Berry, J. A. (2008). Carbon isotopes and water use efficiency: sense and sensitivity. *Oecologia*, 155(3), 441-454.
- Tomás, M., Medrano, H., Escalona, J. M., Martorell, S., Pou, A., Ribas-Carbó, M., & Flexas, J. (2014). Variability of water use efficiency in grapevines. *Environmental and Experimental Botany*, 103, 148-157.
- von Caemmerer, S., & Farquhar, G. D. (1981). Some relationships between the biochemistry of photosynthesis and the gas exchange of leaves. *Planta*, 153(4), 376-387.
- Wanek, W., Heintel, S., & Richter, A. (2001). Preparation of starch and other carbon fractions from higher plant leaves for stable carbon isotope analysis. *Rapid Communications in Mass Spectrometry*, 15(14), 1136-1140.
- Weigt, R. Bränlich, S., Zimmermann, L., Saurer, M., Grams, T.E.E., Dietrich, H.-P., ... Nikolova, P.S. (2015). Comparison of  $\delta^{18}\text{O}$  and  $\delta^{13}\text{C}$  values between tree-ring whole wood and cellulose in five species growing under two different site conditions. *Rapid Communications in Mass Spectrometry*, 29(23), 2233-2244.
- Winter, K., Aranda, J., & Holtum, J. A. M. (2005). Carbon isotope composition and water-use efficiency in plants with crassulacean acid metabolism. *Functional Plant Biology*, 32(5), 381.

**Authors:** Goldsmith GR<sup>1</sup>, Berry ZC<sup>1</sup>, Lehmann MM<sup>2</sup>

**Reviewer:** Cernusak LA<sup>3</sup>

### Affiliations

<sup>1</sup> Schmid College of Science and Technology, Chapman University, Orange, USA

<sup>2</sup> Forest Dynamics, Swiss Federal Institute for Forest, Snow and Landscape Research WSL, Birmensdorf, Switzerland

<sup>3</sup> College of Science and Engineering, James Cook University, Cairns, Australia

## 5.16 Leaf hydraulic vulnerability to dehydration

**Authors:** Scoffoni C<sup>1</sup>, Sack L<sup>2</sup>

**Reviewer:** Dickman LT<sup>3</sup>, Johnson DM<sup>4</sup>

**Measurement unit:**  $K_{leaf}$  in  $\text{mmol m}^{-2} \text{s}^{-1} \text{MPa}^{-1}$ , and  $P_{50}$  in MPa; **Measurement scale:** leaf; **Equipment costs:** \$\$\$; **Running costs:** €; **Installation effort:** low; **Maintenance effort:** low; **Knowledge need:** medium; **Measurement mode:** data logger

A leaf hydraulic vulnerability curve represents the response of the leaf hydraulic conductance ( $K_{leaf}$  – a measure of how efficiently water can move through the leaf) to increasing dehydration for a given species. The leaf hydraulic vulnerability curve is typically depicted by plotting  $K_{leaf}$  against leaf water potential ( $\Psi_{leaf}$ ) (Figure 5.16.1). Because water moves through both the vein xylem and living cells outside the xylem, during soil or atmospheric drought, several phenomena can lead to  $K_{leaf}$  decline: embolism of xylem conduits (i.e. they become filled with air, decreasing the conductance through the xylem; Johnson et al., 2012; Brodribb et al., 2016b), xylem wall collapse (Cochard et al., 2004; Zhang et al., 2016), or cell volume changes (Scoffoni et al., 2014) which are associated with reduced aquaporin activity (Kim & Steudle, 2007; Shatil-Cohen et al., 2011; Sade et al., 2014). While the decline in  $K_{leaf}$  with dehydration has most typically been associated with xylem embolism (Scoffoni & Sack, 2017), recent work using x-ray microcomputed tomography and novel methods to partition the xylem and outside-xylem vulnerabilities shows that xylem embolism typically occurs only with very strong dehydration, and changes in outside-xylem pathways can play a major role in  $K_{leaf}$  decline (Trifilo et al., 2016; Scoffoni et al., 2017a). Several functional traits can be extrapolated from the leaf hydraulic vulnerability curve: the leaf water potential at which  $K_{leaf}$  declined by 50% ( $P_{50}$ ) or 80% ( $P_{80}$ ), the initial slope of the leaf vulnerability curve, and the maximum leaf hydraulic conductance (Scoffoni et al., 2012). These traits vary widely across species and growth forms and are importantly linked with plant adaptation across biomes (Scoffoni & Sack, 2017). They can shed light on expected responses to more frequent occurrences of drought episodes projected for many regions around the world.

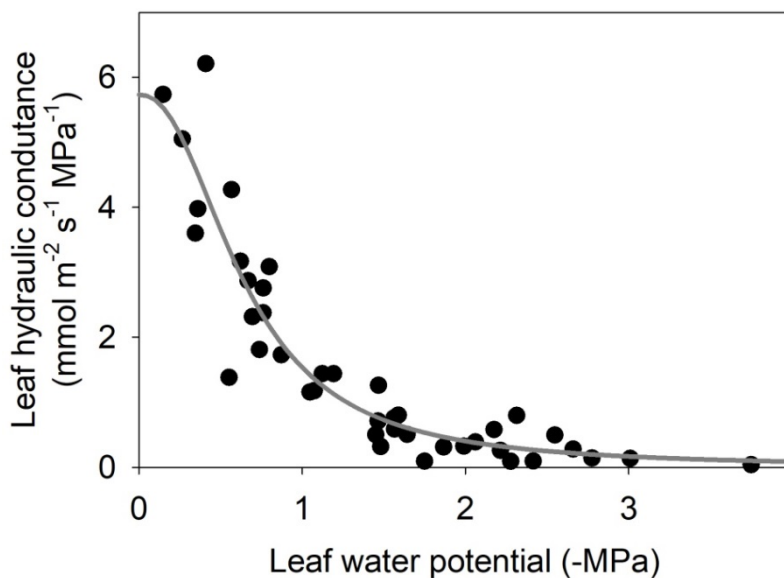


**Figure 5.16.1** Leaf vulnerability curve of *Hedera canariensis*. Note that each point on the figure represents a different leaf measurement. Leaf water potential on the x-axis is the most negative water potential that the leaf has experienced (either prior to, or at the end of the measurement).

### 5.16.1 What and how to measure?

There are three methods currently in use to construct leaf hydraulic vulnerability curves: the evaporative flux method, the rehydration method, and the vacuum pump method. The **evaporative flux method** (EFM) has the advantage of mimicking the natural pathways of water movement in the leaf, including the outside-xylem pathways and therefore is the only method described here. Measuring  $K_{leaf}$  for dehydrated leaves is similar to measuring  $K_{leaf}$  for fully hydrated leaves as described in [protocol 5.10 Maximum leaf hydraulic conductance](#): the main difference is that branches are dehydrated prior to measurement.  $K_{leaf}$  is calculated by dividing flow rate by the leaf water potential at the end of the measurement, but is typically plotted against the most negative water potential it experienced (whether initially after dehydration prior to measurement, or at the end of the measurement if it dehydrated further on the system) to construct leaf hydraulic vulnerability curves. It can take 2–10 days to construct a vulnerability curve for a given species, depending on the number of measurement systems, how vulnerable the species is, and how variable  $K_{leaf}$  is within a given range of water potential. Step-by-step protocols and videos are available (Sack & Scoffoni, 2012).

Branches can be collected in the field the day prior to measurements and placed in large dark plastic bags filled with wet paper towels. Plant material can be transported to the lab in a cooler. In the lab, at least two nodes should be cut under water to ensure the removal of any embolized conduits (as a result of cutting shoots off individuals in air in the field), and the shoots should be left to rehydrate in pure water overnight, with two dark plastic bags filled with wet paper towels covering them, ensuring high atmospheric humidity around the rehydrating samples. Alternatively, if working with greenhouse plants, whole pots can be transported to the lab the evening prior to measurements, watered to saturation and covered in two dark plastic bags filled with wet paper towers. The next day, branches of at least three leaves are placed to dehydrate on the bench (or over a fan) for different amounts of time to obtain a range of initial leaf water potentials ( $\Psi_{initial}$ ). The branch is then bagged and left to equilibrate for 30 min. Initial water potentials are measured for the top and bottom leaf of the branch. If the two leaves differ by  $>0.2$  MPa, the branch is discarded. The remaining middle leaf is then attached to the EFM apparatus and  $K_{leaf}$  is measured following the instructions from [protocol 5.10 Maximum leaf hydraulic conductance](#). At the end of the measurement, leaf temperature is recorded, and the leaf taken off the system and its petiole dabbed dry. The leaf is quickly placed in a bag to equilibrate for 30 min before the final leaf water potential is measured ( $\Psi_{final}$ ).  $K_{leaf}$  is calculated by dividing the steady-state flow rate (normalised by leaf area and temperature to correct for water viscosity) by  $\Psi_{final}$ . To construct the leaf hydraulic vulnerability curve,  $K_{leaf}$  is plotted against the most negative water potential it experienced (either  $\Psi_{initial}$  or  $\Psi_{final}$ ). Generally, 6 points per 0.5 MPa intervals are recommended to obtain a species' vulnerability curve (although the interval can be reduced if the species is very drought sensitive, and the number of points within intervals can be increased if the variation within that interval is too large). Because both linear and non-linear responses of  $K_{leaf}$  to dehydration can be found across species (Brodrribb & Holbrook, 2006; Scoffoni et al., 2012), we recommend using a maximum likelihood approach to select and parameterise the best fitting response from at least four functions (linear, sigmoidal, logistic, exponential), all of which have been used in past studies (Scoffoni et al., 2012). From the selected model, the water potential at 50 and 80% loss of  $K_{leaf}$ , as well as the initial slope, can be extrapolated.

### **Where to start**

Guyot et al. (2012), Sack & Scoffoni (2012), Scoffoni & Sack (2017), Scoffoni et al. (2012, 2017a)

#### **5.16.2 Special cases, emerging issues, and challenges**

It is imperative to construct vulnerability curves using high light acclimated leaves. This is easily (and typically) done with the EFM and vacuum pump method by placing a bright light source above the leaf (Sack et al., 2002). Studies have shown a strong interaction of the light enhancement of  $K_{leaf}$  with the dehydration response, with species typically showing greater vulnerability in their  $K_{leaf}$  responses under high light between full turgor and turgor loss point (Guyot et al., 2012). Notably, studies using the rehydration kinetics method are typically performed under lab light conditions (e.g. Blackman et al., 2010; Johnson et al., 2012) or under  $50\text{--}100 \mu\text{mol quanta m}^{-2} \text{s}^{-1}$  for only a few minutes while the leaf is rehydrating (e.g. Brodribb et al., 2016b), which could greatly influence the shape and intensity of the response of  $K_{leaf}$  to dehydration. Thus caution is needed when comparing the rehydration kinetics method to the EFM. While a study found the two methods produce comparable results in olive and almond (Hernandez-Santana et al., 2016), not all species respond to light at the same intensity, and further tests are needed to compare these two methods.

One emerging issue has been linked to the interpretation of the causes behind the decline observed in  $K_{leaf}$ . A recent meta-analysis of the literature revealed that the bulk of the species studied ( $> 300$ ) decline by more than 50% prior to turgor loss point (Scoffoni & Sack, 2017). The majority of studies have assumed that the decline in  $K_{leaf}$  relates to embolism in the vein xylem, as has been widely demonstrated for stems. However, on average across species, 57% of the resistance of the hydraulic pathway is located outside the vein xylem (Scoffoni & Sack, 2017). Recent studies imaging embolism formation in the veins of dehydrated leaves (using either a simple scanner or x-ray microcomputer tomography) reveal that embolism only occurs in strongly dehydrated leaves, typically past their wilting point when stomata are shut (Brodribb et al., 2016a; Hochberg et al., 2017; Scoffoni et al., 2017b), and hydraulics experiments show that strong declines of  $K_{leaf}$  are driven by changes in outside-xylem pathways (Trifilo et al., 2016; Scoffoni et al., 2017a). However, because many processes occur outside the xylem during leaf dehydration (such as aquaporin deactivation, tissue shrinkage, abscisic acid (ABA) signalling, changes in the volume of intercellular airspaces, collapse of xylem conduits in the minor veins), it has been challenging to determine the main cause, although spatially explicit modelling of the outside-xylem pathways have given important insights, pointing especially to a role of declining membrane permeability (Buckley et al., 2017; Scoffoni et al., 2017a).

#### **5.16.3 References**

##### **Theory, significance, and large datasets**

Blackman et al. (2010), Brodribb et al. (2016a), Hernandez-Santana et al. (2016), Scoffoni & Sack (2017), Trifilo et al. (2016)

### **More on methods and existing protocols**

Guyot et al. (2012), Sack & Scoffoni (2012), Scoffoni et al. (2012)

### **All references**

- Blackman, C. J., Brodribb, T. J., & Jordan, G. J. (2010). Leaf hydraulic vulnerability is related to conduit dimensions and drought resistance across a diverse range of woody angiosperms. *New Phytologist*, 188(4), 1113-1123.
- Brodribb, T. J., & Holbrook, N. M. (2006). Declining hydraulic efficiency as transpiring leaves desiccate: two types of response. *Plant, Cell & Environment*, 29(12), 2205-2215.
- Brodribb, T. J., Biénaime, D., & Marmottan, P. (2016a). Revealing catastrophic failure of leaf networks under stress. *Proceedings of the National Academy of Sciences USA*, 113(17), 4865-4869.
- Brodribb, T. J., Skelton, R. P., McAdam, S. A. M., Biénaime, D., Lucani, C. J., & Marmottan, P. (2016b). Visual quantification of embolism reveals leaf vulnerability to hydraulic failure. *New Phytologist*, 209(4), 1403-1409.
- Buckley, T. N., John, G. P., Scoffoni, C., & Sack, L. (2017). The sites of evaporation within leaves. *Plant Physiology*, 173, 1763-1782.
- Cochard, H., Froux, F., Mayr, F. F. S., & Coutand, C. (2004). Xylem wall collapse in water-stressed pine needles. *Plant Physiology*, 134(1), 401-408.
- Guyot, G., Scoffoni, C., & Sack, L. (2012). Combined impacts of irradiance and dehydration on leaf hydraulic conductance: insights into vulnerability and stomatal control. *Plant, Cell & Environment*, 35, 857-871.
- Hernandez-Santana, V., Rodriguez-Dominguez, C. M., Fernández, J. E., & Diaz-Espejo, A. (2016). Role of leaf hydraulic conductance in the regulation of stomatal conductance in almond and olive in response to water stress. *Tree Physiology*, 36(6), 725-735.
- Hochberg, U., Windt, C. W., Ponomarenko, A., Zhang, Y.-J., Gersony, J., Rockwell, F. E., & Holbrook, N. M. (2017). Stomatal closure, basal leaf embolism, and shedding protect the hydraulic integrity of grape stems. *Plant Physiology*, 174(2), 764-775.
- Johnson, D. M., McCulloh, K. A., Woodruff, D. R., & Meinzer, F. C. (2012). Evidence for xylem embolism as a primary factor in dehydration-induced declines in leaf hydraulic conductance. *Plant, Cell & Environment*, 35(4), 760-769.
- Kim, Y. X., & Steudle, E. (2007). Light and turgor affect the water permeability (aquaporins) of parenchyma cells in the midrib of leaves of *Zea mays*. *Journal of Experimental Botany*, 58(15-16), 4119-4129.
- Sack, L., & Scoffoni, C. (2012). Measurement of leaf hydraulic conductance and stomatal conductance and their responses to irradiance and dehydration using the evaporative flux methods (EFM). *Journal of Visualized Experiments*, 70, e4179.

- Sack, L., Melcher, P. J., Zwieniecki, M. A., & Holbrook, N. M. (2002). The hydraulic conductance of the angiosperm leaf lamina: a comparison of three measurement methods. *Journal of Experimental Botany*, 53(378), 2177-2184.
- Sade, N., Shatil-Cohen, A., Attia, Z., Maurel, C., Boursiac, Y., Kelly, G., ... Moshelion, M. (2014). The role of plasma membrane aquaporins in regulating the bundle sheath-mesophyll continuum and leaf hydraulics. *Plant Physiology*, 166(3), 1609-1620.
- Scoffoni, C., & Sack, L. (2017). The causes and consequences of leaf hydraulic decline with dehydration. *Journal of Experimental Botany*, 68(16), 4479-4496.
- Scoffoni, C., McKown, A. D., Rawls, M., & Sack, L. (2012). Dynamics of leaf hydraulic conductance with water status: quantification and analysis of species differences under steady-state. *Journal of Experimental Botany*, 63, 643-658.
- Scoffoni, C., Vuong, C., Diep, S., Cochard, H., & Sack, L. (2014). Leaf shrinkage with dehydration: coordination with hydraulic vulnerability and drought tolerance. *Plant Physiology*, 164, 1772-1788.
- Scoffoni, C., Albuquerque, C., Brodersen, C. R., Townes, S. T., John, G. P., Bartlett, M. K., ... Sack, L. (2017a). Outside-xylem tissue vulnerability, not xylem embolism, controls leaf hydraulic decline with dehydration across diverse angiosperms. *Plant Physiology*, 173, 1197-1210.
- Scoffoni, C., Albuquerque, C., Brodersen, C. R., Townes, S. T., John, G. P., Cochard, H., ... Sack, L. (2017b). Leaf vein xylem conduit diameter influences susceptibility to embolism and hydraulic decline. *New Phytologist*, 213, 1076-1092.
- Shatil-Cohen, A., Attia, Z., & Moshelion, M. (2011). Bundle-sheath cell regulation of xylem-mesophyll water transport via aquaporins under drought stress: a target of xylem-borne ABA? *Plant Journal*, 67(1), 72-80.
- Trifilo, P., Raimondo, F., Savi, T., Lo Gullo, M. A., & Nardini, A. (2016). The contribution of vascular and extra-vascular water pathways to drought-induced decline of leaf hydraulic conductance. *Journal of Experimental Botany*, 67(17), 5029-5039.
- Zhang, Y. J., Rockwell, F. E., Graham, A. C., Alexander, T., & Holbrook, N. M. (2016). Reversible leaf xylem collapse: a potential "circuit breaker" against cavitation. *Plant Physiology*, 172(4), 2261-2274.

**Authors:** Scoffoni C<sup>1</sup>, Sack L<sup>2</sup>

**Reviewer:** Dickman LT<sup>3</sup>, Johnson DM<sup>4</sup>

## Affiliations

<sup>1</sup> Department of Biological Sciences, California State University, Los Angeles, USA

<sup>2</sup> Department of Ecology and Evolutionary Biology, University of California Los Angeles, Los Angeles, USA

Halbritter et al. (2020) The handbook for standardised field and laboratory measurements in terrestrial climate-change experiments and observational studies (ClimEx). *Methods in Ecology and Evolution*, 11(Issue) Pages.

<sup>3</sup> Earth and Environmental Sciences Division, Los Alamos National Laboratory, Los Alamos, USA

<sup>4</sup> Warnell School of Forestry and Natural Resources, University of Georgia, Athens, USA